

# **Modulation of Cell-Matrix Adhesions to Affect Mechanotransduction**

**Inauguraldissertation**

zur

Erlangung der Würde eines Doktors der Philosophie

vorgelegt der

Philosophisch-Naturwissenschaftlichen Fakultät

der Universität Basel

von

**Roman Lutz**

aus Basel, Schweiz

Leiter der Arbeit

Prof. Dr. M. Chiquet

Friedrich Miescher Institute for Biomedical Research

Basel, Switzerland, 2010

Genehmigt von der Philosophisch-Naturwissenschaftlichen Fakultät auf Antrag von

Matthias Chiquet, Matthias Lütolf, Markus Rüegg

Basel, den 22.06.2010

Prof. E. Parlow  
Dekan

## Acknowledgements

Many people directly and indirectly supported and helped me and my projects throughout these years. However, first and most special thanks go to **Matthias Chiquet** who never hesitated to help me with his broad knowledge and scientific skills to proceed the projects. His constant support at all levels made him literally deserve the term “Doktorvater”.

Many thanks also go to **Ruth Chiquet-Ehrismann** who gave me the possibility to start and carry out my thesis in her lab. I always appreciated her interest in my project and fruitful comments in lab meetings.

Big thanks also go all present and past members of the **Chiquet-lab** that crossed my time at the FMI. I will miss funny and relaxing lunch breaks as well as being interpersonally entertained during lab-work. Thanks also go to all other **friends at the FMI** from all around the world giving this international place its nice atmosphere.

I would also like to thank our **collaborators Matthias Lütolf, Jürgen Brugger, Markus Textor** and the members of their labs especially **Mirjam Ochsner** and **Kristopher Pataky** for the constant supply and production of micro and nanopatterns.

I am also very thankful for support and helpful comments of **Matthias Lütolf** and **Markus Rüegg** and for being part of my thesis committee.

Many thanks also go to my **friends** especially Mäge, Sticky and Ric.

A big thank you and all my love go to my girlfriend **Lana**.

At this point I would like to give my deepest and most sincere thanks to **my family**, especially to my parents **Helena and Rudolf**, my sister **Estelle** and my lovely **grandmother** who showed me from the beginning what love means. I know I would never have reached this point without them and I'm more than grateful for their support in every aspect throughout my whole life.

## Table of Contents

<b>I. SUMMARY</b>	<b>3</b>
<b>II. INTRODUCTION</b>	<b>6</b>
II.1 Extracellular Matrix .....	7
II.2 Integrins and cell-matrix adhesions .....	8
II.3 Different types of cell-matrix adhesions.....	10
II.4 Fibronectin and the $\alpha_5\beta_1$ integrin receptor .....	13
II.5 Vitronectin and the $\alpha_v\beta_3$ integrin receptor .....	16
II.6 Small GTPases of the Rho-family .....	16
II.7 The Cytoskeleton .....	18
II.8 Actin Stress Fibers .....	19
II.9 Rho, Rac and Cdc42 regulate the organization of the actin cytoskeleton .....	21
II.10 MAL/MKL-1 .....	23
II.11 Tenascin-C .....	24
II.12 Mechanical stress and ECM regulation .....	25
II.13 Cyclic strain as a model system for mechanotransduction .....	26
II.14 Responses of fibroblasts to mechanical stress .....	28
<b>III. AIM OF THE WORK</b>	<b>30</b>
<b>IV. RESULTS</b>	<b>32</b>
IV.1 Tenascin-C induction by cyclic strain requires integrin-linked kinase .....	33
IV.2 Identification of a fibronectin interaction site in the extracellular matrix protein ameloblastin .....	47
IV.3 Pericellular fibronectin is required for RhoA-dependent responses to cyclic strain in fibroblasts .....	59
IV.4 Pericellular fibronectin is required for RhoA-dependent responses to cyclic strain in fibroblasts (high quality figures and supplementary material).....	71

---

IV.4 Limiting Growth of Focal Complexes Inhibits their Maturation and Induces Lamellipodia Formation.....	84
IV.4.1 Summary .....	86
IV.4.2 Introduction .....	87
IV.4.3 Results .....	88
IV.4.4 Discussion .....	94
IV.4.5 Material and Methods .....	97
IV.4.6 Figures with legends.....	100
VI.4.7 References .....	106
<b>V. DISCUSSION</b>	<b>108</b>
V.1 Integrating our results in the context of mechanotransduction .....	109
V.2 Integrating our results in the context of cell adhesion maturation .....	111
V.3 Fibronectin and Rho-dependent responses in cancer.....	114
<b>VI. APPENDIX</b>	<b>116</b>
VI.1 References.....	117
VI.2 Abbreviations.....	127
VI.3 Curriculum Vitae.....	128

# **SUMMARY**

# I. Summary

In cultured fibroblasts three types of cell-matrix adhesion with specific cellular localization and protein composition can be distinguished: focal complexes, focal adhesions and fibrillar adhesions. The formation of fibrillar adhesions is known to be required for fibronectin fibrillogenesis. However, little is known about specific signaling from these adhesion sites. Previous experiments showed that ILK (integrin-linked kinase) knockout fibroblasts are defective in RhoA-dependent responses to cyclic strain. In addition these cells did not form fibrillar adhesions and did not assemble fibronectin. We therefore speculated that pericellular fibronectin and the fibrillar adhesions are important to activate the RhoA/ROCK pathway by mechanical stress. To test this hypothesis, we generated fibronectin knockdown fibroblasts and analyzed their ability to activate specific RhoA dependent responses to cyclic strain in the absence and presence of exogenous fibronectin. Normal fibroblasts seeded on vitronectin in fibronectin-depleted medium deposited their own fibronectin matrix and in response to cyclic strain, activated RhoA, formed stress fibers, translocated MAL (megakaryocytic leukemia protein) to the nucleus, and induced tenascin-C. By contrast, these responses were suppressed in fibronectin knockdown or knockout cells grown under identical conditions. Interestingly, on vitronectin substrate, fibronectin-deficient cells lacked integrin  $\alpha_5\beta_1$ -positive fibrillar adhesions. However, when fibronectin-deficient fibroblasts were plated on exogenous fibronectin, their defects in adhesions and mechanotransduction were restored. Studies with fibronectin fragments indicated that both, the RGD-synergy site and the adjacent heparin-binding region were required for full activity in mechanotransduction, but not its ability to self-assemble. In contrast to RhoA-mediated responses, activation of Erk1/2 and PKB/Akt by cyclic strain was not affected in fibronectin-deficient cells. Our results indicate

that activation of the RhoA/ROCK pathway by mechanical stress originates from fibrillar adhesions connected to fibronectin in the extracellular matrix.

In a second project we tried to get more insight in signaling by focal complexes. These cell-matrix adhesions are the first to be formed by adhering fibroblasts. They are clearly smaller than more mature focal adhesions and are uniquely found at the cell border of lamellipodia. Using patterns with square-shaped, RGD-coupled gold dots of a limited size, we attempted to inhibit maturation of focal complexes into focal adhesions. Indeed, on RGD-coated gold-squares smaller than  $1\mu\text{m}$ , cells uniquely formed focal complexes indicated by low recruitment of  $\alpha_5$  integrin. Cells formed excessive amounts of lamellipodia and assembled actin only into a fine meshwork. However, on squares equal or larger than  $1\mu\text{m}$  cells exhibited focal adhesions, spread normally and assembled actin into thick fibers. Our results show that at the level of focal complexes cell adhesion maturation can be inhibited by restricting size. In addition, according to the lamellipodia which are seen with cells on patterns smaller than  $1\mu\text{m}$ , let suggest increased Rac signaling deriving from these focal complexes.



# **INTRODUCTION**

## II. Introduction

Mechanical stress is important for tissue homeostasis (Chiquet et al., 2009). At cell-matrix adhesions transmembrane proteins called integrins join the extracellular matrix with the intracellular actin cytoskeleton. Mechanical signals that are transmitted through the extracellular matrix are converted into intracellular biochemical signals at cell adhesions (Geiger et al., 2009). Thereby growth factor receptors work in concert with integrins to modulate signaling cascades that affect cellular structures and gene regulation (Alam et al., 2007). Cellular signaling often involves activation of small GTPases of the ras superfamily and protein phosphorylation by kinases. Mechanical stress thereby affects the actin cytoskeleton leading to actin polymerization and contraction. This again leads to nuclear translocation of MAL/MKL-1, a transcriptional co-activator regulating gene expression (Miralles et al., 2003). Mechanisms and structure of the most important players involved in mechanotransduction and intracellular signaling are explained in the following paragraphs.

### II.1 Extracellular Matrix

The extracellular matrix (ECM) is an intricate network of macromolecules that surrounds cells and anchors them in tissues. This matrix is composed of a variety of highly glycosylated proteins that are secreted locally and assembled into an organized meshwork in direct association with the surface of the cells that produced them.

Proteins in the ECM are normally grouped as glycoproteins, proteoglycans and collagens. The oligosaccharides of glycoproteins like elastins, laminins or fibronectins are added and processed along the secretory pathway in the endoplasmatic reticulum and the Golgi. Proteoglycans contain long charged glycosaminoglycan (GAG) chains that are also added in

the golgi. An exception represents hyaluronan, which is a GAG chain without core protein that is "spun out" by enzymes at the cell surface directly into the extracellular space. Collagens are defined as glycoproteins or proteoglycans with one or more collagenous domains. These domains are built from three type II helices forming a right handed superhelix. The sequence is composed of repeating GXY in which proline is frequently found in X-position and hydroxyproline in Y-position. Dependent on the requirement of the tissue, collagens can be aligned as bundles to bear tensile stress (e.g. in tendons) or be arranged as meshwork with incorporated proteoglycans acting as water cushion (e.g. in cartilage). Also in other tissues GAG side chains are highly hydrated and form a gel to resist compressive forces and allow fast diffusion of micromolecules.

Not only the components of the ECM but also their organization is controlled by the cells embedded and varies among different tissues. Thereby cells influence the matrix in a dynamic process including protein secretion, matrix modulation and proteolysis.

Many extracellular matrix glycoproteins are unusually large molecules with extended conformations spanning distances of several hundred nanometers. They are considered to have evolved by exon shuffling and therefore often consist of similar protein domains. Some of these proteins serve as ligands for cell attachment and activate intracellular signaling pathways within cells, thereby regulating cell proliferation, survival and differentiation.

(Alberts, 2008; Kjaer, 2004; Reichardt, 1999)

## **II.2 Integrins and cell-matrix adhesions**

In all tissues the extracellular matrix provides a scaffold for cellular support. Cells interact with specific proteins in the matrix by means of specialized adhesion sites. At these sites integrins anchor the cell to the matrix. Integrins are heterodimeric transmembrane proteins

generated by selective pairing between 18  $\alpha$  and 8  $\beta$  subunits (Luo et al., 2007). There are 24 distinct integrin receptors that bind various ECM ligands with different affinities. With their cytoplasmic domain integrins join to the actin cytoskeleton by a variety of anchor proteins (Figure 1).

Integrins are involved in mechanotransduction, a classical outside-in signaling in which extracellular mechanical signals are converted into intracellular biochemical activation. However integrins also signal from the inside to the outside. This is particularly important during the initial step of cell-matrix adhesion formation (Ratnikov et al., 2005). Thereby the adaptor protein talin is binding an NPxY peptide motif in the cytosolic domain of  $\beta$  integrins. This promotes clustering and activation of integrins leading to binding of extracellular matrix proteins. Activation involves a large conformational change of integrin ectodomains from a bent to an extended shape. Thus, adaptor proteins like talin not only mediate a direct interaction between integrin and actin but also have a regulatory function. Recruitment of proteins into adhesion sites depends on competition, conformational state and tyrosine phosphorylation of potential binding partners (Zamir and Geiger, 2001). Together these factors build a scaffold to stabilize the adhesion site and to allow interaction with kinases like Src and FAK forming a platform for early steps of signaling via various pathways. The functional mechanism of how physical stimuli are converted into biochemical signaling is largely unknown. However, a possible mechanism was proposed for the adaptor protein p130Cas, which was shown to expose tyrosine sites upon mechanical stretching allowing access for phosphorylation by Src (Sawada et al., 2006).

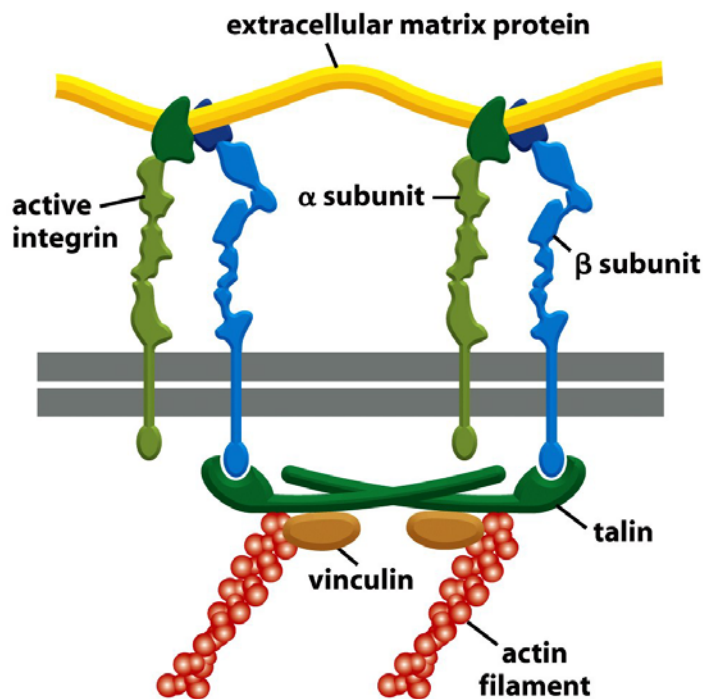


Figure 19-45 Molecular Biology of the Cell 5/e (© Garland Science 2008)

### Figure 1: First proteins in cell-matrix adhesion sites.

Binding of talin to the cytosolic NPXY motif in the  $\beta$ -subunit activates integrins. In the active conformation integrins bind extracellular matrix proteins. Actin polymerization is then initiated and the primary complex is stabilized by adaptor proteins like vinculin,  $\alpha$ -actinin, and filamin. (Image taken from Alberts, 2008).

## II.3 Different types of cell-matrix adhesions

Cell-matrix adhesions are assembled in a hierarchical way (Zaidel-Bar et al., 2004). In fibroblasts cultured on 2D substrates three distinct stages of integrin-based adhesions can be distinguished, each consisting of a specific protein composition and localization within the cell (figure 2, 3). Initial contact between the cell and ECM, however, is mediated independently of integrins by cell-associated hyaluronan (Zimmerman et al., 2002). This rather transient interaction is replaced by focal complexes. They are composed of talin, paxillin and  $\alpha_v\beta_3$  integrin interacting with several extracellular matrix proteins containing an RGD peptide motif. Later on, vinculin, FAK,  $\alpha$ -actinin and Arp2/3 are recruited to build late focal complexes. These highly dynamic adhesion sites are found as dot-like structures ( $0.25 \mu\text{m}^2$ ) at the border of ruffling lamellipodia (Ballestrem et al., 2001; Zaidel-Bar et al., 2003). After persisting a few minutes (meanwhile the leading edge further advances and new focal complexes are formed in front) some of them eventually mature into focal adhesions by

recruiting additional proteins like integrin  $\alpha_5\beta_1$ , tensin and zyxin. This transition depends on formation of actin bundles and their contractility, which applies force at cell-matrix adhesions. Thus, focal adhesions can only form on a mechanically stable (stiff) substrate. Contraction requires active RhoA and induces growth of these adhesions (Alexandrova et al., 2008; Riveline et al., 2001). Even though  $\alpha_5\beta_1$  and tensin are recruited, these proteins are modestly found in mature focal adhesions. Further actomyosin contraction pulls them out of focal adhesions thereby forming fibrillar adhesions. During this process, pericellular fibronectin bound to its receptor  $\alpha_5\beta_1$  is stretched, thereby exposing self assembly sites for fibronectin fibrillogenesis (Zamir et al., 2000).

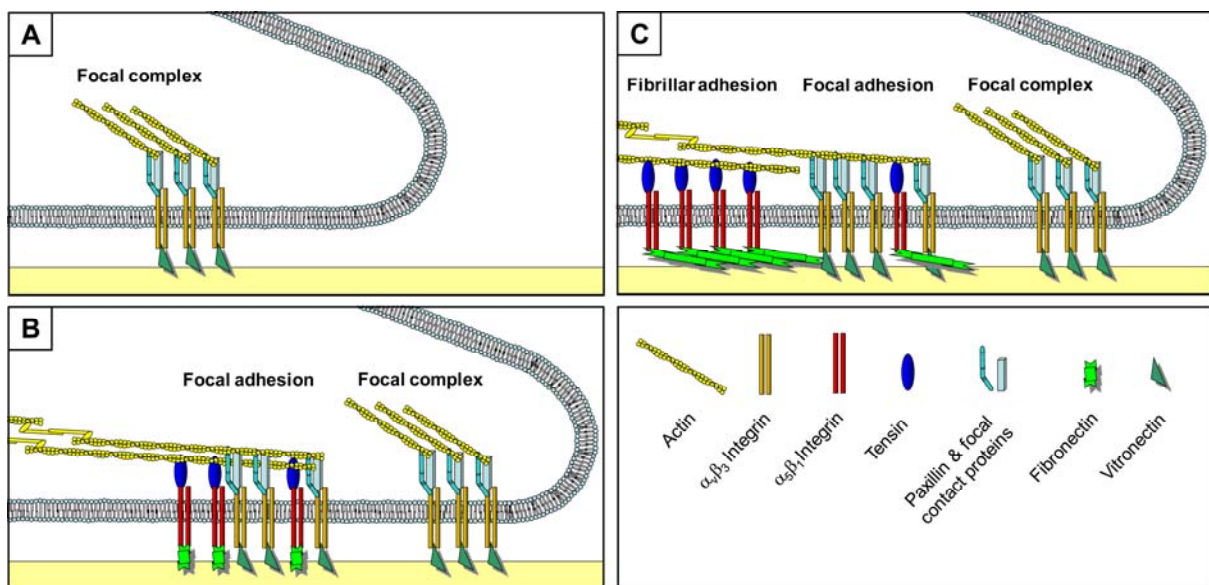


**Figure 2: Cell-matrix assembly is linked to fibronectin fibrillogenesis.**

(A) Focal complexes represent the initial cell-matrix adhesion structures. They are assembled at the cell border of ruffling lamellipodia. (B) As focal complexes mature into early focal adhesions the cell pushes to the front and new focal complexes are formed. Maturation includes actomyosin contraction and recruitment of  $\alpha_5\beta_1$  integrin and tensin. (C) Further tension pulls  $\alpha_5\beta_1$  integrin and tensin out of early focal adhesions to form fibrillar adhesions and late focal adhesions. During this process fibronectin bound to  $\alpha_5\beta_1$  integrin is stretched and thereby enables assembly of fibronectin fibrils. (Scheme: R.Lutz; published in Chiquet et al., 2009).

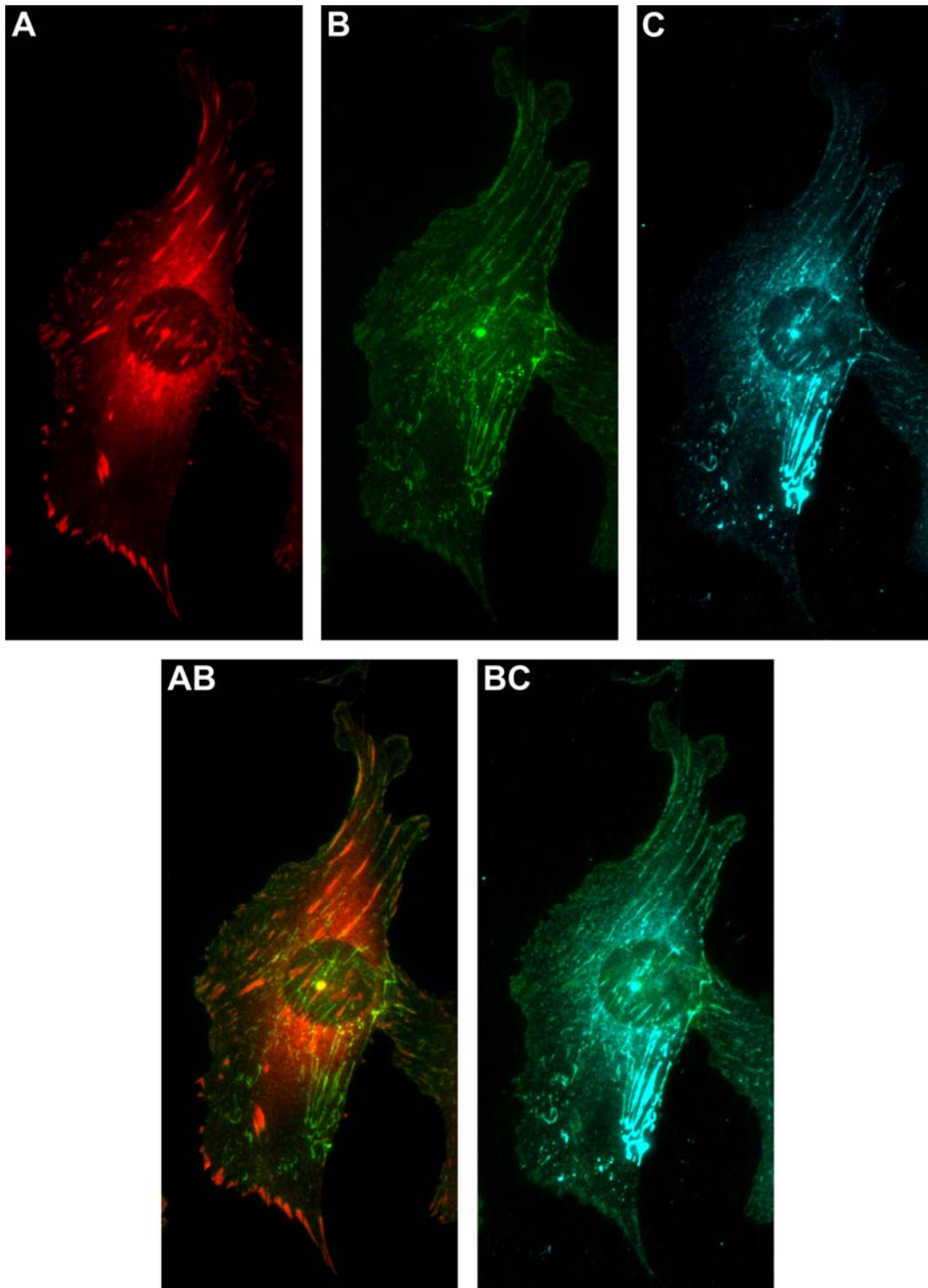


**Figure 3: Distinct subcellular localization of focal and fibrillar adhesions in fibroblasts.** Staining for vinculin (A) shows localization of focal adhesions. Also some focal complexes are stained at the border of the lamellipodia (top). Staining for  $\alpha_5\beta_1$  integrin (B) reflects fibrillar adhesions. In the colocalization picture of these two channels (AB) the origin of  $\alpha_5\beta_1$  integrin is visible as they are often adjacent to focal adhesions. Fibronectin staining is shown

in (C) and strongly colocalizes with  $\alpha_5\beta_1$  integrin in fibrillar adhesions (BC). (Pictures: R.Lutz, unpublished).

## II.4 Fibronectin and the $\alpha_5\beta_1$ integrin receptor

Fibronectin (FN) is a dimeric glycoprotein ubiquitously found in extracellular matrix (Wierzbicka-Patynowski and Schwarzbauer, 2003). Also in blood plasma a high concentration of FN is found, which is secreted in the liver by hepatocytes. While FN in the extracellular matrix serves as adhesion protein, plasma FN is important in wound healing as it interacts with fibrin and platelets to form a hemostatic clot (Sakai et al., 2001). FN knockout mice die around embryonic day 8.5. Deficits in mesodermal migration, adhesion and proliferation have been proposed (George et al., 1993).

FN is secreted as disulfide-bonded dimer primarily composed of FN type I, II and III modules. Sets of these modules form domains to bind distinct extracellular and cell surface molecules including heparin, fibrin, collagen, integrins and FN itself (figure 4A, B). Binding to heparin is mediated by two binding sites, a weaker one at the N-terminal end and a strong one towards the C-terminal end of FN which also binds to chondroitin sulfate. Collagen binding is mediated by FN type I and II repeats at the N-terminus. However, these sites bind far more effectively to denaturated collagen. Therefore a physiological role in the ECM is controversial (Pankov and Yamada, 2002). However, a function of these sites in clearance of denaturated collagens from the blood has been suggested (Pankov and Yamada, 2002). FN also contains two major fibrin-binding sites at the N- and C-terminus. Interaction between FN and fibrin is thought to be important for cell adhesion or cell migration into fibrin clots during wound healing (Pankov and Yamada, 2002). FN can also assemble with itself, which is probably its most important interaction in the ECM. Self assembly, however, is not possible in its secreted, compact conformation. For fibrillogenesis FN must be activated in a process



involving the FN receptor integrin  $\alpha_5\beta_1$  to expose self assembly sites (Wierzbicka-Patynowski and Schwarzbauer, 2003). Integrin  $\alpha_5\beta_1$  thereby specifically recognizes the RGD motif (Arg-Gly-Asp) located in FN's 10<sup>th</sup> typeIII domain (figure 4C). Interaction also involves an adjacent synergy site (PHSRN) in FN's 9<sup>th</sup> type III domain which renders fibronectin binding specific for  $\alpha_5\beta_1$  (Nagai et al., 1991). Binding of this synergy site, however, is induced upon force application and switches  $\alpha_5\beta_1$  into a tensioned state with increased bond strength (Friedland et al., 2009). Initial integrin-binding of FN induces expansion of the compact dimer that, in combination with actin contraction during fibrillar adhesion formation, allow FN fibrillogenesis by exposing FN self assembly sites (figure 4D). In matrices FN is thereby found in different degrees of partially unfolded structures (Smith et al., 2007).

FNs are generated in a variety of different splice variants. More than 20 different isoforms are known. The variant region close to the C-terminus can be alternatively spliced in many different ways. In addition, the exons coding for extra domains EDA and EDB are either fully spliced in or totally excluded. Fibronectins including the EDA exon have been observed in wounds and lung fibrosis (White et al., 2008).

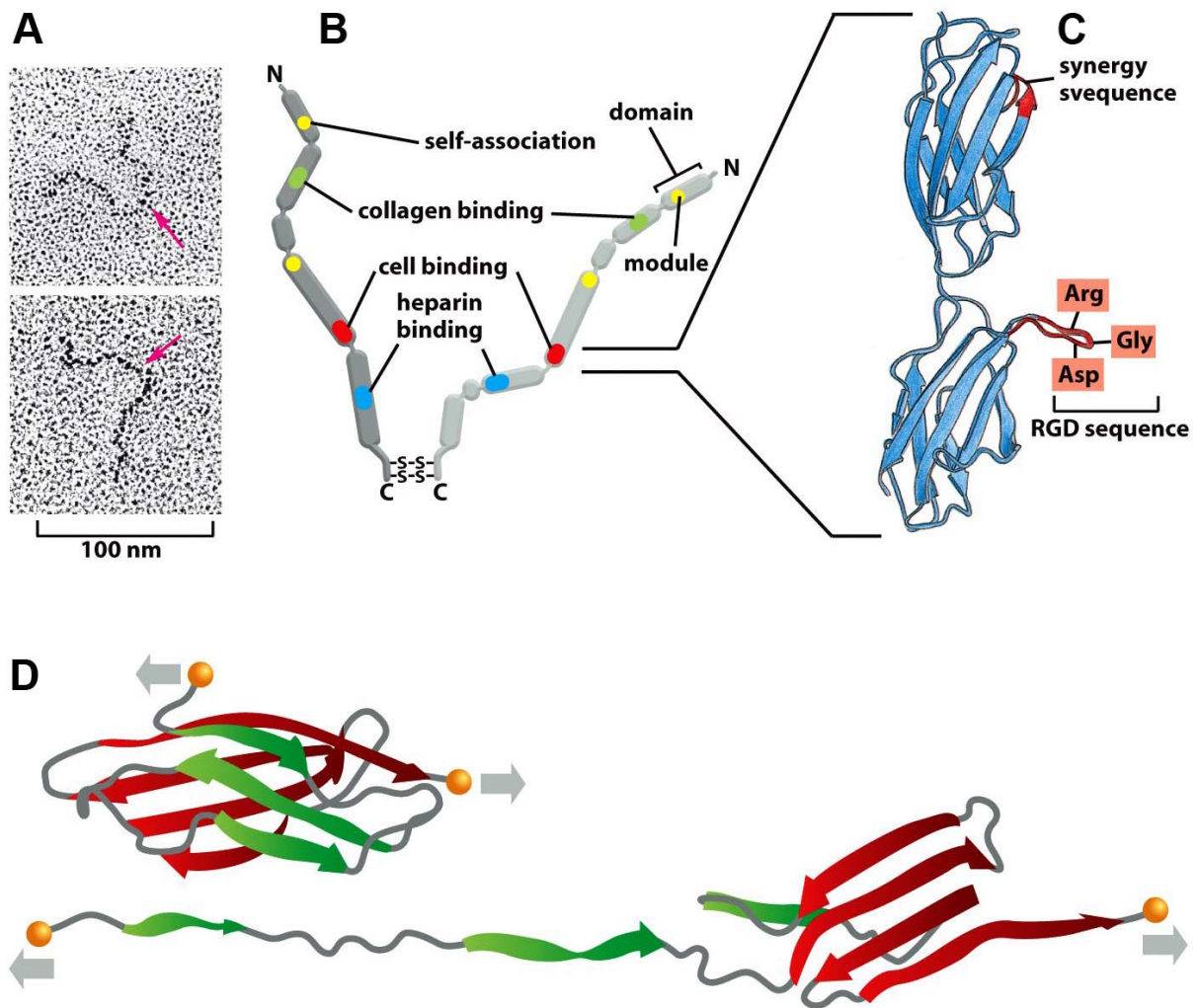


**Figure 4: Structure of fibronectin.**

(A) Electron micrographs of individual fibronectin dimer molecules shadowed with platinum; red arrows mark the C-termini. (B) Two fibronectin polypeptide chains are joined by two disulfide bonds near the C-termini. Each chain is folded into different domains that contain binding modules for various molecules. (C) The cell binding domain exposes a loop consisting of the RGD motif which is recognized by different integrins. The adjacent synergy site, however, is specific for binding to  $\alpha_5\beta_1$  integrin. (D) Fibronectin consists of several type III domains that can be stretched by application of force. Some of these domains expose cryptic binding sites that cause the stretched molecule to assemble into filaments. (Image taken from Alberts, 2008).

## II.5 Vitronectin and the $\alpha_v\beta_3$ integrin receptor

Vitronectin is an abundant glycoprotein in blood plasma and is synthesized in the liver (Horton, 1997; Schwartz et al., 1999). It binds plasminogen, urokinase-receptor and complement implicating its participation on the immune response and in the regulation of clot formation. Vitronectin is also present in the extracellular matrix, where it is anchored by binding to collagen and heparin. It directly interacts with cells by its N-terminal RGD motif that bind different integrins such as  $\alpha_v\beta_1$ ,  $\alpha_v\beta_3$ ,  $\alpha_v\beta_5$ ,  $\alpha_v\beta_6$ ,  $\alpha_v\beta_8$ . In fibroblasts vitronectin is mainly bound by  $\alpha_v\beta_3$  which is also called “vitronectin receptor”. However,  $\alpha_v\beta_3$  does not only bind vitronectin but generally recognizes RGD-motifs that are present in various ECM proteins.

## II.6 Small GTPases of the Rho-family

The Rho proteins belong to the Ras superfamily of small, monomeric GTPases that comprise more than 150 members. They are molecular switches that cycle between an active (GTP-bound) and an inactive (GDP-bound) state (Etienne-Manneville and Hall, 2002) (figure 5). In the active state, GTPases recognize target proteins and generate a response until GTP hydrolysis returns them back to the inactive form. However most Rho-family proteins have weak GTPase activity and are therefore supported by GTPase-activating proteins (GAPs). To be activated again Rho proteins must bind to guanine nucleotide exchange factors (GEF), which replace the hydrolysed GDP by GTP. In the human genome there are more than 60 GEFs and over 70 GAPs to carefully regulate activation of the small GTPases. At the C-terminus Rho proteins are geranylated. In the inactive state this prenyl-tail is covered by a guanosine nucleotide exchange inhibitor (GDI). Upon activation by a GEF the Rho GTPases

undergo conformational changes. Thereby GDI dissociate and the prenyl-tail gets exposed allowing Rho to attach to the plasma membrane.

The Rho family of GTPases consists of 16 members. Besides the best-characterized members Rho, Rac and Cdc42 few functional data are currently available on the other members of this family. Rho, Rac and Cdc42 are all represented by different isoforms. Rho for example exists in the isoforms RhoA, RhoB and RhoC. While RhoA is clearly the best studied isoform, few is known about function of RhoB and RhoC. However, different effector binding and localization in the cell indicate different functions of these isoforms (Wheeler and Ridley, 2004).

Every GTPase can be activated by many different GEFs and one GEF may activate several GTPases. However the mechanisms by which specificity is determined remains to be unraveled (Sinha and Yang, 2008). Rho GTPase GEFs are characterized by their conserved Dbl Homology (DH) / Pleckstrin Homology (PH) domains. The DH domain directly interacts with the Rho GTPases, which results in the dissociation of GDP, while the PH domain modulates the activities of the DH domain and targets the complex to the membrane.

Rho, Rac and Cdc42 regulate the polymerization of actin to produce stress fibers, lamellipodia and filopodia respectively. Thereby they control cell contractility and migration but also influence phagocytosis, proliferation and regulated secretion (Etienne-Manneville and Hall, 2002).

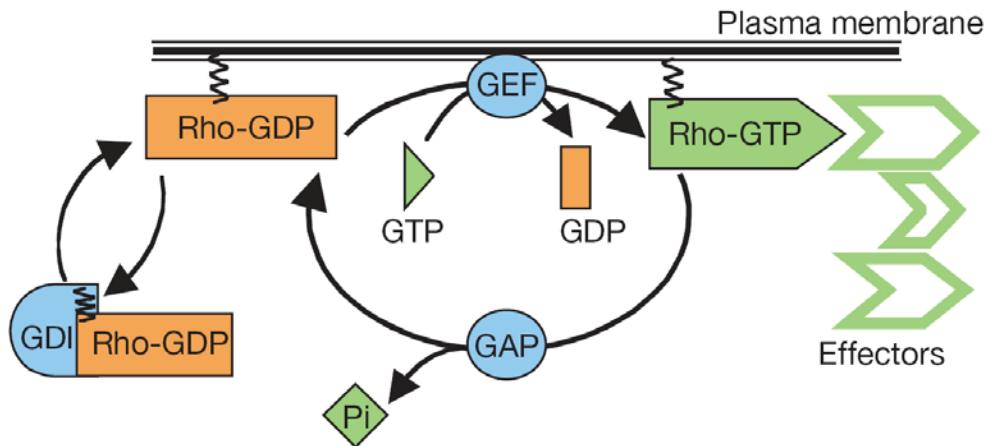


**Figure 5: The Rho GTPase cycle.**

In the inactive (GDP-bound) state Rho GTPases are bound by a guanine nucleotide exchange inhibitors (GDIs). Upon activation by a guanine nucleotide exchange factor (GEF) the GDI dissociates from Rho and the active GTPase is recruited and attached to the plasma membrane by help of its prenyl tail. At the membrane, active Rho can interact with different effectors. GTPase-activating proteins (GAPs) stimulate hydrolysis, leading to inactivation, and detachment from the membrane. (Taken from Etienne-Manneville and Hall, 2002).

## II.7 The Cytoskeleton

The cytoskeleton is a network of protein filaments that spatially organizes the cytoplasm of eukaryotic cells. Functions include cell stabilization, migration, cell division and intracellular transport. It consists of three types of structures (actin filaments, microtubules and intermediate filaments), each with different mechanical properties and dynamics.

Actin filaments are double-helical polymers formed from globular actin monomers (G-actin). The monomers are ATPases that polymerize at the end of the filaments upon binding of ATP. Actin filaments are polarized and the speed of polymerization is higher at the “plus” than at the “minus” end. Shortly after binding to the filament the ATP is hydrolyzed. Since ATP concentration is 10-fold higher than ADP, growth of actin filaments is favoured. However,

endogenous proteins like thymosin and profilin slow down and thereby control polymerization.

A similar system is used by microtubules, which are stiff, hollow cylinders made up from the globular GTPases  $\alpha$  and  $\beta$  tubulin. Upon polymerization GTP is hydrolyzed which slows down binding of further monomers. Fast growing microtubules therefore have a cap of GTP-bound monomers. Cell-derived factors help to stabilize or destabilize microtubules and thereby control their growth.

Intermediate filaments are reinforcing woven structures made from filamentous proteins with  $\alpha$ -helical coiled-coil structures. In most animal cells an extensive network of intermediate filaments surrounds the nucleus and extends out to the cell periphery, where they interact with the plasma membrane. There is a variety of tissue-specific forms of intermediate filaments like keratin filaments (epithelial cells), desmin filaments (muscle), vimentin filaments (fibroblasts) and neurofilaments (neurons). Intermediate filaments mainly have a structural and tension-bearing role within cells (Alberts, 2008).

## II.8 Actin Stress Fibers

The stress fibers of fibroblasts are composed of bundles of approximately 10-30 actin filaments which are held together by the actin-crosslinking protein  $\alpha$ -actinin (Cramer et al., 1997). In some stress fibers, actin filament polarity is uniform. In others, the filaments show random plus and minus orientation (Cramer et al., 1997). Stress fibers disassemble in response to the clostridium botulinum C3 toxin, which targets RhoA, RhoB and RhoC (Chardin et al., 1989). On the other hand, microinjection of activated recombinant RhoA into fibroblasts leads to rapid and extensive formation of stress fibers (Paterson et al., 1990). The link thereby lies in the activation of RhoA-effectors.

RhoA-GTP activates Rho-dependent kinase ROCK, which phosphorylates myosin light chain to induce actomyosin contractility (figure 6). However, activation of ROCK alone does not generate the thick, parallel stress fibers seen after RhoA activation; the activity of the actin-binding protein mDia1 is also required (Pellegrin and Mellor, 2007). The function of mDia1 is to initiate the polymerization of actin filaments from cell-matrix adhesions to form a short actin bundle that can then be elongated into a stress fiber. This activating effect of mDia1 on actin polymerization is thought to be regulated by interaction with profilin (Watanabe et al., 1999). In addition, actin polymerization can also be facilitated by phosphorylation and inactivation of the actin depolymerizing factor cofilin, which is a substrate of activated LIM-kinase (Arber et al., 1998). LIM-kinase 1 in turn is activated by ROCK (Bernard, 2007).

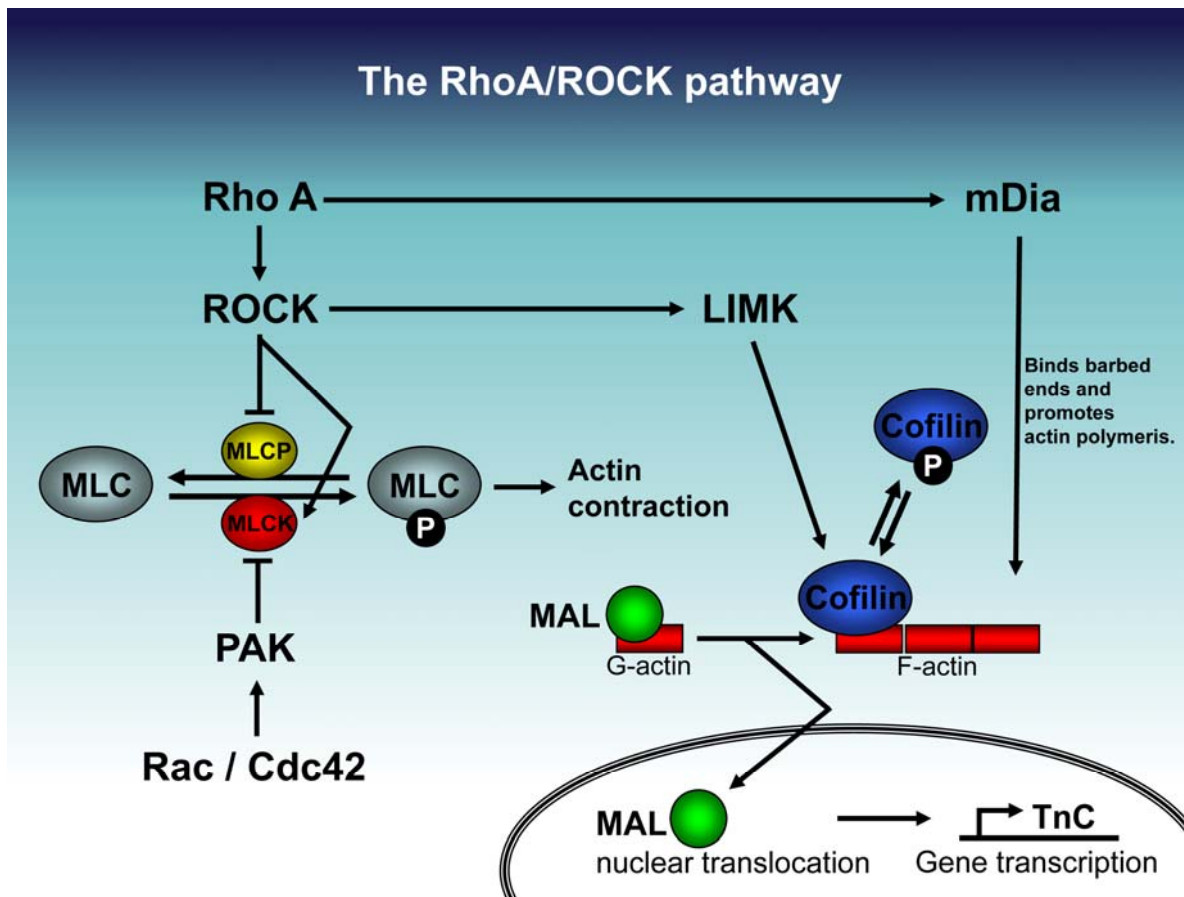


**Figure 6: The RhoA/ROCK pathway controls actin polymerization and contraction.** RhoA stimulates ROCK to promote myosin light chain phosphorylation, which leads to actin contraction. An active RhoA/ROCK pathway also supports actin polymerization via mDia or

LIM-kinase and cofilin. The transcriptional co-activator MAL/MKL-1 has affinity for G-actin and is translocated to the nucleus upon actin assembly. There it has been implicated in activation of promoters of genes like tenascin-C. (Scheme: R. Lutz)

## **II.9 Rho, Rac and Cdc42 regulate the organization of the actin cytoskeleton**

Polymerized actin in fibroblasts is organized into three major types of filamentous arrays, each linked to the cell membrane and the underlying matrix via integrin receptors (Hall, 1998). Lamellipodia are sheetlike cell protrusions containing a cross-linked meshwork of actin filaments. These structures are predominantly found in the front of a moving cell. Filopodia are fingerlike extensions at the cell border stabilized by thin parallel bundles of actin filaments. Actin structures of both lamellipodia and filopodia are linked to focal complexes. At the rear of the cell's leading edge actin filament bundles (stress fibers) are found. These structures merge in focal adhesions.

Much insight into how actin structures are controlled derives from the laboratory of Alan Hall, who used microinjection of specific proteins and inhibitors into fibroblasts (figure 7). Thereby Cdc42, Rac-1 and RhoA were postulated to be activated in this hierarchical order when a cell interacts with ECM (Nobes and Hall, 1995). Rac-1 was shown to induce stress fiber formation through activation of RhoA (Ridley et al., 1992). In addition, injection of activated Cdc42 together with dominant negative Rac-1 and the Rho inhibitor C3 caused extensive formation of filopodia (Nobes and Hall, 1995). With injection of only activated Cdc42 and C3 cells also produced lamellipodia. In these experiments focal complexes associated with filopodia and lamellipodia while focal adhesions were only observed with stress fibers. It was concluded that Cdc42 leads to the induction of filopodia, Rac-1 induces



lamellipodia and RhoA activation stimulates formation of stress fibers (Hall, 1998). In scratch-wound assays it was also found that Rac-1 is essential for cell movement while Cdc42 is supporting migration by establishing cell polarity (Nobes and Hall, 1999). On the other hand, RhoA-dependent stress fibers and focal adhesions are not required for cell migration, but these structures must undergo dynamic turnover in order to not inhibit cell movement.

The assumption that Rac-1 activates RhoA was later on modified by the idea of an antagonism between RhoA and Rac-1 (Rottner et al., 1999). This hypothesis arose from the fact that the ROCK-inhibitor Y27632 caused a shift from focal adhesions to peripheral focal complexes. In addition, injection of active Rac-1 caused a reduction in focal adhesion size whereas dominant-negative Rac-1 induced growth of focal complexes (Rottner et al., 1999). Thereby Rac-1 activation would turn a cell into a motile phenotype with lamellipodia and dynamic focal complexes while active RhoA would induce a sessile phenotype anchored with firm focal adhesions and a tensioned cytoskeleton.

As discussed in a previous paragraph, actin stress fibers are controlled mainly by the Rho/ROCK pathway. However, filamentous actin as observed in lamellipodia or associated with filopodia is regulated differently. WASP is a target of Cdc42 and binds the Arp2/3 complex (Millard et al., 2004). In this manner Arp2/3 is activated and attaches to actin structures. There it serves as new nucleation site for actin polymerization, thus creating a branched network. WAVE is a homologue of WASP that forms a ternary complex with active Rac-1 and Arp2/3 thereby stimulating actin branching in lamellipodia (Takenawa and Miki, 2001). Both, WAVE and WASP also have a binding site for profilin, which accelerates the exchange of ADP/ATP on actin and promotes actin polymerization.

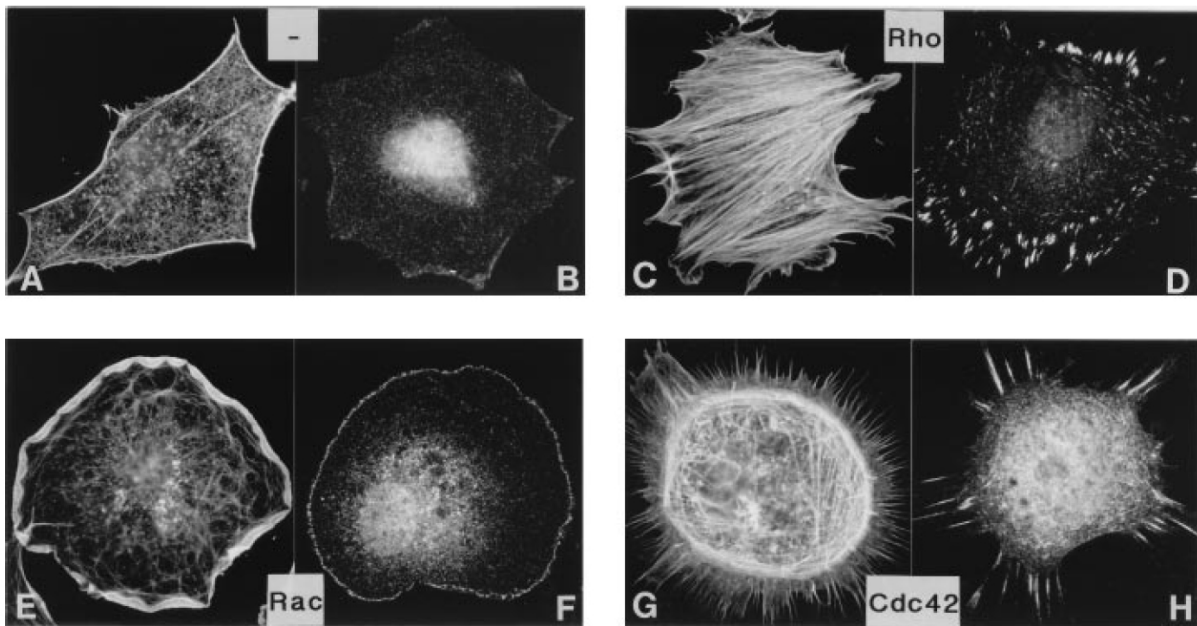


**Figure 7: Rho, Rac, and Cdc42 control the assembly and organization of the actin cytoskeleton.**

Serum-starved Swiss 3T3 fibroblast (-) contain few organized actin filaments (A) and small vinculin containing cell adhesions (B). Addition of the growth factor lysophosphatidic acid activates RhoA, which leads to stress fibers (C) and focal adhesions (D). Microinjection of Rac-1 induces lamellipodia (E) and associated focal complexes (F). Microinjection of FGD1, an exchange factor for Cdc42, leads to formation of filopodia (G) and the associated focal complexes (H). Taken from Hall, 1998

## II.10 MAL/MKL-1

Changes in actin dynamics are monitored by MAL (megakaryocytic acute leukemia) protein, also known as myocardin-related transcription factor A (MRTF-A), megakaryoblastic leukemia 1 (MKL1), or BSAC (basic, SAP, and coiled-coil domain) (Asparuhova et al., 2009). MAL was shown to physically interact with serum response factor (SRF) to activate SRF-dependent transcription (Miralles et al., 2003). In the N-terminal region, MAL contains two or three RPEL motifs (depending on the isoform). These motifs have been implicated in actin-association and RhoA-dependent nuclear import of MAL (Miralles et al., 2003). Two

basic boxes are important for nuclear localization of MAL whereas basic region 1 is also required for MAL binding to SRF (Miralles et al., 2003; Wang et al., 2001). A highly conserved leucine-zipper-like domain mediates homo- or heterodimerization among myocardin family members.

MAL directly interacts with unpolymerized actin (G-actin) (Posern et al., 2004). It has been demonstrated that in unstimulated cells, MAL is predominantly localized in the cytoplasm through an interaction of its N-terminal RPEL motifs with G-actin. As discussed previously, activation of RhoA increases polymerization of G-actin into actin filaments (F-actin). Upon stimulations that increase RhoA activity (e.g. serum, lysophosphatidic acid or transfection with active RhoA or mDia), G-actin recruited into actin filaments frees MAL to enter the nucleus, where it can stimulate SRF-dependent transcription (Miralles et al., 2003).

SRF is a transcription factor that binds the CArG box motif in gene promoters (Posern and Treisman, 2006). Binding is controlled to a large extent by its interaction with cofactors. Besides the proposed interaction with MAL, SRF can also interact with members of the ternary complex factor (TCF) family. These proteins make sequence-specific DNA contact with Ets motifs adjoining the CArG box. While interaction of SRF with MAL is dependent on the RhoA/ROCK pathway, binding to TCFs is controlled by the MAPK pathway (Posern and Treisman, 2006).

## **II.11 Tenascin-C**

Tenascin-C was discovered in 1984 as myotendinous antigen (Chiquet and Fambrough, 1984). It was the founding member of the family of tenascins that consists of the four members tenascin-C, tenascin-R, tenascin-X and tenascin-W (Chiquet-Ehrismann, 2004; Chiquet-Ehrismann and Chiquet, 2003). Tenascin-C has six identical subunits built from

variable numbers of repeated domains. N-terminal cysteins join the six subunits to form a six-armed molecule. Expression of the protein can be induced by certain homeobox-genes. High expression levels of tenascin-C are therefore found during embryogenesis. In the adult the protein is largely absent from most tissues. However, it reappears under pathological conditions caused by infections, inflammation or during tumorigenesis. Continuous expression of tenascin-C is found in tendons and at myotendinous junctions. A reason for this may be its induction by mechanical stress (Chiquet et al., 2004; Fluck et al., 2000). Induction by cyclic strain is not observed in  $\beta 1$  integrin and ILK knockdown cells (Chiquet et al., 2007), is abolished by the ROCK inhibitor Y27623 (Sarasa-Renedo et al., 2006) and correlates with nuclear translocation of MAL (Maier et al., 2008). Thus, induction of tenascin-C by mechanical stress seems to depend on the RhoA/ROCK pathway. Functionally, tenascin-C was shown to interfere with fibroblast attachment to fibronectin (Chiquet-Ehrismann et al., 1988). Later it was demonstrated that tenascin-C interacts with the 13<sup>th</sup> fibronectin type III repeat (FNIII13) of fibronectin. This interaction inhibited fibronectin binding to syndecan-4 (Huang et al., 2001), a co-receptor of the  $\alpha_5\beta_1$  integrin that is necessary for full spreading of fibroblasts on fibronectin (Woods and Couchman, 1994). Tenascin-C was also shown to inhibit cell mediated contraction of fibronectin/fibrinogen-matrices (Midwood and Schwarzbauer, 2002) and to suppress Rho activation during cell spreading (Wenk et al., 2000).

## **II.12 Mechanical stress and ECM regulation**

Mechanical forces are essential for homeostasis of all tissues (Chen, 2008). Some tissues, however, are influenced in special ways by mechanical signals. Pressure and shear stress from the circulation influence the morphology and pathology of the heart and vasculature.

Bone is shaped by forces generated from gravity and muscle contraction. Hearing and balance are based on mechanical sensors, and these are only examples. In tissues, the ECM plays an important role in transmission of mechanical forces. Physical properties of the matrix can differ drastically among different tissues and shield cells by modulating the strain. Composition of the matrix not only differs locally but also temporally, meaning that the ECM is not static (Bosman and Stamenkovic, 2003). Constant expression and secretion of proteins and their degradation by proteases form a dynamic matrix that is controlled by the embedded cells. Tenascin-C and the major collagens are among ECM components whose deposition is strongly influenced by mechanical stress (Chiquet et al., 2004; Fluck et al., 2000; Kjaer, 2004).

While reasons for the upregulation of tenascin-C upon mechanical stress are less clear, a tissue is strengthened by increased deposition of collagen. However, since tenascin-C was shown to interfere with fibronectin binding (Chiquet-Ehrismann et al., 1988; Fischer et al., 1997; Huang et al., 2001) a function in reducing matrix adhesion of cells to escape mechanical overload has been discussed.

## **II.13**

### **Cyclic strain as a model system for mechanotransduction**

To study integrin signaling and mechanotransduction, many studies have used the approach of observing cells in the first hours after plating on a substrate (Danen et al., 2002; Huvneers et al., 2008; Midwood and Schwarzbauer, 2002; Midwood et al., 2004; Wenk et al., 2000). However this is only a transient state and rather rare in physiology. To use externally applied strain represents a more sophisticated system, since fully spread cells are examined in which a large integrin pool is already activated and engaged with ligands. In addition, cells can be

given time to secrete ECM proteins forming a more physiological environment. The principle of cyclic strain is a valid model to analyze mechanotransduction. Many tissues like arterial vessels, lung, heart or tendons are exposed to cycles of strain and relaxation. Also in culture, cells respond to cyclic strain of amplitude and frequency in the range found in these tissues (Chiquet et al., 2004; Lehoux et al., 2006; Magnusson et al., 2008).

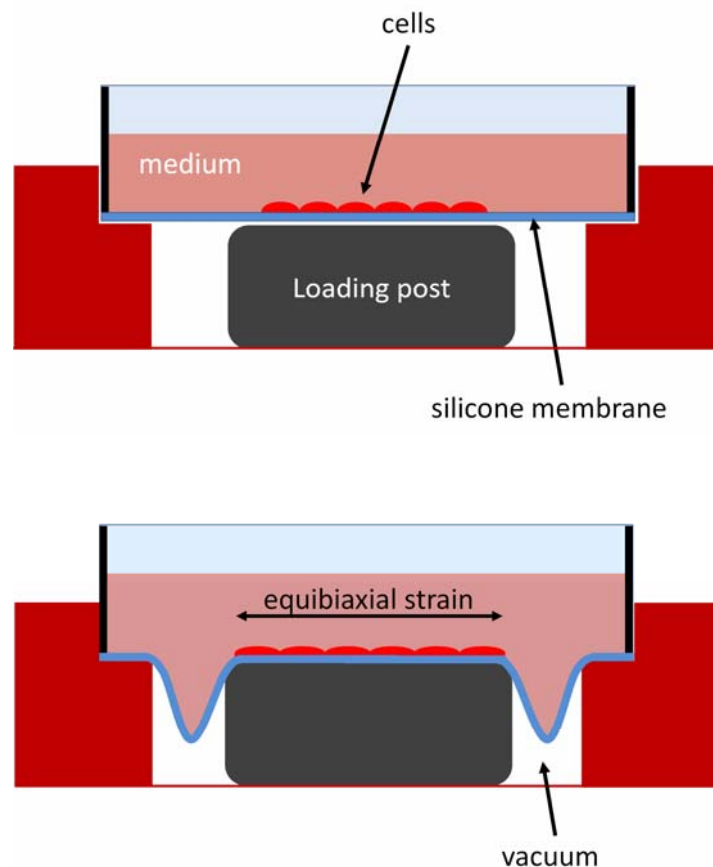


**Figure 8: Device to apply biaxial cyclic strain in vitro**

Cells are cultured in specialized wells that consist of a silicone membrane as bottom. To be able to let cells attach, the membrane is coated with the desired extracellular matrix proteins (e.g. fibronectin or vitronectin). Cells are then seeded and cultured until cyclic strain is applied. During cycles of strain a vacuum is created that sucks the silicone membrane around the disk-shaped loading post. Thereby cells can be biaxially strained with desired frequency and amplitude. (Scheme: R. Lutz)

## II.14 Responses of fibroblasts to mechanical stress

Mechanotransduction is defined as the process by which physical stimulation is converted intracellularly into various types of electrical or chemical signals (Chiquet et al., 2009). Responses to mechanical stimulation are versatile and vary among cell types. Besides activation of the RhoA/ROCK pathway as described previously, other events can be triggered in fibroblasts. Calcium has long been recognized as an important second messenger for biological processes and was also found to increase in the cytoplasm after stretch (Munevar et al., 2004). This influx was inhibited by gadolinium, an inhibitor of stretch-activated ion channels. Uni-axial stretch also caused translocation of the transcription factor NF- $\kappa$ B, which activated an NF- $\kappa$ B-inducible promoter (Inoh et al., 2002). Both, translocation and activation were also inhibited by gadolinium indicating activation by stretch-activated ion channels. Cyclic strain also led to an upregulation of cyclooxygenase (COX)-2 to produce reactive oxygen species (Amma et al., 2005). This was followed by phosphorylation of I $\kappa$ B kinase (IKK). I $\kappa$ B, the substrate of IKK, is an inhibitor of NF- $\kappa$ B that dissociates upon phosphorylation. Upon addition of gadolinium or in the absence of extracellular calcium phosphorylation of IKK was blocked.

Mechanical stretch can also activate the MAPK-pathway (Li and Xu, 2000; Rychly et al., 1998). Initial steps include phosphorylation of the focal adhesion kinase (FAK) which thereby creates a binding site for Src-family kinases. Src phosphorylates multiple constituents of the focal adhesion complex, including FAK at another tyrosine residue. This again creates an SH2 docking site for the recruitment of Grb2 and Sos, thereby linking integrins to the Ras/Raf/ERK cascade.

Less evidence exists about induction of the PKB/Akt pathway by mechanical strain. However, involvement of the epidermal growth factor receptor (EGFR) has been suggested (Kippenberger et al., 2005)



## **AIM OF THE WORK**

### **III. Aim of the work**

In fibroblasts, different types of cell-matrix adhesions exist. Fibrillar adhesions are known to be important for fibronectin fibrillogenesis but little is known about the importance of these adhesion sites in cellular signaling. Previous experiments showed that fibroblasts lacking ILK (an adaptor protein of focal and fibrillar adhesions) were defective in activation of the RhoA/ROCK pathway upon cyclic strain. In addition they failed to assemble fibronectin into a matrix and lacked fibrillar adhesions. We therefore speculated that the pericellular fibronectin meshwork and fibrillar adhesions might be involved in transduction of cyclic strain into the RhoA/ROCK pathway. To address this hypothesis we generated fibronectin knockdown fibroblasts and analyzed their mechanotransduction in the presence and absence of fibronectin.

Focal complexes on the other hand were shown to be induced by Rac activation and to correlate with cellular structures used for migration. These assumptions derived from studies that modulated the activity of monomeric G-proteins like Rac, Cdc42 and Rho. However, the present literature hardly addressed questions about specific signaling arising from focal complexes. To get more insight how focal complexes affect cell morphology we analyzed fibroblasts that were only allowed to form this type of adhesions. To do so we tried to arrest the maturation of focal complexes by limiting their growth. By help of our collaborators we generated specific nano- and micropatterned substrates with RGD-coupled gold squares of different sizes in the range of cell-matrix adhesions. We plated fibroblasts on these patterns and studied their adhesion sites, the actin cytoskeleton, and fibronectin fibrillogenesis.

## **RESULTS**

## **IV. Results**

### **IV.1 Tenascin-C induction by cyclic strain requires integrin-linked kinase**

Silke Maier, Roman Lutz, Laurent Gelman, Ana Sarasa-Renedo, Susanne Schenk, Carsten Grashoff and Matthias Chiquet

Biochimica et biophysica Acta (BBA), 2008

My contribution: Experiments and data for figure 2a, 5b and 9c

Available online at [www.sciencedirect.com](http://www.sciencedirect.com)

Biochimica et Biophysica Acta 1783 (2008) 1150–1162

[www.elsevier.com/locate/bbamcr](http://www.elsevier.com/locate/bbamcr)

## Tenascin-C induction by cyclic strain requires integrin-linked kinase

Silke Maier<sup>a</sup>, Roman Lutz<sup>a</sup>, Laurent Gelman<sup>a</sup>, Ana Sarasa-Renedo<sup>b</sup>,  
Susanne Schenk<sup>a</sup>, Carsten Grashoff<sup>c</sup>, Matthias Chiquet<sup>a,\*</sup>

<sup>a</sup> Friedrich Miescher Institute for Biomedical Research, Novartis Research Foundation, CH-4058 Basel, Switzerland

<sup>b</sup> ITI Research Institute for Dental and Skeletal Biology, University of Bern, CH-3001 Bern, Switzerland

<sup>c</sup> Max Planck Institute of Biochemistry, D-82152 Martinsried, Germany

Received 18 October 2007; received in revised form 11 January 2008; accepted 14 January 2008

Available online 26 January 2008

### Abstract

Induction of tenascin-C mRNA by cyclic strain in fibroblasts depends on RhoA and Rho dependent kinase (ROCK). Here we show that integrin-linked kinase (ILK) is required upstream of this pathway. In ILK-deficient fibroblasts, RhoA was not activated and tenascin-C mRNA remained low after cyclic strain; tenascin-C expression was unaffected by ROCK inhibition. In ILK wild-type but not ILK  $-/-$  fibroblasts, cyclic strain-induced reorganization of actin stress fibers and focal adhesions, as well as nuclear translocation of MAL, a transcriptional co-activator that links actin assembly to gene expression. These findings support a role for RhoA in ILK-mediated mechanotransduction. Rescue of ILK  $-/-$  fibroblasts by expression of wild-type ILK restored these responses to cyclic strain. Mechanosensation is not entirely abolished in ILK  $-/-$  fibroblasts, since cyclic strain activated Erk-1/2 and PKB/Akt, and induced c-fos mRNA in these cells. Conversely, lysophosphatidic acid stimulated RhoA and induced both c-fos and tenascin-C mRNA in ILK  $-/-$  cells. Thus, the signaling pathways controlling tenascin-C expression are functional in the absence of ILK, but are not triggered by cyclic strain. Our results indicate that ILK is selectively required for the induction of specific genes by mechanical stimulation via RhoA-mediated pathways.

© 2008 Elsevier B.V. All rights reserved.

**Keywords:** Mechanotransduction; Tenascin-C; RhoA/ROCK; Integrin-linked kinase; c-fos

### 1. Introduction

Adaptation to mechanical loads is an important function of connective tissue. In response to mechanical stimulation, fibroblasts change the expression of extracellular matrix (ECM) proteins [1,2] and of ECM-degrading enzymes and their inhibitors [3,4]. Among the ECM proteins regulated by mechanical stress, tenascin-C is one of the most prominent both in vivo [5–8] and in vitro [9–12]. In fibroblasts attached to elastic membranes, 10% cyclic strain at 0.3 Hz leads to a significant increase in the tenascin-C mRNA level within 2–6 h [11,12]. Early responses of fibroblasts to mechanical signals are the secretion of paracrine factors like transforming growth factor- $\beta$  [13], the activation of

mitogen activated protein kinases (MAPK) e.g. Erk-1/2 [14–16], and the induction of transcription factors such as c-fos, c-jun or egr-1 [16–18]. The increase in c-fos and c-jun mRNA in stretched cells depends at least in part on MAPK pathways [18]. While the induction of major ECM components such as collagen I is secondary to such early signaling events [13], up-regulation of tenascin-C mRNA seems to be a direct response to strain, since it can occur in the absence of de novo protein synthesis and does not require paracrine factors [11]. There is also no evidence that MAPK are involved [11]. Rather, we found that induction of tenascin-C by cyclic strain depends on an intact cytoskeleton and on actin contractility, which is controlled by the small GTPase RhoA and its target, Rho dependent protein kinase (ROCK) [12]. Interestingly, when cytoskeletal tension was stimulated via the RhoA/ROCK pathway before applying strain, this caused a super-induction of tenascin-C mRNA, i.e. it seemed to increase cellular mechanosensitivity [12].

\* Corresponding author. Friedrich Miescher Institute, Maulbeerstrasse 66, CH-4058 Basel, Switzerland. Tel.: +41 61 697 2494; fax: +41 61 697 3976.

E-mail address: [matthias.chiquet@fmi.ch](mailto:matthias.chiquet@fmi.ch) (M. Chiquet).

Via its ability to induce actin polymerization, RhoA also regulates the transcriptional activity of serum response factor (SRF). As co-activators of SRF, megakaryocytic acute leukemia proteins MAL/MKL1 [19,20] and MAL16/MKL2 [20,21] were identified in fibroblasts. The mouse homologues MRTF-A (MKL1) and -B (MKL2) potentiate SRF activity [22] and a mouse MAL isoform, BSAC, was isolated [23]. RhoA-dependent actin assembly regulates the subcellular localization of MAL [24]. MAL is predominantly cytoplasmic in serum-starved cells, but accumulates in the nucleus following serum stimulation. The activation of the RhoA-actin signaling pathway is necessary and sufficient to promote MAL nuclear accumulation [24]. Very recently, it has been shown that application of force by collagen-coated magnetic beads leads to the activation of RhoA, nuclear translocation of MAL and finally increased transcription of  $\alpha$ -smooth muscle actin in rat cardiac fibroblasts [25].

Despite of increasing information concerning the signaling pathways triggered by mechanical stress and the resulting changes in gene expression [2,12–15], the question remains how exactly non-excitable cells such as fibroblasts sense mechanical forces [26]. Recently, cell-ECM adhesion sites (mainly focal adhesions of cultured cells) received much attention as putative sites of mechanotransduction. Integrins are their transmembrane components, and there is ample evidence that mechanical signaling is integrin-dependent [26–28]. Recent data indicate that integrin-associated focal adhesion proteins undergo conformational changes in response to mechanical force and thereby expose hidden phosphorylation and/or binding sites recognized by other signaling components [26,29–31].

Integrin-linked kinase (ILK) is an integrin-binding molecule and a prominent component of focal adhesions [32–37]. ILK has been shown to be involved most notably in the activation of the PKB/AKT pathway [38]. However, since critical catalytic residues within the kinase domain of ILK are not conserved, its function as a kinase *in vivo* is still disputed [35,39]. Nevertheless, as an important adaptor protein ILK is indispensable for early embryonic development [40]. In a heterotrimeric complex with the adaptor protein PINCH and the F-actin binding protein parvin, ILK connects integrins with the cytoskeleton and presumably with adjacent receptor tyrosine kinases [34,35]. ILK-deficient cells have severe defects in cell adhesion, migration and polarization [40–43], and these deficits have been related to abnormal Rac1- and RhoA-dependent actin dynamics [41,44–47]. Because of its important role in integrating signals at cell-ECM contacts and in organizing the cytoskeleton we compared the ability of wild-type, ILK knockout and rescued fibroblasts to activate the RhoA/ROCK and Erk-1/2 MAPK signaling pathways in response to cyclic strain. In addition, we tested whether the absence of ILK affected the mechanical induction of the mRNAs for tenascin-C and c-fos, putative target genes of these two pathways. Our results indicate that ILK-deficient cells are not entirely insensitive to mechanical stimulation. Rather, ILK is essential for the force-induced expression of tenascin-C and a critical mediator of a RhoA-dependent mechanotransduction pathway.

## 2. Materials and methods

### 2.1. Cell culture

The following cell lines were used [41]. A clonal fibroblast line was derived from the kidney of a 4-week-old male mouse containing a floxed ILK gene [40] and immortalized by stable transfection with SV40 large T-antigen (ILK wt). Transduction of Cre into these cells led to the deletion of the ILK gene and the generation of a knockout cell line (ILK  $-/-$ ). ILK rescued cell lines were produced as follows. Murine ILK cDNA was generated by PCR and inserted into the p3xFLAG vector (Sigma, Buchs, Switzerland). The ILK-3xFLAG cDNA was amplified by PCR and inserted into pCLMFG (Imgenex, San Diego, CA), resulting in pCLILKFLAG. On the other hand recombinant retroviruses carrying a GFP-tagged wild-type ILK cDNA (pCLILKGFP) were generated. Infection of ILK-deficient cells with pCLILKFLAG or pCLILKGFP resulted in robust expression of the transduced cDNA [40]. Cells were maintained at 37 °C and 6% CO<sub>2</sub> in Dulbecco's modified Eagle medium (D-MEM; Seromed, Basel, Switzerland) containing 10% fetal calf serum (FCS; Gibco/Invitrogen, Basel, Switzerland). Cells were harvested and plated onto silicone membranes (0.05", gloss/gloss; Specialty Manufacturing Inc., Saginaw MI, USA) mounted into custom-made 6-well dishes [11]. Before seeding cells, membranes were coated with purified horse serum fibronectin (100  $\mu$ g/ml in phosphate buffered saline [PBS]) for 1 h [11]. Alternatively, cells were plated into Flexercell II 6-well dishes (Dunn Labortechnik, Asbach, Germany) that were coated with fibronectin as above. Three hours after plating cells (600,000 per well) in 3% FCS/D-MEM, medium was changed and cultures were maintained in 0.3% (or 0.03% in certain experiments; see figure legends) FCS/D-MEM overnight before use in cyclic strain experiments.

### 2.2. Mechanical loading of cells

30 min before applying cyclic strain, cultures received a medium change (0.3% or 0.03% FCS/D-MEM) and, where indicated, 10  $\mu$ M Y27632 (Calbiochem, JURO Supply GmbH, Switzerland) was added into the same medium. Culture dishes were mounted onto a custom-made stretching device [11] or on a Flexcell FX-4000 machine (Dunn Labortechnik, Asbach, Germany). On either machine, cells were subjected to equibiaxial cyclic strain (10%, 0.3 Hz) at 37 °C for the times indicated (usually 1 h to 6 h). For a given dose of mechanical stimulation, the two machines gave identical results. After the experiment, cells were formaldehyde-fixed for phalloidin and immunofluorescence staining (see below). Alternatively, cells were lysed and total RNA was isolated [11]. For RhoA activation assays, 1.25  $\times 10^6$  mouse fibroblasts were plated per well and washed twice with D-MEM containing 0.3% FCS on the day of plating. On the following day, cells were directly (without medium change) subjected to cyclic strain (10%, 0.3 Hz) at 37 °C for 5–15 min before extraction (see below).

### 2.3. Stimulation of cells with lysophosphatidic acid

Oleoyl- $\alpha$ -lysophosphatidic acid (LPA) was purchased from Sigma (Buchs, Switzerland) and stock solutions were prepared in water. Cells were plated on fibronectin-coated 6-well tissue culture dishes and serum-starved as described above. For stimulation, medium was changed to either D-MEM/0.03% FCS alone, or to the same medium containing 2 or 10  $\mu$ M LPA. Cells were extracted after 5–15 min for determination of RhoA activity, or after 1 and 6 h for quantification of mRNA as described above.

### 2.4. Quantification of mRNA levels from Northern blots

RNA was isolated by the RNeasy procedure (Qiagen, Basel, Switzerland), run on agarose gels, and Northern blots were prepared as described previously [11]. Blots were simultaneously hybridized with [<sup>32</sup>P]dCTP-labeled mouse tenascin-C and rat glyceraldehyde phosphate dehydrogenase (GAPDH) cDNA probes [11]. The tenascin-C to GAPDH mRNA ratio was quantified for each sample by phospho-imaging and densitometric analysis of Northern blots using a Storm 860 phospho-imager and Image Quant software (Molecular Dynamics, Sunnyvale, CA) [11,12]. Data represent the average and standard error of the mean of five independent experiments. Statistical significance was determined by one-way ANOVA and paired Student's *t*-Test. Differences with a value of  $P < 0.05$  were considered significant.

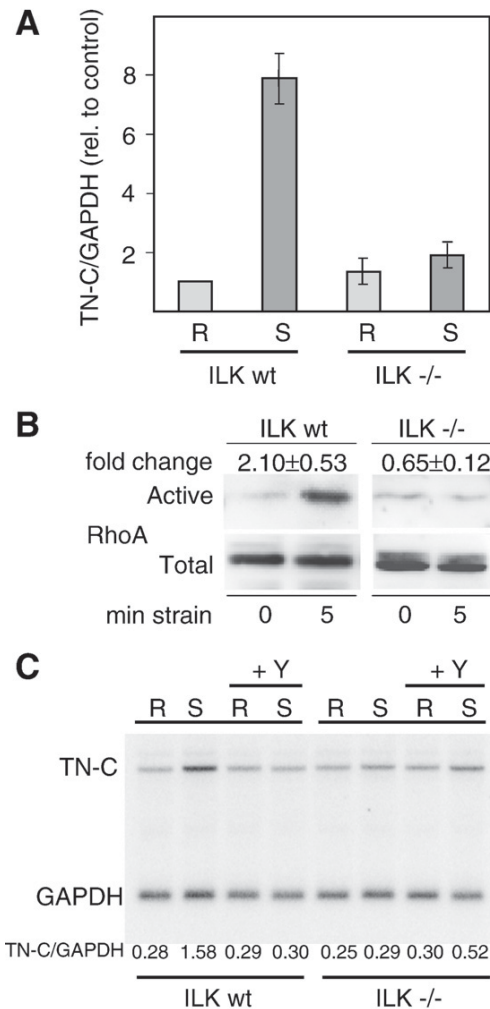


Fig. 1. Cyclic strain activates RhoA and induces tenascin-C (TN-C) mRNA in wild-type but not in ILK-deficient fibroblasts. (A) Wild-type mouse fibroblasts (ILK wt) and their descendants in which the ILK gene was deleted (ILK -/-) were cultured on fibronectin-coated silicone membranes. Cells maintained in 0.3% serum were either left at rest (R) or subjected to cyclic strain (10%, 0.3 Hz) for 6 h (S), total RNA was extracted and Northern blots were hybridized with <sup>32</sup>P-labeled cDNA. TN-C/GAPDH mRNA ratios were quantified by phosphoimaging and densitometry of blots and are expressed relative to the resting control. Bars represent means and standard errors of 5 independent experiments. (B) Activation of RhoA by cyclic strain in wild-type but not in ILK-deficient fibroblasts. ILK wild-type and ILK -/- cells were subjected to cyclic strain (10%, 0.3 Hz) for 5 min. Active RhoA was pulled down from cell lysates (see Materials and methods), and detected on SDS-PAGE by immunoblotting (top panel). For control, total RhoA in the corresponding samples is shown in immunoblots of whole cell lysates (bottom panel). Active RhoA was quantified by densitometry of Western blots and normalized to total RhoA; the fold change in stressed versus resting cells is indicated on top of the figure ( $n=4$ ;  $\pm$ S.E.M.). (C) Effect of ROCK inhibition on tenascin-C mRNA expression levels in wild-type versus ILK-deficient fibroblasts. Wild-type and ILK -/- fibroblasts were subjected to cyclic strain (10%, 0.3 Hz) for 6 h in the absence or presence of ROCK I/II inhibitor Y27632 (10  $\mu$ M). The mean TN-C/GAPDH ratio of three independent experiments is indicated at the bottom of the figure. Note that ROCK inhibition interferes with strain-dependent tenascin-C induction in wild-type cells, but has no effect on tenascin-C mRNA levels in ILK-deficient cells.

## 2.5. Quantification of mRNA levels by real time PCR

RNA was isolated as above and reverse transcribed with a High Capacity cDNA Reverse Transcription Kit (Applied Biosystems, Rotkreuz, Switzerland). TaqMan real time PCR primer/probe mixtures for mouse tenascin-C (Mm00495662\_m1), mouse c-fos (Mm00487425\_m1) and mouse GAPDH (Mm99999915\_g1) as well as TaqMan Universal Master Mix were purchased from Applied Biosystems. For every experimental condition, reverse transcribed cDNA (3 and 6 ng) was amplified for each of the 3 genes on an ABI Prism 7000 real time PCR cycle (Applied Biosystems). Data were analyzed by the  $\Delta$ Ct method [48], i.e. values for tenascin-C and c-fos were normalized to GAPDH for each sample. These data are shown in the graphs, rather than their further normalization to the resting controls ( $\Delta\Delta$ Ct method [48]; “fold increase”). The single normalization used here allows comparison of basic gene expression levels between the different cell lines used in this study. Data represent the average  $\pm$  S.E.M. from five to seven independent experiments. Statistical significance was determined by one-way ANOVA and paired Student's *t*-Test. Differences with a value of  $P < 0.05$  were considered significant.

## 2.6. Isolation of monoclonal antibody against mouse MAL

A His-tagged recombinant fragment of mouse MAL was generated as follows. A cDNA fragment coding for amino acids 611–731 (Acc. No. NP\_694629; NML\_153049.2) was selected and amplified from mouse fibroblast cDNA with a sense primer 5'-CCCGCATGCGAAAGTGGTTTCTCCAGTTGC-3' containing a SphI restriction site and an antisense primer 5'-CCCAAGCTTGCTG-GAAAACCGCTGGGA-3' containing a HindIII restriction site. The PCR product was digested with SphI and HindIII (Roche Diagnostics) and cloned into the pQE30 vector (Qiagen, Hombrechtikon, Switzerland) containing a 6 $\times$ Histidine (6 $\times$ His) tag just upstream of the multiple cloning site. The recombinant fragment was expressed in *E. coli* M15 bacteria and purified from the pellet according to the QIAexpressionist protocol (Qiagen) under denaturing conditions. The purified His-tagged MAL fragment of 13 kDa was analyzed by SDS-polyacrylamide gel electrophoresis (SDS-PAGE). Fractions of the elution peak were pooled and dialysed against PBS. 3 female Balb/c mice were immunized subcutaneously each with 50  $\mu$ g recombinant MAL fragment in 100  $\mu$ l PBS, which was mixed with 25  $\mu$ l of Stimune adjuvant (Prionoc AG, Schlieren-Zurich, Switzerland). After two identical boosts at 3-week intervals, a final injection was made intraperitoneally with 25  $\mu$ g MAL fragment in 150  $\mu$ l PBS without adjuvant. Two days later, the mice were killed, and the splenic lymphocytes were fused to the myeloma cell line P3xAg8.653 (American Type Culture Collection) and cultured in selection medium according to standard protocols. Hybridoma supernatants were tested for secreted antibodies on ELISA plates coated with purified recombinant MAL fragment. Hybridomas showing the best ELISA signals were further analyzed by immunoblotting using bacterial lysates that contained expressed MAL fragment. Finally, supernatants reacting with the recombinant His-tagged 13 kDa MAL peptide were tested on immunoblots against mouse embryo fibroblast extracts. Selected hybridomas specifically recognizing endogenous mouse MAL (160 kDa; [24]) were subcloned twice and rescreened by ELISA and immunoblotting. The isotype of selected monoclonal antibodies (mAbs) was determined (Isostrip; Roche Applied Science); mAb 65F13 is an IgG1 with  $\kappa$  light chains. 65F13 cells were grown in IMDM with 15% FCS to high cell density without medium change to allow mAb accumulation in the tissue culture supernatant. All experiments presented here were done with a single batch of 65F13 culture supernatant diluted 1:10 for immunoblotting and immunofluorescence.

## 2.7. Immunofluorescence and phalloidin staining

Silicone membranes with attached cells were cut out from the bottom of culture wells and placed upside down onto a solution of 4% paraformaldehyde buffered with 20 mM Na-phosphate for 15 min. Fixed cells were washed and blocked overnight at 4  $^{\circ}$ C in PBS containing 3% bovine serum albumin (BSA) and 0.2% Triton X-100. Cells were labeled at room temperature with a monoclonal antibody to vinculin (clone hVIN11-5 ascites fluid; Sigma-Aldrich, Buchs, Switzerland) diluted 1:1250 in PBS/BSA/Triton or with 65F13 supernatant diluted 1:10 for 1 h, washed three times with PBS/BSA/Triton, and then incubated simultaneously with Alexa488- or Alexa568-labeled goat anti-mouse IgG (Cappel/ICN Biomedicals, EGT Chemie, Switzerland; diluted 1:400), Alexa546-labeled phalloidin (Sigma,

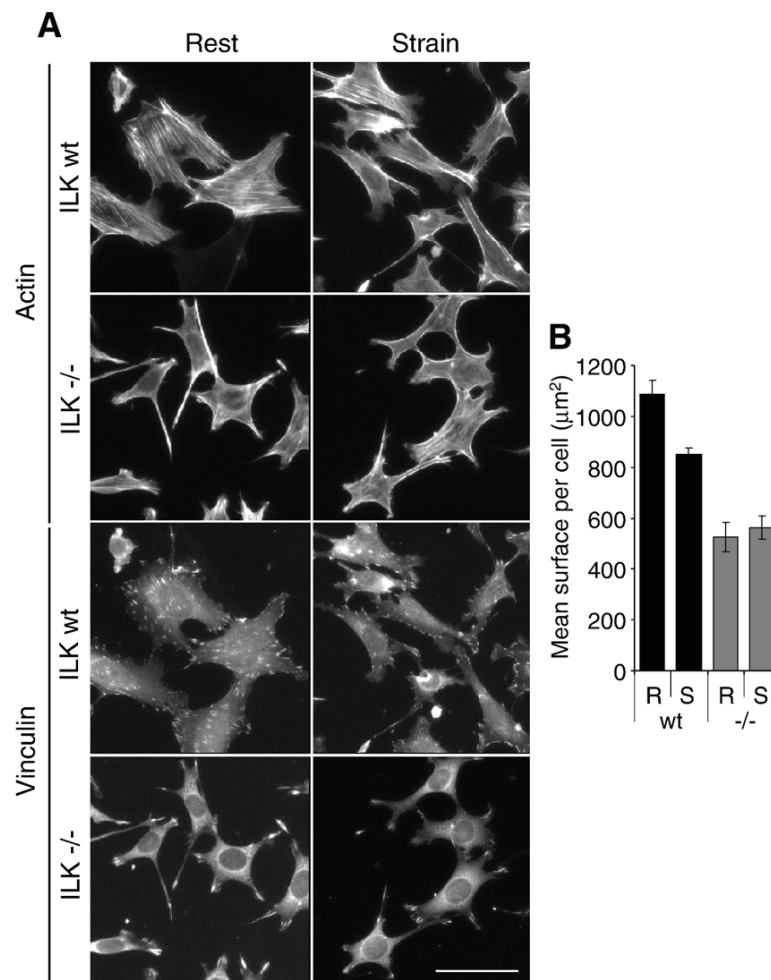


Fig. 2. Cyclic strain stimulates actin stress fiber formation and focal adhesion redistribution in wild-type but not in ILK-deficient fibroblasts. (A) Wild-type and ILK  $-/-$  cells cultured on fibronectin-coated silicone membrane were cyclically strained (10%, 0.3 Hz) for 3 h, fixed with paraformaldehyde, and double-stained with rhodamine-labeled phalloidin for actin stress fibers and an antibody to vinculin to visualize focal adhesion sites. Note the shape change and the strain-induced actin reorganization in wild-type but not in ILK-deficient fibroblasts. Wild-type cells exhibit scattered adhesions that tend to redistribute to the cell margins after cyclic strain. In contrast, resting ILK-deficient cells form focal adhesions only at their periphery, and no redistribution is observed upon strain. The scale bar represents 50  $\mu\text{m}$ . (B) The mean surface of ILK wild-type and ILK  $-/-$  cells was quantified before and after 3 h of cyclic strain (10%, 0.3 Hz) as described in Materials and methods.

Buchs, Switzerland; 1  $\mu\text{g}/\text{ml}$ ) in PBS/BSA/Triton or with Alexa633-labeled goat anti-mouse IgG for 1 h. Cells were again washed three times with PBS/BSA/Triton and mounted in Prolong Gold antifade reagent (Invitrogen, Basel, Switzerland). Slides were observed on a Zeiss Z1 microscope equipped with a 20 $\times$ /0.8 objective, Zeiss filter cubes n $^{\circ}$ 38HE for Alexa488, n $^{\circ}$ 43 for Alexa546 and Alexa568 and n $^{\circ}$ 26 for Alexa633 and a Zeiss MRm camera. Alternatively, cells were observed on a Zeiss LSM510 confocal microscope with a 40 $\times$ /1.3 oil immersion objective. For cell surface measurements cells were directly fixed in the Flexercell dishes and stained with Alexa546-labeled wheat germ agglutinin (WGA) and Hoechst 33342 (Image-iT LIVE plasma membrane and nuclear labeling kit, Invitrogen) for 3 h, then washed 3 times with PBS and mounted in Prolong Gold. Slides were observed on a Zeiss Z1 microscope equipped with a 20 $\times$ /0.8 objective and a Zeiss MRm camera and quantification was done with the ImagePro software.

## 2.8. RhoA activity assay

The activity of RhoA was determined using a rhotekin-Rho-binding domain (RBD) assay as published [49]. Briefly, serum-starved mouse fibroblasts ( $1.5 \times 10^7$  per sample) were subjected to cyclic strain (10%, 0.3 Hz) for 5 min. Cells were washed with ice-cold TBS and lysed in glutathione-S-transferase (GST)-fish buffer

(10% glycerol, 50 mM Tris pH 7.4, 100 mM NaCl, 1% NP-40 and 2 mM  $\text{MgCl}_2$ ) to which protease and phosphatase inhibitors were added. Lysates were cleared in the cold by centrifugation (700  $\times g$ , 5 min) and incubated at 4  $^{\circ}\text{C}$  for 45 min with glutathione-Sepharose 4B beads (Amersham, Braunschweig, Germany) coupled to freshly prepared GST-rhotekin-RBD fusion protein (expression vector obtained from Dr. Jens Stein, Theodor Kocher Institute, Bern, Switzerland). Beads were washed with GST-fish buffer and bound proteins solubilized by the addition of 2 $\times$  Laemmli buffer. Total RhoA in lysates and active (rhotekin-RBD-bound) RhoA were detected by Western blotting with anti-Rho-mouse mAb (Santa Cruz; Lab Force, Nunningen, Switzerland) diluted 1:200 in PBS/BSA/Tween-20. Blots were washed and incubated with peroxidase-labeled goat anti-mouse IgG (1:7000; Cappel/ICN Biomedicals; EGT Chemie, Switzerland) for 1 h. Blots were developed using SuperSignal $^{\text{TM}}$  West-Pico peroxide kit (Pierce; Socochem SA, Switzerland). Chemiluminescence signals were detected using a Bio-Rad VersaDoc $^{\text{TM}}$  Imaging System, Model 3000 (Bio-Rad Laboratories AG, Reinach BL, Switzerland).

## 2.9. Immunoblotting

Wild-type, ILK  $-/-$  and rescued fibroblasts were left at rest or subjected to cyclic strain for 5, 10 and 15 min, respectively. Per sample,  $1.8 \times 10^6$  cells were



1154

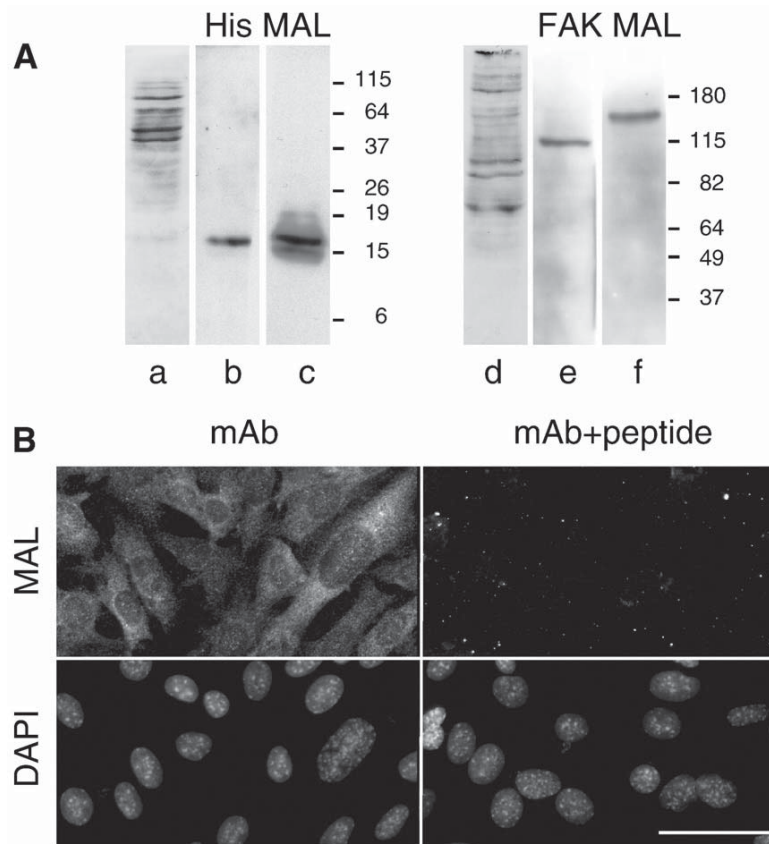
S. Maier et al. / *Biochimica et Biophysica Acta* 1783 (2008) 1150–1162

Fig. 3. Monoclonal antibody 65F13 detects endogenous mouse MAL on immunoblots and by immunofluorescence. (A) A monoclonal antibody was generated using a bacterially expressed mouse MAL peptide with an N-terminal His-tag. A blot of bacterial lysate containing the MAL peptide was stained with amido black (a), anti-His antibody (b) or the newly generated MAL mAb 65F13 (c). Extracts of mouse wild-type fibroblasts were blotted and stained with amido black (d), anti-FAK (e) or mAb 65F13 (f) to detect the endogenous proteins. (B) Mouse wild-type fibroblasts were cultured on fibronectin-coated silicone membranes in 0.03% serum, fixed with paraformaldehyde and stained with mAb 65F13 (top left) or with mAb 65F13 preincubated with a ten-fold excess of immunogen (recombinant mouse MAL peptide) for 2 h (top right). The cell nuclei were localized via DAPI costaining (bottom panels). The scale bar represents 50  $\mu\text{m}$ .

lysed in 600  $\mu\text{l}$  ice-cold RIPA buffer (50 mM Tris-HCl pH 7.4, 150 mM NaCl, 1% NP-40, 0.25% Na-deoxycholate, and 1 mM EDTA) containing protease and phosphatase inhibitors. Lysates were cleared by centrifugation and run on 10% polyacrylamide-SDS gels and blotted to nitrocellulose. Blots were incubated with the following antibodies: a rabbit antibody to Erk-1/2, a mouse mAb to phospho-Erk-1/2, a rabbit antibody to phospho-Akt (S473) (all Cell Signaling; BioConcept, Allschwil, Switzerland), a rabbit antibody Ab10 to PKB [50] or mouse antibodies to FAK and phospho-FAK (Y397) (BD Biosciences). For detecting ILK, the cells at rest were treated as mentioned above and blots were incubated with a mouse antibody to ILK (BD Biosciences). TN-C was detected in lysates and media of fibroblasts stressed for 6 h, using a rat monoclonal anti-TN-C antibody mTn-12 [51]. Bacterial and cell lysates were blotted and probed with our monoclonal anti-MAL antibody 65F13. In all cases an incubation with peroxidase-labeled secondary antibodies (1:10,000; Cappel/ICN Biomedicals; EGT Chemie, Switzerland) followed and blots were developed with SuperSignal<sup>®</sup>WestPico peroxide kit (Pierce, Socochim SA, Switzerland) and exposed to Kodak X-ray film for 1–5 min.

### 3. Results

#### 3.1. RhoA/ROCK-dependent tenascin-C mRNA induction by cyclic strain fails to occur in ILK-deficient fibroblasts

When primary chick embryo fibroblasts are cultured on fibronectin-coated elastic membranes and subjected to cyclic strain, a robust induction of tenascin-C mRNA is a prominent

response [11,12]. We also showed that cyclic strain rapidly activates RhoA, and that the subsequent increase in tenascin-C mRNA requires ROCK and myosin II activity [12]. First, we tested whether immortalized wild-type mouse fibroblasts containing a floxed ILK gene reacted to cyclic strain in a similar manner. Indeed, on Northern blots we observed a several fold increase in the level of tenascin-C mRNA in these cells after stimulating them with 10% equibiaxial cyclic strain at 0.3 Hz for 6 h (Fig. 1A). In the wild-type cells, RhoA was activated after 5 min of cyclic strain (Fig. 1B), and tenascin-C mRNA induction at 6 h of strain was suppressed by ROCK inhibitor Y27632 as expected (Fig. 1C). The parental fibroblasts were then compared to cells in which the floxed ILK gene had been deleted. ILK-deficient fibroblasts exhibited a similar basal tenascin-C mRNA expression level as wild-type cells; however, they completely failed to induce this mRNA under the influence of cyclic strain (Fig. 1A). Moreover, RhoA activity was not stimulated by cyclic strain in fibroblasts lacking ILK (Fig. 1B), and the ROCK inhibitor had no effect on tenascin-C mRNA levels in these cells, neither at rest nor after strain (Fig. 1C). From these results, we conclude that ILK is required for RhoA/ROCK-dependent induction of tenascin-C by cyclic strain.

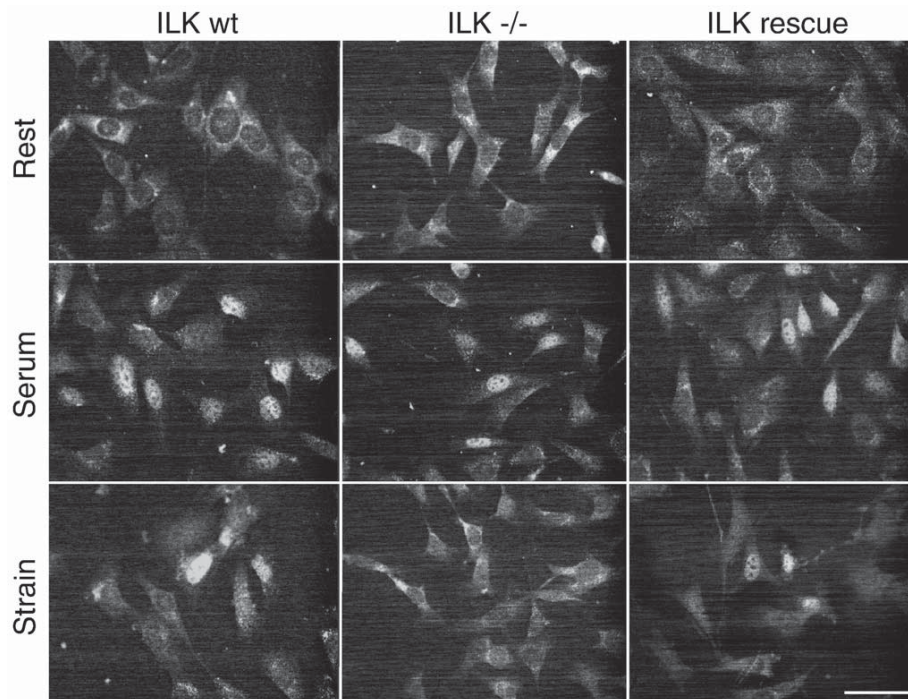


Fig. 4. Cyclic strain induces nuclear translocation of MAL in wild-type but not in ILK  $-/-$  fibroblasts. Wild-type, ILK  $-/-$  and rescued cells were cultured on fibronectin-coated silicone membranes in 0.03% serum and either left at rest, stimulated with 10% serum for 1 h, or subjected to cyclic strain (10%, 0.3 Hz) for 1 h. Cells were fixed with paraformaldehyde and stained with mAb 65F13 to visualize nuclear translocation of MAL. The scale bar represents 50  $\mu$ m.

### 3.2. Cyclic strain leads to rearrangement of actin stress fibers and focal contacts in wild-type but not in ILK-deficient fibroblasts

In primary chick embryo fibroblasts, cyclic strain induces a characteristic change in cell shape and a ROCK-dependent increase and relocation of actin stress fibers [12]. To test whether strain-dependent actin reorganization also required ILK, we subjected wild-type and ILK-deficient mouse fibroblasts to cyclic strain (10%, 0.3 Hz) for 3 h. For wild-type cells, we observed a redistribution of actin stress fibers to the cell margins upon cyclic strain, as evidenced by phalloidin staining (Fig. 2A). At rest, vinculin-positive adhesion contacts were scattered over the basal side of wild-type cells but located preferentially at the cell margins after cyclic strain (Fig. 2A). In parallel to these changes, strain caused a significant decrease of about 20% in the measured surface area of wild-type cells (Fig. 2B), indicating contraction [12]. In contrast, ILK-deficient fibroblasts were considerably less spread already at rest, with a surface area about half as large as that of wild-type cells (Fig. 2B). Resting ILK knockout cells appeared to have an abnormal cytoskeleton with thick actin bundles along their margins, and cyclic strain triggered neither a redistribution of stress fibers nor a change in cell surface area (Fig. 2A, B). Furthermore, ILK-deficient cells at rest exhibited vinculin-containing focal adhesions only at their periphery and this distribution remained unaltered after cyclic strain (Fig. 2A). Thus, the absence of ILK by itself causes a perturbation of cytoskeleton and focal contacts, and cyclic strain fails to induce

a response of these structures. This is in accordance with the suppression of strain-dependent RhoA activation in ILK-deficient cells.

### 3.3. Cyclic strain induces nuclear translocation of MAL in wild-type but not in ILK-deficient fibroblasts

MAL, a co-activator of SRF, is known to translocate to the nucleus in response to RhoA-dependent actin assembly, linking RhoA activity and actin dynamics to gene expression [24]. Because cyclic strain triggers RhoA activation and actin reorganization in wild-type but not ILK-deficient fibroblasts,

Table 1  
Quantification of MAL translocation after cyclic strain

Experiment 1	Rest	Serum	Strain
ILK wt	0	55	35
ILK $-/-$	3	63	11
ILK rescue	2	53	34
Experiment 2	Rest	Serum	Strain
ILK wt	0	90	65
ILK $-/-$	0	100	23
ILK rescue	0	97	84

Wild-type, ILK  $-/-$  and rescued cells were cultured on fibronectin-coated silicone membranes in 0.03% serum and either left at rest, stimulated with 10% serum for 1 h or subjected to cyclic strain (10%, 0.3 Hz) for 1 h. Between 70 and 100 cells were counted per condition, and numbers represent the percentage of cells with nuclear staining for MAL.

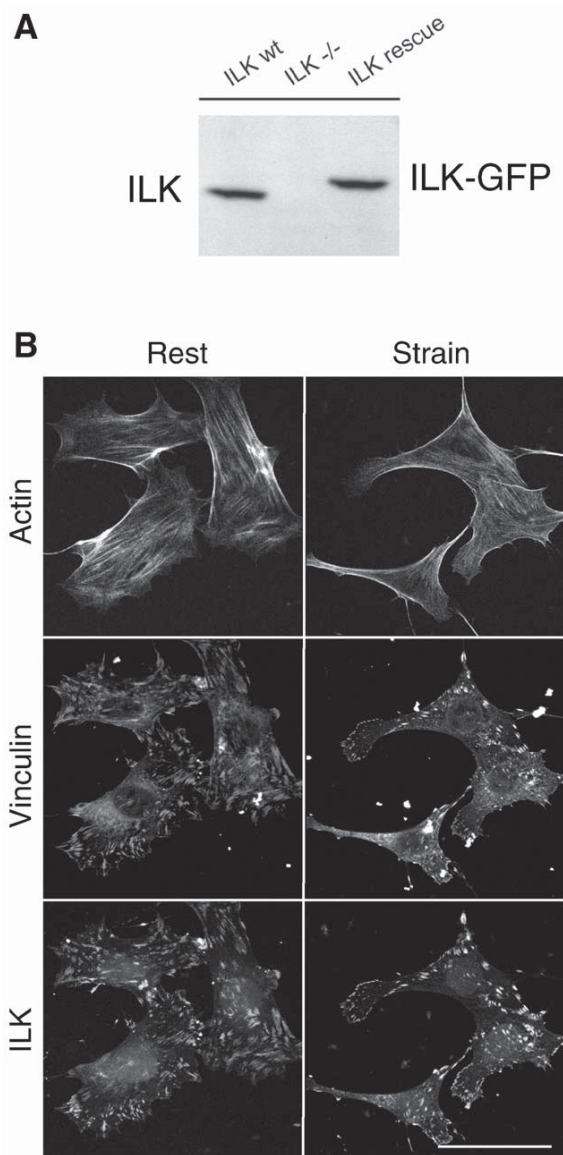


Fig. 5. Actin reorganization and focal adhesion distribution in response to cyclic strain is restored in ILK rescued cells. (A) Wild-type, ILK  $-/-$  and rescued cells were maintained in 0.03% serum, and cell extracts were blotted and incubated with anti-ILK antibody. (B) ILK rescued cells were cyclically strained (10%, 0.3 Hz) for 3 h, fixed with paraformaldehyde, and stained with rhodamin-labeled phalloidin for actin stress fibers and an antibody to vinculin for focal adhesion sites. The expressed ILK was visualized by its GFP-tag. The scale bar represents 50  $\mu$ m.

we asked whether this stimulus would induce nuclear translocation of MAL in an ILK-dependent manner. For these experiments, we generated a monoclonal antibody (mAb 65F13) against a recombinant fragment of mouse MAL expressed in *E. coli*. On immunoblots of bacterial lysates, mAb 65F13 recognized the His-tagged MAL peptide ( $M_r=13,000$ ) used for immunization (Fig. 3A). In mouse fibroblast extracts, the antibody detected a single protein band of  $M_r=160,000$  (Fig. 3A), the correct size for endogenous full length mouse

MAL [24]. By immunofluorescence, mAb 65F13 stained a cytoplasmic protein in serum-starved fibroblasts that was not detected when mAb 65F13 was preincubated with the peptide used for immunization (Fig. 3B). As MAL is expected to translocate to the nucleus upon serum stimulation [24], we stained wild-type and ILK-deficient fibroblasts under serum-starved, serum-stimulated and mechanically strained conditions (Fig. 4). ILK-deficient fibroblasts showed a similar response to the addition of serum as wild-type fibroblasts: the proportion of cells with nuclear MAL staining increased from below 5% to 60–100% after 1 h. When serum-starved wild-type cells were treated with 10% cyclic strain (0.3 Hz), the proportion of nuclei staining for MAL increased with time, peaked at 35–65% after 1 h and decreased again afterwards (Fig. 4; Table 1). However, MAL translocation in response to cyclic strain was greatly diminished in ILK-deficient cells, since only about 10–20% of their nuclei stained positive after 1 h of stimulation (Fig. 4; Table 1). These data suggest that ILK is required for RhoA-dependent actin dynamics stimulated by external tensile strain but not by serum.

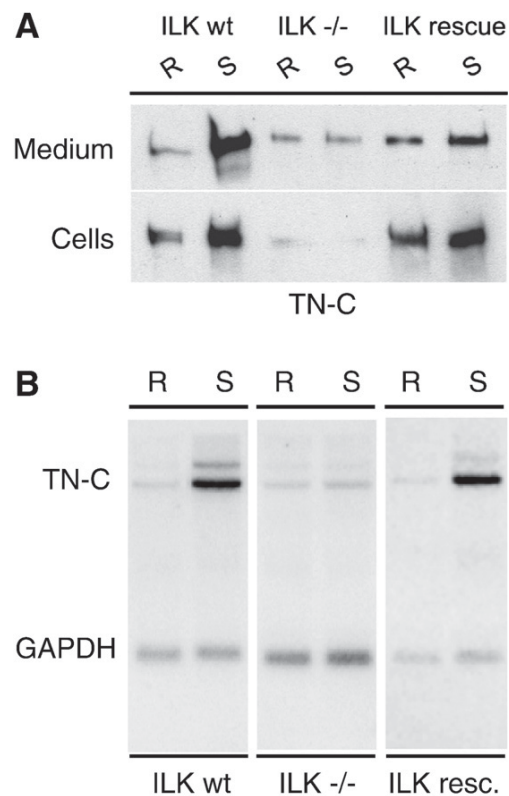


Fig. 6. ILK rescued cells show induction of tenascin-C upon mechanical stress. (A) Wild-type, ILK  $-/-$  and rescued cells were changed to fresh medium containing 0.3% serum and either left at rest (R) or subjected to cyclic strain (10%, 0.3 Hz) for 6 h (S). 18 h later, media were collected and cell extracts prepared. Media and extracts were blotted and incubated with anti-tenascin-C antibody. (B) After 6 h of cyclic strain, total RNA was extracted from all three cell lines and Northern blots were hybridized with  $^{32}$ P-labeled cDNA. A representative blot shows that tenascin-C mRNA is induced by cyclic strain in wild-type but not ILK  $-/-$  cells, and that this response is fully restored in the ILK rescued cells.

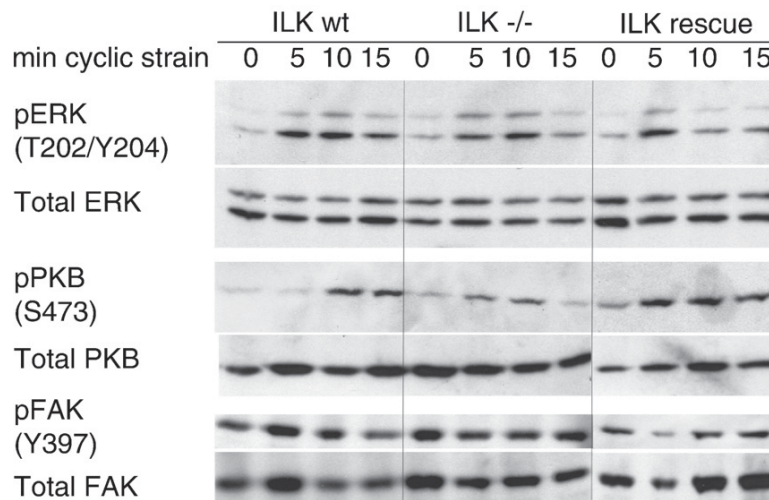


Fig. 7. Cyclic strain activates Erk-1/2 and PKB/Akt in wild-type as well as ILK-deficient fibroblasts. Wild-type, ILK  $-/-$  and rescued cells were subjected to cyclic strain (10%, 0.3 Hz) for 5, 10 and 15 min, cell lysates were run on SDS-PAGE, and immunoblots were developed with antibodies to phospho-(top panel) and total (bottom panel) Erk-1/2, PKB and FAK, respectively. Note that cyclic strain induces the phosphorylation of Erk-1/2 and PKB similarly in all cell types. FAK is phosphorylated even before stretching the cells.

### 3.4. Responses to cyclic strain are restored in ILK rescued cells

To prove that the lack of ILK directly causes the deficits described above, we used ILK-deficient fibroblasts rescued with full length ILK as a control. Fig. 5A shows that cell extracts from ILK knockout cells reveal no trace of ILK protein, whereas rescued cells exhibit an ILK protein expression level comparable to that of wild-type cells. In ILK rescued cells, the extent of MAL nuclear translocation induced by either serum or cyclic strain was nearly identical as in wild-type cells (Fig. 4; Table 1). Moreover, a morphological comparison to wild-type cells (c.f. Fig. 2A) confirmed the strain-dependent actin reorganization and redistribution of vinculin-positive adhesion contacts after cyclic strain (10%, 0.3 Hz) for 3 h in ILK rescued cells (Fig. 5B). In the rescued cells, re-expressed ILK colocalized with vinculin in focal adhesions as expected (Fig. 5B).

The most relevant response to test in the rescued cells was mechanical induction of tenascin-C. Therefore the protein and mRNA levels of all three cell lines were analyzed at rest and after 6 h of cyclic strain. Tenascin-C protein is secreted into the culture medium by all cell types but clearly induced by strain only in wild-type and rescued cells (Fig. 6A). Northern blotting revealed that tenascin-C mRNA levels were increased to the same extent in wild-type and ILK rescued cells after 6 h of cyclic strain, in contrast to what we found for ILK knockout cells (Fig. 6B). These results demonstrate that ILK deficiency indeed accounts for the defects of knockout cells in responding to cyclic strain by actin reorganization, MAL nuclear translocation and tenascin-C induction.

### 3.5. Cyclic strain activates Erk-1/2 and PKB/Akt in wild-type as well as ILK-deficient fibroblasts

To test whether ILK knockout cells are completely insensitive to mechanical stimulation, or whether mechanotransduction

pathways not involving RhoA are still functional in these cells, we determined Erk-1/2, PKB/Akt and FAK activity after applying cyclic strain. As shown in Fig. 7, cyclic strain (10%, 0.3 Hz) led to a similar increase in the level of phospho-Erk-1/2 after 5–15 min in ILK wild-type, knockout and rescued cells, respectively. This shows that ILK is not required for strain-mediated Erk-1/2 activation. In other cell types, ILK has been shown to function upstream of PKB/Akt [37,38,52]. We therefore tested whether strain activated PKB in our three cell lines. Indeed, we observed an increase in PKB (S473) phosphorylation after 5–15 min of cyclic strain not only in wild-type and ILK rescued cells, but also in ILK knockout cells (Fig. 7). Thus, external mechanical stress can activate PKB independently of ILK. For comparison, we also checked the state of FAK (Y397) activation in our cells. On the fibronectin-coated substrates used in this study, we found high phosphorylation levels for FAK (Y397) already at rest and in low serum for all three cell types, and we could not detect any further stimulation by cyclic strain (Fig. 7).

### 3.6. Induction of *c-fos* mRNA by cyclic strain in wild-type as well as ILK-deficient cells

Since ILK-deficient fibroblasts still respond to cyclic strain by activating Erk-1/2 and PKB/Akt, we asked whether genes other than tenascin-C were induced normally by mechanical stimulation in these cells. The AP-1 transcription factor *c-fos* is an early response gene induced by mechanical stress [17,18], and *c-fos* induction is partially inhibited by MAPK antagonists [18]. By real time RT-PCR, we therefore compared *c-fos* and tenascin-C mRNA expression levels between wild-type, ILK-deficient and ILK rescued fibroblasts after applying cyclic strain (Fig. 8). These experiments were carried out with cells starved in 0.03% serum to reduce basic *c-fos* expression levels. Cells were strained for just 1 h because we found *c-fos* mRNA

1158

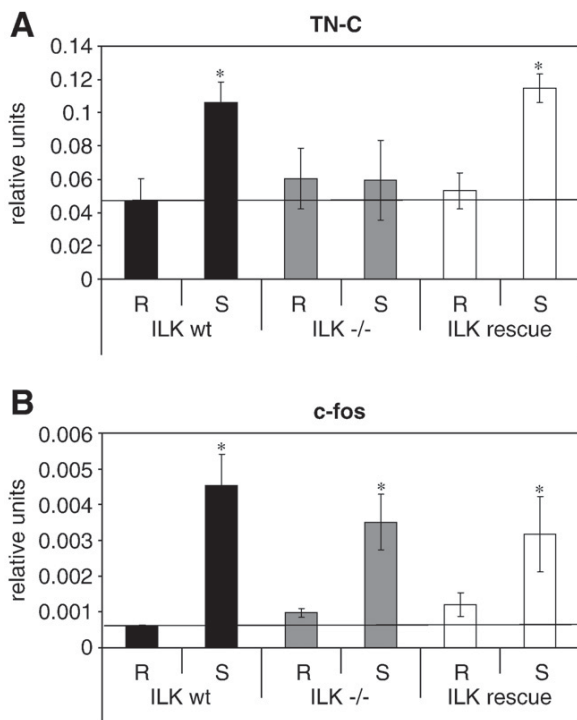
S. Maier et al. / *Biochimica et Biophysica Acta* 1783 (2008) 1150–1162

Fig. 8. Induction of c-fos mRNA by cyclic strain independently of ILK. (A) Wild-type, ILK  $-/-$  and rescued cells maintained in 0.03% serum were subjected to cyclic strain (10%, 0.3 Hz) for 1 h, total RNA was extracted and tenascin-C mRNA levels were determined by real time PCR as described in Materials and methods. Values are normalized to GAPDH expression in the same sample and are expressed as relative units. Bars represent the average  $\pm$  S.E.M. of seven independent experiments. \*Significant difference to the resting control ( $P < 0.05$ ). (B) The same is shown for c-fos mRNA levels.

levels to return to base level after 6 h of cyclic strain (not shown). To allow comparison of basic gene expression levels between cell lines, values were normalized to GAPDH mRNA only ( $\Delta$ Ct method). This showed that whereas basic tenascin-C mRNA levels did not differ significantly in the three cell lines (Fig. 8A), the amount of c-fos mRNA at rest was moderately (about two-fold) increased in ILK knockout as well as ILK rescued cells compared to wild-type fibroblasts (Fig. 8B). One hour of cyclic strain (10%, 0.3 Hz) already induced a two-fold increase of tenascin-C mRNA in wild-type as well as in ILK rescued cells, but not in ILK knockout fibroblasts (Fig. 8B). Thus, whereas tenascin-C mRNA steadily rises between 1 and 6 h of cyclic strain in wild-type cells (cf. Fig. 1; [11]), there is not even a transient induction of this mRNA in ILK-deficient cells. The mRNA for c-fos was induced about nine-fold after 1 h of cyclic strain in wild-type fibroblasts. Because of higher expression at rest, in ILK knockout as well as rescued cells the relative induction of c-fos mRNA by strain was lower (3–4 fold). However, normalized c-fos mRNA levels after 1 h strain were not statistically different between the three cell lines, but all significantly higher than in the respective resting controls. This shows that c-fos induction by cyclic strain does not require ILK, in contrast to what we found for tenascin-C.

### 3.7. Lysophosphatidic acid activates RhoA and induces tenascin-C mRNA in ILK-deficient fibroblasts

We considered the possibility that ILK might not just be required for induction of tenascin-C by cyclic strain, but might have a more general function in the activation of this gene by

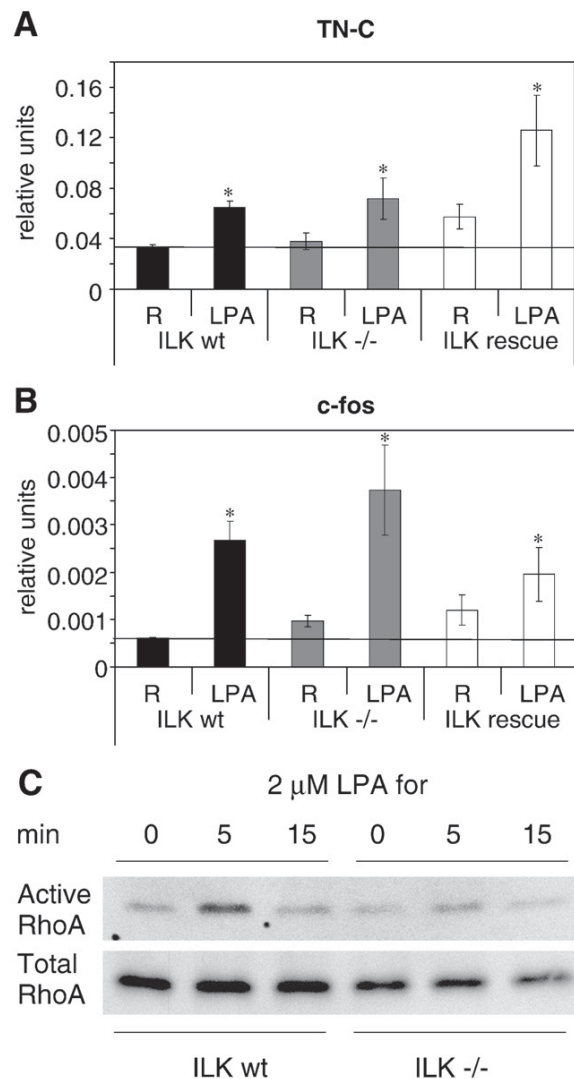


Fig. 9. Activation of RhoA and induction of both, c-fos and tenascin-C mRNA by LPA independently of ILK. (A) Wild-type, ILK  $-/-$  and rescued cells were incubated in 0.03% serum with or without 10  $\mu$ M LPA for 6 h. Total RNA was extracted and tenascin-C mRNA levels were determined by real time PCR as described in Materials and methods. Values are normalized to GAPDH expression in the same sample and are expressed as relative units. Bars represent the average  $\pm$  S.E.M. of four independent experiments. \*Significant difference to the resting control ( $P < 0.05$ ). (B) Levels of c-fos mRNA after 1 h LPA treatment were determined according to A. (C) Wild-type and ILK  $-/-$  cells were incubated in medium containing 2  $\mu$ M LPA for 0, 5 or 15 min. Active RhoA was pulled down from cell lysates (see Materials and methods), and detected on SDS-PAGE by immunoblotting (top panel). For control, total RhoA in the corresponding samples is shown in immunoblots of whole cell lysates (bottom panel).

different stimuli. In chick fibroblasts, tenascin-C mRNA is induced by LPA [12], a serum growth factor that activates both RhoA and MAPK pathways via G-protein coupled receptors [53]. As shown in Fig. 9A, treatment of serum-starved cells with LPA significantly increased tenascin-C mRNA levels in ILK wild-type, ILK-deficient as well as rescued mouse fibroblasts. LPA also induced c-fos mRNA in all three cell types (Fig. 9B). Moreover, addition of LPA led to activation of RhoA in both wild-type and, although to a lesser extent, in ILK-deficient cells after 5 min (Fig. 9C). Thus, a transient activation of RhoA again preceded the induction of tenascin-C mRNA in these experiments. We infer that the absence of ILK does not preclude a RhoA/ROCK-dependent activation of the tenascin-C gene. The downstream signaling required for tenascin-C induction seems to be functional in ILK knockout cells; however, mechanical stimulation cannot trigger this pathway anymore.

#### 4. Discussion

In fibroblasts a direct, integrin-mediated link between the ECM and the cytoskeleton is required for the transduction of mechanical into chemical signals [26,27]. Various intracellular signaling cascades are triggered in response to external mechanical stress via integrins and associated focal adhesion proteins [2,14–16]. Resulting alterations in gene transcription are the basis for the adaptation of connective tissue to changes in mechanical load [1]. A prominent response to tensile strain is the induction of the ECM protein tenascin-C [10–12]. We have demonstrated that in fibroblasts, tenascin-C mRNA induction by cyclic strain occurs in the absence of protein synthesis and does not appear to involve MAPK pathways [11]. Rather, a sustained response of this gene to mechanical stimulation requires an intact actin cytoskeleton and is preceded by RhoA/ROCK- and myosin-dependent actin contraction [12]. We have also shown that the extent of internal cytoskeletal tension is important for the sensitivity of fibroblasts to external strain: stimulation of actin contractility with thrombin or LPA results in a super-induction of tenascin-C mRNA by cyclic strain, whereas inhibition of ROCK attenuates this response [12]. Hence, the steady state level of tenascin-C mRNA in fibroblasts seems to correlate closely with the level of RhoA/ROCK activation.

By these studies, we found that the RhoA/ROCK pathway adjusts mechanosensitivity. However, it was unknown which cellular components record changes in tension between the ECM and the cytoskeleton, and trigger the signals that result in induction of the tenascin-C gene. Recently, an elegant study showed how an adaptor protein in focal adhesions, p130Cas, could act as a “strain gauge” [30]. Physical stretching of this molecule leads to its phosphorylation by Src family kinases, the recruitment of other signaling molecules (Csk and C3G), and the activation of the small GTPase Rap1 [29–31]. In principle, this attractive scheme could apply to other adaptor proteins in focal adhesions. In order to identify components required for transducing mechanical stress into tenascin-C expression, we chose to make use of cell lines lacking specific focal adhesion proteins. We decided to study ILK-deficient cells for several reasons. ILK knockout mouse embryos die at the peri-im-

plantation stage due to adhesion and polarization defects [40]. Importantly, genetic studies in zebrafish implicated ILK as an essential component of a mechanical stretch sensor in vivo [54]. Moreover, ILK-deficient cells in vitro are less spread and have an altered focal adhesion distribution [40,41,43], pointing to its function as an important adaptor protein [34,35]. Finally, ILK has been reported to regulate cell morphology and motility in a Rac1/PAK [46] and RhoA/ROCK [41,45] dependent manner, and cells lacking ILK are not able to assemble a fibronectin matrix [43], another process known to depend on RhoA/ROCK-dependent actin contractility. From these published results, we speculated that ILK might have an important function in mechanotransduction, especially with regard to RhoA-related processes that eventually lead to changes in gene transcription.

In the present experiments we found that, like in primary cells, cyclic strain strongly induced tenascin-C mRNA in immortalized mouse fibroblasts carrying a wild-type ILK gene; however this response was completely lacking in ILK-deficient cells. ILK knockout cells rescued with full length ILK cDNA showed normal induction of tenascin-C mRNA by cyclic strain. In agreement with the known role of the RhoA/ROCK pathway in this specific response [12], ILK-deficient cells also exhibited a defect in the activation of RhoA and an impaired ability to reorganize their actin stress fibers and focal adhesions upon mechanical stimulation. In view of these findings, we speculated that ILK  $-/-$  fibroblasts might also be defective in MAL signaling. MAL, a transcriptional co-activator of SRF, is known to bind to G-actin in the cytoplasm of unstimulated cells and to translocate to the nucleus upon F-actin assembly induced by serum or other activators of RhoA [24,25]. Indeed, we found that cyclic strain triggered nuclear translocation of MAL in wild-type but not in ILK-deficient fibroblasts. Interestingly, however, serum-stimulated MAL trafficking occurred normally in ILK  $-/-$  cells. Moreover, RhoA was still activated and tenascin-C mRNA induced in ILK knockout fibroblasts by LPA. Thus, ILK is required for RhoA-dependent signaling in response to mechanical stress but not to growth factors.

Quite surprisingly in view of the well documented role of ILK in PKB/Akt activation [38,55], cyclic strain-induced normal phosphorylation of this kinase in ILK-deficient cells. Presumably, cyclic strain activates PKB via the classical pathway involving PI3K and PDK1 [37,56], independently of ILK. Moreover, our results clearly show that activation of Erk-1/2 by cyclic strain does not require ILK and, in contrast to tenascin-C, the transcription factor c-fos was still significantly up-regulated by cyclic strain in ILK knockout cells. Thus, cells are still able to sense external strain by triggering various signaling pathways in the absence of ILK, but fail to normally activate RhoA/ROCK-dependent responses. We conclude from these results that ILK has a specific function in relaying external mechanical signals via RhoA-mediated pathways to a subset of mechanoresponsive genes.

The precise role of ILK in this particular mechanotransduction pathway remains to be elucidated. As revealed by LPA stimulation of ILK-deficient cells, ILK is not needed for tenascin-C induction in general, i.e. by signals other than mechanical. Moreover, ILK is not generally required for transducing mechanical signals since the

Erk-1/2 pathway is activated and c-fos is induced normally by cyclic strain in ILK-deficient cells. Rather, ILK might be involved either in regulating RhoA/ROCK-dependent cytoskeletal tension and hence the mechanosensitivity of fibroblasts, or it could act in conjunction with a “strain gauge” similar to p130Cas [30], however upstream of the RhoA/ROCK pathway. Recently published work links ILK to small GTPases of the Rho family [41,44–47]. It has been reported that ILK regulates fibroblast morphology and motility in a RhoA/ROCK-dependent manner [41,45], which positions ILK upstream of this pathway. In another report, overexpression of ILK increased, whereas its silencing decreased the constitutive activity of Rac1 [46]. Since Rac1 and RhoA are known to tune each other’s activity within a cell in space and time [57,58], this might be an indirect way by which ILK controls RhoA. Finally, a recent study investigated the role of ILK in RhoA/ROCK-dependent actin dynamics and gene expression [41]. Treatment of both wild-type and ILK-deficient fibroblasts with LPA led to activation of RhoA and induction of mRNA for connective tissue growth factor (CTGF), similar to what we found for tenascin-C. In contrast, LPA induced cortical actin stress fibers in wild-type but not in ILK  $-/-$  cells, which instead formed thin centripetal actin fibers [41]. The authors conclude that ILK is involved in RhoA-dependent reorganization of the actin cytoskeleton, whereas RhoA activation and RhoA-mediated CTGF expression do not depend on ILK. However, we find that although LPA induces tenascin-C mRNA expression in ILK-deficient cells in a RhoA/ROCK-dependent manner, cyclic strain does not.

In summary, our present results demonstrate an essential function for ILK in the induction of tenascin-C by external cyclic strain. Interestingly, ILK-deficient cells are only partially insensitive towards mechanical stimulation, since other signaling pathways are induced. It is possible that ILK-deficient cells are able to sense static increases in external tension and consequently activate MAPK pathways, but that ILK is required to respond to dynamic strain by RhoA-dependent changes in the actin cytoskeleton; this needs to be addressed further. In addition, our data show that induction of tenascin-C by mechanical stimulation and by growth factors, respectively, can occur by separate pathways, one ILK-dependent but not the other. This finding might help to explain some of the highly restricted expression patterns of tenascin-C in vivo. In normal skeletal muscle, for example, tenascin-C is almost exclusively found at myotendinous junctions [59] and around stretch-sensing muscle spindles [60], locations where mechanical stress is focused during muscle contraction. Under the control of ILK as part of a cell-autonomous mechanosensor, fibroblasts dispersed in muscle and other connective tissue are able to express and secrete tenascin-C very locally, and in part independently from a milieu of growth factors that exerts more global effects. Thus, our studies help to better understand the complex regulation of this important ECM protein during development, wound healing and carcinogenesis [61].

#### Acknowledgements

We gratefully acknowledge the excellent technical assistance of Vildan Tunç-Civelek and her unfailing commitment over the

years. We thank Ruth Chiquet-Ehrismann and Reinhard Fässler for their support and for critically reading the manuscript. This work was funded by the ITI foundation, the Novartis Foundation and by grants from the Swiss National Fund to M.C.

#### References

- [1] M. Kjaer, Role of extracellular matrix in adaptation of tendon and skeletal muscle to mechanical loading, *Physiol. Rev.* 84 (2004) 649–698.
- [2] M. Chiquet, A.S. Renedo, F. Huber, M. Fluck, How do fibroblasts translate mechanical signals into changes in extracellular matrix production? *Matrix Biol.* 22 (2003) 73–80.
- [3] A.L. Bolcato-Bellemin, R. Elkaim, A. Abehsera, J.L. Fausser, Y. Haikel, H. Tenenbaum, Expression of mRNAs encoding for alpha and beta integrin subunits, MMPs, and TIMPs in stretched human periodontal ligament and gingival fibroblasts, *J. Dent. Res.* 79 (2000) 1712–1716.
- [4] J. Deschner, B. Rath-Deschner, S. Agarwal, Regulation of matrix metalloproteinase expression by dynamic tensile strain in rat fibrochondrocytes, *Osteoarthr. Cartil.* 14 (2006) 264–272.
- [5] C.M. Webb, G. Zaman, J.R. Mosley, R.P. Tucker, L.E. Lanyon, E.J. Mackie, Expression of tenascin-C in bones responding to mechanical load, *J. Bone Miner. Res.* 12 (1997) 52–58.
- [6] T.A. Jarvinen, L. Jozsa, P. Kannus, T.L. Jarvinen, M. Kvist, T. Hurme, J. Isola, H. Kalimo, M. Jarvinen, Mechanical loading regulates tenascin-C expression in the osteotendinous junction, *J. Cell Sci.* 112 (Pt 18) (1999) 3157–3166.
- [7] M. Fluck, V. Tunc-Civelek, M. Chiquet, Rapid and reciprocal regulation of tenascin-C and tenascin-Y expression by loading of skeletal muscle, *J. Cell Sci.* 113 (Pt 20) (2000) 3583–3591.
- [8] B. Mikic, M. Wong, M. Chiquet, E.B. Hunziker, Mechanical modulation of tenascin-C and collagen-XII expression during avian synovial joint formation, *J. Orthop. Res.* 18 (2000) 406–415.
- [9] R. Chiquet-Ehrismann, M. Tannheimer, M. Koch, A. Brunner, J. Spring, D. Martin, S. Baumgartner, M. Chiquet, Tenascin-C expression by fibroblasts is elevated in stressed collagen gels, *J. Cell Biol.* 127 (1994) 2093–2101.
- [10] K. Yamamoto, Q.N. Dang, S.P. Kennedy, R. Osathanondh, R.A. Kelly, R.T. Lee, Induction of tenascin-C in cardiac myocytes by mechanical deformation. Role of reactive oxygen species, *J. Biol. Chem.* 274 (1999) 21840–21846.
- [11] M. Chiquet, A. Sarasa-Renedo, V. Tunc-Civelek, Induction of tenascin-C by cyclic tensile strain versus growth factors: distinct contributions by Rho/ROCK and MAPK signaling pathways, *Biochim. Biophys. Acta* 1693 (2004) 193–204.
- [12] A. Sarasa-Renedo, V. Tunc-Civelek, M. Chiquet, Role of RhoA/ROCK-dependent actin contractility in the induction of tenascin-C by cyclic tensile strain, *Exp. Cell Res.* 312 (2006) 1361–1370.
- [13] G.E. Lindahl, R.C. Chambers, J. Papakrivopoulou, S.J. Dawson, M.C. Jacobsen, J.E. Bishop, G.J. Laurent, Activation of fibroblast procollagen alpha 1(I) transcription by mechanical strain is transforming growth factor-beta-dependent and involves increased binding of CCAAT-binding factor (CBF/NF-Y) at the proximal promoter, *J. Biol. Chem.* 277 (2002) 6153–6161.
- [14] J.H. Wang, B.P. Thampatty, J.S. Lin, H.J. Im, Mechanoregulation of gene expression in fibroblasts, *Gene* 391 (2007) 1–15.
- [15] D.A. MacKenna, F. Dolfi, K. Vuori, E. Ruoslahti, Extracellular signal-regulated kinase and c-Jun NH2-terminal kinase activation by mechanical stretch is integrin-dependent and matrix-specific in rat cardiac fibroblasts, *J. Clin. Invest.* 101 (1998) 301–310.
- [16] J.L. Schwachtgen, P. Houston, C. Campbell, V. Sukhatme, M. Braddock, Fluid shear stress activation of egr-1 transcription in cultured human endothelial and epithelial cells is mediated via the extracellular signal-related kinase 1/2 mitogen-activated protein kinase pathway, *J. Clin. Invest.* 101 (1998) 2540–2549.
- [17] N. Yamaguchi, M. Chiba, H. Mitani, The induction of c-fos mRNA expression by mechanical stress in human periodontal ligament cells, *Arch. Oral Biol.* 47 (2002) 465–471.

- [18] D. Kletsas, E.K. Basdra, A.G. Papavassiliou, Effect of protein kinase inhibitors on the stretch-elicited c-Fos and c-Jun up-regulation in human PDL osteoblast-like cells, *J. Cell Physiol.* 190 (2002) 313–321.
- [19] Z. Ma, S.W. Morris, V. Valentine, M. Li, J.A. Herbrick, X. Cui, D. Bouman, Y. Li, P.K. Mehta, D. Nizetic, Y. Kaneko, G.C. Chan, L.C. Chan, J. Squire, S.W. Scherer, J.K. Hitzler, Fusion of two novel genes, RBM15 and MKL1, in the t(1;22)(p13;q13) of acute megakaryoblastic leukemia, *Nat. Genet.* 28 (2001) 220–221.
- [20] T. Mercher, M.B. Coniat, R. Monni, M. Mauchauffe, F. Nguyen Khac, L. Gressin, F. Mugneret, T. Leblanc, N. Dastugue, R. Berger, O.A. Bernard, Involvement of a human gene related to the *Drosophila* spen gene in the recurrent t(1;22) translocation of acute megakaryocytic leukemia, *Proc. Natl. Acad. Sci. U. S. A.* 98 (2001) 5776–5779.
- [21] W.C. Skarnes, B.A. Auerbach, A.L. Joyner, A gene trap approach in mouse embryonic stem cells: the lacZ reported is activated by splicing, reflects endogenous gene expression, and is mutagenic in mice, *Genes Dev.* 6 (1992) 903–918.
- [22] D.Z. Wang, S. Li, D. Hockemeyer, L. Sutherland, Z. Wang, G. Schrott, J.A. Richardson, A. Nordheim, E.N. Olson, Potentiation of serum response factor activity by a family of myocardin-related transcription factors, *Proc. Natl. Acad. Sci. U. S. A.* 99 (2002) 14855–14860.
- [23] T. Sasazuki, T. Sawada, S. Sakon, T. Kitamura, T. Kishi, T. Okazaki, M. Katano, M. Tanaka, M. Watanabe, H. Yagita, K. Okumura, H. Nakano, Identification of a novel transcriptional activator, BSAC, by a functional cloning to inhibit tumor necrosis factor-induced cell death, *J. Biol. Chem.* 277 (2002) 28853–28860.
- [24] F. Miralles, G. Posern, A.I. Zamytidou, R. Treisman, Actin dynamics control SRF activity by regulation of its coactivator MAL, *Cell* 113 (2003) 329–342.
- [25] X.H. Zhao, C. Laschinger, P. Arora, K. Szaszi, A. Kapus, C.A. McCulloch, Force activates smooth muscle alpha-actin promoter activity through the Rho signaling pathway, *J. Cell Sci.* 120 (2007) 1801–1809.
- [26] B. Geiger, A. Bershadsky, Assembly and mechanosensory function of focal contacts, *Curr. Opin. Cell Biol.* 13 (2001) 584–592.
- [27] J.Y. Shyy, S. Chien, Role of integrins in cellular responses to mechanical stress and adhesion, *Curr. Opin. Cell Biol.* 9 (1997) 707–713.
- [28] V. Vogel, M. Sheetz, Local force and geometry sensing regulate cell functions, *Nat. Rev., Mol. Cell Biol.* 7 (2006) 265–275.
- [29] M. Tamada, M.P. Sheetz, Y. Sawada, Activation of a signaling cascade by cytoskeleton stretch, *Dev. Cell* 7 (2004) 709–718.
- [30] Y. Sawada, M. Tamada, B.J. Dubin-Thaler, O. Cherniavskaya, R. Sakai, S. Tanaka, M.P. Sheetz, Force sensing by mechanical extension of the Src family kinase substrate p130Cas, *Cell* 127 (2006) 1015–1026.
- [31] S.E. Lee, R.D. Kamm, M.R. Mofrad, Force-induced activation of Talin and its possible role in focal adhesion mechanotransduction, *J. Biomech.* 40 (2007) 2096–2106.
- [32] G.E. Hannigan, C. Leung-Hagesteijn, L. Fitz-Gibbon, M.G. Coppelino, G. Radeva, J. Filmus, J.C. Bell, S. Dedhar, Regulation of cell adhesion and anchorage-dependent growth by a new beta 1-integrin-linked protein kinase, *Nature* 379 (1996) 91–96.
- [33] S. Dedhar, B. Williams, G. Hannigan, Integrin-linked kinase (ILK): a regulator of integrin and growth-factor signalling, *Trends Cell Biol.* 9 (1999) 319–323.
- [34] C. Grashoff, I. Thievensen, K. Lorenz, S. Ussar, R. Fassler, Integrin-linked kinase: integrin's mysterious partner, *Curr. Opin. Cell Biol.* 16 (2004) 565–571.
- [35] K.R. Legate, E. Montanez, O. Kudlacek, R. Fassler, ILK, PINCH and parvin: the tIPP of integrin signalling, *Nat. Rev., Mol. Cell Biol.* 7 (2006) 20–31.
- [36] G.E. Hannigan, J.G. Coles, S. Dedhar, Integrin-linked kinase at the heart of cardiac contractility, repair, and disease, *Circ. Res.* 100 (2007) 1408–1414.
- [37] M. Delcommenne, C. Tan, V. Gray, L. Rue, J. Woodgett, S. Dedhar, Phosphoinositide-3-OH kinase-dependent regulation of glycogen synthase kinase 3 and protein kinase B/AKT by the integrin-linked kinase, *Proc. Natl. Acad. Sci. U. S. A.* 95 (1998) 11211–11216.
- [38] S. Persad, S. Attwell, V. Gray, N. Mawji, J.T. Deng, D. Leung, J. Yan, J. Sanghera, M.P. Walsh, S. Dedhar, Regulation of protein kinase B/Akt-serine 473 phosphorylation by integrin-linked kinase: critical roles for kinase activity and amino acids arginine 211 and serine 343, *J. Biol. Chem.* 276 (2001) 27462–27469.
- [39] S. Li, R. Bordoy, F. Stanchi, M. Moser, A. Braun, O. Kudlacek, U.M. Wewer, P.D. Yurchenco, R. Fassler, PINCH1 regulates cell-matrix and cell–cell adhesions, cell polarity and cell survival during the peri-implantation stage, *J. Cell Sci.* 118 (2005) 2913–2921.
- [40] T. Sakai, S. Li, D. Docheva, C. Grashoff, K. Sakai, G. Kostka, A. Braun, A. Pfeifer, P.D. Yurchenco, R. Fassler, Integrin-linked kinase (ILK) is required for polarizing the epiblast, cell adhesion, and controlling actin accumulation, *Genes Dev.* 17 (2003) 926–940.
- [41] A. Graness, K. Giehl, M. Goppelt-Struebe, Differential involvement of the integrin-linked kinase (ILK) in RhoA-dependent rearrangement of F-actin fibers and induction of connective tissue growth factor (CTGF), *Cell Signal* 18 (2006) 433–440.
- [42] K. Lorenz, C. Grashoff, R. Torka, T. Sakai, L. Langbein, W. Bloch, M. Aumailley, R. Fassler, Integrin-linked kinase is required for epidermal and hair follicle morphogenesis, *J. Cell Biol.* 177 (2007) 501–513.
- [43] V. Vouret-Craviari, E. Boulter, D. Grall, C. Matthews, E. Van Obberghen-Schilling, ILK is required for the assembly of matrix-forming adhesions and capillary morphogenesis in endothelial cells, *J. Cell Sci.* 117 (2004) 4559–4569.
- [44] F. Acconcia, C.J. Barnes, R.R. Singh, A.H. Talukder, R. Kumar, Phosphorylation-dependent regulation of nuclear localization and functions of integrin-linked kinase, *Proc. Natl. Acad. Sci. U. S. A.* 104 (2007) 6782–6787.
- [45] W.A. Khyrul, D.P. LaLonde, M.C. Brown, H. Levinson, C.E. Turner, The integrin-linked kinase regulates cell morphology and motility in a rho-associated kinase-dependent manner, *J. Biol. Chem.* 279 (2004) 54131–54139.
- [46] E. Boulter, D. Grall, S. Cagnol, E. Van Obberghen-Schilling, Regulation of cell-matrix adhesion dynamics and Rac-1 by integrin linked kinase, *FASEB J.* 20 (2006) 1489–1491.
- [47] G. Hannigan, A.A. Troussard, S. Dedhar, Integrin-linked kinase: a cancer therapeutic target unique among its ILK, *Nat. Rev., Cancer* 5 (2005) 51–63.
- [48] K.J. Livak, T.D. Schmittgen, Analysis of relative gene expression data using real-time quantitative PCR and the 2(-Delta Delta C(T)) Method, *Methods* 25 (2001) 402–408.
- [49] X.D. Ren, M.A. Schwartz, Determination of GTP loading on Rho, *Methods Enzymol.* 325 (2000) 264–272.
- [50] P.F. Jones, T. Jakubowicz, F.J. Pitossi, F. Maurer, B.A. Hemmings, Molecular cloning and identification of a serine/threonine protein kinase of the second-messenger subfamily, *Proc. Natl. Acad. Sci. U. S. A.* 88 (1991) 4171–4175.
- [51] E. Aufderheide, P. Ekblom, Tenascin during gut development: appearance in the mesenchyme, shift in molecular forms, and dependence on epithelial-mesenchymal interactions, *J. Cell Biol.* 107 (1988) 2341–2349.
- [52] T. Fukuda, L. Guo, X. Shi, C. Wu, CH-ILKBP regulates cell survival by facilitating the membrane translocation of protein kinase B/Akt, *J. Cell Biol.* 160 (2003) 1001–1008.
- [53] D.A. Lin, J.A. Boyce, Lysophospholipids as mediators of immunity, *Adv. Immunol.* 89 (2006) 141–167.
- [54] G. Bendig, M. Grimmmler, I.G. Huttner, G. Wessels, T. Dahme, S. Just, N. Trano, H.A. Katus, M.C. Fishman, W. Rottbauer, Integrin-linked kinase, a novel component of the cardiac mechanical stretch sensor, controls contractility in the zebrafish heart, *Genes Dev.* 20 (2006) 2361–2372.
- [55] A.A. Troussard, N.M. Mawji, C. Ong, A. Mui, R. St-Arnaud, S. Dedhar, Conditional knock-out of integrin-linked kinase demonstrates an essential role in protein kinase B/Akt activation, *J. Biol. Chem.* 278 (2003) 22374–22378.
- [56] B. Vanhaesebroeck, D.R. Alessi, The PI3K-PDK1 connection: more than just a road to PKB, *Biochem. J.* 346 (Pt 3) (2000) 561–576.



- [57] Y. Yamaguchi, H. Katoh, H. Yasui, K. Mori, M. Negishi, RhoA inhibits the nerve growth factor-induced Rac1 activation through Rho-associated kinase-dependent pathway, *J. Biol. Chem.* 276 (2001) 18977–18983.
- [58] H. Rosenfeldt, M.D. Castellone, P.A. Randazzo, J.S. Gutkind, Rac inhibits thrombin-induced Rho activation: evidence of a Pak-dependent GTPase crosstalk, *J. Mol. Signal* 1 (2006) 8.
- [59] M. Chiquet, D.M. Fambrough, Chick myotendinous antigen. I. A monoclonal antibody as a marker for tendon and muscle morphogenesis, *J. Cell Biol.* 98 (1984) 1926–1936.
- [60] A. Maier, R. Mayne, Basal lamina development in chicken muscle spindles, *Dev. Dyn.* 202 (1995) 284–293.
- [61] R. Chiquet-Ehrismann, M. Chiquet, Tenascins: regulation and putative functions during pathological stress, *J. Pathol.* 200 (2003) 488–499.

### Glossary

*ROCK*: Rho dependent kinase  
*ILK*: integrin-linked kinase  
*LPA*: lysophosphatidic acid  
*MAPK*: mitogen activated protein kinase  
*ERK-1/2*: extracellular signal-regulated kinases 1/2  
*c-fos*: cellular FBJ murine osteosarcoma viral oncogene homolog  
*GAPDH*: glyceraldehyde-3-phosphate dehydrogenase  
*RBD*: Rho-binding domain  
*TN-C*: tenascin-C  
*CTGF*: connective tissue growth factor  
*FAK*: focal adhesion kinase  
*PKB*: protein kinase B  
*MAL*: megakaryocytic acute leukemia

## **IV.2 Identification of a fibronectin interaction site in the extracellular matrix protein ameloblastin**

Michael Beyeler, Christof Schild, Roman Lutz, Matthias Chiquet, Beat Trueb

Experimental Cell Research (Exp cell res), 2010

My contribution: Generation of fibronectin knockdown fibroblasts (see figure 6A, 6B, and 6C)

available at [www.sciencedirect.com](http://www.sciencedirect.com)[www.elsevier.com/locate/yexcr](http://www.elsevier.com/locate/yexcr)

## Research Article

## Identification of a fibronectin interaction site in the extracellular matrix protein ameloblastin

Michael Beyeler<sup>a</sup>, Christof Schild<sup>a</sup>, Roman Lutz<sup>b</sup>, Matthias Chiquet<sup>c</sup>, Beat Trueb<sup>a,d,\*</sup>

<sup>a</sup>Department of Clinical Research, University of Bern, Murtenstrasse 35, 3010 Bern, Switzerland

<sup>b</sup>Friedrich Miescher Institute for Biomedical Research, Novartis Research Foundation, Maulbeerstrasse 66, 4058 Basel, Switzerland

<sup>c</sup>Department of Orthodontics and Dentofacial Orthopedics, University of Bern, 3010 Bern, Switzerland

<sup>d</sup>Department of Rheumatology, University Hospital, 3010 Bern, Switzerland

## ARTICLE INFORMATION

## Article Chronology:

Received 12 October 2009

Revised version received

11 December 2009

Accepted 21 December 2009

Available online 4 January 2010

## Keywords:

Ameloblastin (AMBN)

Fibronectin (FN)

Enamel

Ameloblast

Cell adhesion

Integrin receptor

## ABSTRACT

Mammalian teeth are composed of hydroxyapatite crystals that are embedded in a rich extracellular matrix. This matrix is produced by only two cell types, the mesenchymal odontoblasts and the ectodermal ameloblasts. Ameloblasts secrete the enamel proteins amelogenin, ameloblastin, enamelin and amelotin. Odontoblasts secrete collagen type I and several calcium-binding phosphoproteins including dentin sialophosphoprotein, dentin matrix protein, bone sialoprotein and osteopontin. The latter four proteins have recently been grouped in the family of the SIBLINGs (small integrin-binding ligand, N-linked glycoproteins) because they display similar gene structures and because they contain an RGD tripeptide sequence that binds to integrin receptors and thus mediates cell adhesion.

We have prepared all the other tooth-specific proteins in recombinant form and examined whether they might also promote cell adhesion similar to the SIBLINGs. We found that only ameloblastin consistently mediated adhesion of osteoblastic and fibroblastic cells to plastic or titanium surfaces. The activity was dependent on the intact three-dimensional structure of ameloblastin and required *de novo* protein synthesis of the adhering cells. By deletion analysis and *in vitro* mutagenesis, the active site could be narrowed down to a sequence of 13 amino acid residues (VPIMDFADPQFPT) derived from exon 7 of the rat ameloblastin gene or exons 7–9 of the human gene. Kinetic studies and RNA interference experiments further demonstrated that this sequence does not directly bind to a cell surface receptor but that it interacts with cellular fibronectin, which in turn binds to integrin receptors.

The identification of a fibronectin-binding domain in ameloblastin might permit interesting applications for dental implantology. Implants could be coated with peptides containing the active

\* Corresponding author. Department of Clinical Research, University of Bern, Murtenstrasse 35, PO Box 43, 3010 Bern, Switzerland. Fax: +41 31 632 49 63.

E-mail address: [beat.trueb@dkf.unibe.ch](mailto:beat.trueb@dkf.unibe.ch) (B. Trueb).

Abbreviations: AMBN, ameloblastin; AMELX, amelogenin; AMTN, amelotin; BSA, bovine serum albumin; BSP, bone sialoprotein; DMEM, Dulbecco's modified Eagle's medium; DMP1, dentin matrix protein; DPP, dentin phosphoprotein; DSP, dentin sialoprotein; DSPP, dentin sialophosphoprotein; ECM, extracellular matrix; ENAM, enamelin; FN, fibronectin; OPN, osteopontin; PBS, phosphate buffered saline; SIBLING, small integrin-binding ligand N-linked glycoprotein

0014-4827/\$ – see front matter © 2009 Elsevier Inc. All rights reserved.

doi:10.1016/j.yexcr.2009.12.019

sequence, which in turn would recruit fibronectin from the patient's blood. The recruited fibronectin should then promote cell adhesion on the implant surface, thereby accelerating osseointegration of the implant.

© 2009 Elsevier Inc. All rights reserved.

## Introduction

Mammalian teeth consist of two mineralized tissues that represent the hardest tissues of the body, namely dentin and enamel. The development of these tissues requires reciprocal interactions between the oral epithelium and the ectomesenchyme and results in the differentiation of enamel-producing ameloblasts and dentin-producing odontoblasts [1]. The odontoblasts secrete mainly collagen type I, which makes up nearly 90% of the dentin, but also several non-collagenous glycoproteins, including dentin sialophosphoprotein (DSPP), dentin matrix protein (DMP1), bone sialoprotein (BSP), osteopontin (SPP1/OPN), osteocalcin, osteonectin and matrix Gla protein [2]. The ameloblasts on the other hand do not produce any collagens, but secrete primarily the enamel proteins amelogenin (AMELX), ameloblastin (AMBN), enamelin (ENAM) [2] and amelotin (AMTN) [3–5].

Eight years ago, Fisher et al. [6] proposed to group the calcium-binding phosphoproteins of teeth and bone in the family of the SIBLINGs (small integrin-binding ligand, N-linked glycoproteins). Today, this family encompasses six members (BSP, OPN, DMP1, DSPP, MEPE and ENAM) [7]. Although the SIBLINGs do not show much similarity at the amino acid sequence level, a detailed comparison of their gene structures and of the chromosomal locations reveals a closer relationship. All the genes are clustered on the long arm of human chromosome 4, in bands 4q13–4q22. The majority of the polypeptides is encoded by the last one or two exons and this region contains the motif RGD that interacts with integrin receptors on cell surfaces. When the sequence of the human genome was completed it became evident that the genes for AMBN and AMTN are also located on human chromosome 4, next to the SIBLING cluster [8,9]. Furthermore, the gene for AMELX shares many features with the SIBLING genes except that it is not found on chromosome 4 but on the X chromosome. It should be emphasized that the enamel proteins AMBN, AMELX and AMTN lack the integrin-binding sequence RGD. Based on the related gene structures it has been speculated that all the secreted, calcium-binding phosphoproteins may have evolved from a common ancestor by tandem gene duplication and that the AMELX gene was later translocated to the X chromosome [8,9].

Most if not all of the proteins from the extracellular matrix (ECM) of teeth are involved in the mineralization of dentin and enamel [10]. Therefore it is not surprising that mouse models with a targeted deletion or mutation in one of the corresponding genes display severe defects in tooth development that resemble human tooth malformations such as amelogenesis imperfecta (e.g. AMELX, AMBN, ENAM) or dentinogenesis imperfecta (e.g. DSPP) [11,12]. In addition to this important function in biomineralization, the SIBLING proteins are involved in the promotion of cell adhesion [7,13]. For this purpose they possess the RGD tripeptide motif that interacts with integrin receptors as mentioned above [13–15]. Although AMELX, AMBN and AMTN are devoid of such an RGD sequence, they have still been implicated in cell adhesion. AMELX promoted adhesion of osteoblastic cells in a dose-

dependent manner when coated on plastic dishes [16]. Likewise, AMBN bound specifically to dental epithelial cells and inhibited cell proliferation [17]. AMTN was found to be located at the interphase between ameloblasts and enamel where it might also support cell adhesion [4]. Moreover, an extract prepared from the enamel of porcine teeth, which consists mainly of AMELX, is commercially distributed under the brand name Emdogain®. This extract has been shown to promote proliferation, migration and adhesion of various cell types and to stimulate periodontal regeneration when administered to the roots of teeth [18]. It is conceivable that other tooth-specific proteins have similar activities which would be beneficial for the osseointegration of dental implants.

Here we have systematically examined the ECM proteins of teeth for their ability to promote cell adhesion. We found that AMBN was the most promising candidate, although it lacks the RGD integrin-binding motif. Very recently, Sonoda et al. [19] demonstrated that AMBN contains several heparin-binding domains, which might be responsible for the interaction of AMBN with the surface of dental epithelial cells. However, these authors were not able to demonstrate a specific binding of AMBN to heparan-sulfate containing cell surface proteins such as syndecan or glypican. Furthermore, deletions of the heparin-binding sequences from AMBN did not abolish all the adhesive capacity of the protein. It was therefore concluded that another domain, which is independent of the heparin-binding region, must exist and promote cell adhesion. Here we identify such an adhesion promoting domain and demonstrate that it interacts with fibronectin (FN). FN is a multifunctional glycoprotein of the ECM produced by a variety of cell types including fibroblasts, hepatocytes, endothelial cells and some epithelial cells [20,21]. It is involved in cell adhesion, growth, migration and differentiation and consequently it is essential for many biological processes such as wound healing and embryonic development. To fulfill its functions, FN interacts with various molecules including heparin, collagen, fibrin and integrin receptors. The FN binding domain of AMBN may therefore explain the adhesion promoting activity observed with AMBN.

## Materials and methods

### Cell culture

Since no established cell lines of odontoblastic or ameloblastic origin are commercially available and since primary cells show large variabilities between different preparations, all our experiments were performed with well characterized osteoblastic and fibroblastic cell lines. Most of these cell lines were purchased from the American Type Culture Collection: human osteosarcoma cells MG63 (CRL-1427), human osteosarcoma cells SAOS-2 (HTB-85), human fetal lung fibroblasts IMR-90 (CCL-186), mouse embryonic fibroblasts 3T3 (CCL-163) and human embryonic kidney cells

HEK293 (CRL-1573). The rat osteosarcoma cells (ROS) were a kind gift of Prof. Dr. J. Caverzasio from the University of Geneva. Immortalized mouse embryo fibroblasts (MEFs) were used to produce stable FN knock-down cells (MEF shFN). For this purpose, the cells were transfected with purified DNA plasmids encoding shRNA against mouse FN (MISSION shRNA Bacterial Glycerol Stock from Sigma, Buchs, Switzerland) and clones resistant to puromycin (2 µg/ml) were selected [22]. All cells were maintained at 37 °C under an atmosphere of 5% CO<sub>2</sub> in Dulbecco's modified Eagle's medium (DMEM) supplemented with 10% fetal bovine serum, 100 units/ml penicillin and 100 µg/ml streptomycin. The media for HEK293 cells under Zeocin selection and for MEF cells under puromycin selection were further enriched with non-essential amino acids.

### Expression of recombinant proteins

The cDNA clones for rat AMBN, AMELX, AMTN, ENAM, DSP and DPP originated from a tooth-specific cDNA library that was previously described in detail [21]. An EST clone for human AMBN (IMAGE ID: 40033703) was obtained from the HGMP Resource Centre in Cambridge, UK. All proteins were expressed as mature, full-length polypeptides except for ENAM. In the case of ENAM, only the most stable proteolytic fragment spanning amino acids 248–360 (32 kDa fragment) was generated. FN used as a positive control was purified from human blood plasma (Swiss Red Cross) by affinity chromatography on gelatin Sepharose [23].

For expression in mammalian cells, the cDNA sequences were ligated into the *Bam*HI/*Xho*I site of the expression vector pSecTag2B (Invitrogen) upstream of the His-tag sequence. HEK293 cells were transfected with the resulting plasmids using Metafectene (Biontex, Martinsried, Germany). The transfected cells were cultivated in the presence of 200 µg/ml Zeocin (Invitrogen) until resistant colonies became visible (~4 weeks). The resistant colonies were pooled into one oligoclonal Zeocin resistant batch. Subcultures of this batch were grown to confluence, washed with phosphate buffered saline (PBS) and then kept in serum free medium for 4 days. The conditioned media were dialyzed against 100 mM NaCl, 50 mM Tris, pH 8.0. Recombinant proteins were purified from the dialyzed media by affinity chromatography on nickel agarose (His-select HC nickel affinity gel, Sigma) as suggested by the supplier.

For the expression in bacteria, the cDNA sequences were ligated into the *Bam*HI/*Xho*I restriction site of the expression vector pGEX-5X (GE Healthcare) downstream of the GST gene and transformed into competent bacteria (*Escherichia coli* BL21). Fusion proteins were expressed after induction with isopropyl-β-D-thiogalactopyranoside as suggested by the supplier of the GST gene fusion system (GE Healthcare). The bacteria were collected by centrifugation and lysed by sonication. Fusion proteins were purified from the lysates by affinity chromatography on reduced glutathione Sepharose, followed by dialysis against 2 M urea, 100 mM NaCl, 50 mM Tris, pH 8.0.

### Gel electrophoresis and immunoblotting

The purity of the recombinant proteins was analyzed on 10% SDS polyacrylamide gels. The gels were stained with Coomassie Brilliant Blue R250. For Western blots, the proteins were transferred by electroblotting to nitrocellulose membranes. The

membranes were incubated with mouse monoclonal antibodies against the His-tag or goat polyclonal antibodies against the GST-fusion protein (GE Healthcare), followed by secondary, alkaline phosphatase-conjugated antibodies against mouse or goat IgG (Sigma), respectively. Bound antibodies were detected by reaction with bromochloroindolyl phosphate and nitroblue tetrazolium substrate.

### Cell adhesion experiments

For the quantitative assay, three droplets (10 µl each) of a solution containing the corresponding protein at 0.4 µM in PBS with 1 M urea were spotted onto bacterial (non-tissue culture) plastic dishes (Sarstedt 35 mm Petri Dish, number 82.1135) and dried overnight under vacuum (Speed Vac SC110, Savant). Residual sites of the plastic surface were blocked for 1 h at 37 °C with 10 mg/ml bovine serum albumin (BSA) in PBS. Exponentially growing cells were harvested by trypsin treatment and washed once with serum containing medium to inactivate the enzyme and then three times with serum free medium before they were applied to the coated plates in DMEM (~1 × 10<sup>6</sup> cells/plate). The plates were incubated at 37 °C for 120 min unless otherwise stated. Non-adherent cells were removed by shaking the plates on an orbital shaker at 100 rpm for 1 min, followed by 3 washing steps with PBS. For quantification, the adherent cells were incubated with 300 µl of a solution containing 3.75 mM p-nitrophenyl-N-acetyl-β-D-glucosaminide, 50 mM sodium citrate, 0.25% Triton X-100, pH 5.0. The reaction was stopped after 45 min by addition of 600 µl of 50 mM glycine, 5 mM EDTA, pH 10.4. Finally, the absorbance of the yellow reaction mixture was determined at 405 nm. All quantitative assays were performed in duplicate and repeated at least once (*n* = 4).

For the qualitative assay, droplets of the protein solutions were spotted onto the plastic dishes or onto machined titanium disks (1 × 15 mm) as described above. Residual sites were blocked with BSA and cells were seeded on the pretreated surfaces. After thorough washing, the adherent cells were fixed for 10 min with 4% paraformaldehyde in PBS. Cells on bacterial dishes were then stained for 5 min with crystal violet (1 mg/ml). Cells on titanium disks were permeabilized for 10 min with 0.2% Triton X-100 in PBS, washed and stained with TRITC-labeled phalloidin (Sigma) and DAPI (Invitrogen) according to the manufacturer's suggestions. Finally, pictures were taken under an Axiovert 10 microscope equipped with epifluorescence optics (Carl Zeiss, Germany).

## Results

### Cell adhesion to different tooth proteins

In order to systematically search for matrix proteins of teeth that would be able to facilitate cell adhesion, we expressed several clones from our previously described tooth-specific cDNA library [5] in a bacterial expression system. To this end, full-length clones for AMBN, AMELX, AMTN, DSP and DPP as well as a clone for the stable ENAM fragment of 32 kDa were selected and fusion proteins with GST were produced. Collagen type I, DMP1, BSP and OPN were not included in our investigations because the adhesion promoting activity of these proteins has already been described in the literature in detail [7,13,14].

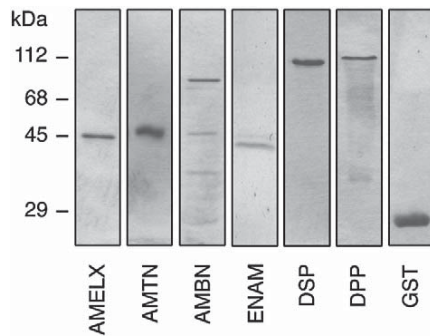


**Fig. 1 – Purity of expressed fusion proteins. Individual cDNA sequences were expressed as GST-fusion proteins in a bacterial expression system and purified by affinity chromatography on Glutathione Sepharose. The purified proteins were separated on SDS polyacrylamide gels and stained with Coomassie blue. The mobility of globular protein markers is indicated in the left margin.**

The six recombinant proteins migrated with the expected mobility on a polyacrylamide gel (Fig. 1). AMBN revealed some traces of proteolytic degradation, which increased with the duration of storage. All the other proteins migrated as single, clean bands on the gel. Fresh preparations of the six fusion proteins were examined in a qualitative assay for their ability to promote cell adhesion. To this end, individual droplets of the protein solutions were applied to bacterial plastic dishes and completely dried overnight. Residual sites on the plastic dishes were blocked with BSA. MG63 cells from a human osteosarcoma were seeded on the pretreated dishes and incubated at 37 °C. We found that the cells adhered after 20–30 min on the spots coated with FN, as previously described in the literature (Fig. 2A) [21,24]. On AMBN, the cells started to adhere after 1 h. After 2 h, they had firmly attached to this substratum so that the dishes could be vigorously washed on an orbital shaker without losing the cells. A similar adhesion promoting activity was also found for AMELX and to a lesser extent for AMTN. In contrast DSP, DPP and ENAM as well as GST and BSA that were included as negative controls did not facilitate cell adhesion under these conditions (Fig. 2A).

Since many dental implants are manufactured of titanium, we also tested our recombinant proteins on this material. When applied to titanium disks as described above, FN and AMBN were found to promote adhesion of MG63 cells as demonstrated by staining of the attached cells with fluorescently labeled phalloidin (Fig. 2B). In contrast, titanium disks coated with AMELX, AMTN, ENAM, DSP, DPP, GST or BSA showed only occasional, small clumps of adherent cells after an incubation period of 2 h (shown only for AMELX in Fig. 2B).

In the next step, we quantified the extent of cell adhesion on pretreated plastic dishes. The adherent cells were lysed and the activity of the endogenous enzyme hexosaminidase, which is proportional to the cell number, was determined with a colorimetric assay. Five different cell lines were used for these quantitative measurements, the osteoblast-like cells MG63, SAOS-2 and ROS as well as the fibroblast-like cells IMR-90 and 3T3. When the hexosaminidase values were normalized to the extent of adhesion observed with FN, results very similar to those

of the qualitative assay were obtained (Fig. 3). All the five cell types adhered firmly on AMBN. In the case of MG63, IMR-90 and 3T3 cells, the signal observed with AMBN was even higher (110–127%) than that obtained with FN. Using SAOS-2 and ROS cells, the signal was still 60% and 75%, respectively. On the other hand, DPP, DSP, ENAM, GST and BSA were not able to facilitate adhesion of any one of the five different cell types. AMTN was found to promote some adhesion of MG63 and ROS cells and a signal of about 50% was observed. AMELX facilitated adhesion of all the cell types except SAOS-2 and yielded a signal of 41–92% depending on the actual cell line used.

Taken together, the quantitative and the qualitative assays demonstrate that AMBN is the only protein of the six tested candidates that is capable of promoting stable adhesion of different cell types on plastic as well as titanium surfaces. In the following we therefore focused on the elucidation of the molecular mechanism of the interaction between cells and AMBN.

#### Dependence on AMBN structure

In the next experiments, we examined whether AMBN depends on metal ions for its adhesion promoting activity. In fact, when the protein was spotted onto the plastic dishes in the presence of EDTA, it was no longer able to facilitate adhesion of MG63 cells (Fig. 4A). In contrast, FN did not lose its adhesion promoting activity when treated with EDTA. To further test the dependence on an intact three-dimensional structure, we denatured AMBN by heating to 95 °C before applying it to the plastic dishes. Again, this treatment drastically reduced the activity of AMBN to facilitate cell adhesion (Fig. 4A). In contrast, FN did not lose its adhesion promoting activity by a brief heating step. Thus, an intact conformation is crucial for AMBN to mediate cell adhesion.

As noted in our initial experiments (see above), MG63 cells required up to 2 h for stable adhesion on AMBN, while only 20–30 min were needed to attach to FN. We therefore examined whether *de novo* protein synthesis by the plated cells would be required for adhesion to AMBN. In fact, when cycloheximide, a potent inhibitor of protein synthesis, was added to the cells during the incubation period, adhesion of MG63 cells on AMBN was completely abolished (Fig. 4B). Thus, we concluded that *de novo* synthesis of another protein must be required to mediate cell adhesion to AMBN.

#### Interaction partner of AMBN

The protein that facilitates cell adhesion to AMBN could either be a transmembrane receptor, which has to be replenished after trypsin treatment of the cells, or another adhesive protein, which interacts with AMBN and indirectly mediates binding of a transmembrane receptor to AMBN. We first examined the second possibility and tested whether other known adhesive ECM proteins would decrease the required adhesion time from 2 h to 30 min. To this end, AMBN was coated on plastic dishes and residual sites were blocked with BSA as described above. Putative interaction partners were then added to the AMBN coated plates and incubated for 1 h. After thorough rinsing, MG63 cells were added to the pretreated plates, but this time the plates were incubated for only 30 min before they were vigorously washed on the orbital shaker. Within this short time period, the cells firmly adhered to the positive control FN and as expected the cells did

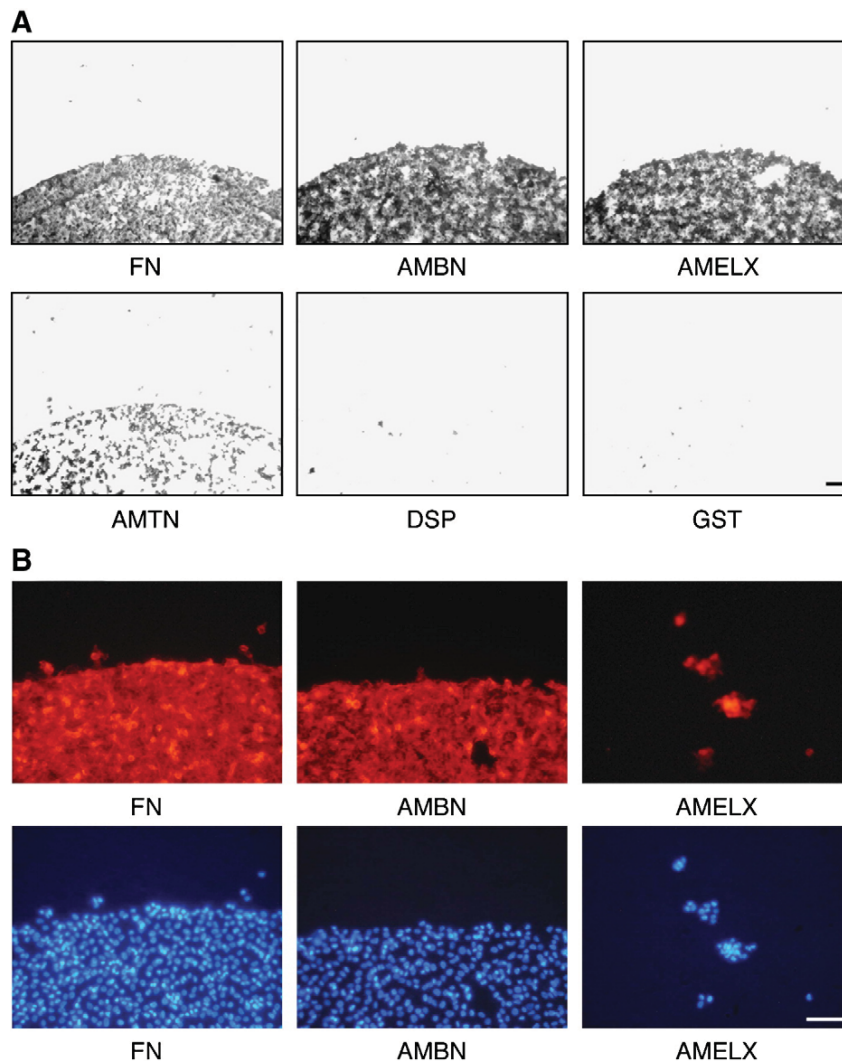


**Fig. 2 – Cell adhesion to recombinant tooth proteins.** Droplets of different protein solutions, as indicated below the individual panels, were applied to bacterial plastic dishes (A) or to machined titanium disks (B) and completely dried. Residual sites on the plastic or titanium surface were blocked with BSA. MG63 osteosarcoma cells were seeded on the pretreated surfaces and incubated for 2 h. After thorough washing, the adherent cells were fixed with paraformaldehyde and (A) stained with crystal violet or (B) permeabilized and stained with TRITC-labeled phalloidin (red) and DAPI (blue). Fibronectin and AMBN promoted cell adhesion on both surfaces. AMELX, and to some extent also AMTN, promoted cell adhesion on the plastic dishes but not on the titanium disks. DSP, DPP, GST and BSA did not promote cell adhesion, neither on the plastic dishes nor on the titanium disks. Bar = 100  $\mu$ m.

not adhere to untreated AMBN because 2 h would be required for stable adhesion in this case (Fig. 5). However, when the AMBN coated dishes were incubated with FN prior to the addition of the cells, most of the adhesion promoting activity could be restored. Since all sites of the plastic dishes had been blocked with BSA and since no adhesion was observed outside of the AMBN coated area, this result suggests that FN directly interacts with AMBN. This effect was specific and could not be repeated with vitronectin, another well-known adhesive ECM molecule (Fig. 5) [25]. Likewise it could not be achieved by heparin, a glycosaminoglycan often involved in cell adhesion. Thus, AMBN must specifically bind to FN.

To definitively prove that FN was the protein partner, which mediated adhesion of MG63 cells to AMBN and which had to be secreted during the 2-h incubation period, we repeated the above experiment with cells deficient in FN production. For this purpose, we used fibroblasts that had been stably transfected with a short hairpin RNA construct, which specifically inhibited the transcription of the FN gene by RNA interference (MEF shFN cells). These cells could be grown in culture like the original wild-type cells (MEF cells), but they displayed a slightly different phenotype and they depended on the presence of FN from fetal bovine serum for proper adhesion (Fig. 6A). When confluent dishes of such MEF shFN cells were cultivated for 2 days in medium without serum,

the conditioned medium contained almost no FN as indicated by Western blotting (Fig. 6B). In contrast, the medium conditioned by wild-type cells contained high levels of FN as shown by the

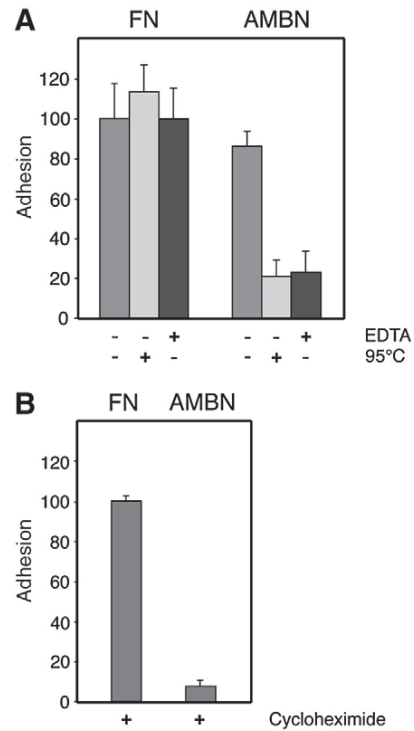
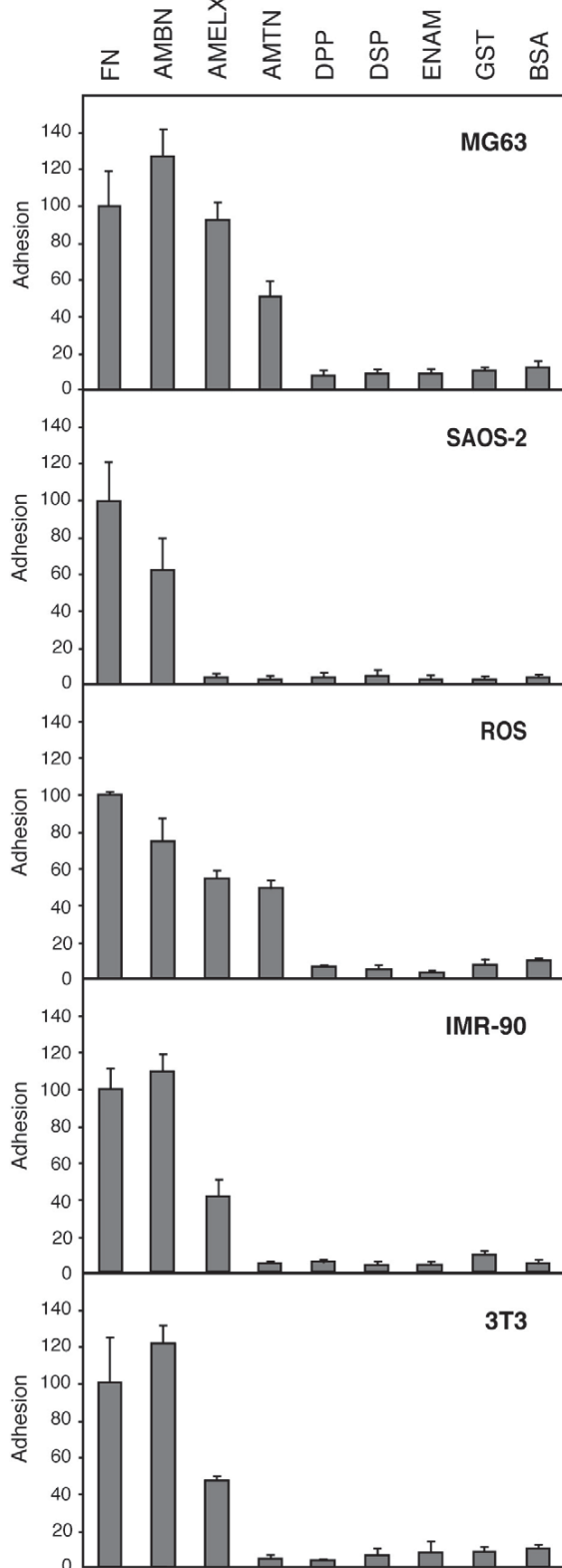


**Fig. 4 – Interference with cell adhesion to AMBN. (A) Influence of divalent ions and three-dimensional structure on promotion of cell adhesion.** Solutions of AMBN and FN were treated with EDTA (1 mM) or heated for 5 min to 95 °C as indicated and then administered to bacterial plastic dishes as described in the legend to Fig. 3. After blocking of residual sites with BSA, MG63 cells were added to the pretreated dishes and incubated for 2 h. After a thorough washing step, adherent cells were quantified by measuring the activity of the endogenous enzyme hexosaminidase. The results show that cell adhesion to AMBN is dependent on divalent ions and on the correct three-dimensional structure of the protein, whereas this is not the case for adhesion to FN. (B) Influence of *de novo* protein synthesis on adhesion to AMBN. MG63 cells were seeded on protein spots of FN or AMBN as above and incubated for 2 h in the presence of cycloheximide (50 µg/ml), a potent inhibitor of protein synthesis. Adherent cells were quantified after washing as above. *De novo* protein synthesis was required for adhesion to AMBN, but not for adhesion to FN.

**Fig. 3 – Quantification of cell adhesion on different tooth proteins.** Recombinant tooth proteins were administered to bacterial plastic dishes as described in the legend to Fig. 2. Different osteoblastic (MG63, SAOS-2, ROS) and fibroblastic (IMR-90, 3T3) cells were allowed to adhere to the pretreated plastic surface. Non-adherent cells were washed off. Adherent cells were quantified by measuring the activity of the endogenous enzyme hexosaminidase. The results are given in relation to the adhesion on FN (100%) ± SE (n = 4, except for MG63 where n = 14). Only FN and AMBN promoted adhesion of all different cell lines.



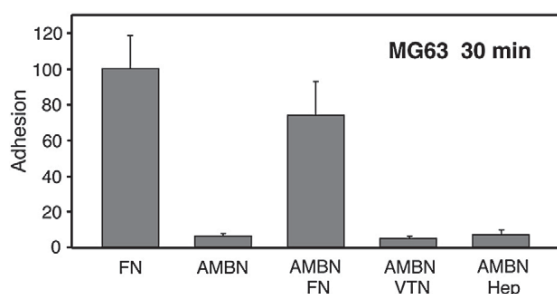


**Fig. 5 – Identification of the binding partner of AMBN.** AMBN and FN were spotted onto plastic dishes and residual sites were blocked with BSA. Some of the AMBN spots were subsequently treated for 1 h with solutions (10  $\mu$ g/ml) of FN, vitronectin (VTN) or heparin (Hep). After thorough washing, MG63 cells were incubated on the pretreated plastic dishes for 30 min. This incubation period allowed the cells to adhere to FN, but not to AMBN. However, when the AMBN spots had been treated with FN prior to the incubation with cells, they promoted cell adhesion within 30 min. This effect was specific for FN since treatment of the AMBN spots with VTN or Hep did not improve cell adhesion.

presence of the broad smear on the Western blot. When the FN deficient cells were seeded on AMBN coated dishes and incubated for 2 h as above, they could not adhere on this substratum (Fig. 6C). In contrast, the wild-type cells readily adhered on AMBN under the same conditions. Furthermore, the FN deficient cells adhered similar to wild-type cells on FN coated dishes that were included as positive control. These experiments clearly demonstrate that the cells do not directly adhere on AMBN, but rather require FN, which in turn interacts with AMBN. AMBN must therefore possess a FN-binding domain.

#### Localization of the FN-binding domain in AMBN

We tried several different assays to demonstrate a direct interaction of AMBN with FN, including ELISA, blot overlays and GST pull-down assays. Unfortunately, all our efforts remained fruitless. Obviously, AMBN and FN are both very sticky proteins. Without inclusion of Triton X-100 in all buffers, we always observed unspecific interactions, and after addition of detergent we could not observe any binding anymore (data not shown). These negative results suggest that hydrophobic interactions might be involved in the binding of FN to AMBN.

Nevertheless, in order to localize the binding site of FN in AMBN, we resorted to the cell adhesion assay described above, which had consistently yielded robust results (Fig. 7). The full-length AMBN sequence was divided into four overlapping fragments. Each of these fragments was expressed in the bacterial expression system and tested separately for its adhesion promoting activity. This experiment demonstrated that the FN-binding domain must reside in the N-terminal half of AMBN since the two fragments spanning the C-terminal half (residues 263–365 and 360–422) were negative, while the two fragments spanning the N-terminal half (residues 27–212 and 177–265) were positive. Two additional fragments spanning residues 27–183 and 197–422 were also found to be negative, whereas a fragment covering the central portion of

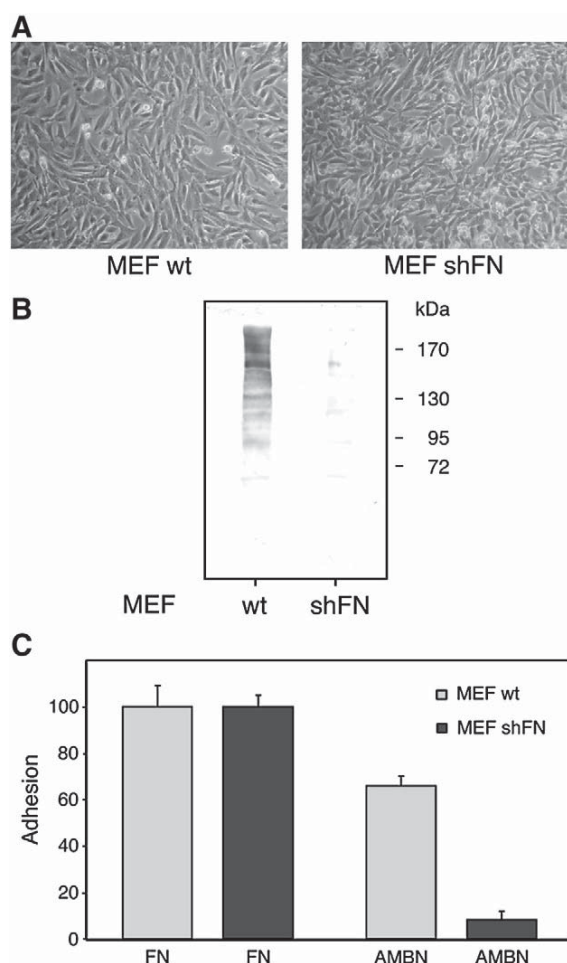


**Fig. 6 – Verification of FN as the binding partner of AMBN.** Adhesion experiments were performed with mouse embryonic fibroblasts (MEF) that had been stably transfected with a short hairpin RNA construct (MEF shFN), which specifically inhibits the synthesis of FN. (A) In the presence of fetal bovine serum, MEF shFN cells grew on plastic dishes with a phenotype similar to MEF wild-type cells. (B) If kept in serum-free medium for 2 days, the MEF shFN cells barely produced any FN when compared to wild-type cells, which produced large amounts. FN accumulated in the conditioned media was concentrated by gelatin Sepharose beads and identified by immunoblotting with a rabbit anti-FN antibody. (C) MEF cells adhered to FN and to AMBN within 2 h. However, MEF shFN cells adhered only to FN, not to AMBN, since they were not able to produce any FN by their own.

AMBN (residues 104–246) was positive. We therefore concluded that the active domain of AMBN must be located around residues 183–197. Consequently, the putative interaction site was deleted from the active central fragment. In fact, the resulting fragment lacking residues 184–196 had lost all its activity (Fig. 7).

To exclude the possibility that posttranslational modifications would affect the FN-mediated adhesion of cells to AMBN, we also expressed the full-length sequence as well as two selected fragments in a eukaryotic expression system involving HEK293

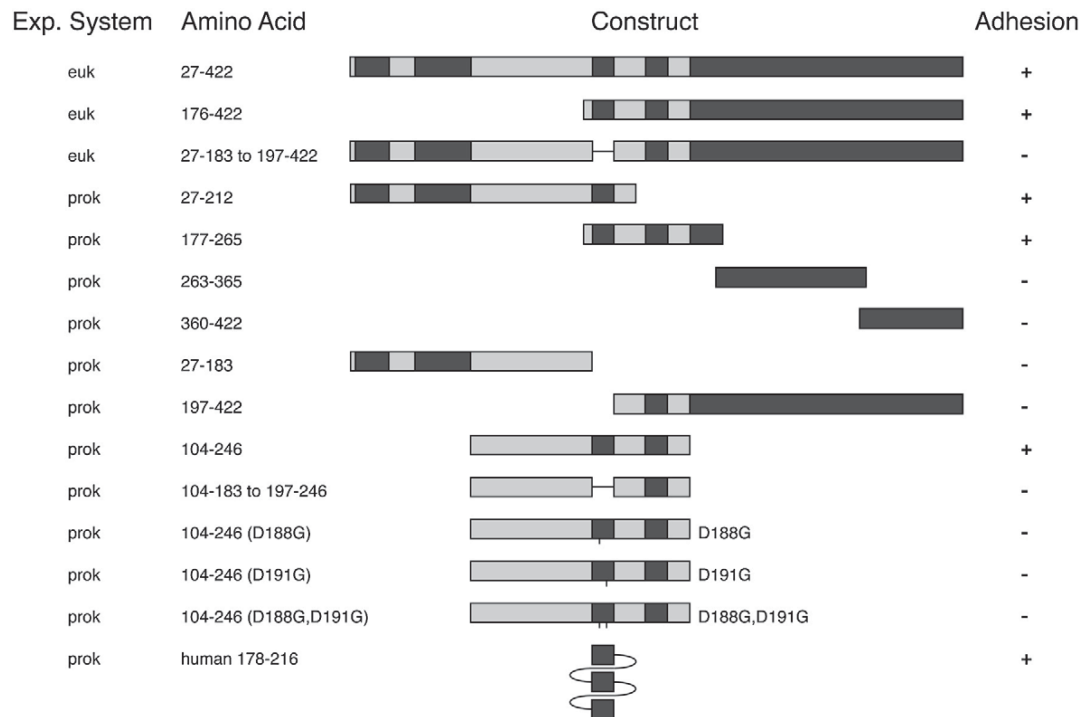


**Fig. 7 – Localization of the FN binding site in AMBN.** Various fragments of AMBN were expressed in *E. coli* (prok) or HEK293 (euk) cells and tested for their activity (+ or –) in the quantitative cell adhesion assay with MG63 cells. The location of the individual fragments relative to the full-length sequence of rat AMBN is schematically drawn by horizontal bars. Alternating shades of grey show the exon structure. The exact amino acid residues that are covered by the individual fragments are given on the left. Residues 1–26 have not been included in the constructs since they correspond to the signal peptide. A single line between two bars marks the position of a deletion. In some fragments, critical amino acids were exchanged by *in vitro* mutagenesis (D188G, D191G). A fragment corresponding to exons 7–9 of human AMBN was also included in the analysis. Note that the human AMBN gene displays a triplication of exon 7 when compared to the rat gene.

cells. Virtually identical results were obtained with these proteins. The two polypeptides containing the active sequence (residues 184–196) promoted cell adhesion, but a polypeptide with a deletion of the active sequence had lost its adhesion promoting activity. These results indicate that the active domain of AMBN must reside within residues 184–196 and that no posttranslational modifications are required for activity.

It is interesting to note that the active sequence corresponds exactly to exon 7 of the rat AMBN gene. To emphasize this correlation, the relative location of the 10 exons along the AMBN protein sequence is highlighted in Fig. 7 by alternating shades of grey. Exon 7 is transcribed and translated into an amino acid sequence of only 13 residues (184-VPIMDFADPQFPT-196). A comparison of the AMBN sequences from human, rat, mouse, pig, guinea pig and bovine showed that the 4 central residues DFAD are conserved in all species (Supplementary Fig. 1) [26]. Since the results presented in Fig. 4A (see above) had implicated metal ions in the promotion of cell adhesion and since the two aspartic acid residues 188 and 191 could theoretically complex metal ions, we exchanged these residues by *in vitro* mutagenesis [27]. In fact, the central AMBN fragment (residues 104–246) lost all of its activity when either one of the two aspartates or both in concert were mutated to glycine (Fig. 7). Thus, aspartic acids 188 and 191 are essential for interaction of AMBN with FN.

The comparison of the AMBN sequences from different vertebrates (Supplementary Fig. 1) also revealed another striking result. The sequence of exon 7 in the rat gene has obviously become triplicated in the human gene during evolution. Thus, exons 7–9 of the human AMBN gene display a nearly perfect triplication of the 13 residue sequence mentioned above. In the final experiment, we therefore expressed the triplicated human sequence in the bacterial expression system and examined the resulting peptide in our adhesion assay. In fact, the 39 residue peptide showed the same activity as the full-length AMBN protein. Taken together, these results clearly demonstrate that the sequences translated from exon 7 of the rat AMBN gene and from exons 7–9 of the human gene interact with FN and thus indirectly mediate cell adhesion.

## Discussion

Adhesion of various cell types to the ECM is often accomplished by surface receptors of the integrin family [15]. In many instances, the versatile matrix protein FN is involved in this process [20,21,24]. Here we demonstrated with a set of biochemical and cell biological experiments that this principle also holds true for the enamel protein AMBN that is found in the ECM of mammalian teeth.

When coated on plastic dishes or titanium disks, recombinant AMBN promotes stable adhesion of osteoblastic and fibroblastic cells. Other tooth proteins including ENAM, AMTN, DSP and DPP or negative control proteins like GST and BSA do not show this feature. The adhesion promoting activity of AMBN could be narrowed down to a peptide of 13 amino acids (VPIMDFADPQFPT) derived from exon 7 of the rat AMBN gene. This sequence corresponds to exons 7–9 of the human gene as the human gene has experienced a triplication of the active exon during evolution. Three observations may document the importance of the short sequence in cell adhesion: (1) When the 13 amino acids are deleted from rat AMBN, the resulting protein loses all adhesion promoting activity; (2) a peptide corresponding to exons 7–9 of human AMBN has the same activity as the full-length protein; (3) when a single aspartate from the sequence is mutated, the activity of the entire polypeptide is abolished.

Additional experiments demonstrate that this sequence does not directly bind to a novel cell surface receptor but that it rather interacts with FN, which in turn binds to the cell surface receptor integrin. The following observations support this conclusion: (1) *de novo* protein synthesis is necessary for cell adhesion on AMBN as demonstrated with the protein synthesis inhibitor cycloheximide; (2) stable cell adhesion on AMBN requires up to 2 h, a time period that might be used for the synthesis of another adhesive ECM protein; (3) when AMBN is treated with a solution of FN, the cells require only 30 min for stable adhesion. This effect is specific for FN and cannot be observed with a solution of vitronectin or heparin; (4) when the synthesis of FN is specifically repressed by RNA mediated interference, the cells do not adhere to AMBN; (5) when an antibody against FN is added during incubation of the cells with AMBN, the adhesion is reduced by at least 30% (M. Beyeler, unpublished results).

Taken together these observations allow us to draw a detailed model of how AMBN mediates cell adhesion (Fig. 8). FN which is synthesized by the cells during the 2-h incubation period binds to AMBN, more specifically to the active sequence of 13 residues. For this interaction the correct three-dimensional structure of the substrate is required since denaturation of AMBN or depletion of divalent ions abolishes the interaction. Bound FN interacts then with the corresponding integrin receptor on the cell membrane and mediates adhesion.

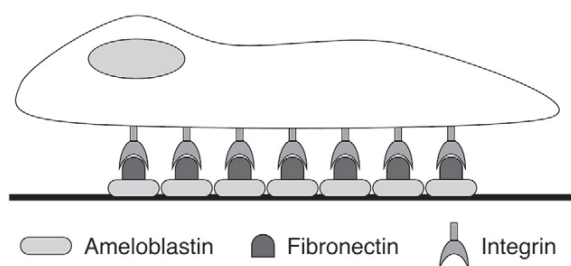


**Fig. 8 – Illustration of the adhesion mechanism on AMBN. The plastic surface of a Petri dish has been coated with AMBN. The bridging molecule FN binds to AMBN (more precisely to the sequence corresponding to exon 7). Finally, the cells adhere to FN via their integrin receptors, which results in attachment and spreading of the cells on the plastic surface.**

FN is synthesized by a great variety of cell types, including fibroblasts, chondrocytes, hepatocytes, endothelial cells and many epithelial cells [20]. It represents a natural component of basement membranes and of the ECM of tendons, muscles, bone, cartilage and skin. During the pre-secretory stage of amelogenesis, FN is present in the basement membrane on which the ameloblasts reside. During the secretory stage when the ameloblasts do no longer touch the basement membrane, they are surrounded by a pericellular matrix consisting of FN. It is likely that these ameloblasts still produce FN since enamel has been shown to react with anti-FN antibodies [28]. Moreover, FN supports and accelerates the growth and differentiation of ameloblasts *in vitro* [29]. When grown for 9 days in culture, the cells produce crystal-like structures that are reminiscent of the enamel matrix.

When we tried to demonstrate a direct interaction of AMBN and FN by different approaches, we encountered irresolvable difficulties. We used ELISA and coated AMBN or FN onto microtiter plates. Alternatively, we used blot overlays and transferred one of the two components to nitrocellulose membranes and probed the blot with the second, labeled component. In a third approach, we immobilized one of the interaction partners on Sepharose beads and tried to pull down the other partner from solution. In all these experiments we did observe binding of AMBN to FN, but we also observed binding to the other tooth proteins that do not promote cell adhesion (DSP, DPP, ENAM) as well as to the negative control protein GST. When we inhibited unspecific interactions by the addition of detergents such as Triton X-100 or NP-40, the specific interaction could no longer be detected. These results indicate that both interaction partners must represent very sticky proteins. On the other hand, they suggest that hydrophobic interactions might be involved in the binding process. An additional reason why we are not able to conclusively demonstrate a direct interaction might be that a third protein partner exists, which stabilizes the interaction of FN and AMBN on the cell surface and which is missing in our *in vitro* assays.

The observation that tooth proteins facilitate the adhesion of osteoblast-like cells is not novel, but has previously been described in the literature. OPN, BSP and DMP1 possess RGD tripeptide sequences similar to FN. With these RGD sequences they bind to the integrin receptor  $\alpha\beta_3$  and thus mediate cell adhesion [7,13,14]. AMELX has also been shown to represent a cell adhesion protein, although it lacks the RGD tripeptide sequence [16]. The activity was dependent on divalent ions and could not be blocked by antibodies against integrins. It is possible that in this case a lectin-like activity ascribed to AMELX by Ravindranath et al. [30] is involved in the facilitation of cell adhesion. In 2005, Fukumoto et al. [17] demonstrated that AMBN is a cell adhesion molecule, which is required for maintaining the differentiation state of ameloblasts. The authors showed that dental epithelial cells adhered in a dose-dependent manner to dishes coated with recombinant AMBN. In their hands, the effect was specific for ameloblasts and could not be repeated with other cell lines such as 3T3, HeLa and MDCK. Very recently, Sonoda et al. [19] from the same group found three heparin-binding domains in AMBN and suggested that AMBN promoted cell adhesion through these sites.

In our study, we could not detect any heparin-binding sites in AMBN, but we observed adhesion of various osteoblastic and fibroblastic cells, including 3T3, to AMBN. We also found that a FN binding site is involved in the adhesion process, rather than three heparin-binding sites. Some of the apparent discrepancies might

be explained by differences in the experimental procedures used between the two studies to measure cell adhesion. While Sonoda et al. [19] incubated their cells with the substrate for only 60 min, we routinely incubated our cells for 2 h. After 1 h, we could barely notice any adhesion. Furthermore, the other authors washed their microtiter plates just briefly with PBS, whereas we selected for a robust interaction by stringent washing on an orbital shaker at 100 rpm for one min. However, Sonoda et al. [19] also described a few observations that they were not able to explain. They assumed that AMBN promoted cell adhesion through the three heparin-binding sites, but deletion of these sites did not abolish all the cell binding activity. Moreover, virtually all cells are known to possess heparan-sulfate containing proteoglycans on their surfaces. It is therefore difficult to understand why the interaction with AMBN should be specific for primary dental epithelial cells and why 3T3, HeLa and MDCK cells should not interact. As a matter of fact, the authors were not able to detect any binding of AMBN to lymphoid cell lines which were manipulated to express individual heparan-sulfate proteoglycans such as syndecan-1,-2 and-4 on their membrane. Since Sonoda et al. [19] could not abolish all the cell binding activity by deletion of the heparin-binding sites, they concluded that there must exist another “heparin-insensitive” cell binding region. Based on their deletion studies, they speculated that this additional cell binding site must be located N-terminal to the heparin-binding domains. This is exactly the region where we found our cell-binding region. It is therefore conceivable that the two independent observations, the heparin-binding site described by Sonoda et al. [19] and the FN binding site described in our study, are not mutually exclusive but are working in concert. This would eventually explain how a low affinity binding would be converted into a robust interaction as observed in our cell binding assays.

The identification of a FN binding site in AMBN offers interesting applications. Many researchers have tried to improve and/or accelerate the integration of dental implants in the jaw by biomimetic coating of the implant surfaces with adhesive proteins, cytokines or functional peptides [31,32]. Utilization of the active peptide described in our study might offer a possibility with several advantages. Since the peptide is derived from the natural matrix protein AMBN, it should not evoke any immune response. Coating of dental implants with this peptide would recruit endogenous FN that is abundant in the patient's plasma to the site of wound healing. Once that stable osseointegration has occurred, FN and the peptide would be removed under physiological conditions by normal turnover. It remains to be determined whether coatings with peptides derived from AMBN as described above will show improvements over existing methods.

### Appendix A. Supplementary data

Supplementary data associated with this article can be found, in the online version, at doi:10.1016/j.yexcr.2009.12.019.

### REFERENCES

- [1] I. Thesleff, P. Sharpe, Signalling networks regulating dental development, *Mech. Dev.* 67 (1997) 111–123.
- [2] P.G. Robey, Vertebrate mineralized matrix proteins: structure and function, *Connect. Tissue Res.* 35 (1996) 131–136.
- [3] K. Iwasaki, E. Bajenova, E. Somogyi-Ganss, M. Miller, V. Nguyen, H. Nourkeyhani, Y. Gao, M. Wendel, B. Ganss, Amelotin—a novel secreted, ameloblast-specific protein, *J. Dent. Res.* 84 (2005) 1127–1132.
- [4] P. Moffatt, C.E. Smith, R. St-Arnaud, D. Simmons, J.T. Wright, A. Nanci, Cloning of rat amelotin and localization of the protein to the basal lamina of maturation stage ameloblasts and junctional epithelium, *Biochem. J.* 399 (2006) 37–46.
- [5] B. Trueb, S. Taeschler, C. Schild, N.P. Lang, Expression of phosphoproteins and amelotin in teeth, *Int. J. Mol. Med.* 19 (2007) 49–54.
- [6] L.W. Fisher, D.A. Torchia, B. Fohr, M.F. Young, N.S. Fedarko, Flexible structures of SIBLING proteins, bone sialoprotein, and osteopontin, *Biochem. Biophys. Res. Commun.* 280 (2001) 460–465.
- [7] L.W. Fisher, N.S. Fedarko, Six genes expressed in bones and teeth encode the current members of the SIBLING family of proteins, *Connect. Tissue Res.* 44 (Suppl. 1) (2003) 33–40.
- [8] K. Kawasaki, K.M. Weiss, Mineralized tissue and vertebrate evolution: the secretory calcium-binding phosphoprotein gene cluster, *Proc. Natl. Acad. Sci. U. S. A.* 100 (2003) 4060–4065.
- [9] N.L. Huq, K.J. Cross, M. Ung, E.C. Reynolds, A review of protein structure and gene organisation for proteins associated with mineralised tissue and calcium phosphate stabilisation encoded on human chromosome 4, *Arch. Oral Biol.* 50 (2005) 599–609.
- [10] J. Caton, A.S. Tucker, Current knowledge of tooth development: patterning and mineralization of the murine dentition, *J. Anat.* 214 (2009) 502–515.
- [11] J.C. Hu, J.P. Simmer, Developmental biology and genetics of dental malformations, *Orthod. Craniofac. Res.* 10 (2007) 45–52.
- [12] M. MacDougall, Dental structural diseases mapping to human chromosome 4q21, *Connect. Tissue Res.* 44 (Suppl. 1) (2003) 285–291.
- [13] Z. von Marschall, L.W. Fisher, Dentin matrix protein-1 isoforms promote differential cell attachment and migration, *J. Biol. Chem.* 283 (2008) 32730–32740.
- [14] A. Bellahcène, V. Castronovo, K.U. Ogbureke, L.W. Fisher, N.S. Fedarko, Small integrin-binding ligand N-linked glycoproteins (SIBLINGs): multifunctional proteins in cancer, *Nat. Rev. Cancer* 8 (2008) 212–226.
- [15] R.O. Hynes, Cell-matrix adhesion in vascular development, *J. Thromb. Haemost.* 5 (Suppl. 1) (2007) 32–40.
- [16] A.M. Hoang, R.J. Klebe, B. Steffensen, O.H. Ryu, J.P. Simmer, D.L. Cochran, Amelogenin is a cell adhesion protein, *J. Dent. Res.* 81 (2002) 497–500.
- [17] S. Fukumoto, T. Kiba, B. Hall, N. Iehara, T. Nakamura, G. Longenecker, P.H. Krebsbach, A. Nanci, A.B. Kulkarni, Y. Yamada, Ameloblastin is a cell adhesion molecule required for maintaining the differentiation state of ameloblasts, *J. Cell Biol.* 167 (2004) 973–983.
- [18] S. Gestrelus, S.P. Lyngstadaas, L. Hammarstrom, Emdogain- periodontal regeneration based on biomimicry, *Clin. Oral Investig.* 4 (2000) 120–125.
- [19] A. Sonoda, T. Iwamoto, T. Nakamura, E. Fukumoto, K. Yoshizaki, A. Yamada, M. Arakaki, H. Harada, K. Nonaka, S. Nakamura, Y. Yamada, S. Fukumoto, Critical role of heparin binding domains of ameloblastin for dental epithelium cell adhesion and ameloblastoma proliferation, *J. Biol. Chem.* 284 (2009) 27176–27184.
- [20] R.O. Hynes, K.M. Yamada, Fibronectins: multifunctional modular glycoproteins, *J. Cell Biol.* 95 (1982) 369–377.
- [21] R. Pankov, K.M. Yamada, Fibronectin at a glance, *J. Cell Sci.* 115 (2002) 3861–3863.
- [22] R. Lutz, M. Chiquet, Involvement of the pericellular fibronectin matrix of fibroblasts in cyclic strain transduction, *Mol. Biol. Cell* 19 (Suppl.) (2008) Abstract M-L44.
- [23] E. Engvall, E. Ruoslahti, Binding of soluble form of fibroblast surface protein, fibronectin, to collagen, *Int. J. Cancer* 20 (1977) 1–5.
- [24] F. Grinnell, M.K. Feld, Initial adhesion of human fibroblasts in serum-free medium: possible role of secreted fibronectin, *Cell* 17 (1979) 117–129.

- [25] I. Schvartz, D. Seger, S. Shaltiel, Vitronectin, *Int. J. Biochem. Cell Biol.* 31 (1999) 539–544.
- [26] J. Vymetal, I. Slaby, A. Spahr, J. Vondrasek, S.P. Lyngstadaas, Bioinformatic analysis and molecular modelling of human ameloblastin suggest a two-domain intrinsically unstructured calcium-binding protein, *Eur. J. Oral Sci.* 116 (2008) 124–134.
- [27] A. Aiyar, Y. Xiang, J. Leis, Site-directed mutagenesis using overlap extension PCR, *Methods Mol. Biol.* 57 (1996) 177–191.
- [28] C. Garbarsch, M.E. Matthiessen, B.E. Olsen, D. Moe, S. Kirkeby, Immunohistochemistry of the intercellular matrix components and the epithelio-mesenchymal junction of the human tooth germ, *Histochem. J.* 26 (1994) 110–118.
- [29] M.J. Tabata, T. Matsumura, T. Fujii, M. Abe, K.J. Kurisu, Fibronectin accelerates the growth and differentiation of ameloblast lineage cells *in vitro*, *Histochem. Cytochem.* 51 (2003) 1673–1679.
- [30] R.M. Ravindranath, W.Y. Tam, P. Nguyen, A.G. Fincham, The enamel protein amelogenin binds to the *N*-acetyl-*D*-glucosamine-mimicking peptide motif of cytokeratins, *J. Biol. Chem.* 275 (2000) 39654–39661.
- [31] Y. Liu, J.P. Li, E.B. Hunziker, K. de Groot, Incorporation of growth factors into medical devices via biomimetic coatings, *Philos. Transact. A Math. Phys. Eng. Sci.* 364 (2006) 233–248.
- [32] G. Avila, K. Misch, P. Galindo-Moreno, H.L. Wang, Implant surface treatment using biomimetic agents, *Implant. Dent.* 18 (2009) 17–26.

### **IV.3 Pericellular fibronectin is required for RhoA-dependent responses to cyclic strain in fibroblasts**

Roman Lutz, Takao Sakai, and Matthias Chiquet

Journal of Cell Science (J Cell Sci), 2010

My contribution: All experiments presented (except generation of fibronectin knockout fibroblasts: T. Sakai)

# Pericellular fibronectin is required for RhoA-dependent responses to cyclic strain in fibroblasts

Roman Lutz<sup>1</sup>, Takao Sakai<sup>2,\*</sup> and Matthias Chiquet<sup>3,†</sup>

<sup>1</sup>Friedrich Miescher Institute for Biomedical Research, CH-4056 Basel, Switzerland

<sup>2</sup>Max-Planck Institute of Biochemistry, Department of Molecular Medicine, D-82152 Martinsried, Germany

<sup>3</sup>Department of Orthodontics and Dentofacial Orthopedics, University of Bern, Freiburgrasse 7, CH-3010 Bern, Switzerland

\*Present address: Cleveland Clinic, Department of Biomedical Engineering, Cleveland, OH 44195, USA

†Author for correspondence ([matthias.chiquet@zmk.unibe.ch](mailto:matthias.chiquet@zmk.unibe.ch))

Accepted 11 February 2010

Journal of Cell Science 123, 1511–1521

© 2010. Published by The Company of Biologists Ltd

doi:10.1242/jcs.060905

## Summary

To test the hypothesis that the pericellular fibronectin matrix is involved in mechanotransduction, we compared the response of normal and fibronectin-deficient mouse fibroblasts to cyclic substrate strain. Normal fibroblasts seeded on vitronectin in fibronectin-depleted medium deposited their own fibronectin matrix. In cultures exposed to cyclic strain, RhoA was activated, actin-stress fibers became more prominent, MAL/MKL1 shuttled to the nucleus, and mRNA encoding tenascin-C was induced. By contrast, these RhoA-dependent responses to cyclic strain were suppressed in fibronectin knockdown or knockout fibroblasts grown under identical conditions. On vitronectin substrate, fibronectin-deficient cells lacked fibrillar adhesions containing  $\alpha 5$  integrin. However, when fibronectin-deficient fibroblasts were plated on exogenous fibronectin, their defects in adhesions and mechanotransduction were restored. Studies with fragments indicated that both the RGD-synergy site and the adjacent heparin-binding region of fibronectin were required for full activity in mechanotransduction, but not its ability to self-assemble. In contrast to RhoA-mediated responses, activation of Erk1/2 and PKB/Akt by cyclic strain was not affected in fibronectin-deficient cells. Our results indicate that pericellular fibronectin secreted by normal fibroblasts is a necessary component of the strain-sensing machinery. Supporting this hypothesis, induction of cellular tenascin-C by cyclic strain was suppressed by addition of exogenous tenascin-C, which interferes with fibronectin-mediated cell spreading.

**Key words:** Fibronectin, Mechanotransduction, Cyclic strain, RhoA, Actin, MAL/MKL1/MRTF-A, Tenascin-C

## Introduction

Cellular responses to mechanical cues are essential for tissue homeostasis, and mechanical stress is linked to the development and progression of several diseases, such as fibrosis, arteriosclerosis and cancer (Butcher et al., 2009; Hahn and Schwartz, 2009; Wipff et al., 2007). Cells constantly integrate mechanical signals into information about the physical properties of their environment (Chen, 2008; Geiger et al., 2009). To study mechanotransduction and signaling pathways triggered by mechanical stress, cells can be cultured on extracellular matrix (ECM)-coated elastic membranes and cyclically strained (Chiquet et al., 2004; Hsieh et al., 2000). This is a physiologically relevant model to analyze mechanotransduction because cellular responses can be measured after mechanical strain of amplitude and frequency within the ranges found in many tissues (e.g. arterial vessels, lung, heart or tendons) (Lehoux et al., 2006; Magnusson et al., 2008). Among other responses, tissues adapt to mechanical load by remodeling their extracellular matrix (ECM). For example, the ECM protein tenascin-C is strongly expressed in tissues bearing high tensile stress, and is induced by dynamic tensile strain both in vivo (Fluck et al., 2000) and in vitro (Chiquet et al., 2004).

Several types of cell-ECM adhesion structures are crucial for mechanotransduction via integrin-dependent signaling (Geiger et al., 2009). Focal complexes are formed during initial contact of fibroblasts with an ECM substrate. Some mature into focal adhesions that contain mainly  $\alpha v \beta 3$  integrin, which binds to vitronectin and other ECM components with RGD peptide motifs (Horton, 1997; Zamir et al., 2000). During cell spreading,

fibroblasts rapidly develop fibrillar adhesions characterized by the presence of mainly  $\alpha 5 \beta 1$  integrin, which are involved in the assembly of a pericellular fibronectin matrix (Zamir et al., 2000). Activation of major intracellular signaling pathways by mechanical stress, such as NF $\kappa$ B, MAPK and RhoA/ROCK, is both adhesion- and integrin-dependent (Inoh et al., 2002; Orr et al., 2006; Stupack and Cheresch, 2002). The induction of tenascin-C by cyclic strain requires  $\beta 1$  integrins (Chiquet et al., 2007), but does not depend on MAPK signaling (Chiquet et al., 2004). Instead, induction is abolished after actin disassembly or inhibition of RhoA-dependent kinase (ROCK) (Sarasa-Renedo et al., 2006). Upregulation of tenascin-C by cyclic strain also correlates with an increase in actin-stress fibers and the translocation of MAL/MKL1/MRTF-A to the nucleus (Maier et al., 2008). MAL is a transcriptional co-activator of serum response factor that links RhoA activation and actin dynamics to gene expression (Miralles et al., 2003). Thus, induction of tenascin-C by mechanical stress appears to be controlled primarily by the RhoA-ROCK pathway.

In a previous study, we showed that in fibroblasts deficient for integrin-linked kinase (ILK), activation of RhoA, nuclear translocation of MAL and tenascin-C induction by cyclic strain were all abolished (Maier et al., 2008). The defect was specific for RhoA-dependent responses, because the MAPK Erk1/2 was activated normally and the *Fos* gene was induced by mechanical stress in ILK-knockout cells. ILK is an adaptor protein in cell-matrix adhesion sites that forms a complex with PINCH and parvin, joining the cytosolic part of  $\beta 1$  and  $\beta 3$  integrins to the actin cytoskeleton (Legate et al., 2006). ILK<sup>-/-</sup> fibroblasts do not

assemble fibronectin into fibrils, and classical fibrillar adhesions are absent, indicating an important function for ILK in the formation of these structures (Legate et al., 2006). We speculated that the missing RhoA-ROCK activation upon mechanical stress in ILK<sup>-/-</sup> cells was due to lack of a fibronectin matrix and of fibrillar adhesions, rather than to a direct involvement of ILK in the activation of this pathway. In this case, the pericellular fibronectin matrix (in conjunction with fibrillar adhesions) would itself be part of the machinery that transduces cyclic (i.e. dynamic) mechanical stress. To test this hypothesis, we prepared stable fibronectin-knockdown fibroblast lines and monitored their RhoA-ROCK-dependent responses to cyclic strain in the presence or absence of exogenous fibronectin. Indeed, when plated on vitronectin, such cells had defects in mechanotransduction that were very similar to those in ILK-deficient fibroblasts. In contrast to ILK<sup>-/-</sup> cells, however, fibronectin-knockdown cells could be rescued by adding exogenous fibronectin to the culture. Based on our results, we propose a model for mechanotransduction in which cyclic strain activates the RhoA-ROCK pathway mainly via attachment of cells to their own pericellular fibronectin matrix.

## Results

### Fibronectin-deficient fibroblasts can assemble exogenous fibronectin

To test whether the fibronectin matrix is important for mechanotransduction, we isolated stable fibronectin-knockdown cell lines and tested them for their ability to activate canonical signaling pathways in response to mechanical stress. Fibronectin knockdown was carried out in immortalized wild-type mouse embryo fibroblasts (MEFs) by stable transfection with shRNA. Two clones (1.2 and 8.3) were analyzed further. Clone 1.2 was transfected with one type of shRNA to knockdown fibronectin; however, this clone expressed and secreted normal amounts of fibronectin and was therefore used as a control (Fig. 1A,B). For clone 8.3, another type of shRNA targeting mRNA encoding

fibronectin was used, that effectively reduced fibronectin expression to 10% of the original level in wild type MEFs (Fig. 1B). We also tested fibronectin-knockout MEFs (FN<sup>-/-</sup>) and the matched fibronectin-expressing control cells (FN<sup>f/f</sup>). Unlike in control cells, staining for fibronectin was not detected in either fibronectin-knockdown clone 8.3 or the fibronectin-knockout MEFs grown for 2 days on tissue culture plastic (Fig. 1A) or vitronectin (supplementary material Fig. S1) in fibronectin-depleted medium. However, both cell lines showed distinct fibronectin fibrils upon addition of 100 µg/ml soluble fibronectin to the plating medium (Fig. 1A), indicating that the machinery for fibronectin fibrillogenesis was still intact. This assumption was confirmed by the fact that expression levels of integrin  $\alpha_v$ ,  $\alpha_5$  and  $\beta_1$  were similar in all cell lines tested (Fig. 1C).

### Cyclic-strain-induced activation of RhoA requires pericellular fibronectin

Amongst many other stimuli, mechanical stress is known to increase intracellular levels of active RhoA (Sarasa-Renedo et al., 2006; Smith et al., 2003). To test whether a pericellular fibronectin matrix is required for activation of RhoA by cyclic strain, we plated fibronectin-expressing (FN<sup>f/f</sup>) or fibronectin-deficient (FN<sup>-/-</sup>) MEFs on silicone membranes coated with either vitronectin or fibronectin. Cells were cultured for 24 hours and then subjected to biaxial cyclic strain (10%, 0.3 Hz) for 5 minutes. Levels of active (GTP-bound) RhoA were detected by Rhotekin-RBD binding assays as described in the Materials and Methods. On vitronectin, a clear increase in the amount of active RhoA could be detected in the fibronectin-expressing control cells after 5 minutes of cyclic strain (Fig. 2A,B). However, this activation was absent in fibronectin-knockout cells grown on vitronectin. Interestingly, after plating on fibronectin, a robust activation of RhoA could be detected for both cell lines, indicating that fibronectin as extracellular substrate is necessary for this effect.

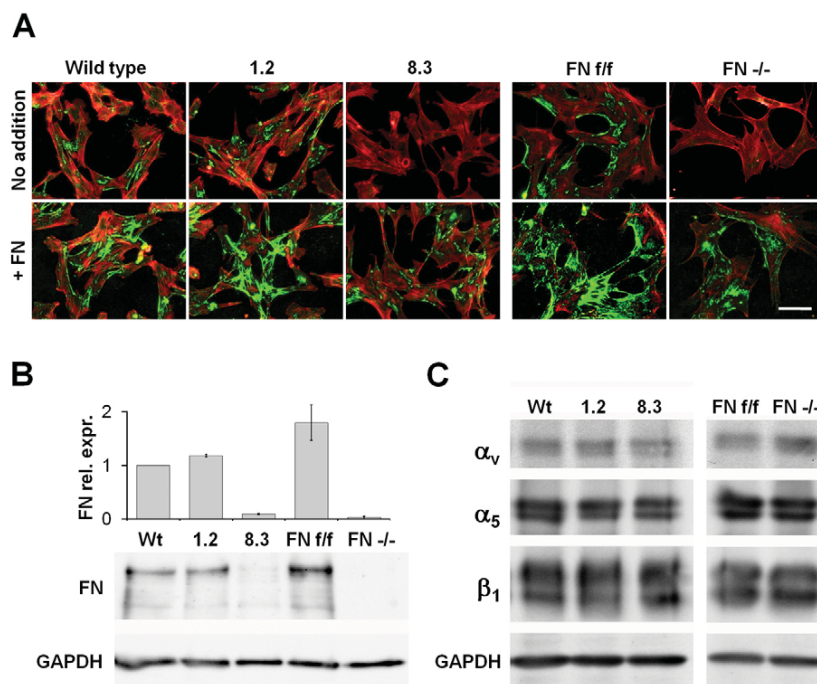


**Fig. 1. Fibronectin expression levels and integrin profiles of fibronectin-knockdown, fibronectin knockout and control MEFs.** (A) Cells were plated on cell culture plastic and grown for 48 hours in DMEM containing 3% fibronectin-depleted FCS, either without (top) or with fibronectin added at 100 µg/ml (bottom). Cells were subsequently fixed and double-stained with phalloidin (red) and anti-fibronectin (green). Scale bar: 50 µm. Note that clone 8.3 and FN<sup>-/-</sup> cells assembled pericellular fibronectin fibrils only in the presence of exogenous fibronectin. (B) Cells were grown for 48 hours on tissue culture plastic and subsequently detached from the matrix by detergent. Matrices were scraped into Laemmli buffer and analyzed by immunoblotting against fibronectin. Cell lysates were blotted for GAPDH as a loading control. Graph shows the average relative expression (mean ± s.e.m.) of fibronectin to GAPDH quantified from independent experiments. (C) Cell extracts were immunoblotted for  $\alpha_v$ ,  $\alpha_5$  and  $\beta_1$  integrins to check their expression levels; GAPDH was detected as a loading control.



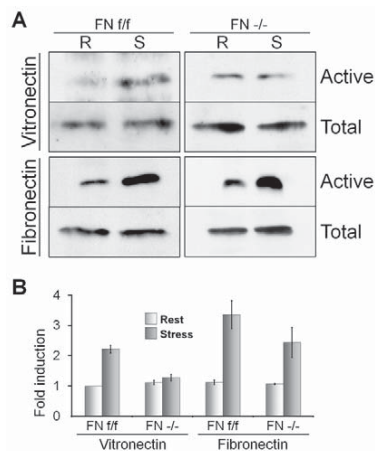


**Fig. 2. Cyclic strain activates RhoA only in the presence of pericellular fibronectin.** (A) Fibronectin-knockout (FN<sup>-/-</sup>) and control MEFs (FN<sup>fl/fl</sup>) were cultured on either vitronectin (top) or fibronectin (bottom) for 48 hours. Cells were then cyclically strained (10%, 0.3 Hz) for 5 minutes and active RhoA levels were determined by Rho pull-down experiments. (B) Graph showing average levels of active RhoA from independent experiments. Values (mean ± s.e.m.) are normalized to levels in FN<sup>fl/fl</sup> cells at rest on vitronectin.

### Cyclic-strain-induced actin reorganization requires a pericellular fibronectin matrix

In embryonic fibroblasts cultured on fibronectin-coated elastomer membranes, cyclic strain induces a characteristic change in cell shape and a RhoA-ROCK-dependent increase and relocation of actin-stress fibers (Maier et al., 2008; Sarasa-Renedo et al., 2006). To analyze whether the fibronectin matrix is required for this actin reorganization, we plated fibronectin-expressing or fibronectin-knockdown clone 8.3 on vitronectin-coated silicone membranes. After 2 days in culture, cells were subjected to 6 hours of cyclic strain and subsequently stained with fluorescently labeled phalloidin. After mechanical stress, fibronectin-deficient cells remained triangular or multipolar, without prominent stress fibers (Fig. 3A,B). Conversely, fibronectin-expressing and secreting control cells (wild type and clone 1.2) both assumed a more bipolar shape and formed distinct bundles of stress fibers and actin foci within 6 hours of cyclic strain on a vitronectin substrate. Strong stress-fiber bundles formed predominantly along the cell edges, whereas thinner actin fibers in the central area of the cell disappeared (Fig. 3A,B). Similarly to fibronectin-knockdown clone 8.3, fibronectin-knockout fibroblasts did not respond to cyclic strain by actin rearrangement when cyclically strained for 6 hours on vitronectin (Fig. 3C,D). By contrast, their fibronectin-expressing parental cells (FN<sup>fl/fl</sup>) formed distinct stress fibers under these conditions. Interestingly, the missing response to strain of either of the fibronectin-deficient cell lines (clone 8.3 or FN<sup>-/-</sup>) was restored when these cells were plated on exogenous fibronectin and cyclically strained. Similarly to fibronectin-expressing control cells, central thinner actin structures in clone 8.3 and FN<sup>-/-</sup> fibroblasts were replaced by peripheral thick actin-stress fibers after 6 hours of cyclic strain on this substrate. These peripheral actin-stress fiber bundles are easily distinguishable from other actin structures, and were therefore used to quantify our observations (Fig. 3B,D).

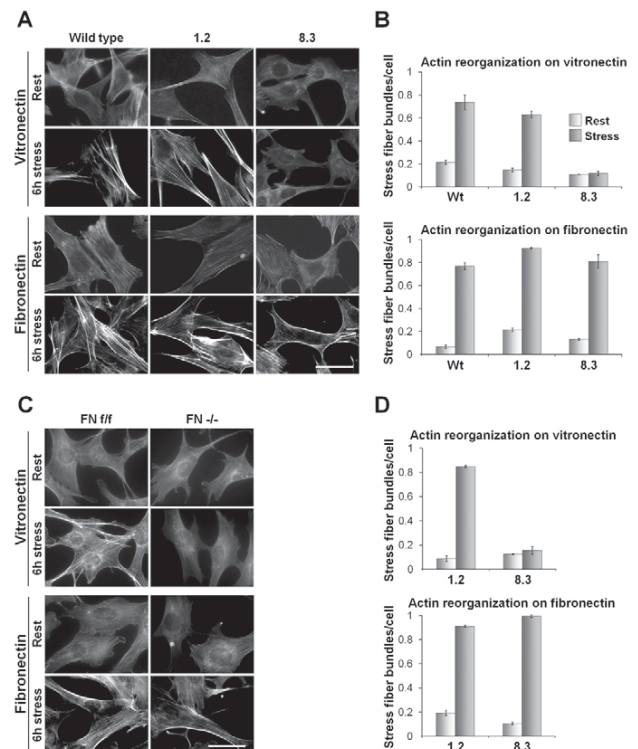


**Fig. 3. Cyclic-strain-induced actin reorganization requires a pericellular fibronectin matrix.** (A) Wild-type MEFs, the fibronectin-expressing clone 1.2 and the fibronectin-knockdown clone 8.3 were seeded on vitronectin-coated (top) or fibronectin-coated (bottom) silicone membranes. Two days after plating in DMEM plus 0.3% fibronectin-depleted FCS, cells were cyclically strained (10%, 0.3 Hz) for 6 hours and subsequently stained for the actin cytoskeleton. (B) Statistical analysis of different independent experiments as depicted in A. For every experiment, 100 cells per condition were analyzed and number of peripheral actin-stress-fiber bundles per cell was determined (mean ± s.e.m.). Peripheral actin bundles were defined as locations where single visible stress fibers merged in the cell periphery into larger and thicker, bright foci. (C) Fibronectin-knockout MEFs (FN<sup>-/-</sup>) and the matched fibronectin-expressing control cells (FN<sup>fl/fl</sup>). (D) The statistical analysis of different independent experiments shown in C. Note the missing actin reorganization in the fibronectin-deficient clones 8.3 and FN<sup>-/-</sup> on the vitronectin, but not on the fibronectin substrate. Scale bars: 50 μm.

### Pericellular fibronectin is required for cyclic-strain-induced MAL translocation to the nucleus

MAL (MKL-1; MRTF-A) is a transcriptional co-activator of serum response factor (SRF) that cycles between the cytoplasm and the nucleus under the control of RhoA-dependent actin dynamics (Asparuhova et al., 2009; Miralles et al., 2003). Mechanical strain stimulates actin reorganization and was shown to promote a shift of MAL from the cytoplasm to the nucleus in serum-starved cells (Maier et al., 2008; Zhao et al., 2007). Nuclear translocation of MAL after cyclic strain depends on activation of RhoA, because it was abolished in the presence of the specific inhibitor C3 transferase (supplementary material Fig. S2). Since actin dynamics in response to cyclic strain were clearly affected in fibronectin-deficient fibroblasts plated on vitronectin, we expected to find a similar effect on MAL shuttling. Cyclic strain for 1 hour stimulated

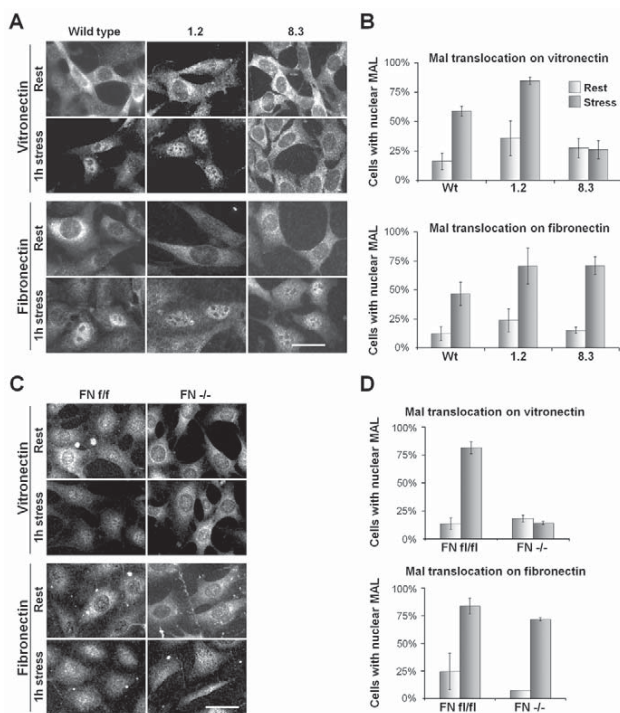


**Fig. 4. Pericellular fibronectin is necessary for the cyclic-strain-induced translocation of MAL to the nucleus.** (A) Wild-type MEFs, the fibronectin-expressing clone 1.2 and the fibronectin-knockdown clone 8.3 were seeded on either vitronectin (top) or fibronectin (bottom). Two days after plating, cells were cyclically strained for 1 hour and subsequently fixed and stained for MAL. Scale bar: 50  $\mu$ m. (B) Statistical analysis of three independent experiments as depicted in A. For every experiment, 100 cells per condition were analyzed and MAL staining was scored as either nuclear or cytoplasmic. The graph shows the mean percentage of cells with nuclear MAL ( $\pm$  s.e.m.). Light columns represent values before and dark columns values after 1 hour of cyclic strain. (C) Fibronectin-knockout MEFs (FN<sup>-/-</sup>) and the matched fibronectin-expressing control cells (FN<sup>fl/fl</sup>). Scale bar: 50  $\mu$ m. (D) Statistical analysis of the results from three independent experiments shown in C. Note the absence of MAL translocation in response to cyclic strain in the fibronectin-deficient clones 8.3 and FN<sup>-/-</sup>, when plated on vitronectin, but not on fibronectin.

translocation of MAL in wild-type MEFs and in fibronectin-expressing clone 1.2; the shift of MAL to the nucleus was observed not only on fibronectin, but also on vitronectin substrate (Fig. 4A,B). Conversely, in fibronectin-knockdown clone 8.3 cells grown on vitronectin, MAL did not translocate to the nucleus after 1 hour of cyclic strain. However, plating these cells on fibronectin and straining them for 1 hour clearly raised the percentage of cells with nuclear MAL from 15% at rest to 71% after strain (Fig. 4A,B).

To confirm these results, we also analyzed the localization of MAL in fibronectin-knockout cells. Fibronectin-knockout fibroblasts plated on vitronectin showed no increase in nuclear MAL upon cyclic strain, in contrast to the matched wild-type cells (Fig. 4C,D). However, for both knockout and wild-type cells, MAL translocation was observed after strain when fibronectin was used as a substrate. Our findings indicate that on vitronectin substrate, the fibronectin matrix deposited by wild-type cells themselves is required for translocation of MAL after cyclic strain, because

fibronectin-deficient cells depended on exogenous fibronectin for this process.

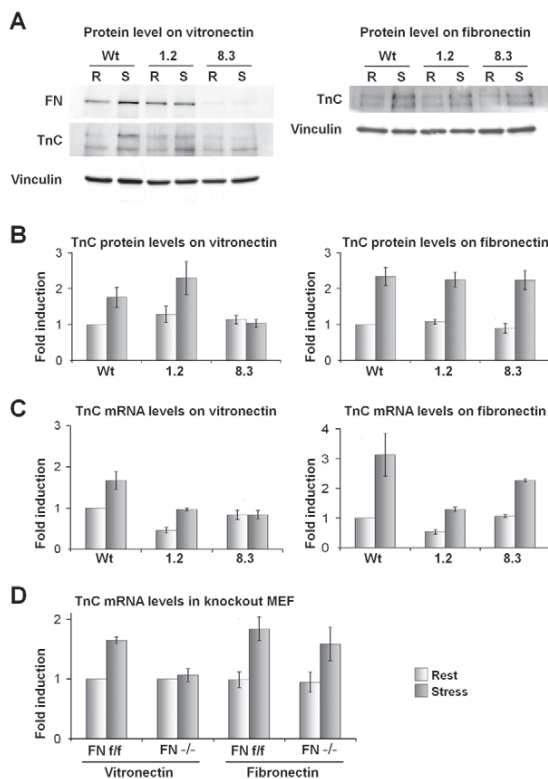
#### mRNA and protein levels of tenascin-C are induced by cyclic strain only in the presence of pericellular fibronectin

Tenascin-C is a glycoprotein of the extracellular matrix whose expression is induced by cyclic strain (Chiquet et al., 2004). We have shown that this response depends on RhoA-ROCK-induced actin assembly and correlates with translocation of MAL to the nucleus (Maier et al., 2008; Sarasa-Renedo et al., 2006). We therefore investigated tenascin-C expression levels in response to cyclic strain in fibronectin-expressing and non-expressing fibroblasts. Cells were cultured with fibronectin-depleted serum on either vitronectin or fibronectin. Fibroblasts were then cyclically strained for 6 hours and cultured for an additional 18 hours, during which time tenascin-C was deposited. Immunoblotting of cell lysates showed higher amounts of tenascin-C protein in both wild-type MEFs and fibronectin-expressing clone 1.2 after straining, than in the resting control (Fig. 5A,B). This effect did not depend on the respective ECM substrates. However, a response to mechanical stress by the fibronectin-knockdown clone 8.3 was again only observed when cells were plated on fibronectin. On vitronectin, tenascin-C accumulation by clone 8.3 fibroblasts did not change after strain, indicating that the absence of the fibronectin matrix prevented this cellular response.

By quantitative PCR, the induction of tenascin-C by cyclic strain was also analyzed at the mRNA level. After only 1 hour of cyclic strain (10%, 0.3 Hz), there was a significant increase in levels of mRNA encoding tenascin-C ( $P < 0.05$ ) in cell lines plated on fibronectin (Fig. 5C,D). However, tenascin-C (*Tnc*) mRNA remained at resting levels when fibronectin-deficient cells (clone 8.3 and FN<sup>-/-</sup>) were plated and strained on vitronectin. By contrast, *Tnc* mRNA was upregulated in fibronectin-expressing control cells (wild type, clone 1.2, FN<sup>fl/fl</sup>) after cyclic strain, also on a vitronectin substrate (Fig. 5C,D). Thus, as in previous experiments, responses were consistent between fibronectin-knockdown and fibronectin-knockout fibroblasts. Induction of *Tnc* mRNA by cyclic strain appears to depend on pericellular fibronectin, either provided exogenously or deposited by the fibroblasts themselves.

#### Activation of ERK and PKB/Akt by cyclic strain does not depend on the presence of pericellular fibronectin

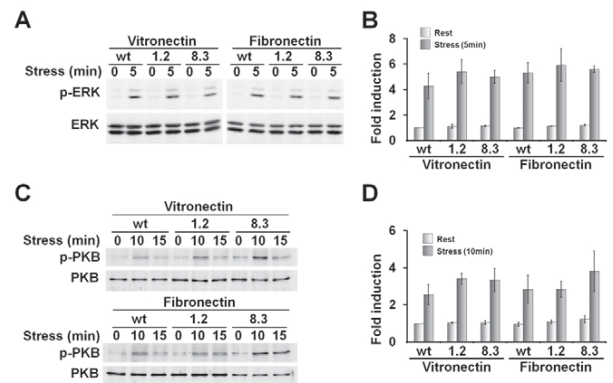
We showed that the presence of pericellular fibronectin was required for reorganization of the actin cytoskeleton, translocation of MAL to the nucleus, and upregulation of tenascin-C protein and mRNA in response to cyclic strain. As reported previously (Chiquet et al., 2004; Sarasa-Renedo et al., 2006; Zhao et al., 2007), these events all depended on RhoA-ROCK, indicating that the fibronectin matrix is essential for the activation of this signaling pathway by mechanical stress. To test whether mechanotransduction was affected in general in the absence of fibronectin, we analyzed other pathways known to be triggered by mechanical stress. Erk1/2 was phosphorylated upon 5 minutes of cyclic strain, independently of the cell type and the underlying ECM substrate, indicating that activation of the MAPK pathway by mechanical stress does not require the presence of fibronectin (Fig. 6A,B). As with wild-type fibroblasts and clone 1.2, an analysis of the time-course of PKB/Akt phosphorylation showed a robust signal of phosphorylated PKB/Akt in fibronectin-knockdown clone 8.3 after strain, independently of whether cells adhered to vitronectin or fibronectin (Fig. 6C,D).



Taken together, these results show that activation of the MAPK and the PKB/Akt pathways by mechanical stress does not depend on the presence of fibronectin.

**The response of fibroblasts to cyclic strain depends on the amount of deposited fibronectin**

Stable shRNA transfection of a rat embryo fibroblast cell line (REFs) resulted in a partial fibronectin-knockdown clone (R2A). These cells built up a fibronectin matrix only slowly over a few days. R2A cultures showed only faint intracellular staining for fibronectin 24 hours after plating (Fig. 7A). However, after 48 hours, intracellular staining was more intense and extracellular fibronectin fibrils appeared. By contrast, normal fibronectin-



expressing REFs showed staining of distinct extracellular fibronectin fibrils by 24 hours after plating. The intensity of fibronectin-matrix staining correlated with the responsiveness of the cells to mechanical stress in terms of tenascin-C induction. Upregulation of *Tnc* mRNA after 1 hour of cyclic strain was generally higher in REFs than in MEFs. Both, wild-type and knockdown REFs on fibronectin, showed a six- to eightfold induction compared with the respective cells at rest. The induction levels were similar when cells were cyclically strained for 1 hour, after 24 hours or 48 hours in culture (Fig. 7B). Interestingly, in clone R2A grown on vitronectin, *Tnc* mRNA was induced only ~2.5-fold by cyclic strain 24 hours after plating, correlating with the poor fibronectin deposition at this time point. However, tenascin-C induction after 1 hour of strain increased almost sixfold when cells were allowed a further 24 hours for fibronectin deposition.

**The cell-binding site and adjacent heparin-binding region of fibronectin are necessary for full induction of *Tnc* mRNA by cyclic strain**

As shown so far, pericellular fibronectin is necessary for cyclic-strain-induced activation of RhoA, reorganization of actin, MAL translocation to the nucleus and induction of tenascin-C. We then asked which domains of fibronectin were required for activation of this pathway. We therefore tested the response of fibronectin-knockout MEFs on different fibronectin fragments. Stable cell- and heparin-binding fragments of fibronectin (160 and 135 kDa) were generated from serum fibronectin by mild digestion with chymotrypsin (Ehrismann et al., 1982) (supplementary material Fig. S3A). These fragments lacked the 60 kDa N-terminal gelatin-binding, self-assembly region and part of the C-terminal domain, including the interchain disulfide bridge; thus, they could not

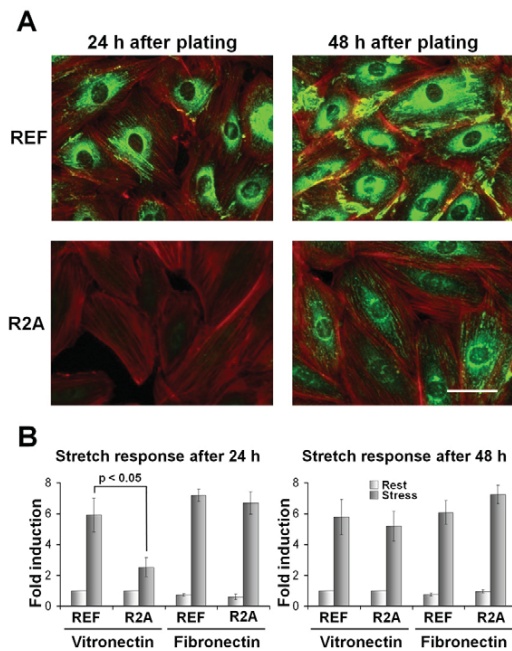


**Fig. 7. Response of rat embryo fibroblasts to cyclic strain depends on the time endogenous fibronectin has been allowed to accumulate in the matrix.** R2A is a partial fibronectin-knockdown clone derived from REFs. (A) Immunofluorescence staining of actin (red) and endogenous fibronectin (green) of detergent-permeabilized REFs and R2A plated on tissue culture plastic. Cells were fixed 24 hours (left) or 48 hours (right) after plating. Scale bar: 50  $\mu$ m. (B) REFs and R2A cells were plated on vitronectin or fibronectin and strained for 1 hour after 24 or 48 hours in culture. Induction of *Tnc* mRNA was measured by qPCR. Light columns represent values before and dark columns values after 1 hour of cyclic strain. Note the correlation between fibronectin matrix accumulation on vitronectin and the level of tenascin-C induction in R2A cells.

dimerize or form fibrils. However, these large fragments contained the RGD and the synergy site (FNIII 9-10) required for integrin  $\alpha$ 5 $\beta$ 1 binding, as well as a major heparin-binding site (FNIII 13-14) known to be recognized by cellular syndecan-4 (Mao and Schwarzbauer, 2005). A second smaller fragment of fibronectin type III repeats 7-11 (which contains the RGD and the synergy but not the heparin-binding site) was expressed in bacteria (Bloom et al., 1999) and purified on glutathione-Sepharose beads (supplementary material Fig. S3B). To analyze their ability to trigger induction of tenascin-C upon cyclic strain, the fragments were coated on silicone membranes. Fibronectin-knockout MEFs were seeded, cultured for 2 days and subsequently strained for 1 hour. Induction of *Tnc* mRNA on the large cell- and heparin-binding fragment of fibronectin (FN CHB) reached a similar level as seen on full-length fibronectin (FN) (Fig. 8A). Interestingly, even though cells attached and spread normally on the fibronectin type III 7-11 (FN 7-11) fragment (Fig. 9), induction was clearly diminished (Fig. 8A). In agreement with these data, addition of soluble heparin (100  $\mu$ g/ml) inhibited induction of *Tnc* mRNA on native fibronectin after 1 hour of cyclic strain (Fig. 8A). This supports the notion that the heparin-binding site is important for full induction. On a substrate of fibrillar collagen I, fibronectin-knockout MEFs attached, but did not fully spread (not shown).

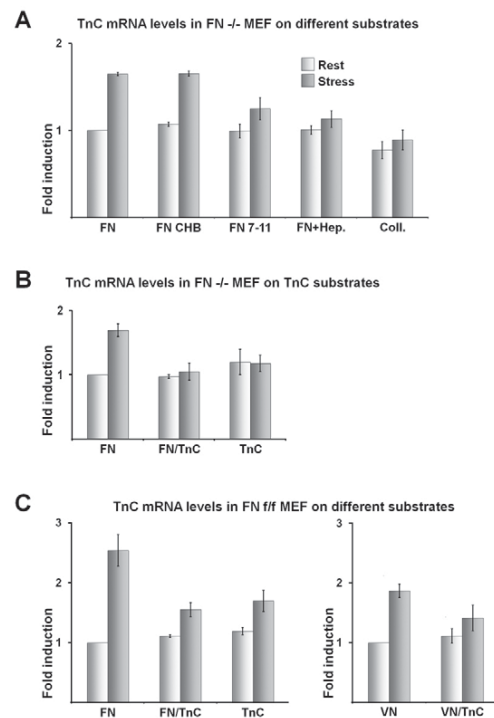


**Fig. 8. The cell-binding site and adjacent heparin-binding region of fibronectin are necessary for full induction of *Tnc* mRNA by cyclic strain.** (A) Fibronectin-knockout MEFs (FN<sup>-/-</sup>) were plated on elastic silicone membranes coated with either fibronectin (FN), fibronectin 160 and 135 kDa chymotrypsin fragments (FN CHB), fibronectin type 3 domain 7-11 (FN 7-11) or collagen I (Coll) and cultured for 48 hours. In FN+Hep cells were plated on fibronectin and soluble heparin was added at 100  $\mu$ g/ml 24 hours after plating. For all conditions, cells were then kept at rest or subjected to 1 hour of cyclic strain. *Tnc* mRNA levels were measured by quantitative PCR relative to *Gapdh* and normalized to the rest-values on fibronectin. Light columns represent values before and dark columns values after 1 hour of cyclic strain. (B) FN<sup>-/-</sup> MEFs were plated on elastic silicone membranes coated with either fibronectin (50  $\mu$ g/ml), fibronectin and tenascin-C (50  $\mu$ g/ml and 50  $\mu$ g/ml) or tenascin-C (50  $\mu$ g/ml). (C) Fibronectin-expressing MEFs (FN<sup>+/+</sup>). Tenascin-C induction was also measured on vitronectin (20  $\mu$ g/ml) or vitronectin and tenascin-C (20  $\mu$ g/ml and 50  $\mu$ g/ml).

Induction of *Tnc* mRNA was not observed (Fig. 8A), indicating the specificity of the response for fibronectin.

Tenascin-C was shown to interfere with fibroblast spreading on fibronectin (Chiquet-Ehrismann et al., 1988) by interacting with the 13th type III repeat which is part of the heparin-binding site (Huang et al., 2001). We therefore asked whether substrate-bound tenascin-C also affected its own induction upon cyclic strain. To address this question, silicone membranes were coated with either fibronectin, a 1:1 mixture of fibronectin and tenascin-C, or tenascin-C alone. Indeed, *Tnc* mRNA was not induced after cyclic strain in fibronectin-knockout cells either on tenascin-C alone or on mixed tenascin-C and fibronectin substrates (Fig. 8B). This indicates that substrate-bound tenascin-C could quench the effect of exogenous fibronectin on mechanotransduction. By analyzing fibronectin-expressing MEFs on the same substrates, we found a clearly decreased response on tenascin-C and mixed substrates compared with fibronectin substrates, but no full inhibition (Fig. 8C). This indicates that at least

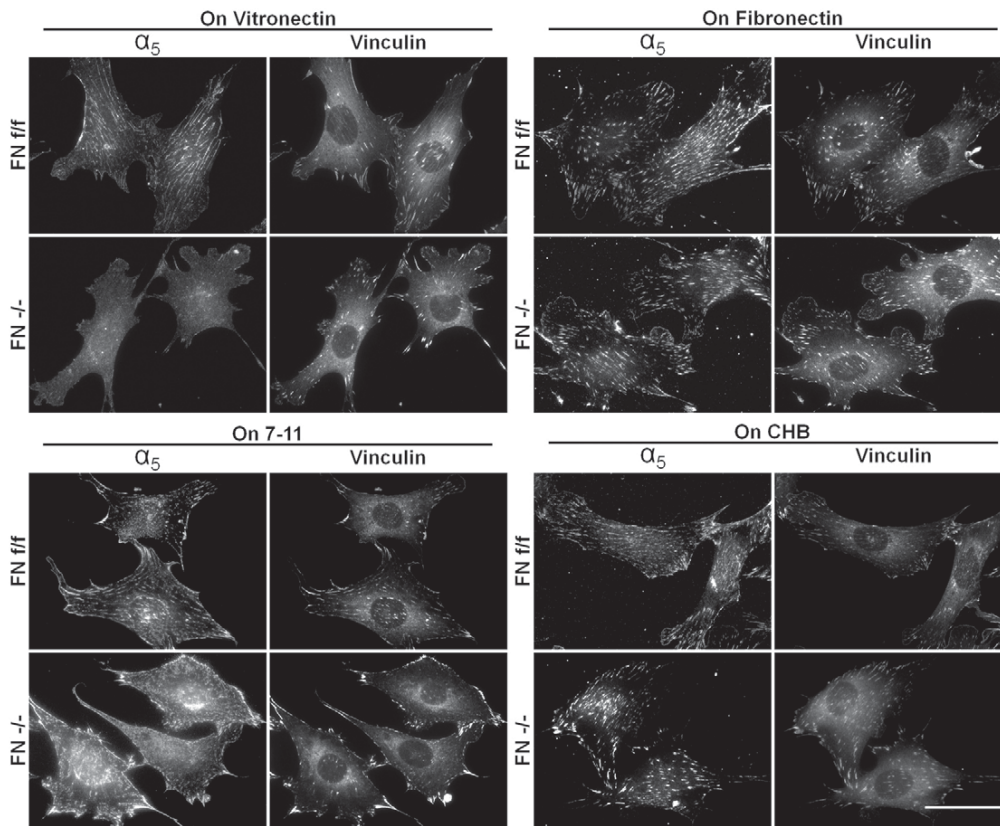


**Fig. 9. Fibronectin-deficient MEFs lack integrin- $\alpha_5$ -containing fibrillar adhesions when plated on vitronectin.** Fibronectin-expressing (FN<sup>fif</sup>) and deficient (FN<sup>-/-</sup>) MEFs were grown on vitronectin (upper left), fibronectin (upper right), the fibronectin type III repeat 7-11 fragment (7-11, lower left) or the fibronectin cell-binding and adjacent heparin-binding site fragment (CHB, lower right) for 48 hours. Cells were then fixed and subsequently stained for vinculin and  $\alpha_5$  integrin. Note that fibronectin-deficient cells do not form  $\alpha_5$ -integrin-containing fibrillar adhesions on vitronectin. Scale bar: 50  $\mu$ m.

part of the endogenously expressed fibronectin could not be inhibited by substrate-bound tenascin-C. This assumption was confirmed by straining fibronectin-expressing cells on vitronectin and mixed vitronectin and tenascin-C substrates (Fig. 8C).

#### Fibronectin-deficient MEFs lack fibrillar adhesions containing $\alpha_5$ integrin and tensin when plated on vitronectin

Since fibronectin-deficient fibroblasts showed clear defects in mechanotransduction in the absence of pericellular fibronectin, we asked whether matrix adhesion sites might also be altered. To address this question we cultured fibronectin-expressing and fibronectin-deficient cells on different substrates for 48 hours. Cells were then co-stained for the cell-matrix adhesion components vinculin and  $\alpha_5$  integrin, a subunit of the fibronectin receptor that is enriched in fibrillar adhesions (Zaidel-Bar et al., 2004; Zamir et al., 2000). On fibronectin (Fig. 9, upper right panel) as well as on its large cell- and heparin-binding (CHB) fragment (Fig. 9, lower right panel), both cell lines formed adhesions that were rather homogeneous in shape and generally stained equally well for both vinculin and  $\alpha_5$  integrin. On vitronectin, however, two types of cell-matrix adhesions could be found (Fig. 9, upper left). One adhesion type was rather oval in shape, and stained strongly for vinculin but faintly for  $\alpha_5$  integrin ('focal adhesions'). This type could be found in both fibronectin-expressing and fibronectin-deficient cells. The other type of cell matrix adhesion was thin and elongated in shape and strongly stained for  $\alpha_5$  integrin ('fibrillar adhesions'). Interestingly, on vitronectin, these fibrillar adhesions could only be found in fibronectin-expressing cells. In

fibronectin-deficient cells on this substrate,  $\alpha_5$  integrin localized very faintly to vinculin-positive focal adhesions, but staining was mostly diffuse, and no elongated fibrillar adhesions were observed (Fig. 9, second row left). To further analyze adhesion sites in these cells, we studied the localization of tensin, an adaptor protein that is enriched in fibrillar adhesions (Katz et al., 2000; Zamir et al., 2000). To do so, we transfected fibronectin-expressing and fibronectin-deficient cells with tensin-GFP and grew them on fibronectin or vitronectin substrates for 48 hours. Cells were then fixed and co-stained for vinculin and fibronectin (supplementary material Fig. S4). In wild-type cells plated on vitronectin, tensin was present in elongated adhesions that colocalized with extracellular fibronectin fibrils. By contrast, we could not detect tensin-GFP in cell-matrix adhesions of fibronectin-deficient cells on vitronectin (supplementary material Fig. S4), in accordance with their diffuse staining for  $\alpha_5$  integrin. However, tensin clearly localized to adhesion sites in the deficient cells when plated on fibronectin. These results suggest a correlation between the lack of fibrillar adhesions rich in  $\alpha_5$  integrin and tensin, and the defective mechanotransduction observed in the absence of fibronectin.

When fibronectin-deficient cells were stretched on substrate coated with fibronectin type III domain 7-11 fragment, tenascin-C induction was diminished (Fig. 8A). Interestingly, cells on this substrate stained for  $\alpha_5$  integrin in bright, irregular patches on their lower surface (Fig. 9, lower left) rather than in elongated adhesion structures. Together, these results indicate that  $\alpha_5$  integrin has to be organized in fibrillar adhesions for efficient RhoA-dependent mechanotransduction. Experiments with fibronectin-

knockdown clone 8.3 and control cells confirmed this (data not shown).

### Discussion

The mechanism by which mechanical stress is transduced into the altered expression of specific genes has received much attention in recent years, but is still not fully understood. Although several signaling pathways are activated by cyclic strain in fibroblasts (Chiquet et al., 2009), reorganization and increase in actin-stress fibers as a result of RhoA activation is a prominent response (Sarasa-Renedo et al., 2006). Recent evidence indicates that mechanical stress might regulate a specific group of genes directly via a change in RhoA-dependent actin dynamics, among them are genes encoding  $\alpha$ -smooth muscle actin, CTGF/CCN1, Cyr61/CCN2 and tenascin-C (Chaqour and Goppelt-Struebe, 2006; Chaqour et al., 2007; Schild and Trueb, 2004; Zhao et al., 2007). We have shown previously that induction of tenascin-C by cyclic strain requires the presence of  $\beta$ 1 integrin (Chiquet et al., 2006) and ILK (Maier et al., 2008), the activation of RhoA (Sarasa-Renedo et al., 2006), actin reorganization (Sarasa-Renedo et al., 2006), and that it correlates with translocation of MAL to the nucleus (Maier et al., 2008). The results presented here show that the mechanotransduction machinery requires pericellular fibronectin for a complete response to cyclic strain. In the absence of exogenous fibronectin, fibroblasts deficient for this protein have defects in RhoA-dependent mechanotransduction identical to those of ILK-knockout cells: in cells subjected to cyclic strain, RhoA is not activated, the actin cytoskeleton is not reorganized, MAL is not translocated to the nucleus, and tenascin-C protein and mRNA are not induced. Nevertheless, similarly to ILK-knockout cells, Erk1/2 and PKB/Akt are still activated in fibronectin-deficient fibroblasts after cyclic strain, indicating that the defect is specific for RhoA-mediated responses. ILK<sup>-/-</sup> fibroblasts secrete normal amounts of fibronectin into the medium but fail to assemble it on the cell surface and the substrate, which might explain their similar phenotype.

On any artificial or ECM substrate, a fibronectin matrix is rapidly deposited from normal wild-type fibroblasts (Grinnell and Feld, 1979). There is increasing evidence that fibronectin-specific integrin  $\alpha$ 5 $\beta$ 1 is involved in the activation of RhoA in the process of fibroblast adhesion and spreading. RhoA activation was promoted during spreading of cells with elevated levels of  $\alpha$ 5 and  $\beta$ 1 chains, but not of cells predominantly expressing the vitronectin receptor  $\alpha$ v $\beta$ 3 (Danen et al., 2002). The absence of  $\alpha$ 5 and  $\beta$ 1 integrin chains also affected the RhoA-dependent process of fibronectin fibrillogenesis (Danen et al., 2002; Huvencers et al., 2008). Moreover, fibronectin was the only substrate to stimulate RhoA activity, and thereby cell-cycle progression, upon plating (Danen et al., 2000). These data clearly indicate that activation of RhoA is dependent on fibronectin and  $\alpha$ 5 $\beta$ 1 integrin during interaction of fibroblasts with their substrate. Our data reveal a requirement for fibronectin in other RhoA-dependent responses, namely those induced by cyclic substrate strain in fully spread cells, in which a large integrin pool is already activated and engaged with ligands.

Different types of cell-matrix adhesions can be distinguished in cultured fibroblasts and these are assembled in a hierarchical manner (Zaidel-Bar et al., 2004). Early focal complexes contain mainly integrin  $\alpha$ v $\beta$ 3, talin and paxillin. Later, the adaptor protein vinculin is recruited and helps to stabilize focal complexes (Ziegler et al., 2006). Cytoskeletal force and the recruitment of additional proteins such as zyxin, tensin and  $\alpha$ 5 $\beta$ 1 integrin lead to the

formation of early focal adhesions. From these structures, specific proteins such as  $\alpha$ 5 $\beta$ 1 integrin and tensin are pulled out by actomyosin contraction and form fibrillar adhesions (Zamir et al., 2000). The latter are essential for the assembly of the pericellular fibronectin fibrils to which they are attached (Mao and Schwarzbauer, 2005). We observed that in fibronectin-deficient MEFs,  $\alpha$ 5 integrin and tensin-GFP were integrated in elongated matrix contacts when cells were plated on fibronectin, but not on a vitronectin substrate. This indicates that on vitronectin these cells do not form fibrillar adhesions and suggests that RhoA-mediated responses to cyclic strain depend on the presence of these adhesions (Fig. 10). Fibrillar adhesions are also absent in ILK<sup>-/-</sup> fibroblasts that fail to assemble fibronectin (Vouret-Craviari et al., 2004) and show a similar defect in mechanotransduction (Maier et al., 2008).

The RhoA-dependent responses to cyclic strain measured on vitronectin depended on the secretion of fibronectin and are therefore likely to be mediated mainly via integrin  $\alpha$ 5 $\beta$ 1 in fibrillar adhesions. By contrast, activation of ERK and PKB/Akt by cyclic strain was also observed in fibronectin-deficient cells in the absence of exogenous fibronectin, indicating that the triggering of these pathways is independent of fibrillar adhesions.

Activity of the fibronectin receptor  $\alpha$ 5 $\beta$ 1 is known to be influenced by force. Externally applied tension switches  $\alpha$ 5 $\beta$ 1 from a relaxed to a tensioned state, which engages the fibronectin synergy site and shows increased bond strength (Friedland et al., 2009; Kong et al., 2009). However, application of external force leads to a lesser activation of  $\alpha$ 5 $\beta$ 1 on soft substrates in comparison to rigid substrates, indicating that a resistant counterforce is needed to trigger the integrin switch (Friedland et al., 2009). Our finding that substrate-bound fibronectin is important for activation of RhoA-dependent responses by cyclic strain is likely to be linked to the fact that actin contraction induced upon RhoA activation counteracts the applied strain. More stress resulting from increased external and internal forces might trigger the catch-bond character of  $\alpha$ 5 $\beta$ 1.

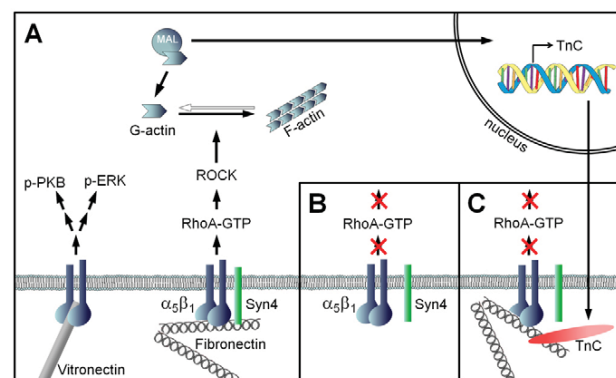


**Fig. 10. Schematic model representing activation of RhoA-mediated responses by cyclic strain and induction of a negative-feedback loop.**

(A) Phosphorylation of PKB/Akt and ERK by cyclic strain is not dependent on the presence of fibronectin and might be mediated mainly by  $\alpha$ v $\beta$ 3 integrins that are enriched in focal adhesions. Induction of RhoA-mediated responses such as actin reorganization, MAL translocation and upregulation of tenascin-C by cyclic strain require fibronectin, which is mainly bound to  $\alpha$ 5 $\beta$ 1 in fibrillar adhesions. (B) In the absence of fibronectin, these RhoA-mediated responses are not induced. (C) In the presence of fibronectin, the tenascin-C synthesized and deposited in response to cyclic strain might suppress RhoA activation on further mechanical stress and negatively regulate its own induction.

Experiments with a small fibronectin fragment (type III domains 7-11) indicated that the RGD and the adjacent synergy site are not sufficient for a full response to cyclic strain in terms of induction of tenascin-C. By contrast, 160 and 135 kDa chymotryptic fibronectin fragments that contained in addition a major heparin-binding site, led to full induction of tenascin-C by cyclic strain in fibronectin-deficient cells; cell-adhesion sites appeared normal on this substrate. However, on intact fibronectin substrates, mechanotransduction was suppressed when soluble heparin was added to the medium. These experiments strongly suggest the involvement of the respective heparin-binding site of fibronectin in RhoA-dependent responses to cyclic strain. This region of fibronectin also contains an interaction site for syndecan-4, a co-receptor of  $\alpha 5 \beta 1$  integrin that is necessary for full spreading of fibroblasts (Woods and Couchman, 1994). Interestingly, the ECM protein tenascin-C interacts with the 13th type III repeat of fibronectin, which is part of this heparin-binding site, and thereby inhibits fibronectin interaction with syndecan-4 (Huang et al., 2001). This might be the reason why tenascin-C interferes with fibroblast attachment to fibronectin (Chiquet-Ehrismann et al., 1988). Tenascin-C is induced by mechanical stress via the RhoA-ROCK pathway (Chiquet et al., 2007; Maier et al., 2008; Sarasa-Renedo et al., 2006). We show here that the induction of tenascin-C by cyclic strain also depends on the presence of pericellular fibronectin. Tenascin-C was shown to suppress RhoA activation (Wenk et al., 2000) and inhibit cell-mediated contraction of mixed fibronectin and fibrinogen matrices (Midwood and Schwarzbauer, 2002). In addition, several other functions of tenascin-C were reported to depend on the presence of syndecan-4 (Midwood et al., 2004). We now demonstrate that addition of exogenous tenascin-C protein to coated fibronectin interferes with the induction of endogenous *Tnc* mRNA following cyclic strain. Together with our previous results, this further strengthens our hypothesis that pericellular fibronectin is crucial for the activation of the RhoA-ROCK pathway by mechanical stimuli. In addition, tenascin-C expressed upon mechanical stimulation could interfere with fibronectin binding and thereby prevent further activation of the RhoA-ROCK pathway brought about by future bouts of mechanical stress (Fig. 10). This feedback loop, in which tenascin-C protein negatively regulates its own induction, might avoid mechanical overload of the cell that results from excess adhesion to a strained substrate.

Our data indicate that the pericellular fibronectin matrix is fundamental to the activation of RhoA and RhoA-dependent responses to cyclic mechanical stress. Three different mechanically induced events reported to depend on RhoA activation (Chiquet et al., 2004; Maier et al., 2008; Miralles et al., 2003; Sarasa-Renedo et al., 2006; Zhao et al., 2007) were shown to be defective in the absence of fibronectin. All effects occurred in both fibronectin-knockdown and fibronectin-knockout fibroblasts. However, the normal activation of ERK and PKB/Akt following mechanical stress in the absence of fibronectin indicates that mechanotransduction is not affected in general. Experiments made with fibronectin fragments and addition of soluble heparin showed that RhoA-dependent responses to cyclic strain depend on a major heparin-binding site of fibronectin. This fact and the inhibitory effect of tenascin-C protein on its own induction by mechanical stress both seem to indicate the possible involvement of syndecan-4 in the observed responses. The precise role and putative co-operation of fibronectin receptor  $\alpha 5 \beta 1$  integrin and syndecan-4 (Fig. 10) have to be addressed in future experiments. Nonetheless,

our present results implicate pericellular fibronectin in the activation of a specific pathway that changes cytoskeletal structure and gene expression in response to external mechanical stress, and they suggest ways in which this pathway is regulated.

## Materials and Methods

### Cell culture

A kidney MEF cell line immortalized by stable transfection with SV40 large-T antigen was used to produce stable fibronectin-knockdown mouse embryo fibroblasts (MEFs) (Graness et al., 2006). Cells were transfected with purified plasmid DNA encoding shRNA against mouse fibronectin (MISSION shRNA Bacterial Glycerol Stock from Sigma, Buchs, Switzerland) by means of the MEF nucleofactor kit (Amaxa, Lonza, Basel, Switzerland). Transfected cells were seeded and clones resistant to puromycin were selected. By the same procedure, fibronectin-knockdown REFs were generated from wild-type REFs. A kidney MEF cell line containing a floxed fibronectin gene ( $FN^{fl}$ ) and a fibronectin-knockout MEF cell line ( $FN^{-/-}$ ) (Fontana et al., 2005; Sakai et al., 2001) were obtained from Michael Leiss and Reinhard Fässler (Max-Planck Institute for Biochemistry, Martinsried, Germany). The original cells were maintained at 37°C with 6% CO<sub>2</sub> in Dulbecco's modified Eagle medium (DMEM; Seromed, Basel, Switzerland) containing 10% fetal calf serum (FCS; Gibco/Invitrogen, Basel, Switzerland). Fibronectin-knockdown clones were maintained in the same medium to which puromycin was added at 2  $\mu$ g/ml.

### Generation of fibronectin fragments

160- and 135-kDa cell-binding fragments of fibronectin were generated as described (Ehrismann et al., 1982) (supplementary material Fig. S3A). Briefly, fibronectin from 50 ml horse serum was adsorbed to gelatin-Sepharose and digested on the column with 20  $\mu$ g/ml crystalline chymotrypsin (Serva, Heidelberg, Germany) for 5 minutes. Eluted (non-gelatin binding) fragments were collected into tubes containing protease inhibitors, pooled, and adsorbed to heparin-Sepharose to remove chymotrypsin and protease inhibitors. Bound 160 and 135 kDa fragments were eluted from the heparin affinity column with 1 M NaCl, 20 mM sodium phosphate, pH 7.4. A fibronectin fragment comprising type III domains 7-11 was expressed as described (Bloom et al., 1999). Briefly *E. coli* strain DH5a harboring the expression vector (obtained from Gertraud Orend, University of Strasbourg, Strasbourg, France) was grown to late log-phase and induced with 1 mM IPTG for 4 hours. Cells were harvested, lysed by sonification in lysis buffer (50 mM NaH<sub>2</sub>PO<sub>4</sub>, 150 mM NaCl, pH 7.2, 1 mM DTT, 1 mM EDTA, 1% Triton X-100, 1 mg/ml lysozyme, protease inhibitors (Roche, Basel, Switzerland), and the GST-tagged recombinant fragment was purified using glutathione-Sepharose beads (Qiagen, Basel, Switzerland).

### Matrix coating and plating of cells

For cyclic strain experiments, silicone membranes of Flexercell II six-well plates were coated for 3 hours with purified horse serum fibronectin at 50  $\mu$ g/ml in Dulbecco's phosphate buffered saline (PBS) (Chiquet et al., 2004). Alternatively, silicone membranes were coated with vitronectin at 20  $\mu$ g/ml (Abcam, Cambridge, UK) for 90 minutes and then allowed to air dry. Concentrations used for coating were saturating for cell adhesion and roughly adjusted to the molecular mass of the respective proteins. Air drying was used because a more homogeneous coating of the very hydrophobic silicone membrane was achieved, and no loss of adhesive activity was observed compared with coating glass or culture plastic without drying. In some experiments tenascin-C, purified from chick embryo fibroblast conditioned medium (Chiquet-Ehrismann et al., 1988), was mixed with fibronectin or vitronectin during coating. Concentrations used for coating of tenascin-C (TnC)-containing substrates were: FN and TnC (50  $\mu$ g/ml and 50  $\mu$ g/ml), TnC (50  $\mu$ g/ml), VN and TnC (20  $\mu$ g/ml and 50  $\mu$ g/ml). Other matrix proteins were used at the following coating concentrations: FN CHB (30  $\mu$ g/ml), FN 7-11 (20  $\mu$ g/ml), Collagen (Serva, Heidelberg, Germany; 2 mg/ml). For inhibition experiments, porcine intestinal mucosa heparin (Sigma, Buchs, Switzerland) was added at 100  $\mu$ g/ml 24 hours before applying strain. For immunofluorescence experiments, 40,000 cells and, for biochemical experiments 90,000 cells were plated in DMEM containing 3% FCS depleted of fibronectin by two passages over gelatin-Sepharose (Amersham, Wädenswil, Switzerland). Cells were allowed to attach, spread and deposit their own matrix for 20 hours. After washing with serum-free medium, cells were starved for a further 20 hours in DMEM containing a low concentration of fibronectin free serum (0.03% to determine tenascin-C protein and mRNA, 0.3% for all other experiments) and cells were subsequently subjected to cyclic strain in this medium. For analyzing tenascin-C deposition into the matrix, cells were kept in culture for a further 18 hours after straining.

### Mechanical loading of cells

Culture dishes were mounted on a Flexcell FX-4000 machine (Dunn Labortechnik, Asbach, Germany) and cells were subjected to equibiaxial cyclic strain (10%, 0.3 Hz) at 37°C for the times indicated (5 minutes to 6 hours). After mechanical stimulation, cells were fixed with 4% paraformaldehyde for phalloidin and immunofluorescence staining (see below). Alternatively, cells were lysed in RNA isolation buffer from an RNA purification kit (RNeasy, Qiagen, Basel, Switzerland).

If used, cell-permeable C3-transferase at 0.25 µg/ml (Cytoskeleton, LuBioScience, Luzern, Switzerland) was added 30 minutes before cyclic strain.

#### Rho-activity assay

Silicone membranes with attached cells were washed with cold TBS, lysed and Rho activity was measured using a previously described method (Ren and Schwartz, 2000). Briefly, cells were lysed in cold lysis buffer (50 mM Tris-HCl, pH 7.2, 1% Triton X-100, 0.5% sodium deoxycholate, 0.1% SDS, 500 mM NaCl, 10 mM MgCl<sub>2</sub>, 10 µg/ml each of leupeptin and aprotinin, and 1 mM PMSF) and GTP-Rho was affinity precipitated using Rhotekin-GST-Sepharose beads (for production of beads and precipitation see Ren and Schwartz (Ren and Schwartz, 2000) and Sarasa-Renedo et al. (Sarasa-Renedo et al., 2006). Affinity precipitated RhoA was quantified in parallel with total cellular RhoA from cell lysates by western blot analysis with an antibody against RhoA (Santa Cruz Biotechnology, Santa Cruz, CA) at 1:75 in TBS, 5% BSA, 0.1% Tween.

#### Immunofluorescence and phalloidin staining

Silicone membranes with attached, fixed cells were permeabilized and incubated at room temperature for 30 minutes in PBS containing 3% BSA and 0.1% Triton X-100. Rabbit polyclonal antiserum to horse serum fibronectin (crossreacting with mouse) (Wehrle and Chiquet, 1990) and monoclonal antibody 65F13 against mouse MAL (Maier et al., 2008) were described previously. Cells were then stained for 1 hour at room temperature with anti-fibronectin antiserum diluted 1:300, anti-MAL mAb 65F13 supernatant diluted 1:10, anti-vinculin 1:1000 (Sigma, Buchs, Switzerland) and/or anti-α5-integrin 1:500 (BD Pharmingen, Basel, Switzerland) in PBS containing 3% BSA and 0.1% Triton X-100. After staining, cells were washed three times with PBS, 0.1% Triton X-100, incubated for 1 hour with Alexa Fluor 546-labeled phalloidin (Sigma) and either Alexa Fluor 488-labeled goat anti-rabbit or Alexa Fluor 488-labeled goat anti-mouse IgG (Sigma). Cells were again washed three times with PBS, 0.1% Triton X-100 and mounted in Prolong Gold antifade reagent (Invitrogen, Basel, Switzerland). Slides were examined with a Zeiss Z1 microscope equipped with a 20×/0.8 NA objective, Zeiss filter cubes no. 38HE for Alexa Fluor 488, no. 43 for Alexa Fluor 546 and a Zeiss MRm camera.

#### Immunoblotting

Wild-type, clone 1.2 and clone 8.3 cells were left at rest or subjected to cyclic strain for 5, 10 and 15 minutes, respectively. Cells were then immediately washed with ice-cold PBS and subsequently scraped in RIPA buffer (50 mM Tris-HCl, pH 7.4, 150 mM NaCl, 1% NP-40, 0.25% sodium deoxycholate and 1 mM EDTA) containing protease and phosphatase inhibitors (Roche, Basel, Switzerland). Lysates were cleared by centrifugation, resolved on 10% polyacrylamide-SDS gels and blotted to nitrocellulose. Blots were incubated with one of the following antibodies diluted in TBS (0.1% Tween, 3% BSA): rabbit antibody against Erk1/2 (1:1000), mouse mAb against phosphorylated Erk1/2 (1:1000), rabbit antibody against phosphorylated Akt (S473) (1:1000) (all Cell Signaling; BioConcept, Allschwil, Switzerland) or rabbit antibody Ab10 against PKB/Akt (1:500) (Jones et al., 1991). Tenascin-C in cell or cell-matrix lysates was detected using the rat monoclonal anti-tenascin-C antibody mTn-12 (1:500) (Aufderheide and Ekblom, 1988). For detection of fibronectin, blots were incubated with polyclonal antiserum against fibronectin (see above) diluted 1:300. Non-reducing gels were run to analyze integrin expression levels. After blotting to PVDF membranes, α5 integrin (rat monoclonal, 1:250, BD Bioscience, Allschwil, Switzerland), αv integrin (mouse anti-CD51, 1:250, BD Biosciences) and β1 integrin (rat monoclonal, 1:1500, BD Bioscience) were used for detection. In all cases, blots were washed and subsequently incubated with peroxidase-labeled secondary antibodies (1:2000; Cappel/ICN Biomedicals; EGT Chemie, Switzerland) and developed with ECL reagent (Amersham, Wädenswil, Switzerland).

#### Quantification of mRNA levels by real-time PCR

RNA was isolated from scraped cell lysates by the RNeasy procedure (Qiagen, Basel, Switzerland). RNA was then reverse-transcribed with a High Capacity cDNA Reverse Transcription Kit (Applied Biosystems, Rotkreuz, Switzerland). TaqMan real-time PCR primer/probe mixtures for mouse tenascin-C (Mm00495662\_m1), and mouse GAPDH (Mm9999915\_g1) as well as TaqMan Universal Master Mix were purchased from Applied Biosystems. For each experimental condition, reverse-transcribed cDNA was amplified for each gene on an ABI Prism 7000 real-time PCR cycler (Applied Biosystems). Data were analyzed by the ΔCt method (Livak and Schmittgen, 2001), i.e. values for tenascin-C were normalized to GAPDH for each sample. These data are shown in the graphs rather than data produced by further normalization to the resting controls [ΔΔCt method (Livak and Schmittgen, 2001)]. Data are the means ± s.e.m. of 3–4 independent experiments. Statistical significances between rest and stressed conditions were determined by two-way ANOVA. Differences of *P* < 0.05 were considered significant.

We thank Michael Leiss and Reinhard Fässler for the fibronectin-knockout and control fibroblasts, Ken Yamada and Richard Hynes for GFP-tensin and FNIII-7-11 expression plasmids, respectively, Gertraud Orend for the FNIII-7-11-expressing bacteria, Patrick King for critical reading of the manuscript, and Ruth Chiquet-Ehrismann for many

discussions and continuing support. This work was supported by the Novartis Research Foundation and by grants from the Swiss National Fund to M.C.

Supplementary material available online at <http://jcs.biologists.org/cgi/content/full/123/9/1511/DC1>

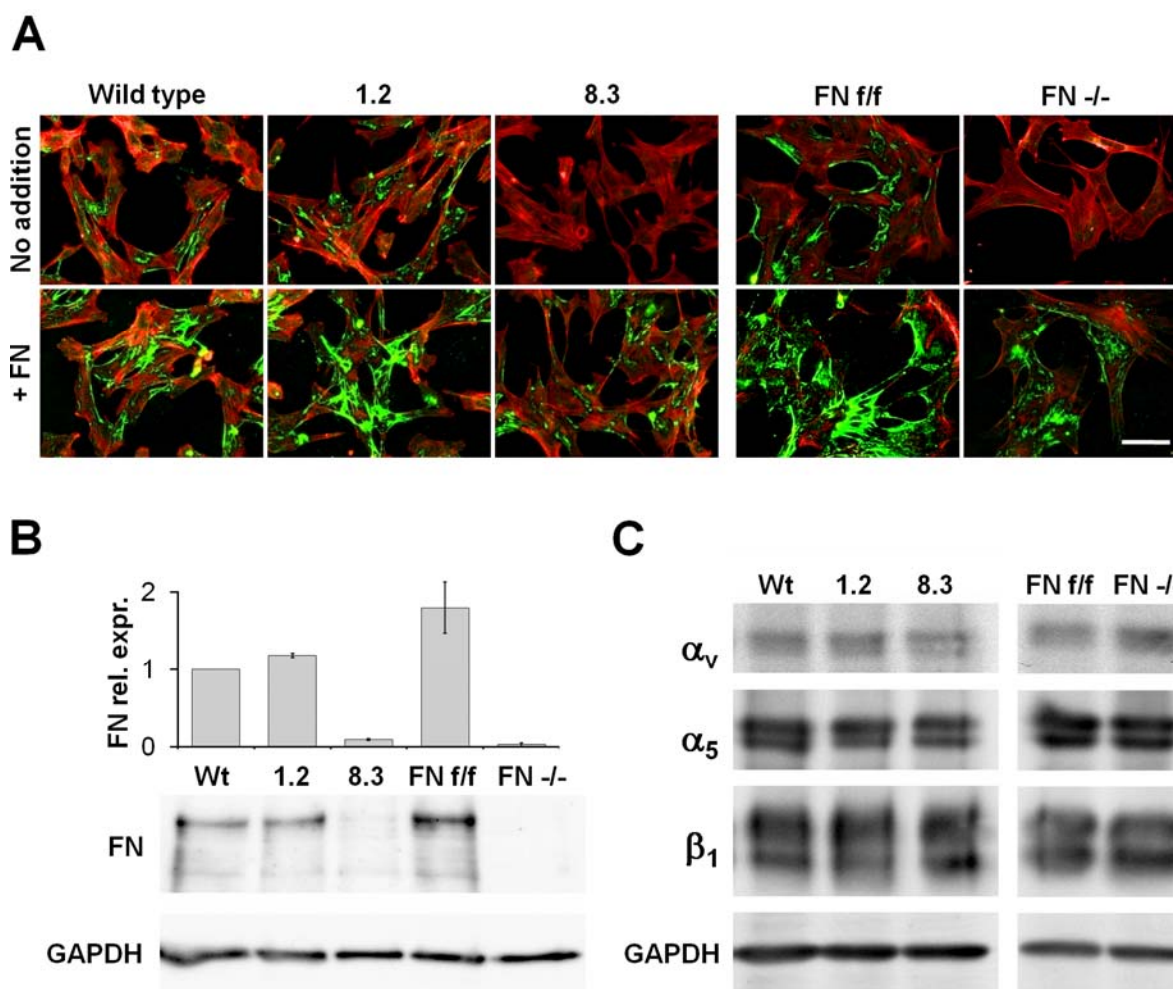
#### References

- Asparuhova, M. B., Gelman, L. and Chiquet, M. (2009). Role of the actin cytoskeleton in tuning cellular responses to external mechanical stress. *Scand. J. Med. Sci. Sports*, **19**, 490–499.
- Aufderheide, E. and Ekblom, P. (1988). Tenascin during gut development: appearance in the mesenchyme, shift in molecular forms, and dependence on epithelial-mesenchymal interactions. *J. Cell Biol.* **107**, 2341–2349.
- Bloom, L., Ingham, K. C. and Hynes, R. O. (1999). Fibronectin regulates assembly of actin filaments and focal contacts in cultured cells via the heparin-binding site in repeat III13. *Mol. Biol. Cell* **10**, 1521–1536.
- Butcher, D. T., Alliston, T. and Weaver, V. M. (2009). A tense situation: forcing tumour progression. *Nat. Rev. Cancer* **9**, 108–122.
- Chaquor, B. and Goppelt-Strube, M. (2006). Mechanical regulation of the Cyr61/CCN1 and CTGF/CCN2 proteins. *FEBS J.* **273**, 3639–3649.
- Chaquor, B., Yang, R. and Sha, Q. (2006). Mechanical stretch modulates the promoter activity of the profibrotic factor CCN2 through increased actin polymerization and NF-κappaB activation. *J. Biol. Chem.* **281**, 20608–20622.
- Chen, C. S. (2008). Mechanotransduction—a field pulling together? *J. Cell Sci.* **121**, 3285–3292.
- Chiquet, M., Sarasa-Renedo, A. and Tunc-Civelek, V. (2004). Induction of tenascin-C by cyclic tensile strain versus growth factors: distinct contributions by Rho/ROCK and MAPK signaling pathways. *Biochim. Biophys. Acta* **1693**, 193–204.
- Chiquet, M., Tunc-Civelek, V. and Sarasa-Renedo, A. (2007). Gene regulation by mechanotransduction in fibroblasts. *Appl. Physiol. Nutr. Metab.* **32**, 967–973.
- Chiquet, M., Gelman, L., Lutz, R. and Maier, S. (2009). From mechanotransduction to extracellular matrix gene expression in fibroblasts. *Biochim. Biophys. Acta* **1793**, 911–920.
- Chiquet-Ehrismann, R., Kalla, P., Pearson, C. A., Beck, K. and Chiquet, M. (1988). Tenascin interferes with fibronectin action. *Cell* **53**, 383–390.
- Danen, E. H., Sonneveld, P., Sonnenberg, A. and Yamada, K. M. (2000). Dual stimulation of Ras/mitogen-activated protein kinase and RhoA by cell adhesion to fibronectin supports growth factor-stimulated cell cycle progression. *J. Cell Biol.* **151**, 1413–1422.
- Danen, E. H., Sonneveld, P., Brakebusch, C., Fassler, R. and Sonnenberg, A. (2002). The fibronectin-binding integrins alpha5beta1 and alphavbeta3 differentially modulate RhoA-GTP loading, organization of cell matrix adhesions, and fibronectin fibrillogenesis. *J. Cell Biol.* **159**, 1071–1086.
- Ehrismann, R., Roth, D. E., Eppenberger, H. M. and Turner, D. C. (1982). Arrangement of attachment-promoting, self-association, and heparin-binding sites in horse serum fibronectin. *J. Biol. Chem.* **257**, 7381–7387.
- Fluck, M., Tunc-Civelek, V. and Chiquet, M. (2000). Rapid and reciprocal regulation of tenascin-C and tenascin-Y expression by loading of skeletal muscle. *J. Cell Sci.* **113**, 3583–3591.
- Fontana, L., Chen, Y., Prijatelj, P., Sakai, T., Fassler, R., Sakai, L. Y. and Rifkin, B. R. (2005). Fibronectin is required for integrin alphavbeta6-mediated activation of latent TGF-beta complexes containing LTBP-1. *FASEB J.* **19**, 1798–1808.
- Friedland, J. C., Lee, M. H. and Boettiger, D. (2009). Mechanically activated integrin switch controls alpha5beta1 function. *Science* **323**, 642–644.
- Geiger, B., Spatz, J. P. and Bershadsky, A. D. (2009). Environmental sensing through focal adhesions. *Nat. Rev. Mol. Cell Biol.* **10**, 21–33.
- Granness, A., Giehl, K. and Goppelt-Strube, M. (2006). Differential involvement of the integrin-linked kinase (ILK) in RhoA-dependent rearrangement of F-actin fibers and induction of connective tissue growth factor (CTGF). *Cell. Signal.* **18**, 433–440.
- Grinnell, F. and Feld, M. K. (1979). Initial adhesion of human fibroblasts in serum-free medium: possible role of secreted fibronectin. *Cell* **17**, 117–129.
- Hahn, C. and Schwartz, M. A. (2009). Mechanotransduction in vascular physiology and atherogenesis. *Nat. Rev. Mol. Cell Biol.* **10**, 53–62.
- Horton, M. A. (1997). The alpha v beta 3 integrin “vitronectin receptor”. *Int. J. Biochem. Cell Biol.* **29**, 721–725.
- Hsieh, A. H., Tsai, C. M., Ma, Q. J., Lin, T., Banes, A. J., Villarreal, F. J., Akeson, W. H. and Sung, K. L. (2000). Time-dependent increases in type-III collagen gene expression in medical collateral ligament fibroblasts under cyclic strains. *J. Orthop. Res.* **18**, 220–227.
- Huang, W., Chiquet-Ehrismann, R., Moyano, J. V., Garcia-Pardo, A. and Orend, G. (2001). Interference of tenascin-C with syndecan-4 binding to fibronectin blocks cell adhesion and stimulates tumor cell proliferation. *Cancer Res.* **61**, 8586–8594.
- Huveeners, S., Truong, H., Fassler, R., Sonnenberg, A. and Danen, E. H. (2008). Binding of soluble fibronectin to integrin alpha5 beta1-link to focal adhesion redistribution and contractile shape. *J. Cell Sci.* **121**, 2452–2462.
- Inoh, H., Ishiguro, N., Sawazaki, S., Amma, H., Miyazu, M., Iwata, H., Sokabe, M. and Naruse, K. (2002). Uni-axial cyclic stretch induces the activation of transcription factor nuclear factor kappaB in human fibroblast cells. *FASEB J.* **16**, 405–407.
- Jones, P. F., Jakubowicz, T., Pitossi, F. J., Maurer, F. and Hemmings, B. A. (1991). Molecular cloning and identification of a serine/threonine protein kinase of the second-messenger subfamily. *Proc. Natl. Acad. Sci. USA* **88**, 4171–4175.

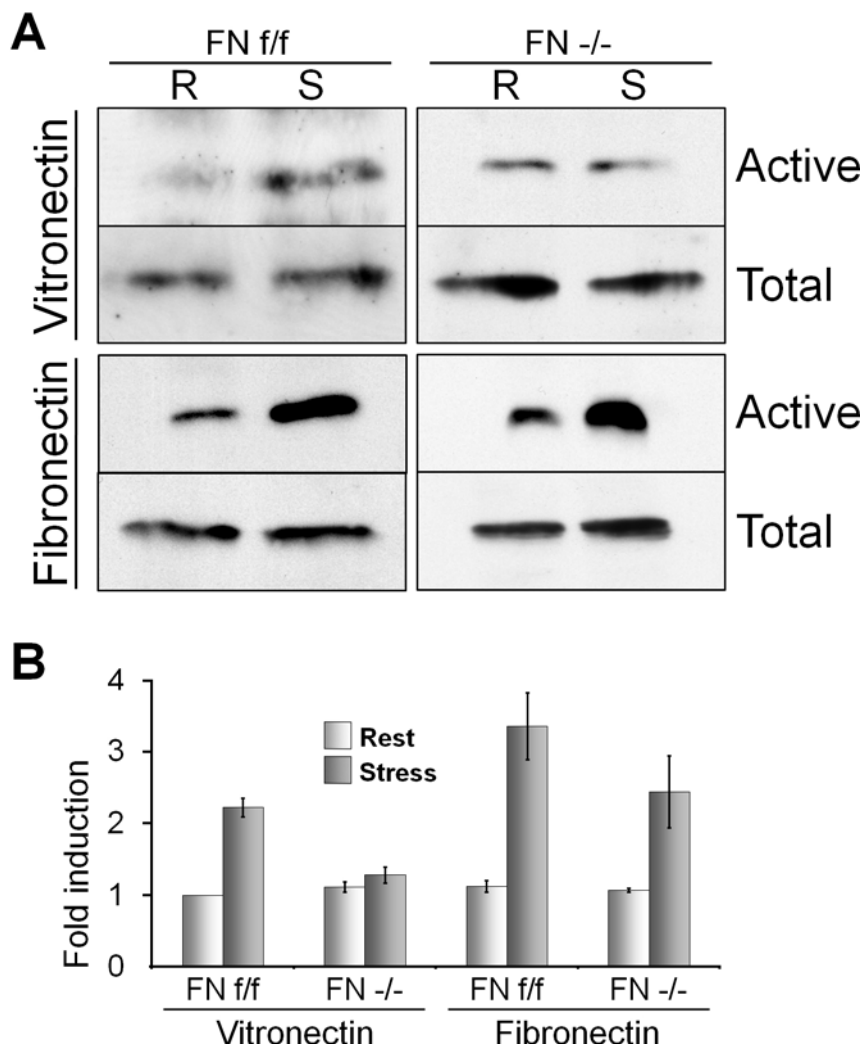


- Katz, B. Z., Zamir, E., Bershadsky, A., Kam, Z., Yamada, K. M. and Geiger, B. (2000). Physical state of the extracellular matrix regulates the structure and molecular composition of cell-matrix adhesions. *Mol. Biol. Cell* **11**, 1047-1060.
- Kong, F., Garcia, A. J., Mould, A. P., Humphries, M. J. and Zhu, C. (2009). Demonstration of catch bonds between an integrin and its ligand. *J. Cell Biol.* **185**, 1275-1284.
- Legate, K. R., Montanez, E., Kudlacek, O. and Fassler, R. (2006). ILK, PINCH and parvin: the tIPP of integrin signalling. *Nat. Rev. Mol. Cell Biol.* **7**, 20-31.
- Lehoux, S., Castier, Y. and Tedgui, A. (2006). Molecular mechanisms of the vascular responses to haemodynamic forces. *J. Intern. Med.* **259**, 381-392.
- Livak, K. J. and Schmittgen, T. D. (2001). Analysis of relative gene expression data using real-time quantitative PCR and the 2(-Delta Delta C(T)) method. *Methods* **25**, 402-408.
- Magnusson, S. P., Narici, M. V., Maganaris, C. N. and Kjaer, M. (2008). Human tendon behaviour and adaptation, in vivo. *J. Physiol.* **586**, 71-81.
- Maier, S., Lutz, R., Gelman, L., Sarasa-Renedo, A., Schenk, S., Grashoff, C. and Chiquet, M. (2008). Tenascin-C induction by cyclic strain requires integrin-linked kinase. *Biochim. Biophys. Acta.* **1783**, 1150-1162.
- Mao, Y. and Schwarzbauer, J. E. (2005). Fibronectin fibrillogenesis, a cell-mediated matrix assembly process. *Matrix Biol.* **24**, 389-399.
- Midwood, K. S. and Schwarzbauer, J. E. (2002). Tenascin-C modulates matrix contraction via focal adhesion kinase- and Rho-mediated signaling pathways. *Mol. Biol. Cell* **13**, 3601-3613.
- Midwood, K. S., Valenick, L. V., Hsia, H. C. and Schwarzbauer, J. E. (2004). Coregulation of fibronectin signaling and matrix contraction by tenascin-C and syndecan-4. *Mol. Biol. Cell* **15**, 5670-5677.
- Miralles, F., Posern, G., Zaromytidou, A. I. and Treisman, R. (2003). Actin dynamics control SRF activity by regulation of its coactivator MAL. *Cell* **113**, 329-342.
- Orr, A. W., Helmke, B. P., Blackman, B. R. and Schwartz, M. A. (2006). Mechanisms of mechanotransduction. *Dev. Cell* **10**, 11-20.
- Ren, X. D. and Schwartz, M. A. (2000). Determination of GTP loading on Rho. *Methods Enzymol.* **325**, 264-272.
- Sakai, T., Johnson, K. J., Murozono, M., Sakai, K., Magnuson, M. A., Wieloch, T., Cronberg, T., Isshiki, A., Erickson, H. P. and Fassler, R. (2001). Plasma fibronectin supports neuronal survival and reduces brain injury following transient focal cerebral ischemia but is not essential for skin-wound healing and hemostasis. *Nat. Med.* **7**, 324-330.
- Sarasa-Renedo, A., Tunc-Civelek, V. and Chiquet, M. (2006). Role of RhoA/ROCK-dependent actin contractility in the induction of tenascin-C by cyclic tensile strain. *Exp. Cell Res.* **312**, 1361-1370.
- Schild, C. and Trueb, B. (2004). Three members of the connective tissue growth factor family CCN are differentially regulated by mechanical stress. *Biochim. Biophys. Acta* **1691**, 33-40.
- Smith, P. G., Roy, C., Zhang, Y. N. and Chaudhuri, S. (2003). Mechanical stress increases RhoA activation in airway smooth muscle cells. *Am. J. Respir. Cell Mol. Biol.* **28**, 436-442.
- Stupack, D. G. and Chersesh, D. A. (2002). Get a ligand, get a life: integrins, signaling and cell survival. *J. Cell Sci.* **115**, 3729-3738.
- Vouret-Craviari, V., Boulter, E., Grall, D., Matthews, C. and Van Obberghen-Schilling, E. (2004). ILK is required for the assembly of matrix-forming adhesions and capillary morphogenesis in endothelial cells. *J. Cell Sci.* **117**, 4559-4569.
- Wehrle, B. and Chiquet, M. (1990). Tenascin is accumulated along developing peripheral nerves and allows neurite outgrowth in vitro. *Development* **110**, 401-415.
- Wenk, M. B., Midwood, K. S. and Schwarzbauer, J. E. (2000). Tenascin-C suppresses Rho activation. *J. Cell Biol.* **150**, 913-920.
- Wipff, P. J., Rifkin, D. B., Meister, J. J. and Hinz, B. (2007). Myofibroblast contraction activates latent TGF-beta1 from the extracellular matrix. *J. Cell Biol.* **179**, 1311-1323.
- Woods, A. and Couchman, J. R. (1994). Syndecan 4 heparan sulfate proteoglycan is a selectively enriched and widespread focal adhesion component. *Mol. Biol. Cell* **5**, 183-192.
- Zaidel-Bar, R., Cohen, M., Addadi, L. and Geiger, B. (2004). Hierarchical assembly of cell-matrix adhesion complexes. *Biochem. Soc. Trans.* **32**, 416-420.
- Zamir, E., Katz, M., Posen, Y., Erez, N., Yamada, K. M., Katz, B. Z., Lin, S., Lin, D. C., Bershadsky, A., Kam, Z. et al. (2000). Dynamics and segregation of cell-matrix adhesions in cultured fibroblasts. *Nat. Cell Biol.* **2**, 191-196.
- Zhao, X. H., Laschinger, C., Arora, P., Szasz, K., Kapus, A. and McCulloch, C. A. (2007). Force activates smooth muscle alpha-actin promoter activity through the Rho signaling pathway. *J. Cell Sci.* **120**, 1801-1809.
- Ziegler, W. H., Liddington, R. C. and Critchley, D. R. (2006). The structure and regulation of vinculin. *Trends Cell Biol.* **16**, 453-460.

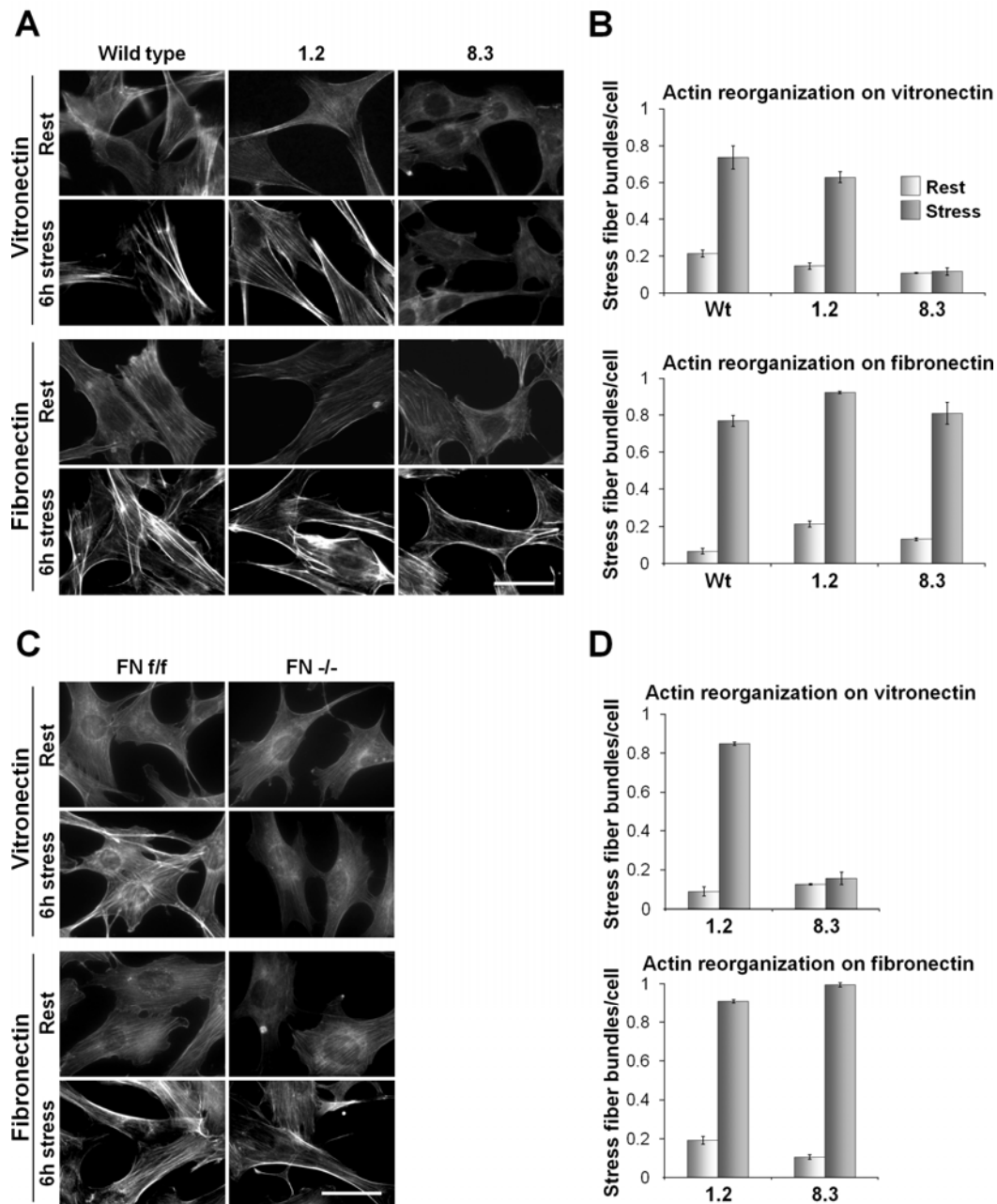
#### IV.4 Pericellular fibronectin is required for RhoA-dependent responses to cyclic strain in fibroblasts (high quality figures and supplementary material)



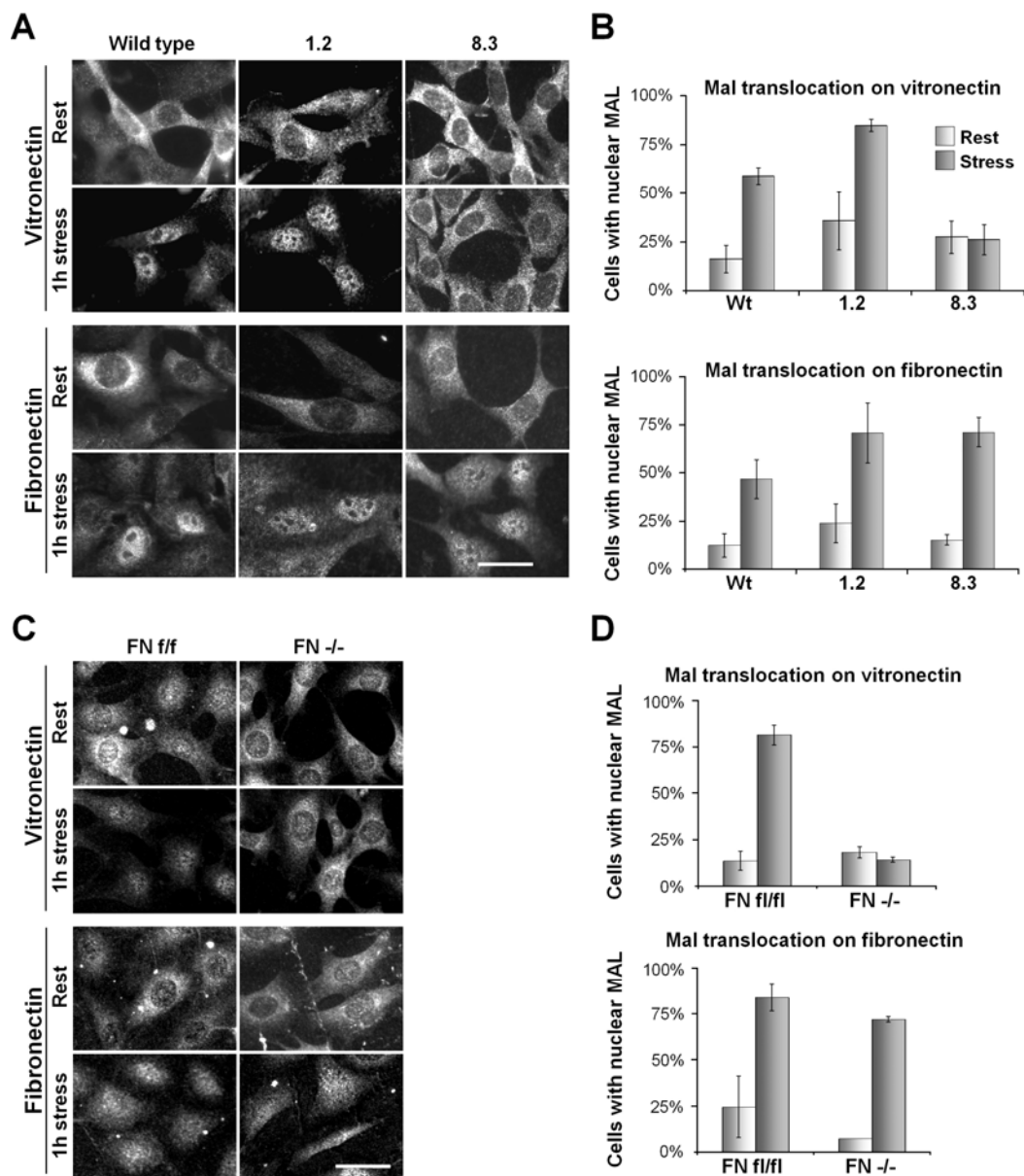
**Fig. 1. Fibronectin expression levels and integrin profiles of fibronectin knockdown (8.3), fibronectin knockout (FN<sup>-/-</sup>), and control (FN<sup>f/f</sup>, 1.2, wild type) MEF. (A)** Cells were plated on cell culture plastic and grown for 48 hours in DMEM containing 3% fibronectin-depleted FCS, either without (top) or with fibronectin added at 100 µg/ml (bottom). Cells were subsequently fixed and double-stained with phalloidin (red) and anti-fibronectin (green). Scale bar is 50 µm. Note that 8.3 and FN<sup>-/-</sup> assembled pericellular fibronectin fibrils only in the presence of exogenous fibronectin. **(B)** Cells were grown for 48 hours on tissue culture plastic and subsequently detached from the matrix by detergent. Matrices were scraped into Laemmli buffer and analyzed by immunoblotting against fibronectin. Cell lysates were blotted for GAPDH as a loading control. Graph shows the average relative expression of fibronectin to GAPDH quantified from independent experiments. **(C)** Cell extracts were immunoblotted for  $\alpha_v$ ,  $\alpha_5$  and  $\beta_1$  integrins to check their expression levels; GAPDH was used as a loading control.



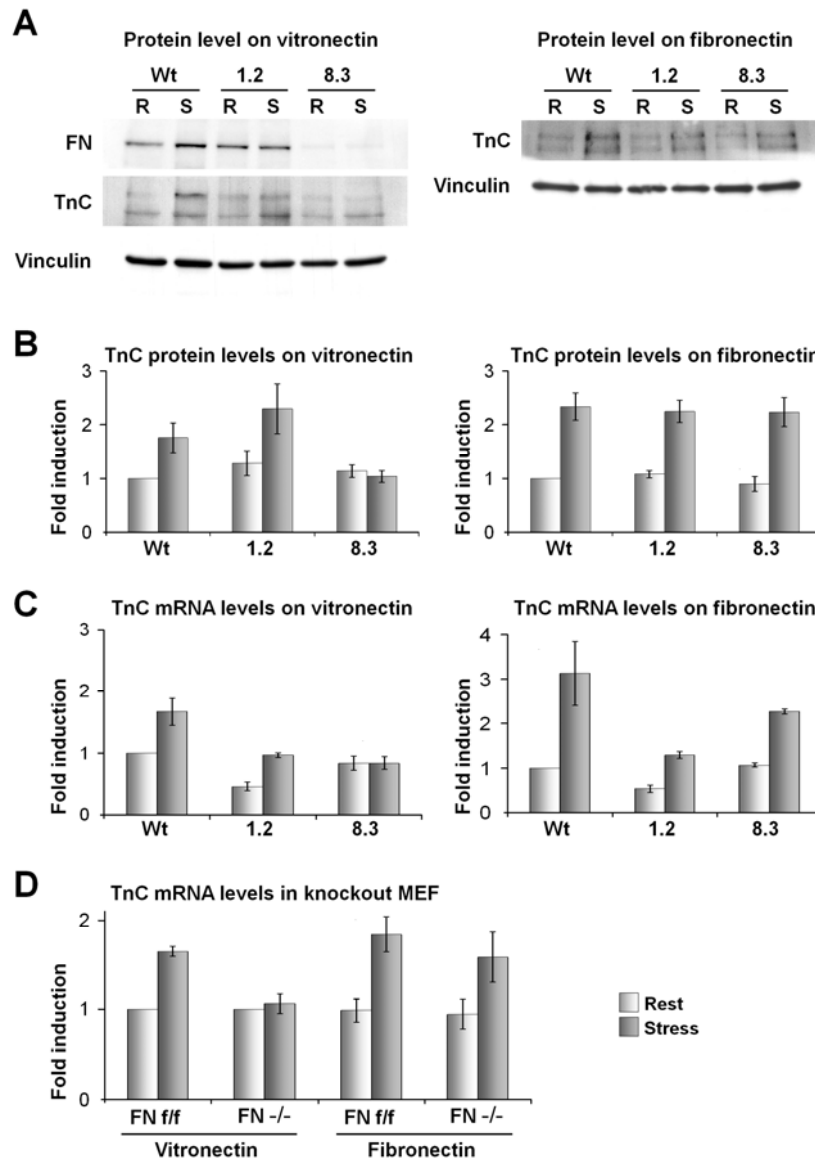
**Fig. 2. Cyclic strain activates RhoA only in the presence of pericellular fibronectin.** (A) Fibronectin knockout (FN<sup>-/-</sup>) and control MEF (FN<sup>f/f</sup>) were cultured on either vitronectin (top) or fibronectin (bottom) for 48 hours. Cells were then cyclically strained (10%, 0.3Hz) for 5 minutes and active RhoA levels were determined by Rho pull down experiments. (B) Graph showing average levels of active RhoA from independent experiments. Values are normalized to levels in FN<sup>f/f</sup> cells at rest on vitronectin.



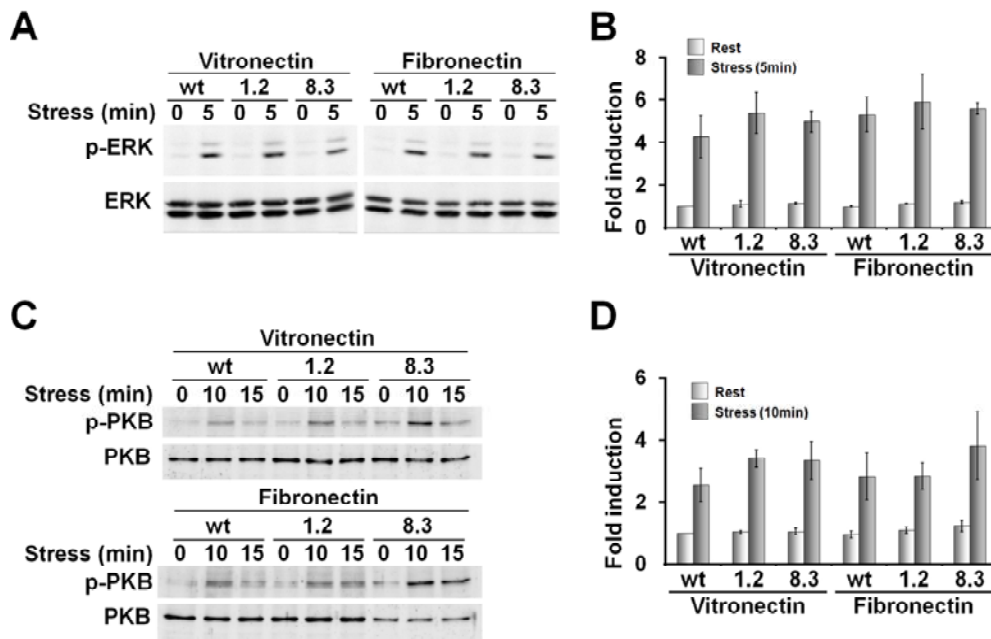
**Fig. 3. Cyclic strain-induced actin reorganization requires a pericellular fibronectin matrix. (A)** Wild type MEF, the fibronectin-expressing clone 1.2 and the fibronectin knockdown clone 8.3 were seeded on vitronectin (top) or fibronectin coated (bottom) silicone membranes. Two days after plating in DMEM plus 0.3% fibronectin-depleted FCS, cells were cyclically strained (10%, 0.3Hz) for 6 hours and subsequently stained for the actin cytoskeleton. **(B)** Statistical analysis of different independent experiments as depicted in A. For every experiment, 100 cells per condition were analyzed and peripheral actin stress fiber bundles per cell were determined. Peripheral actin bundles were defined as locations where single visible stress fibers merged in the cell periphery into larger and thicker, bright foci. **(C)** The experiment described in A carried out with fibronectin knockout MEF (FN<sup>-/-</sup>) and the matched fibronectin-expressing control cells (FN<sup>f/f</sup>). **(D)** The statistical analysis described in B carried out on the results of different independent experiments shown in C. Note the missing actin reorganization in the fibronectin-deficient clones 8.3 and FN<sup>-/-</sup> on the vitronectin, but not on the fibronectin substrate. Scale bars are 50  $\mu$ m.



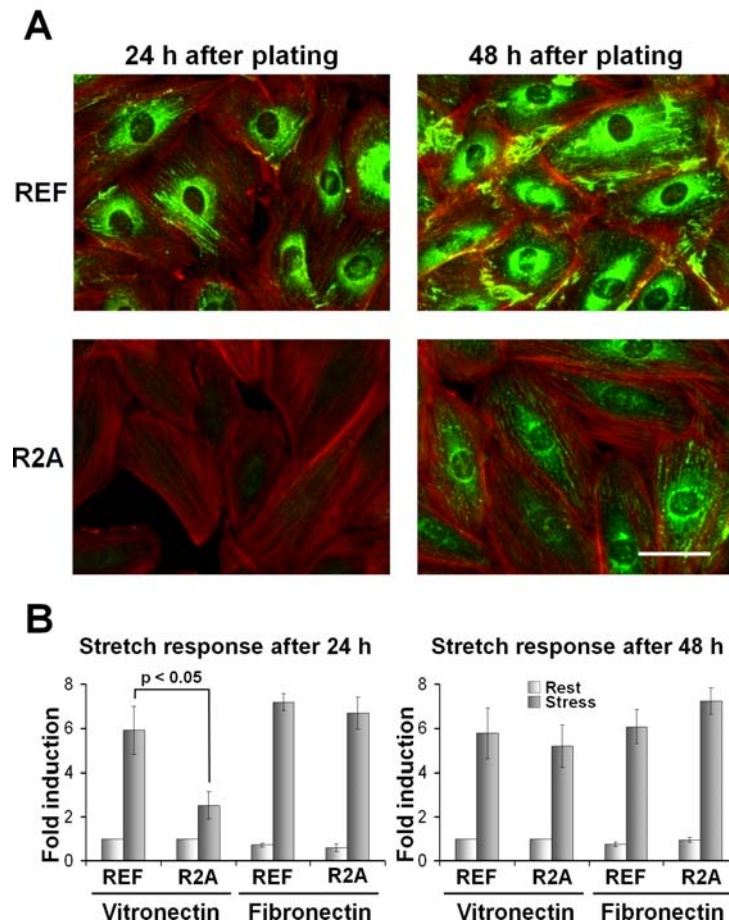
**Fig. 4. Pericellular fibronectin is necessary for the cyclic strain-induced translocation of MAL/MKL1 to the nucleus.** (A) Wild type MEF, the fibronectin-expressing clone 1.2 and the fibronectin knockdown clone 8.3 were seeded on either vitronectin (top) or fibronectin (bottom). Two days after plating, cells were cyclically strained for 1 hour and subsequently fixed and stained for MAL. Scale bar is 50  $\mu$ m. (B) Statistical analysis of three independent experiments as depicted in A. For every experiment, 100 cells per condition were analyzed and MAL staining was scored as either nuclear or cytoplasmic. The graph shows the mean percentage of cells with nuclear MAL ( $\pm$  SEM). Light columns represent values before and dark columns values after 1 hour of cyclic strain. (C) The experiment described in A carried out with fibronectin knockout MEF (FN<sup>-/-</sup>) and the matched fibronectin-expressing control cells (FN<sup>f/f</sup>). (D) The statistical analysis described in B carried out on the results from three independent experiments shown in C. Note the absence of MAL translocation in response to cyclic strain in the fibronectin-deficient clones 8.3 and FN<sup>-/-</sup> when plated on vitronectin but not on fibronectin.



**Fig. 5. Tenascin-C mRNA and protein levels are induced by cyclic strain only in the presence of pericellular fibronectin.** (A, B) Wild type MEF (Wt), the fibronectin-expressing MEF clone 1.2 and the fibronectin knockdown MEF clone 8.3 were seeded on (left) vitronectin or (right) fibronectin coated silicone membranes and grown for 48 hours. Cells were then left at rest (R) or subjected to cyclic strain (S) for 6 hours followed by a further 18 hours at rest, during which tenascin-C was deposited into the matrix. (A) Lysates were immunoblotted for fibronectin (FN), tenascin-C (TnC) and vinculin as standard. (B) The ratios of tenascin-C to vinculin were calculated from densitometry measurements on immunoblots from three independent experiments. Light bars represent rest and dark bars strained conditions. (C) Wt, 1.2 and 8.3 cells were seeded on vitronectin (left) or fibronectin (right), cultured for 48 hours as above and then subjected to 1 hour of cyclic strain. Tenascin-C mRNA levels were measured by quantitative PCR relative to GAPDH and normalized to the values of wild type cells at rest. (D) As in C but with fibronectin knockout (FN<sup>-/-</sup>) and control (FN<sup>f/f</sup>) MEF. Due to variation in basal tenascin-C levels, FN<sup>f/f</sup> and FN<sup>-/-</sup> were normalized individually to their respective rest values on vitronectin.

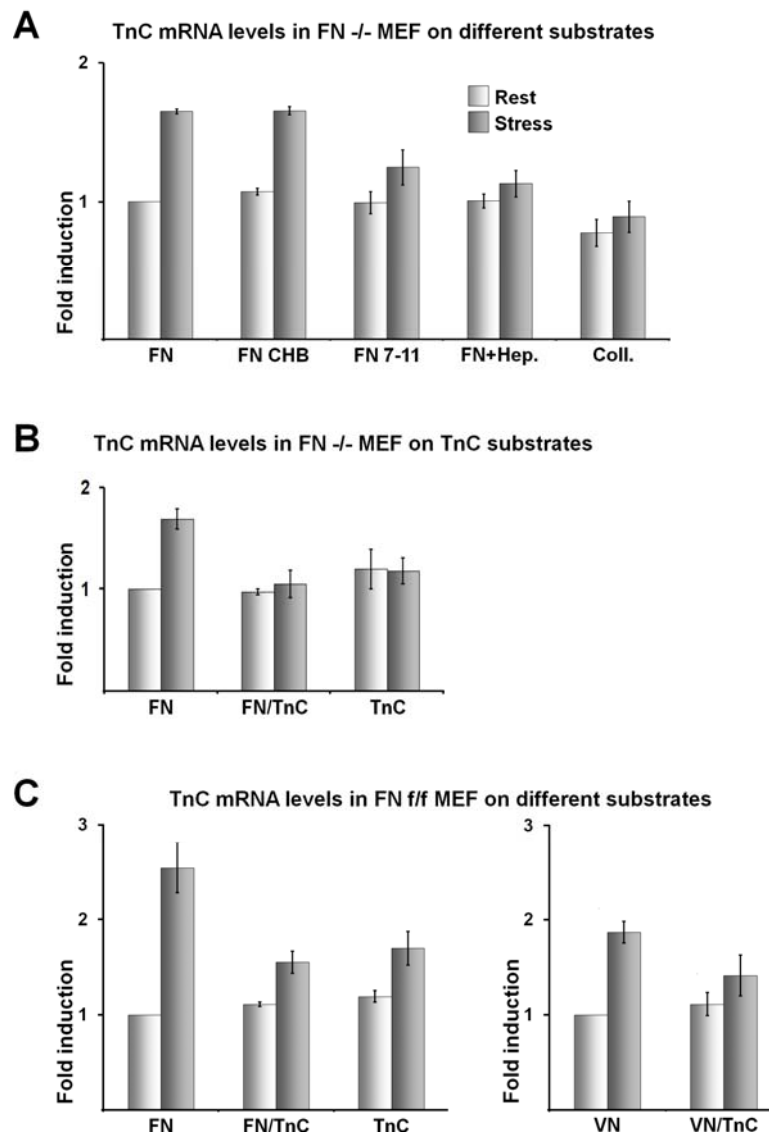


**Fig. 6. Activation of ERK and PKB/Akt by cyclic strain does not depend on the presence of pericellular fibronectin.** As in the previous experiments, fibronectin wild type and deficient MEF were cultured on vitronectin- or fibronectin-coated silicone membranes and cyclically strained for the indicated times (min). **(A)** Immunoblots of ERK and phosphorylated ERK (p-ERK) at rest (0) and after 5 minutes of cyclic strain. **(B)** The ratios of p-ERK to total ERK were calculated from densitometry measurements on immunoblots from three independent experiments. Light bars represent rest and dark bars strained conditions (5 minutes). **(C)** Immunoblot of PKB/Akt and phosphorylated PKB/Akt (p-PKB) at rest (0) and after 10 and 15 minutes of cyclic strain. **(D)** The statistical analysis described in B carried out on the results from three independent experiments shown in C. Light bars represent rest and dark bars strained conditions (10 minutes).



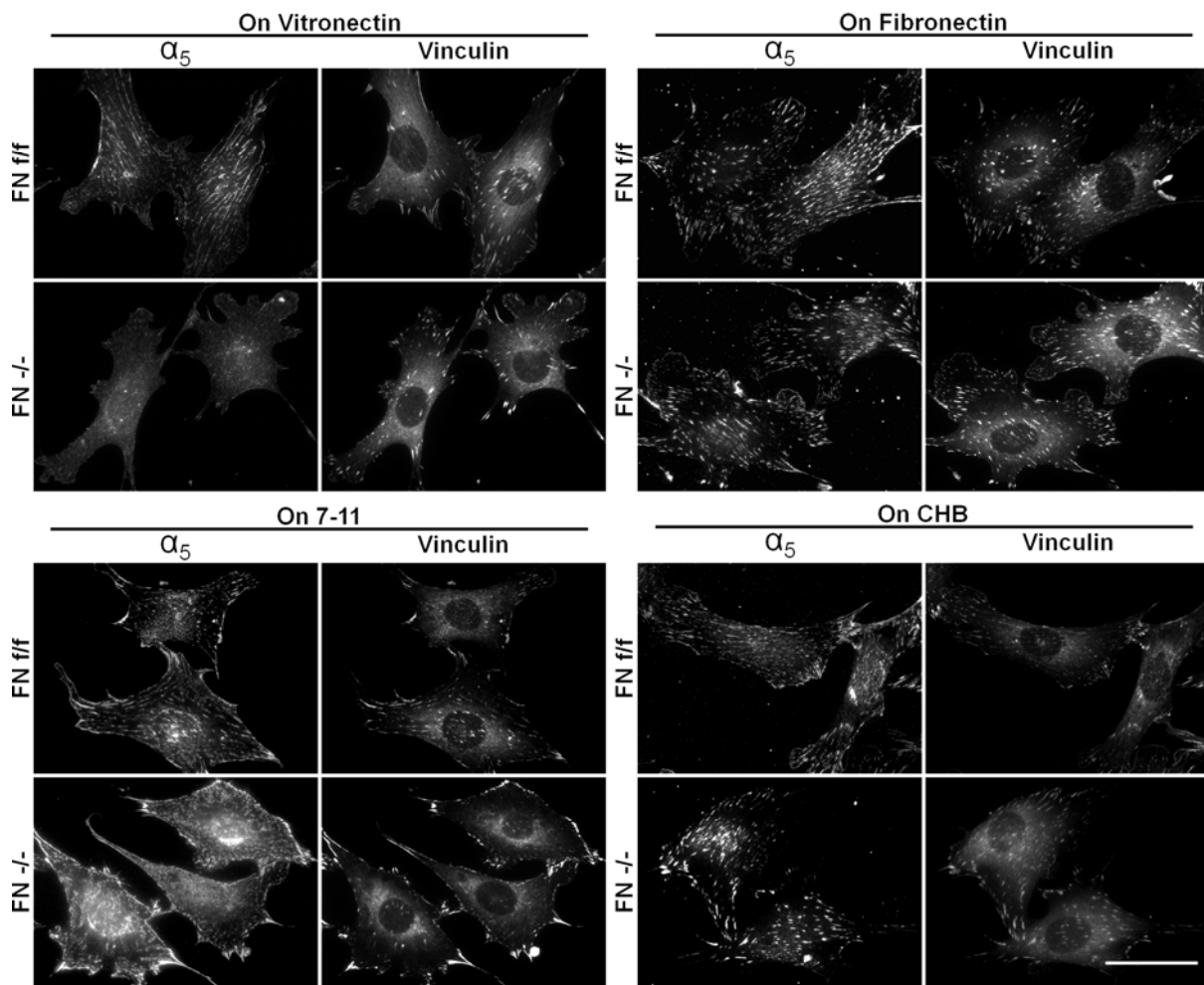
**Fig. 7. Response of rat embryo fibroblasts (REF) to cyclic strain depends on the time endogenous fibronectin has been allowed to accumulate in the matrix.** R2A is a partial fibronectin knockdown clone derived from REF. **(A)** Immunofluorescence staining of actin (red) and endogenous fibronectin (green) of detergent-permeabilized REF and R2A plated on tissue culture plastic. Cells were fixed 24 hours (left) or 48 hours (right) after plating. Scale bar is 50 $\mu$ m. **(B)** REF and R2A were plated on vitronectin or fibronectin and strained for 1 hour after 24 or 48 hours in culture. Induction of tenascin-C mRNA was measured by qPCR. Light columns represent values before and dark columns values after 1 hour of cyclic strain. Note the correlation between fibronectin matrix accumulation on vitronectin and the level of tenascin-C induction in R2A cells.



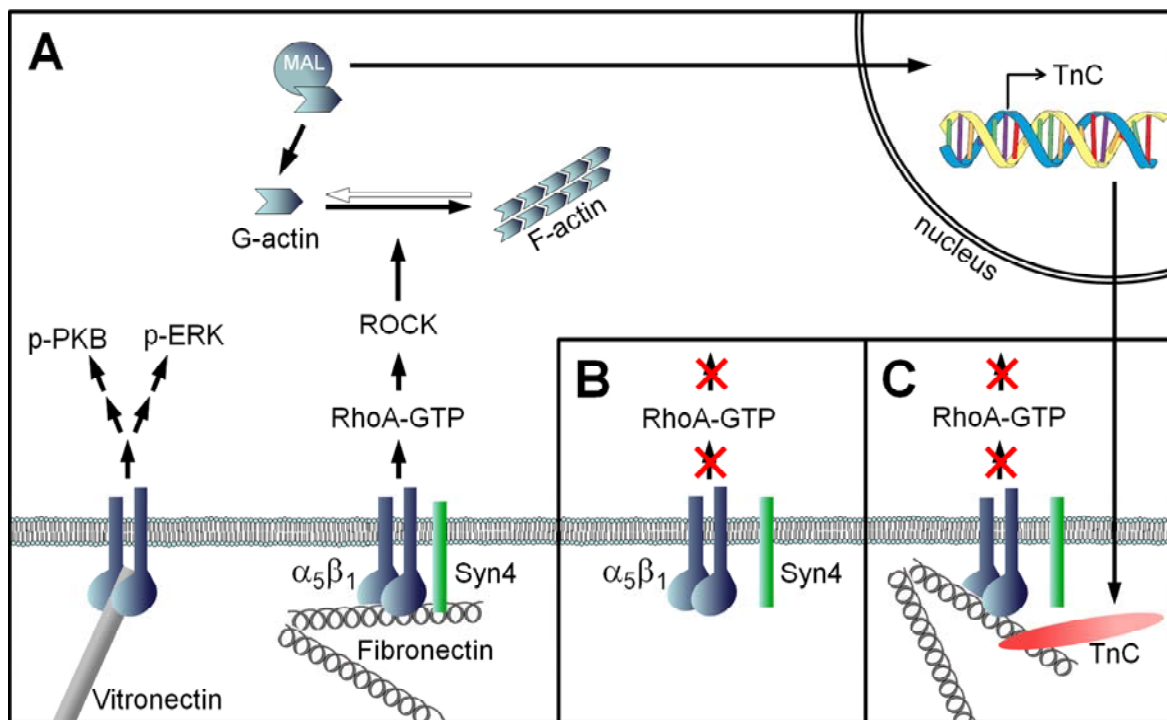


**Fig. 8. The cell binding site and adjacent heparin binding region of fibronectin are necessary for full induction of tenascin-C mRNA by cyclic strain.**

(A) Fibronectin knockout MEF (FN<sup>-/-</sup>) were plated on elastic silicone membranes coated with either fibronectin (FN), fibronectin 160/135 kDa chymotrypsin fragments (FN CHB), fibronectin type 3 domain 7-11 (FN 7-11) or collagen I (Coll) and cultured for 48 hours. In FN+Hep cells were plated on fibronectin and soluble heparin was added at 100  $\mu$ g/ml 24h after plating. For all conditions cells were then kept at rest or subjected to 1 hour of cyclic strain. Tenascin-C mRNA levels were measured by quantitative PCR relative to GAPDH and normalized to the rest-values on fibronectin. Light columns represent values before and dark columns values after 1 hour of cyclic strain. (B) As above but FN<sup>-/-</sup> MEF were plated on elastic silicone membranes coated with either fibronectin (50  $\mu$ g/ml), fibronectin/tenascin-C (50  $\mu$ g/ml / 50  $\mu$ g/ml) or tenascin-C (50  $\mu$ g/ml). (C) As B but fibronectin-expressing MEF (FNf/f) were used. In addition tenascin-C induction was also measured on vitronectin (20  $\mu$ g/ml) or vitronectin/tenascin-C (20  $\mu$ g/ml / 50  $\mu$ g/ml).

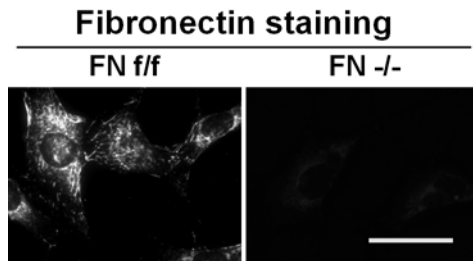


**Fig. 9. Fibronectin-deficient MEF lack integrin  $\alpha_5$ -containing fibrillar adhesions when plated on vitronectin.** Fibronectin-expressing (FNf/f) and deficient (FN-/-) MEF were grown on either vitronectin (upper left), fibronectin (upper right), the fibronectin type III repeat 7-11 fragment (7-11, lower left) or the fibronectin cell and adjacent heparin binding site fragment (CHB, lower right) for 48 hours. Cells were then fixed and subsequently stained for vinculin and  $\alpha_5$  integrin. Note that fibronectin-deficient cells do not form  $\alpha_5$  integrin-containing fibrillar adhesions on vitronectin. Scale bar is 50  $\mu\text{m}$ .



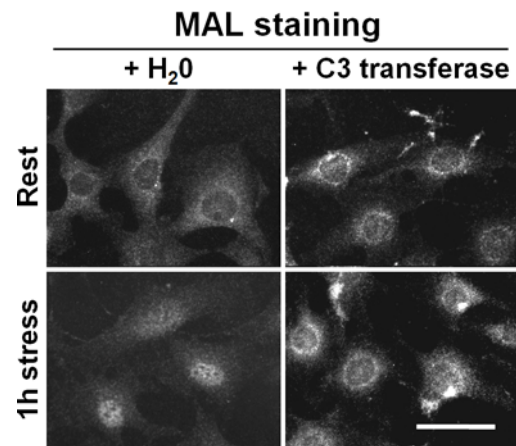
**Fig. 10. Schematic model representing activation of RhoA-mediated responses by cyclic strain and induction of a negative feedback loop.** (A) Phosphorylation of PKB/Akt and ERK by cyclic strain is not dependent on the presence of fibronectin and may be mediated mainly by  $\alpha_v\beta_3$  integrins that are enriched in focal adhesions. Induction of RhoA-mediated responses such as actin reorganization, MAL translocation and upregulation of tenascin-C by cyclic strain require fibronectin, which is mainly bound to  $\alpha_5\beta_1$  in fibrillar adhesions. (B) In the absence of fibronectin these RhoA-mediated responses are not induced. (C) In the presence of fibronectin, the tenascin-C synthesized and deposited in response to cyclic strain may suppress RhoA activation on further mechanical stress and negatively regulate its own induction.

Figure S1



**Fig. S1. Normal MEF cultured on a vitronectin substrate secrete fibronectin and assemble it into a matrix.** MEF were plated on elastic silicone membranes coated with 20  $\mu\text{g}/\text{ml}$  vitronectin and cultured in DMEM containing 3% fibronectin-depleted serum for 48 hours. Cells were subsequently fixed and stained with anti-fibronectin antibody. Scale bar is 50  $\mu\text{m}$ .

Figure S2



**Fig. S2. Cyclic strain-induced translocation of MAL depends on activation of RhoA.** MEF were cultured on fibronectin and starved overnight in low serum. Cell permeable C3 transferase was added at 0.25  $\mu\text{g}/\text{ml}$  30 minutes prior to applying cyclic strain for 1 hour. Cells were subsequently fixed in paraformaldehyde and stained for MAL. Scale bar is 50  $\mu\text{m}$ .

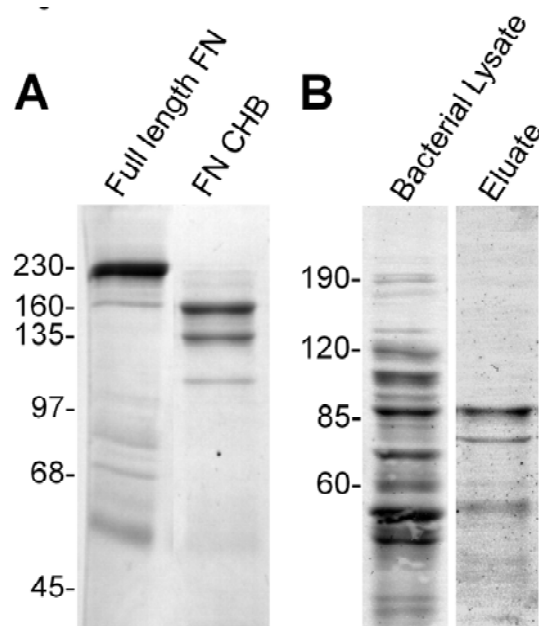


**Fig. S3. Coomassie gels of purified fibronectin type III 7-11 fragment (FN 7-11) and 160/135 kDa chymotryptic fibronectin fragments (FN CHB).** (A) Coomassie gel of full length fibronectin (left) and the chymotryptic fragments appearing in the flowthrough of the gelatin-Sepharose column (right). (B) Coomassie gel of bacterial lysate (left) and the FN 7-11 fragment isolated by adsorption to glutathione-Sepharose. For details of purification, see Materials and Methods.

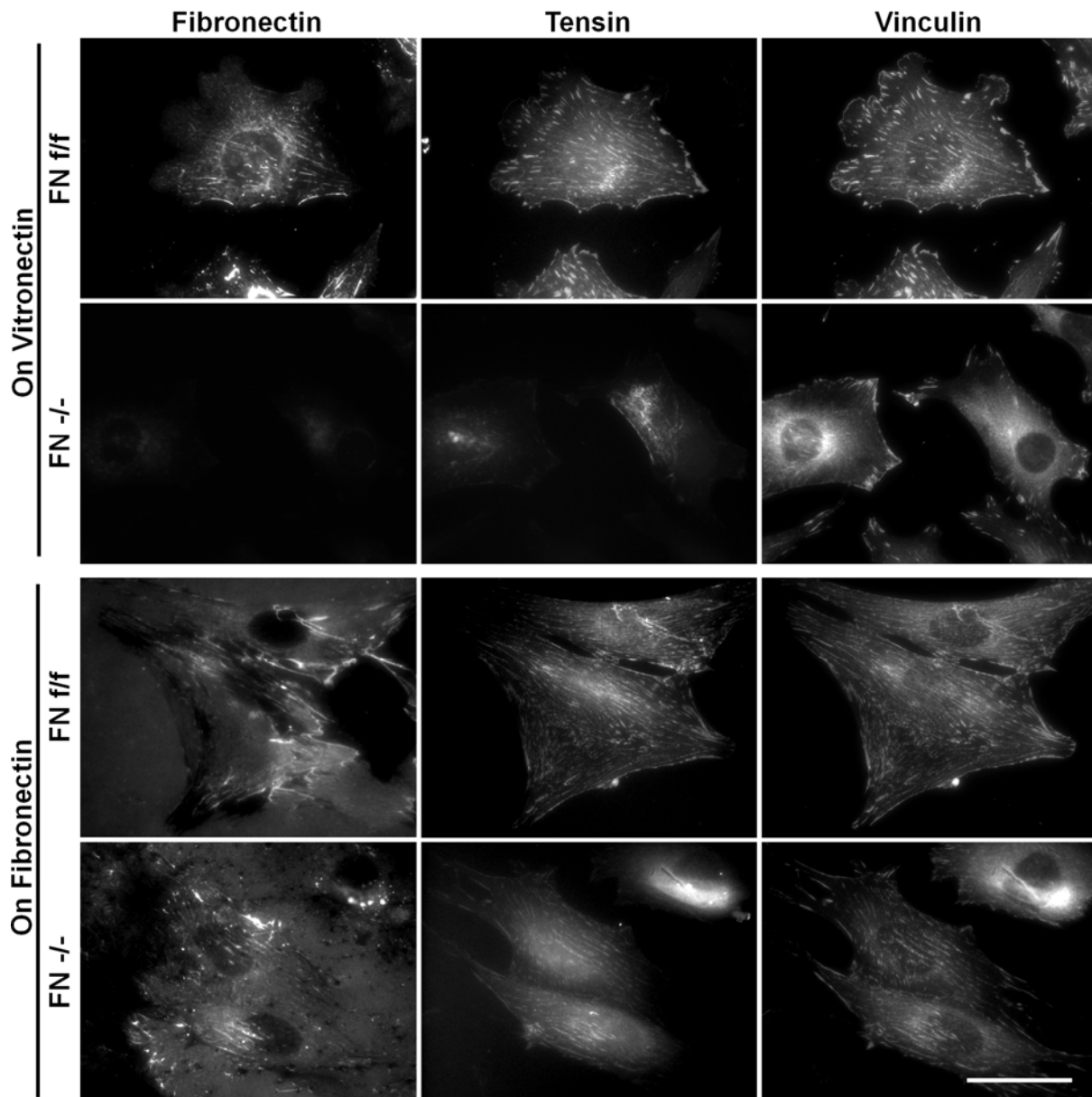


**Fig. S4. Fibronectin-deficient MEF do not form tensin-positive adhesions on a vitronectin substrate.** Fibronectin-expressing (FNf/f) and deficient (FN-/-) MEF were transfected with GFP-tensin and grown on fibronectin or vitronectin-coated glass slides for 48 hours. Cells were then fixed and subsequently stained for vinculin and fibronectin. Normally, tensin and vinculin co-localize in matrix adhesions. However, note that in fibronectin-deficient cells on vitronectin substrate, transfected tensin is not assembled into adhesion sites but forms intracellular aggregates. Scale bar is 50  $\mu\text{m}$ .

## **IV.4 Limiting Growth of Focal Complexes Inhibits their Maturation and Induces Lamellipodia Formation**

Roman Lutz, Kristopher Pataky, Jürgen Brugger, Matthias Chiquet

(Ready for submission)

My contribution: All experiments (except generation of nanopatterned gold substrates: K. Pataky)

## **Limiting Growth of Focal Complexes Inhibits their Maturation and Induces Lamellipodia Formation**

Roman Lutz<sup>1</sup>, Kris Pataky<sup>2</sup>, Jürgen Brugger<sup>2</sup>, Matthias Chiquet<sup>3</sup>

<sup>1</sup> *Friedrich Miescher Institute for Biomedical Research, Basel, Switzerland*

<sup>2</sup> *Ecole Polytechnique Fédérale de Lausanne, Lausanne, Switzerland*

<sup>3</sup> *Department of Orthodontics and Dentofacial Orthopedics, University of Bern, Bern Switzerland*

Corresponding author:

Matthias Chiquet, Ph.D.,  
Department of Orthodontics and Dentofacial Orthopedics  
School of Dental Medicine  
University of Bern  
Freiburgstrasse 7  
CH-3010 Bern, Switzerland  
Phone: +41-31-632-9882  
Fax: +41-31-632-9869  
e-mail: [matthias.chiquet@zmk.unibe.ch](mailto:matthias.chiquet@zmk.unibe.ch)



### IV.4.1 Summary

Cells adhere to substrates by means of cell-matrix adhesions, where integrins join extracellular matrix (ECM) proteins to the intracellular actin cytoskeleton by means of adaptor proteins. In fibroblasts three major types of matrix adhesions can be distinguished. They are assembled in a hierarchical way, thereby gaining in protein complexity and size. However, whether matrix adhesion maturation can be inhibited by restricting their size, and how this affects cell morphology is not known. Using stenciled gold-patterns with covalently linked RGD-peptides in the sub-micrometer range, we managed to restrict matrix adhesion length at different levels between 250 nm and 2  $\mu$ m. Here we show that restriction of matrix adhesion growth to a length of 500 nm or less lead to a disruption in maturation of focal complexes into focal adhesions, as indicated by poor recruitment of  $\alpha_5$  integrin to these adhesion sites. Fibroblasts on such nano-patterned substrates were absent in classical fibrillar adhesions and showed altered fibronectin fibrillogenesis. In addition, cells remained roundish, formed excessive numbers of lamellipodia, and polymerized actin only into a fine meshwork but lacked stress fibers. However, migration speed was clearly reduced versus fibroblasts on 2000 nm RGD-coupled gold pattern. The method of RGD-coupled gold-patterns presented here constitutes a powerful tool to manipulate cell attachment. Our results indicate that specific signaling deriving from focal complexes affect actin dynamics at a basic level which influences cell morphology, cell adhesion maturation, fibronectin fibrillogenesis and migration.

## IV.4.2 Introduction

Cell adhesion to a substrate is mediated via adhesion receptors, mainly integrins, that play key roles in transmembranal signaling processes regulating cell behavior and fate (Geiger et al., 2009). Integrins are composed of type I transmembrane  $\alpha$  and  $\beta$  subunits that bind, depending on their composition, a variety of extracellular matrix proteins with different affinity. Intracellularly, integrins are linked to the actin cytoskeleton by means of specialized adaptor proteins (Zamir and Geiger, 2001). Most of the latter contain multiple domains through which they can interact with different molecular partners, forming a dense and heterogenous protein network. Recruitment of adaptor proteins into adhesion sites depends on competition, conformational state and tyrosine phosphorylation of potential binding partners (Zamir and Geiger, 2001). Interaction partners also involve kinases like Src and FAK that build a platform for early steps of signaling by various pathways. At cell-matrix adhesion sites fibroblast constantly integrate mechanical stimuli into chemical signals. A signaling cascade that is well established to be activated by mechanical stimuli is the RhoA/ROCK pathway (Sarasa-Renedo et al., 2006; Smith et al., 2003). RhoA is a small GTPase that promotes actin stress fiber formation when activated. Evidence is growing that integrin  $\alpha_5\beta_1$  and its ligand fibronectin are responsible for activation of RhoA by mechanical signals (Danen et al., 2002; Lutz et al., 2010). Rac, another Rho-family GTPase, is seen as an opponent of RhoA (Rottner et al., 1999) stimulating the assembly of a fine meshwork of actin filaments at cell borders and the production of extending lamellipodia (Hall, 1998; Nobes and Hall, 1995). A lamellipodium represents the “leading edge” of a moving or spreading cell and is the birthplace of cell-matrix adhesions called focal complexes. These small, dot-like adhesions are less than  $1 \mu\text{m}^2$  in area and characterized by the colocalization of  $\alpha_v\beta_3$  integrin, paxillin, talin, vinculin, FAK and phosphotyrosine (Geiger et al., 2001; Harjanto and Zaman,

; Wolfenson et al., 2009). Focal complexes are highly ephemeral, and either disassemble or mature into focal adhesions by growing in size and recruiting additional proteins like zyxin, tensin, and  $\alpha_5\beta_1$  integrin. This maturation is dependent on myosin-II and can be arrested with inhibitors of the RhoA/ROCK pathway (Alexandrova et al., 2008; Wolfenson et al., 2009). Further traction on focal adhesions by means of the actin cytoskeleton pulls out  $\alpha_5\beta_1$  integrin and tensin from them, initiating the formation of fibrillar adhesions (Zamir et al., 2000). During this process fibronectin bound to  $\alpha_5\beta_1$  is stretched and exposes self-assembly sites leading to the formation of fibronectin fibrils. As described above, the different cell-matrix adhesions are assembled in a hierarchical way. The results presented in this article show that cell-matrix adhesion maturation can be arrested by restricting their size and hence their growth. This affects cell morphology, the actin cytoskeleton, fibronectin fibrillogenesis, the recruitment of  $\alpha_5$  integrin into adhesion sites and migration behavior suggesting a distinct signaling from the different stages of cell-matrix adhesions during maturation.

### IV.4.3 Results

#### Design of the gold-pattern

During cell adhesion and migration fibroblasts form cell-matrix adhesions in a hierarchical manner (Zaidel-Bar et al., 2004). Thereby these adhesions evolve through different stages, each with different protein composition, shape and size. We asked whether preventing cells from forming adhesion sites above a certain size would inhibit the maturation of focal complexes to focal adhesions. To this aim, cells were grown on gold square patterns in the sub-micrometer range that were applied to glass surfaces with a nanostencil technique (ref). While the area surrounding the gold squares was passivated with PLL-PEG, RGD peptide was covalently linked to the gold to provide restricted and integrin-specific cell attachment.

Four different patterns with gold squares ranging from 250 nm to 2000 nm were designed (figure 1). To ensure that cells on different patterns always had the same area to attach, the patterns were designed in a way that the surface area of RGD-coupled gold was fixed to 25% of the total substrate area. Thereby the only difference between the patterns was the distribution of adhesive RGD-gold ligand. For controls, cells were plated on plain (i.e. unpatterned) RGD-gold or on plain PLL-PEG passivated glass.

### **Cells form adhesion sites only on RGD-coupled gold areas.**

Gold patterns were coupled with 3 mg/ml RGD solution for 24 hours and subsequently passivated with 0.2 mg/ml PLL-PEG in PBS for 2 hours. Patterns were then washed several times with PBS, and mouse embryo fibroblasts (MEF) were plated in 3% FCS/DMEM. The FCS used was depleted of fibronectin to reduce deposition of this adhesive glycoprotein to the passivated areas. Cells were allowed to attach and spread for 4 hours, and subsequently fixed with paraformaldehyde and stained for vinculin (figure 2). Besides the staining around the nucleus that was found on all surfaces, staining for vinculin on plain gold was found in elongated cell adhesions primarily at the cell border with radial orientation towards the cell center. On the 2000 nm and 1000 nm pattern vinculin stained cell adhesion sites that were located on top of the RGD-coupled gold squares. A more intense staining was usually detected in adhesion sites (focal adhesions) in the periphery. However it was also present in more central cell adhesions. On the 250 nm and 500 nm patterns vinculin was assembled in small cell adhesions (focal complexes) around lamellipodias. On all patterns, cell adhesions that stained for vinculin were located on areas coated with RGD-coupled gold. In the absence of gold or without coupling of RGD, cells did neither attach nor spread to the passivated substrate (not shown).

**MEF show an altered morphology on RGD-coupled gold squares smaller than 1000 nm.**

By plating and growing fibroblasts on gold patterns as described in figure 2, we found clear differences in cell morphology on the different patterns already by looking at the cells with a light microscope. To analyze cell-shape more precisely, we fixed cells after 4 hours and co-stained fibroblasts for vinculin and actin. On plain gold as well as on the 2000 nm and the 1000 nm pattern, cells were well spread 4 hours after plating (figure 3). Fibroblasts were polarized with usually 3 to 7 processes and few (1-2) lamellipodia. However, on the 500 nm and the 250 nm pattern the cell morphology changed drastically. Cells assumed a phenotype with an average of 4 to 7 extended lamellipodia per cell but no spike-like processes. Lamellipodia did not localize to a specific side of the cell but rather formed all around the perinuclear cell body. On the 500 nm and the 250 nm pattern cells were also less elongated with an average maximal long axis of 50  $\mu\text{m}$ . The larger the gold-squares of the pattern, the larger the maximal long axis was measured and reached about 100  $\mu\text{m}$  on plain gold.

**Fibroblasts on RGD-coupled gold squares smaller than 1  $\mu\text{m}^2$  form an actin meshwork rather than thick actin stress fibers.**

We found clear differences the number of lamellipodia in fibroblasts grown on different gold pattern (figure 3) and cells showed a different morphology (figure 2). Since actin structures are largely involved in these processes, we wanted to analyze the actin cytoskeleton more precisely. To this aim we prepared gold pattern and plated, grew and fixed fibroblasts as described in figure 2. Cells were then stained with alexa labeled phalloidin and analyzed by fluorescence microscopy. In fibroblasts on plain gold we found thick actin fibers throughout the cell often bundled in the cell center forming actin foci (figure 4). Also on the 2000 nm pattern thick actin structures were identified. Some spanned through the cell but most of them were found along the cell border. This might be a reason why actin foci were hardly found on

these patterns. Fibroblasts on the 1000 nm pattern only exhibited thick actin fibers at the cell border. More proximal actin structures were rather fine but still aligned in a parallel fashion. On the 250 nm and 500 nm pattern thick actin fibers were basically absent. In some cells actin bundles of average thickness were found along the cell border between lamellipodia. However most of the actin was polymerized into a fine meshwork in the lamellipodias and also in the cell body. To quantify our observations, images from three independent experiments with a total of around 50 cells per pattern were used. The threshold of the 8-bit pictures was set at 150 and remaining visible structures with a fibrillar shape were counted as actin stress fibers. The number of these actin fibers increased from almost zero on the 250 nm and 500 nm patterns up to 5 prominent actin fibers in average on plain gold (figure 4 lower panel). The length of these structures gradually increased from 10  $\mu\text{m}$  on the 250 nm pattern to 40  $\mu\text{m}$  on plain gold.

**MEF on RGD-coupled gold squares smaller than 1  $\mu\text{m}^2$  only form short and thin fibronectin fibrils.**

Fibronectin fibrillogenesis is dependent on actomyosin contraction (Wierzbicka-Patynowski and Schwarzbauer, 2003). Since cells on the 250 nm and 500 nm pattern assembled actin into a meshwork rather than forming actin fiber bundles, we asked whether these cells might be able assemble fibronectin into fibrils. Therefore we grew cells on RGD-coupled gold pattern as described in figure 2. Cells were fixed with paraformaldehyde 4 hours after plating and subsequently stained with anti fibronectin antibody (figure 5). Within this short time fibroblasts on plain gold as well as on the 2000 nm and 1000 nm pattern assembled their secreted fibronectin into a few relatively thick fibrils per cell. The fibrils reached a length of 15 to 30  $\mu\text{m}$  in average. Conversely, on the 500 nm and the 250 nm pattern cells assembled more but thin and short fibronectin fibrils. To quantify our results fibrils with a length above

3  $\mu\text{m}$  were scored. On the 250 nm and the 500 nm patterns, cells formed in average 6-7 fibrils with a size longer than 3  $\mu\text{m}$ . On the patterns larger than 500 nm these numbers gradually decreased. However, fibronectin fibrils increased in length. Especially on the small patterns (250 nm and 500 nm) a large number of fibrils shorter than 3  $\mu\text{m}$  were observed. However they were often difficult to distinguish from plaque-like fibronectin aggregates and therefore not included for quantification.

**Integrin  $\alpha_5$  is poorly recruited to matrix adhesions if fibroblasts are plated on RGD-coupled gold squares smaller than 1000 nm.**

Maturation of focal complexes into early focal adhesion is accompanied with a recruitment of  $\alpha_5$  integrin (Zaidel-Bar et al., 2004). In a later stage  $\alpha_5$  integrin is pulled out of early focal adhesions to form fibrillar adhesions leaving late focal adhesions behind with low incorporation of integrin  $\alpha_5$  (Zamir et al., 2000). However  $\alpha_5$  is largely absent from focal adhesions. To analyze the localization of  $\alpha_5$  integrin and to confirm that the small structures detected in fibroblasts on the 250 nm and 500 nm pattern are focal complexes, we observed  $\alpha_5$  integrin by immunofluorescence. To this aim we grew fibroblasts on gold patterns as described in figure 2 and stained cells with an anti integrin  $\alpha_5$  antibody (figure 6). On plain gold as well as on the 2000 nm and 1000 nm pattern, MEF bridged neighboring RGD-gold squares by pulling out  $\alpha_5$  integrin as fibrillar adhesions. Thus, cells overcame growth-restriction of fibrillar adhesions given by pattern. However focal adhesions were still localized to RGD-gold only as seen by the vinculin staining (figure 2). In contrast, on RGD-coupled patterns with dot size smaller than 1000 nm, staining for  $\alpha_5$  integrin in matrix adhesions was clearly decreased. A small amount of  $\alpha_5$  integrin was still found in short fibrillar structures. These structures entirely colocalized with the small fibronectin fibrils seen in figure 5 (not shown).

**Fibroblasts show decreased motility on 500 nm versus 2000 nm RGD-coupled gold squares.**

Fibroblasts on RGD-coupled gold pattern smaller than 1000 nm showed excessive amounts of lamellipodia (figure 3). These structures are found at the leading edge of migrating cells (Hall, 1998). To investigate if these high amounts of lamellipodia also lead to increased motility we plated fibroblasts on RGD-coupled gold patterns (500 nm and 2000 nm) as described in figure 2 and pictured the cells by time-lapse microscopy for 6 hours (see supplementary video). On both patterns it took 1-2 hours until the cells started to flatten and form cell protrusions. These cell protrusions were highly dynamic and found around the cell in different patterns every 2 ½ minutes when a new picture was made. In contrary to cells on the 500 nm pattern that remained in this phenotype, fibroblasts on the 2000 nm pattern assumed a more spread and elongated shape 3 hours after plating. These cells also started to pull themselves along the substrate 3-4 hours after plating. Interestingly, despite the high amounts of lamellipodia found in fibroblasts on 500 nm patterns (figure 3), cells hardly changed position on this substrate. To analyze this phenomenon more precisely we tracked cells 3 hours after plating for 3 hours and thereby determined their speed. For every pattern 3 independent experiments were performed and 12-15 cells per experiment were tracked. The speeds of all cells analyzed are represented in a box plot (figure 7A). Cell tracks of one experiment on each pattern are represented by tracking plots (figure 7B). A representative cell on both the 500 nm and the 2000 nm pattern are shown at 2, 3, 4, 5 and 6 hours after plating (figure 7C). The cell on the 500 nm pattern remains roundish with branching lamellipodia all around the cell body. On the 2000 nm pattern the cell assumes an elongated shape



#### IV.4.4 Discussion

In the present study we used RGD-coupled gold pattern of different sizes to restrict growth of matrix adhesions to 250 nm, 500 nm, 1000 nm and 2000 nm in length and compared them to cells plated on plain RGD-coupled gold. The coverage of RGD-coupled gold on all patterns was set to 25%, making the patterns different only by the size and distribution of adhesive spots. Thereby we showed that limiting cell adhesion size affects cell morphology, the actin cytoskeleton, fibronectin fibrillogenesis. The separation between two different types of cell morphologies occurred between the 500 nm and the 1000 nm pattern. Localization, size and  $\alpha_5$  integrin content of matrix adhesions formed suggest that cells on a pattern smaller than 1000 nm only form focal complexes while on patterns  $\geq 1000$  nm cells are able to mature these focal complexes into focal adhesions. This maturation is accompanied by formation of thick actin fibers, an elongated spreading of the cells, and the generation of long fibrillar adhesions that lead to pronounced fibronectin fibrillogenesis. Analysis of the migration behavior of cells on patterns smaller than 1000 nm showed that fibroblasts rapidly formed and retracted many lamellipodia, however, cells failed to move in a preferred direction. This may be caused by the lack of cell polarization and the absence of strong actin fibers allowing the cells to be pulled along the substrate.

The process of cell-matrix adhesion formation and maturation has been discussed extensively (Wolfenson et al., 2009; Zaidel-Bar et al., 2004; Zamir et al., 2000). However, little is known about specific signaling deriving from the distinct stages of cell adhesions. Several studies describe induction of lamellipodia and focal complexes by activation of Rac (Hall, 1998; Machesky and Hall, 1997; Nobes and Hall, 1995). In our experiments, fibroblasts showed extensive formation of lamellipodia after plating them on our 250 nm and 500 nm patterns, indicating that the formation of only focal complexes but not focal and fibrillar adhesions

was stimulated by these substrate features. This suggests an activation of Rac1 caused by focal complexes rather than vice versa. However, Rac was demonstrated to induce new substrate contacts at the cell front, which are associated with the formation of lamellipodia, whereas RhoA serves in the maturation of existing contacts (Rottner et al., 1999). It is becoming more and more evident that  $\alpha_5\beta_1$  integrin bound to its ligand fibronectin is an initiator of RhoA activation upon plating (Danen et al., 2002; Huvneers et al., 2008) and in response to cyclic strain (Lutz et al., 2010). Integrin  $\alpha_5\beta_1$  is hardly found in focal complexes but is recruited upon their maturation into focal adhesions (Harjanto and Zaman). Activation and signaling through  $\alpha_5\beta_1$  integrin bound to fibronectin would thereby induce RhoA activation leading to actin stress fiber formation and contraction. Actin contraction on the other hand then causes fibrillar adhesion formation and fibronectin fibrillogenesis (Zamir et al., 2000). The large numbers of lamellipodia that fibroblasts form on our 250 nm and 500 nm pattern could be explained by the lack of maturation of focal complexes into  $\alpha_5\beta_1$  containing focal adhesions. Low levels of  $\alpha_5\beta_1$  would cause low activation of RhoA, facilitating further Rac1-dependent lamellipodia formation. This hypothesis is supported by the fact that cells spread more extensively and rapidly when plated on fibronectin than on RGD peptide or vitronectin. On fibronectin,  $\alpha_5\beta_1$  is recruited earlier into focal complexes (unpublished observations), probably leading to a faster cell adhesion maturation and RhoA activation. On substrates different from fibronectin (e.g. collagen, vitronectin) cell spreading can be improved and accelerated by addition of high serum (unpublished observation), which is known to induce RhoA activation (Ren et al., 1999; Sarasa-Renedo et al., 2006). In fact, also cells on the 250 nm and 500 nm RGD-gold patterns changed their phenotype into fully spread cells that could not be distinguished from cells on plain RGD-gold within 24 hours (not shown). Deposition of cellular fibronectin and/or activation of RhoA independently of integrin  $\alpha_5\beta_1$  are likely reasons.

Deficiency of RhoA-activation by cyclic strain in the absence of fibronectin correlated with the lack of fibrillar adhesions (Lutz et al., 2010). Fibroblasts on our 250 nm and 500 nm pattern did not show classical fibrillar adhesions and lacked stress fibers, indicating low RhoA activation. In addition, assembly of fibronectin fibrils on these patterns was clearly affected as only fine short fibrils were found. A similar finely weaved meshwork of fibronectin fibrils was found in endothelial cells upon siRNA silencing of RhoA (Fernandez-Sauze et al., 2009). Together these data indicate that limitation of matrix adhesion size to 500 nm clearly diminishes incorporation of  $\alpha_5\beta_1$  integrin. This might be the reason for an ablated RhoA activation, which is crucial for maturation of focal complexes into focal adhesions, the generation of actin stress fibers, fibrillar adhesions, and a fibronectin matrix consisting of thick long fibers.

In this study we showed that focal complex maturation can be inhibited by limiting matrix adhesion size to a length of less than  $1 \mu\text{m}^2$  by means of RGD-coupled gold patterns. However, inhibition of fibrillar adhesion formation once focal adhesions have formed does not seem to occur with this substrate patterning method. A reason for this might be the fibronectin secreted by adhering fibroblasts and its ability to be stretched and self-assembled into fibrils, allowing old sites of cell attachment to be bridged and new to be formed. Fibronectin knockout cells may help to override this problem, but attempts failed to get such cells attached on our RGD-gold patterns (not shown). It might be possible that a total absence of fibronectin and the consequential lack of  $\alpha_5\beta_1$  integrin recruitment would cause a drop in activation of RhoA below the level needed for cell attachment. However, formation of fibrillar adhesions is clearly inhibited upon limitation of matrix adhesion size to 500 nm indicating that preceding maturation into focal adhesions is necessary for this process.

## IV.4.5 Material and Methods

### Cell culture

Kidney MEF cells were maintained at 37 °C with 6% CO<sub>2</sub> in Dulbecco's modified Eagle medium D-MEM; Seromed, Basel, Switzerland) containing 10% fetal calf serum (FCS; Gibco/Invitrogen, Basel, Switzerland).

### RGD-coupling of gold patterned coverslips

Patterned coverslips were cleaned in a UV-ozone photoreactor (PR-100, UVP, Upland, CA) for 30 minutes. Each coverslips was then placed in a 60 $\mu$ -dish (35mm, high) from Ividi (Vitaris, Baar, Switzerland) and subsequently coated with a solution of the peptide Gly-Arg-Gly-Asp-Ser (GRGDS) (Polypeptide, Boulogne, France) at 3 mg/ml in water for 24 hours. Patterns were then washed 3 times with PBS and passivated with PLL-PEG in water at 0.2 mg/ml for 2 hours. PLL-PEG solution was extensively washed away with PBS and the PBS was then again changed with D-MEM. Fibronectin free FCS was added at 3% and fibroblasts were seeded. Dishes were then kept at 37°C and 6% CO<sub>2</sub> for 4 hours. Cells were then fixed with 4% paraformaldehyde for 10 minutes.

### Plating of cells

For cyclic strain experiments, silicone membranes of Flexercell II 6-well plates were coated for 3 hours with purified horse serum fibronectin at 100  $\mu$ g/ml in Dulbecco's phosphate buffered saline (PBS) (Chiquet et al., 2004). Alternatively silicone membranes were coated with vitronectin at 20  $\mu$ g/ml (Abcam, Cambridge, UK) for 90 minutes and then allowed to air dry. In some experiments tenascin-C, purified from chick embryo fibroblast conditioned medium (Chiquet-Ehrismann et al., 1988), was mixed with fibronectin or vitronectin during

coating. For immunofluorescence experiments, 40'000 cells and, for biochemical experiments 90'000 cells were plated in DMEM containing 3% FCS depleted of fibronectin by two passages over gelatin-Sepharose (Amersham, Wädenswil, Switzerland). Cells were allowed to attach, spread and deposit their own matrix for 20 h. After washing with serum-free medium, cells were starved for a further 20 hours in DMEM containing a low concentration of fibronectin free serum (0.03% for determining tenascin-C protein and mRNA, 0.3% for all other experiments) and cells were subsequently subjected to cyclic strain in this medium. For analyzing tenascin-C deposition into the matrix, cells were kept in culture for a further 18 hours after stretching.

### **Immunofluorescence and phalloidin staining**

Patterned cover slips with attached, fixed cells were permeabilized and passivated at room temperature for 30 minutes in PBS solution containing 3% BSA and 0.1% Triton-X100 (Sigma, Buchs, Switzerland). Rabbit polyclonal antiserum to horse serum fibronectin (cross-reacting with mouse) (Wehrle and Chiquet, 1990) was described previously. Cells were then stained for 1 hour at room temperature with one or several of the following antibodies in PBS containing 3% BSA and 0.1% Triton-X100: Anti-fibronectin antiserum diluted 1:300, anti  $\alpha_5$  integrin diluted 1:500 (BD Pharmingen, Basel, Switzerland), anti-vinculin diluted 1:1000 (Sigma, Buchs, Switzerland), Alexa546-labeled phalloidin (Sigma, Buchs, Switzerland). After staining cells were washed three times with PBS/0.1% TritonX100 and incubated for 1 hour with one or several of the following secondary antibodies: Alexa488-labeled goat anti rabbit IgG, Alexa488-labeled goat anti mouse IgG, Alexa488-labeled goat anti rat IgG, Alexa633-labeled goat anti rabbit (all from Sigma, Buchs, Switzerland). Cells were again washed three times with PBS/0.1% Triton-X100 and mounted in Prolong Gold antifade reagent (Invitrogen, Basel, Switzerland). Slides were examined with a Zeiss Z1 microscope

equipped with a 20x/0.8 objective, Zeiss filter cubes n°38HE for Alexa488, n°43 for Alexa546 and a Zeiss MRm camera.

## IV.4.6 Figures with legends

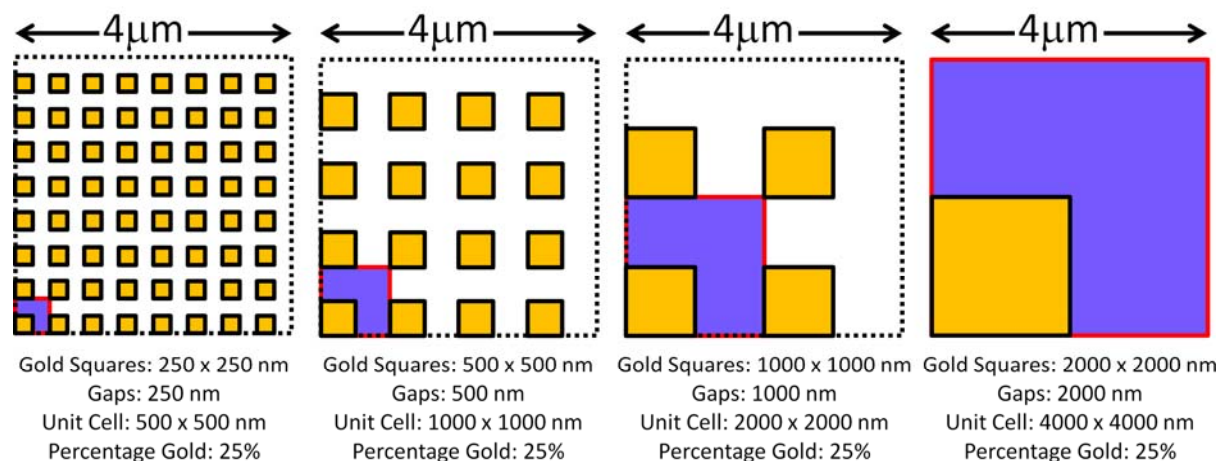


**Fig. 1. Design of gold pattern.**

Gold squares of the indicated sizes were applied to glass surfaces by a nanostencil technique (see material and methods). RGD peptides were then covalently linked to the gold to provide restricted and integrin-specific cell attachment. Background was passivated with PLL-PEG. Unit cells are shown in blue with red frames. Gold squares are represented in gold with black frames. Mind that the patterns were designed in a way that the surface area of RGD-coupled gold was fixed to 25% of the total area.

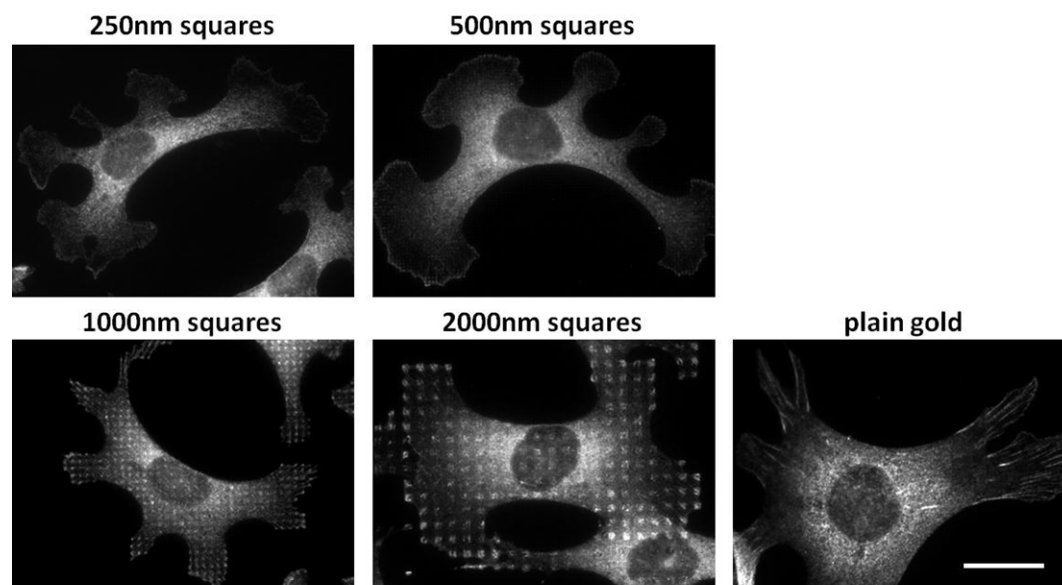


**Fig. 2. Fibroblasts form adhesion sites only on RGD-coupled gold areas.**

Cells were grown on RGD-coupled gold patterns for 4 hours with 3% fibronectin free serum and subsequently fixed and stained with an anti-vinculin antibody. Notice that vinculin in cell adhesions is restricted to gold nano and microsquares while on plain gold restriction omits. Scale bar is 20  $\mu\text{m}$ .

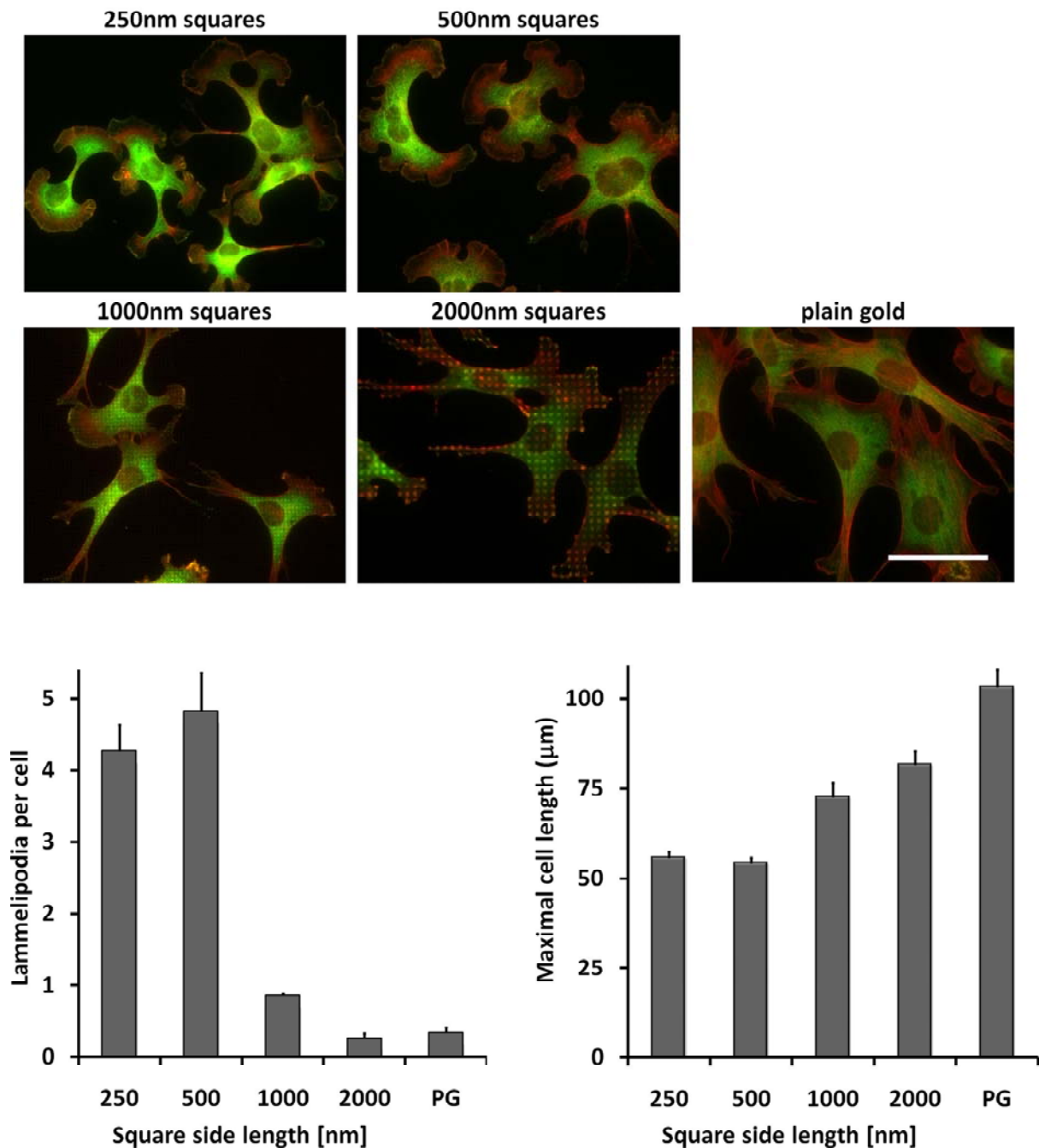


**Fig. 3. Fibroblasts on RGD-coupled gold squares smaller than  $1 \mu\text{m}^2$  show an altered morphology.**

Cells were grown on RGD-coupled gold patterns for 4 hours with 3% fibronectin free serum and subsequently fixed and stained with alexa-labeled phalloidin (red) and anti-vinculin antibody (green). Note the high number of lamellipodia on the 250 nm and the 500 nm patterns in the image as well as in the graph (bottom left). Also maximal cell length was much shorter on these patterns (bottom right). PG = Plain gold. Scale bar is  $50 \mu\text{m}$ .



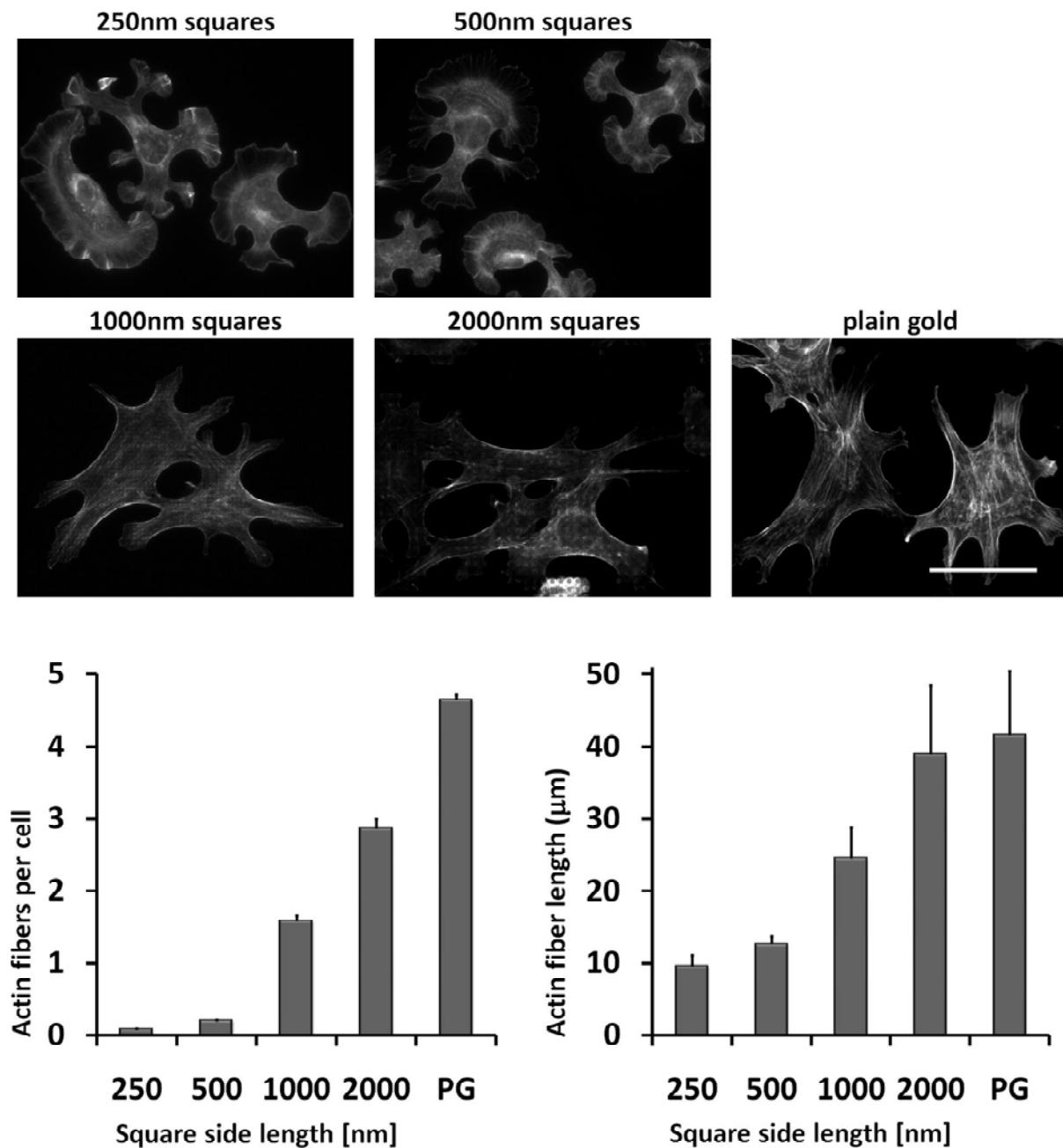


**Fig. 4. Fibroblasts on RGD-coupled gold squares smaller than  $1 \mu\text{m}^2$  form an actin meshwork rather than thick actin stress fibers.**

Cells were grown on RGD-coupled gold patterns for 4 hours with 3% fibronectin free serum and subsequently fixed and stained with alexa-labeled phalloidin. For quantification an intensity threshold was set to determine stress fibers from remaining actin structures. Notice the increased number (bottom left) and length (bottom right) of actin stress fibers on patterns  $\geq 1 \mu\text{m}^2$  and on plain gold (PG). Scale bar is  $50 \mu\text{m}$ .

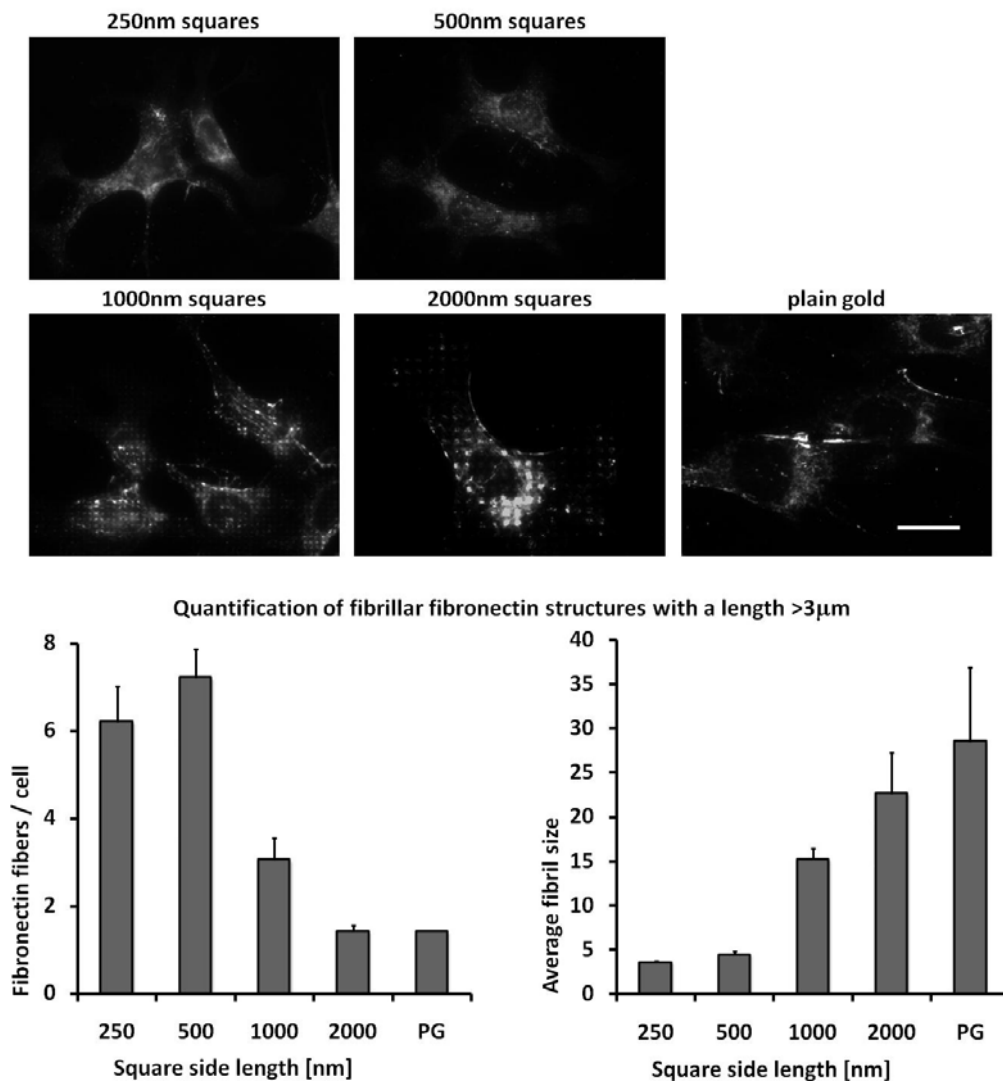


**Fig. 5. Fibroblasts on RGD-coated gold squares smaller than  $1\mu\text{m}^2$  only form short and thin fibronectin fibrils.**

Cells were grown on RGD-coupled gold patterns for 4 hours with 3% fibronectin free serum and subsequently fixed and stained with an anti fibronectin antibody. Be aware of detecting long fibronectin fibrils only on patterns  $\geq 1\mu\text{m}^2$  and on plain gold (PG). Quantifications of the length (bottom right) or number (bottom left) of fibronectin fibrils with a length  $> 3\mu\text{m}$  per cell are shown by graphs. Scale bar is  $20\mu\text{m}$ .

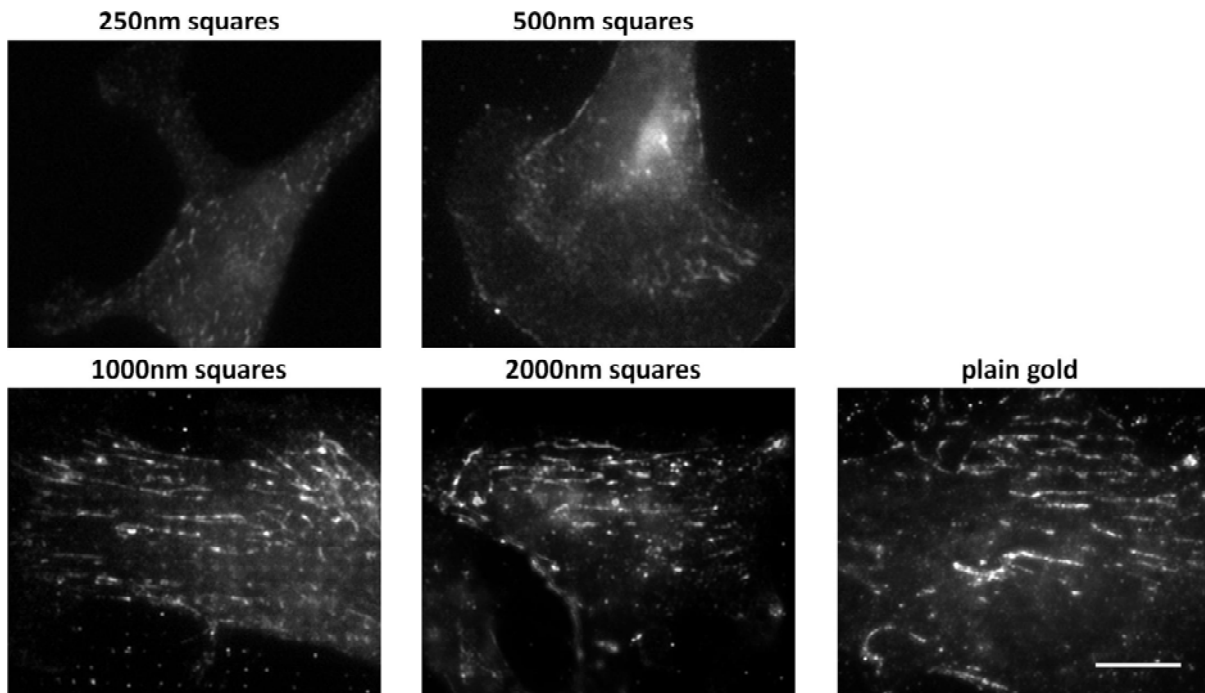


**Fig. 6. Integrin  $\alpha_5$  is poorly recruited to matrix adhesions if fibroblasts are plated on RGD-coupled gold squares smaller than 1000 nm.**

Cells were grown on RGD-coupled gold patterns for 4 hours with 3% fibronectin free serum and subsequently fixed and stained with an anti  $\alpha_5$  integrin antibody. Notice that  $\alpha_5$  integrin is localized in fibrillar adhesions on plain gold and on patterns  $\geq 1 \mu\text{m}^2$  while on smaller patterns it is only modestly recruited into cell adhesions. Scale bar is 10  $\mu\text{m}$ .

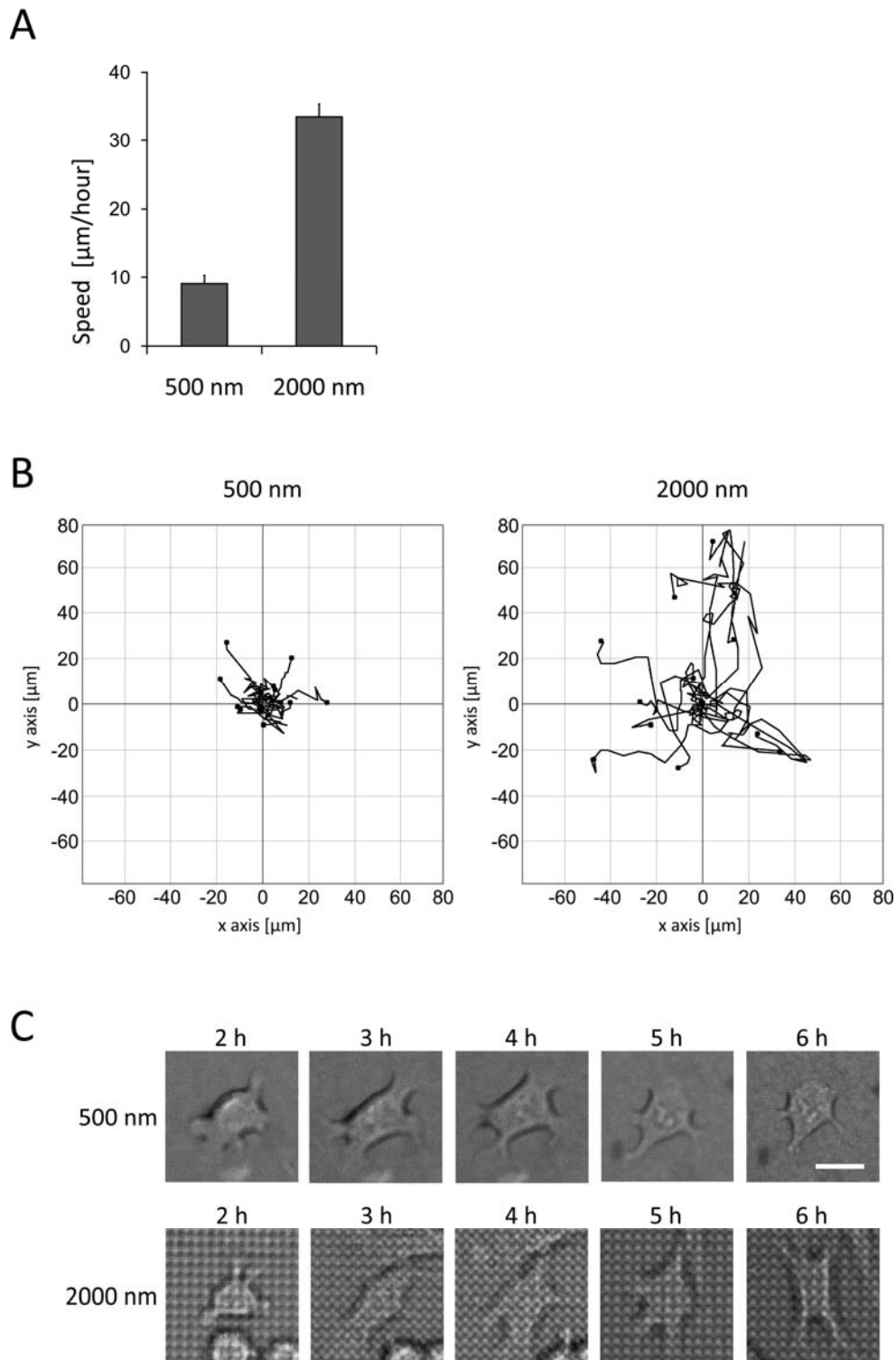


**Fig. 7. MEF migration speed is decreased on 500 nm versus 2000 nm RGD-coupled gold squares.** Cells were plated on RGD-coupled gold patterns in 3% fibronectin free serum and analyzed by time-lapse microscopy for 6 hours A) Three hours after plating cell speed was determined for the following 3 hours. For each pattern (500 nm and 2000nm)  $\geq 40$  cells of three independent experiments were analyzed. B) Cell tracking plots on the 500 nm and the 2000 nm patterns for one of the experiments described in A. C) Differential interference contrast pictures of representative cells on each pattern (500 nm and 2000 nm) are shown. The pictures are taken at 2, 3, 4, 5 and 6 hours after plating. Scale bar is 20  $\mu\text{m}$ .

## VI.4.7 References

- Alexandrova, A. Y., Arnold, K., Schaub, S., Vasiliev, J. M., Meister, J. J., Bershadsky, A. D. and Verkhovsky, A. B. (2008). Comparative dynamics of retrograde actin flow and focal adhesions: formation of nascent adhesions triggers transition from fast to slow flow. *PLoS One* 3, e3234.
- Chiquet-Ehrismann, R., Kalla, P., Pearson, C. A., Beck, K. and Chiquet, M. (1988). Tenascin interferes with fibronectin action. *Cell* 53, 383-90.
- Chiquet, M., Sarasa-Renedo, A. and Tunc-Civelek, V. (2004). Induction of tenascin-C by cyclic tensile strain versus growth factors: distinct contributions by Rho/ROCK and MAPK signaling pathways. *Biochim Biophys Acta* 1693, 193-204.
- Danen, E. H., Sonneveld, P., Brakebusch, C., Fassler, R. and Sonnenberg, A. (2002). The fibronectin-binding integrins alpha5beta1 and alphavbeta3 differentially modulate RhoA-GTP loading, organization of cell matrix adhesions, and fibronectin fibrillogenesis. *J Cell Biol* 159, 1071-86.
- Fernandez-Sauze, S., Grall, D., Cseh, B. and Van Obberghen-Schilling, E. (2009). Regulation of fibronectin matrix assembly and capillary morphogenesis in endothelial cells by Rho family GTPases. *Exp Cell Res* 315, 2092-104.
- Geiger, B., Bershadsky, A., Pankov, R. and Yamada, K. M. (2001). Transmembrane crosstalk between the extracellular matrix--cytoskeleton crosstalk. *Nat Rev Mol Cell Biol* 2, 793-805.
- Geiger, B., Spatz, J. P. and Bershadsky, A. D. (2009). Environmental sensing through focal adhesions. *Nat Rev Mol Cell Biol* 10, 21-33.
- Hall, A. (1998). Rho GTPases and the actin cytoskeleton. *Science* 279, 509-14.
- Harjanto, D. and Zaman, M. H. Matrix mechanics and receptor-ligand interactions in cell adhesion. *Org Biomol Chem* 8, 299-304.
- Huveneers, S., Truong, H., Fassler, R., Sonnenberg, A. and Danen, E. H. (2008). Binding of soluble fibronectin to integrin alpha5 beta1 - link to focal adhesion redistribution and contractile shape. *J Cell Sci* 121, 2452-62.
- Lutz, R., Sakai, T. and Chiquet, M. (2010). Pericellular fibronectin is required for RhoA-dependent responses to cyclic strain in fibroblasts. *J Cell Sci*.
- Machesky, L. M. and Hall, A. (1997). Role of actin polymerization and adhesion to extracellular matrix in Rac- and Rho-induced cytoskeletal reorganization. *J Cell Biol* 138, 913-26.
- Nobes, C. D. and Hall, A. (1995). Rho, rac, and cdc42 GTPases regulate the assembly of multimolecular focal complexes associated with actin stress fibers, lamellipodia, and filopodia. *Cell* 81, 53-62.

Ren, X. D., Kiosses, W. B. and Schwartz, M. A. (1999). Regulation of the small GTP-binding protein Rho by cell adhesion and the cytoskeleton. *EMBO J* 18, 578-85.

Rottner, K., Hall, A. and Small, J. V. (1999). Interplay between Rac and Rho in the control of substrate contact dynamics. *Curr Biol* 9, 640-8.

Sarasa-Renedo, A., Tunc-Civelek, V. and Chiquet, M. (2006). Role of RhoA/ROCK-dependent actin contractility in the induction of tenascin-C by cyclic tensile strain. *Exp Cell Res* 312, 1361-70.

Smith, P. G., Roy, C., Zhang, Y. N. and Chaudhuri, S. (2003). Mechanical stress increases RhoA activation in airway smooth muscle cells. *Am J Respir Cell Mol Biol* 28, 436-42.

Wehrle, B. and Chiquet, M. (1990). Tenascin is accumulated along developing peripheral nerves and allows neurite outgrowth in vitro. *Development* 110, 401-15.

Wierzbicka-Patynowski, I. and Schwarzbauer, J. E. (2003). The ins and outs of fibronectin matrix assembly. *J Cell Sci* 116, 3269-76.

Wolfenson, H., Henis, Y. I., Geiger, B. and Bershadsky, A. D. (2009). The heel and toe of the cell's foot: a multifaceted approach for understanding the structure and dynamics of focal adhesions. *Cell Motil Cytoskeleton* 66, 1017-29.

Zaidel-Bar, R., Cohen, M., Addadi, L. and Geiger, B. (2004). Hierarchical assembly of cell-matrix adhesion complexes. *Biochem Soc Trans* 32, 416-20.

Zamir, E. and Geiger, B. (2001). Molecular complexity and dynamics of cell-matrix adhesions. *J Cell Sci* 114, 3583-90.

Zamir, E., Katz, M., Posen, Y., Erez, N., Yamada, K. M., Katz, B. Z., Lin, S., Lin, D. C., Bershadsky, A., Kam, Z. et al. (2000). Dynamics and segregation of cell-matrix adhesions in cultured fibroblasts. *Nat Cell Biol* 2, 191-6.

## **DISCUSSION**

## V. Discussion

### V.1 Integrating our results

#### in the context of mechanotransduction

Most of our knowledge in mechanotransduction derives from models in which cells are plated on stiff matrices and analyzed in the first hours after plating (for reviews see (Chen, 2008; Chiquet et al., 2009; Geiger et al., 2009)). This approach is based on the fact that ligation of integrins is followed by intracellular signaling (Huveneers et al., 2008; Ren et al., 1999) even without additional external mechanical stimulation. However for cells like fibroblasts this model is quite far away from a physiological condition in which cells are generally spread and attached to a matrix that they secreted and modulated themselves. We therefore use the model of externally applied cyclic strain that allows us to analyze mechanotransduction up to several days after plating. At this time, cells have modulated their matrix and matured their cell adhesions representing a more physiological state.

Involvement of  $\alpha_5\beta_1$  in activation of RhoA during early phases of cell attachment has been demonstrated (Danen et al., 2002; Huveneers et al., 2008). However, we showed here that  $\alpha_5\beta_1$  is not only important in RhoA activation upon plating but plays a general key role in mechanotransduction of fully spread cells. In addition, we demonstrated that activation of RhoA and triggering of RhoA-dependent responses clearly depends on fibronectin. This underlines the intimate relationship of fibronectin with  $\alpha_5\beta_1$  but not  $\alpha_v\beta_3$ . Our findings are strengthened by our observations that  $\alpha_5$  integrin-positive fibrillar adhesions are not formed in the absence of fibronectin while focal adhesions appear normal, indicating that fibrillar adhesions are the key sites of RhoA activation upon mechanical stimulation. Thereby the



machinery for the activation of the RhoA/ROCK pathway by cyclic strain does not start at the cell membrane, but cells project antennas out into the extracellular matrix that are made of fibronectin.

In many cases, however, the approach of analyzing mechanotransduction upon cell plating has its justification. An example for this derives from personal observations that I made working with fibroblasts on different substrates. By culturing fibroblasts on fibronectin substrates cells spread more extensively and form a lot of stress fibers within the first hours after plating pointing to an activated RhoA/ROCK pathway. However on substrates like collagen or vitronectin, cells remain rather small in area and only form little stress fibers. If  $\alpha_5\beta_1$  and fibronectin are required for activation of the RhoA/ROCK pathway one might ask where these stress fibers might come from (even though they are rather thin and little in number). A speculation could be that cells on different substrates modulate their sensitivity in activating the RhoA/ROCK pathway, to compensate for big variations in the amount of fibronectin.

We showed that fibronectin is required for activation of the RhoA/ROCK pathway by cyclic strain. Additionally, in the absence of endogenous and exogenous fibronectin no  $\alpha_5$ -containing fibrillar adhesions were formed, indicating a requirement for fibrillar adhesions and  $\alpha_5\beta_1$  integrin in activation of the RhoA/ROCK pathway upon cyclic strain. If there is a separation in signaling between focal and fibrillar adhesions is not known. We showed that activation of the MAPK- and PKB/Akt-pathway were not affected in the absence of fibronectin and fibrillar adhesions indicating that such signaling could be mediated at focal adhesions by integrin  $\alpha_v\beta_3$ . However there is currently no further evidence for this. Knockdown of vitronectin would make less sense here since  $\alpha_v\beta_3$  binds a variety of different ligands. Knockdown of integrin  $\beta_3$  in fibroblasts, however, could bring more insight.

## V.2 Integrating our results

### in the context of cell adhesion maturation

It is interesting to compare the results of the two main projects and to analyze them in the context of cell spreading. Cells form focal complexes as initial cell-matrix adhesions. On adhesive patterns with a unit size smaller than 1  $\mu\text{m}$ , fibroblasts cannot form mature matrix adhesions. Cells remain with only focal complexes and assume a morphology with many lamellipodia typical for high Rac activity (Nobes and Hall, 1995). This effect is caused only by changing cell-matrix adhesions, indicating that actually focal complexes trigger a Rac-activation that stimulates lamellipodia formation. Focal complexes and Rac could thereby induce themselves in a positive feedback loop. Alternatively, lamellipodia could also be induced indirectly by the missing incorporation of  $\alpha_5\beta_1$  and the lack of active RhoA. Since Rac-1 and RhoA were suggested as antagonistic players (Rottner et al., 1999), low RhoA activation could lead to high levels of Rac-GTP stimulating lamellipodia formation.

In spreading cells with normal cell adhesions, focal complexes recruit (among other factors)  $\alpha_5\beta_1$  integrin. Our results show that  $\alpha_5\beta_1$  and fibronectin are important for activation of the RhoA/ROCK pathway. In fibroblasts RhoA is activated reaching a peak 30-60 minutes after plating on fibronectin (Danen et al., 2002; Ren et al., 1999). Recruitment of  $\alpha_5\beta_1$  and activation upon binding to fibronectin might trigger this RhoA-activation to stimulate actomyosin contraction (Huveneers et al., 2008). Pulling on adhesion sites now allows proteins like p130cas to be phosphorylated upon stretching (Sawada et al., 2006). This again might allow other plaque-proteins to be recruited thereby contributing to adhesion maturation. We noticed that integrin  $\alpha_5\beta_1$  is recruited much earlier to focal complexes if cells were plated on fibronectin than on vitronectin (unpublished observation). This might explain the fact that fibroblasts spread much faster on fibronectin than on other substrates. We also

found that cell spreading can be facilitated and accelerated by addition of fibronectin-free serum especially on substrates other than fibronectin (unpublished observation). In fact serum is known to activate RhoA (Ren et al., 1999) and could thereby compensate for the absence of RhoA-inducing fibronectin.

Actomyosin contraction acting on late focal complexes not only causes maturation into focal adhesions but also induces the separation of fibrillar adhesions. Thereby proteins like  $\alpha_5\beta_1$  and the adaptor protein tensin are pulled out of early focal adhesions to form late focal adhesions and fibrillar adhesions (Zamir et al., 2000). The fact that  $\alpha_5\beta_1$  and tensin are pulled out of early focal adhesions may be explained by the elasticity of fibronectin, the ligand of  $\alpha_5\beta_1$ . Fibronectin is anchored in the extracellular matrix by binding to other proteins like collagens, fibrin, tenascin-C but also proteoglycans (Wierzbicka-Patynowski and Schwarzbauer, 2003). Pulling forces on  $\alpha_5\beta_1$  by actomyosin contraction and anchorage of fibronectin in the matrix elongate the fibronectin molecule to expose self-assembly sites. Binding of other fibronectin molecules in addition with stretching and reorientation could thereby cause the formation and elongation of fibronectin fibrils. Since fibronectin is stretched by the force of actomyosin contraction,  $\alpha_5\beta_1$  bound to the adaptor tensin is pulled in a central direction. Other integrin ligands do not have these stretchable, self-assembling features like fibronectin and are stably anchored in the matrix. Traces of  $\alpha_v\beta_3$  integrin can still be found in fibrillar adhesions. The low affinity binding of fibronectin to  $\alpha_v\beta_3$  (Huvneers et al., 2008) might therefore be an explanation for the high ratio of  $\alpha_5\beta_1$  to  $\alpha_v\beta_3$  in fibrillar adhesions.

Besides the formation of fibronectin fibrils, pulling of  $\alpha_5\beta_1$  integrin towards a more central region of the cell could have another benefit: In a migrating cell, focal complexes are formed at the border of the lamellipodia. Upon recruitment of  $\alpha_5\beta_1$ , focal complexes mature into focal adhesions, which induce actomyosin contraction and are finally pulled towards the cell

center. Thereby also RhoA/ROCK activation would locally move in a proximal direction. Since RhoA and Rac-1 have been postulated to antagonize each other (Rottner et al., 1999), fading RhoA activation would allow high Rac-1-GTP levels to maintain lamellipodial structures at the cell front. In addition, activation of RhoA in the central region of the cell would build up tension to first stabilize the cell and later on to retract the rear part of the cell after disassembling posterior cell adhesions.

Interesting in this respect is also our observation that cell adhesions look different in normal fibroblasts when plated on fibronectin compared to vitronectin (c.f. Fig.9 page 79). It appears that on fibronectin, cells form a hybrid between focal and fibrillar adhesions where vinculin colocalizes with tensin and  $\alpha_5\beta_1$  integrin. It seems plausible that fibroblasts do not need to form fibronectin fibrils if a high amount of accessible fibronectin is already present in the ECM. This raises the question how this mechanism is regulated and whether fibronectin fibrillogenesis is inhibited in the presence of fibrillar fibronectin. However, the absence of fibronectin fibrils and clearly defined fibrillar adhesions on fibronectin substrates could also be an artifact of coated fibronectin. During coating fibronectin might be fixed to the membrane and thereby inhibit fibronectin fibrillogenesis and fibrillar adhesion formation. Nevertheless RhoA is clearly activated by cyclic strain on fibronectin, where cell adhesions form as a hybrid between focal and fibrillar adhesions indicating that  $\alpha_5\beta_1$  does not have to be separated in fibrillar adhesions in mechanotransduction. This, however, is somehow in contradiction to ILK-knockout fibroblasts that also do not separate focal and fibrillar adhesions but are defective in RhoA activation by cyclic strain.

### **V.3 Fibronectin and Rho-dependent responses in cancer**

Activation of RhoA and several RhoA-dependent responses have been implicated in tumor progression and metastasis: Increased RhoA expression was described in various human cancers and often correlated with tumor progression (Karlsson et al., 2009). MAL translocation has been linked with increased expression of  $\beta 1$  integrin and metastasis (Brandt et al., 2009) and tenascin-C is upregulated in all major solid cancers types (Chiquet-Ehrismann and Chiquet, 2003) and has been implicated in metastasis (Tavazoie et al., 2008). Since cyclic stress activates the RhoA pathway it could hypothetically also have an effect on the progression of tumors.

Expression of tenascin-C is high during certain stages of development (Chiquet-Ehrismann and Chiquet, 2003). In healthy adults it is absent or much reduced besides in tendons (Chiquet et al., 2004) where mechanical forces could be the reason for its elevated levels. However, tenascin-C is highly expressed in all major solid cancer types but reasons remain to be unraveled.

In melanomas and glioblastomas, the cancer cells themselves are secreting tenascin-C, whereas in the majority of carcinomas the epithelial cancer cells do not produce tenascin-C, but the cancer-associated fibroblasts of the tumor stroma do (Brellier et al., 2009). A growing tumor exerts mechanical forces to the surrounding tissue and on the cells of the tumor itself. These forces affect intracellular signaling and have been implicated in tumor progression (Butcher et al., 2009). Since tenascin-C is clearly regulated by tensile stress (Chiquet et al., 2004; Fluck et al., 2000), one could speculate that the increased tenascin-C levels found in solid tumors may be due to mechanical forces exerted by the growing tumor on the tumor cells itself or its associated stromal fibroblasts.

Levels of tenascin-C also correlate with metastasis. Downregulation of tenascin-C by miRNA in primary tumors was shown to decrease their ability to colonize the lungs (Tavazoie et al., 2008). Interesting is also the fact that glioblastomas, known to be aggressive and invasive tumors, strongly express tenascin-C, whereas oligodendrogliomas, which are non-invasive, do not or only slightly express tenascin-C. In our experiments we found that tenascin-C in the substrate reduced RhoA activation by cyclic strain. It has been shown before that inhibiting RhoA leads to a disassembly of focal adhesions (Chrzanowska-Wodnicka and Burridge, 1996). Thereby excessive tenascin-C could loosen cell-matrix attachment and facilitate migration and metastasis of cancer cells. However, levels of active RhoA are rather elevated in tumor cells compared to normal cells (Fritz et al., 1999). In fact, increased expression levels of RhoA were described in many human tumors. This correlated with tumor progression (Karlsson et al., 2009). In these cells RhoA levels were not only elevated but RhoA activity was also increased. This might be a reason for the fact that tumors are stiffer than normal tissues and cells are characterized by an altered tissue tensional homeostasis (Paszek et al., 2005). The rigidity of tumors and embedded cells may enhance tumor metastasis. We here confirm that the activation of RhoA correlated with translocation of MAL (Miralles et al., 2003). A recent publication now links MAL translocation to upregulation of  $\beta 1$  integrin and invasion (Brandt et al., 2009).

Taken together activation of RhoA, translocation of MAL and upregulation of tenascin-C are all implicated in tumor progression. We here show that upon induction by cyclic strain, all these events depend on the presence of fibronectin. Interestingly, increased fibronectin expression in tumor matrices is associated with poor prognosis (Yao et al., 2007) and increased mortality (Ioachim et al., 2002). Our results suggest a link between fibronectin in the tumor stroma, the increased activation of RhoA and RhoA-dependent responses and tumor progression.

# **APPENDIX**

## VI. Appendix

### VI.1 References

Alam, N., Goel, H. L., Zarif, M. J., Butterfield, J. E., Perkins, H. M., Sansoucy, B. G., Sawyer, T. K. and Languino, L. R. (2007). The integrin-growth factor receptor duet. *J Cell Physiol* 213, 649-53.

Alberts, J., Walter, Lewis, Raff, Roberts. (2008). In *Molecular Biology of the Cell*. New York: Garland Science, Taylor & Francis Group.

Alexandrova, A. Y., Arnold, K., Schaub, S., Vasiliev, J. M., Meister, J. J., Bershadsky, A. D. and Verkhovsky, A. B. (2008). Comparative dynamics of retrograde actin flow and focal adhesions: formation of nascent adhesions triggers transition from fast to slow flow. *PLoS One* 3, e3234.

Amma, H., Naruse, K., Ishiguro, N. and Sokabe, M. (2005). Involvement of reactive oxygen species in cyclic stretch-induced NF-kappaB activation in human fibroblast cells. *Br J Pharmacol* 145, 364-73.

Arber, S., Barbayannis, F. A., Hanser, H., Schneider, C., Stanyon, C. A., Bernard, O. and Caroni, P. (1998). Regulation of actin dynamics through phosphorylation of cofilin by LIM-kinase. *Nature* 393, 805-9.

Asparuhova, M. B., Gelman, L. and Chiquet, M. (2009). Role of the actin cytoskeleton in tuning cellular responses to external mechanical stress. *Scand J Med Sci Sports*.

Ballestrem, C., Hinz, B., Imhof, B. A. and Wehrle-Haller, B. (2001). Marching at the front and dragging behind: differential alphaVbeta3-integrin turnover regulates focal adhesion behavior. *J Cell Biol* 155, 1319-32.

Bernard, O. (2007). Lim kinases, regulators of actin dynamics. *Int J Biochem Cell Biol* 39, 1071-6.



- Bosman, F. T. and Stamenkovic, I. (2003). Functional structure and composition of the extracellular matrix. *J Pathol* 200, 423-8.
- Brandt, D. T., Baarlink, C., Kitzing, T. M., Kremmer, E., Ivaska, J., Nollau, P. and Grosse, R. (2009). SCAI acts as a suppressor of cancer cell invasion through the transcriptional control of beta1-integrin. *Nat Cell Biol* 11, 557-68.
- Brellier, F., Tucker, R. P. and Chiquet-Ehrismann, R. (2009). Tenascins and their implications in diseases and tissue mechanics. *Scand J Med Sci Sports* 19, 511-9.
- Butcher, D. T., Alliston, T. and Weaver, V. M. (2009). A tense situation: forcing tumour progression. *Nat Rev Cancer* 9, 108-22.
- Chardin, P., Boquet, P., Madaule, P., Popoff, M. R., Rubin, E. J. and Gill, D. M. (1989). The mammalian G protein rhoC is ADP-ribosylated by Clostridium botulinum exoenzyme C3 and affects actin microfilaments in Vero cells. *EMBO J* 8, 1087-92.
- Chen, C. S. (2008). Mechanotransduction - a field pulling together? *J Cell Sci* 121, 3285-92.
- Chiquet-Ehrismann, R. (2004). Tenascins. *Int J Biochem Cell Biol* 36, 986-90.
- Chiquet-Ehrismann, R. and Chiquet, M. (2003). Tenascins: regulation and putative functions during pathological stress. *J Pathol* 200, 488-99.
- Chiquet-Ehrismann, R., Kalla, P., Pearson, C. A., Beck, K. and Chiquet, M. (1988). Tenascin interferes with fibronectin action. *Cell* 53, 383-90.
- Chiquet, M. and Fambrough, D. M. (1984). Chick myotendinous antigen. II. A novel extracellular glycoprotein complex consisting of large disulfide-linked subunits. *J Cell Biol* 98, 1937-46.
- Chiquet, M., Gelman, L., Lutz, R. and Maier, S. (2009). From mechanotransduction to extracellular matrix gene expression in fibroblasts. *Biochim Biophys Acta* 1793, 911-20.

- Chiquet, M., Sarasa-Renedo, A. and Tunc-Civelek, V. (2004). Induction of tenascin-C by cyclic tensile strain versus growth factors: distinct contributions by Rho/ROCK and MAPK signaling pathways. *Biochim Biophys Acta* 1693, 193-204.
- Chiquet, M., Tunc-Civelek, V. and Sarasa-Renedo, A. (2007). Gene regulation by mechanotransduction in fibroblasts. *Appl Physiol Nutr Metab* 32, 967-73.
- Chrzanowska-Wodnicka, M. and Burridge, K. (1996). Rho-stimulated contractility drives the formation of stress fibers and focal adhesions. *J Cell Biol* 133, 1403-15.
- Cramer, L. P., Siebert, M. and Mitchison, T. J. (1997). Identification of novel graded polarity actin filament bundles in locomoting heart fibroblasts: implications for the generation of motile force. *J Cell Biol* 136, 1287-305.
- Danen, E. H., Sonneveld, P., Brakebusch, C., Fassler, R. and Sonnenberg, A. (2002). The fibronectin-binding integrins alpha5beta1 and alphavbeta3 differentially modulate RhoA-GTP loading, organization of cell matrix adhesions, and fibronectin fibrillogenesis. *J Cell Biol* 159, 1071-86.
- Etienne-Manneville, S. and Hall, A. (2002). Rho GTPases in cell biology. *Nature* 420, 629-35.
- Fernandez-Sauze, S., Grall, D., Cseh, B. and Van Obberghen-Schilling, E. (2009). Regulation of fibronectin matrix assembly and capillary morphogenesis in endothelial cells by Rho family GTPases. *Exp Cell Res* 315, 2092-104.
- Fischer, D., Brown-Ludi, M., Schulthess, T. and Chiquet-Ehrismann, R. (1997). Concerted action of tenascin-C domains in cell adhesion, anti-adhesion and promotion of neurite outgrowth. *J Cell Sci* 110 ( Pt 13), 1513-22.
- Fluck, M., Tunc-Civelek, V. and Chiquet, M. (2000). Rapid and reciprocal regulation of tenascin-C and tenascin-Y expression by loading of skeletal muscle. *J Cell Sci* 113 ( Pt 20), 3583-91.
- Friedland, J. C., Lee, M. H. and Boettiger, D. (2009). Mechanically activated integrin switch controls alpha5beta1 function. *Science* 323, 642-4.

Fritz, G., Just, I. and Kaina, B. (1999). Rho GTPases are over-expressed in human tumors. *Int J Cancer* 81, 682-7.

Geiger, B., Bershadsky, A., Pankov, R. and Yamada, K. M. (2001). Transmembrane crosstalk between the extracellular matrix--cytoskeleton crosstalk. *Nat Rev Mol Cell Biol* 2, 793-805.

Geiger, B., Spatz, J. P. and Bershadsky, A. D. (2009). Environmental sensing through focal adhesions. *Nat Rev Mol Cell Biol* 10, 21-33.

George, E. L., Georges-Labouesse, E. N., Patel-King, R. S., Rayburn, H. and Hynes, R. O. (1993). Defects in mesoderm, neural tube and vascular development in mouse embryos lacking fibronectin. *Development* 119, 1079-91.

Hall, A. (1998). Rho GTPases and the actin cytoskeleton. *Science* 279, 509-14.

Harjanto, D. and Zaman, M. H. Matrix mechanics and receptor-ligand interactions in cell adhesion. *Org Biomol Chem* 8, 299-304.

Horton, M. A. (1997). The alpha v beta 3 integrin "vitronectin receptor". *Int J Biochem Cell Biol* 29, 721-5.

Huang, W., Chiquet-Ehrismann, R., Moyano, J. V., Garcia-Pardo, A. and Orend, G. (2001). Interference of tenascin-C with syndecan-4 binding to fibronectin blocks cell adhesion and stimulates tumor cell proliferation. *Cancer Res* 61, 8586-94.

Huveneers, S., Truong, H., Fassler, R., Sonnenberg, A. and Danen, E. H. (2008). Binding of soluble fibronectin to integrin alpha5 beta1 - link to focal adhesion redistribution and contractile shape. *J Cell Sci* 121, 2452-62.

Inoh, H., Ishiguro, N., Sawazaki, S., Amma, H., Miyazu, M., Iwata, H., Sokabe, M. and Naruse, K. (2002). Uni-axial cyclic stretch induces the activation of transcription factor nuclear factor kappaB in human fibroblast cells. *FASEB J* 16, 405-7.

Ioachim, E., Charchanti, A., Briasoulis, E., Karavasilis, V., Tsanou, H., Arvanitis, D. L., Agnantis, N. J. and Pavlidis, N. (2002). Immunohistochemical expression of extracellular matrix components tenascin, fibronectin, collagen type IV and laminin in breast cancer: their prognostic value and role in tumour invasion and progression. *Eur J Cancer* 38, 2362-70.

Karlsson, R., Pedersen, E. D., Wang, Z. and Brakebusch, C. (2009). Rho GTPase function in tumorigenesis. *Biochim Biophys Acta* 1796, 91-8.

Kippenberger, S., Loitsch, S., Guschel, M., Muller, J., Knies, Y., Kaufmann, R. and Bernd, A. (2005). Mechanical stretch stimulates protein kinase B/Akt phosphorylation in epidermal cells via angiotensin II type 1 receptor and epidermal growth factor receptor. *J Biol Chem* 280, 3060-7.

Kjaer, M. (2004). Role of extracellular matrix in adaptation of tendon and skeletal muscle to mechanical loading. *Physiol Rev* 84, 649-98.

Lehoux, S., Castier, Y. and Tedgui, A. (2006). Molecular mechanisms of the vascular responses to haemodynamic forces. *J Intern Med* 259, 381-92.

Li, C. and Xu, Q. (2000). Mechanical stress-initiated signal transductions in vascular smooth muscle cells. *Cell Signal* 12, 435-45.

Luo, B. H., Carman, C. V. and Springer, T. A. (2007). Structural basis of integrin regulation and signaling. *Annu Rev Immunol* 25, 619-47.

Lutz, R., Sakai, T. and Chiquet, M. (2010). Pericellular fibronectin is required for RhoA-dependent responses to cyclic strain in fibroblasts. *J Cell Sci*.

Machesky, L. M. and Hall, A. (1997). Role of actin polymerization and adhesion to extracellular matrix in Rac- and Rho-induced cytoskeletal reorganization. *J Cell Biol* 138, 913-26.

Magnusson, S. P., Narici, M. V., Maganaris, C. N. and Kjaer, M. (2008). Human tendon behaviour and adaptation, in vivo. *J Physiol* 586, 71-81.

Maier, S., Lutz, R., Gelman, L., Sarasa-Renedo, A., Schenk, S., Grashoff, C. and Chiquet, M. (2008). Tenascin-C induction by cyclic strain requires integrin-linked kinase. *Biochim Biophys Acta*.

Midwood, K. S. and Schwarzbauer, J. E. (2002). Tenascin-C modulates matrix contraction via focal adhesion kinase- and Rho-mediated signaling pathways. *Mol Biol Cell* 13, 3601-13.

Midwood, K. S., Valenick, L. V., Hsia, H. C. and Schwarzbauer, J. E. (2004). Coregulation of fibronectin signaling and matrix contraction by tenascin-C and syndecan-4. *Mol Biol Cell* 15, 5670-7.

Millard, T. H., Sharp, S. J. and Machesky, L. M. (2004). Signalling to actin assembly via the WASP (Wiskott-Aldrich syndrome protein)-family proteins and the Arp2/3 complex. *Biochem J* 380, 1-17.

Miralles, F., Posern, G., Zaromytidou, A. I. and Treisman, R. (2003). Actin dynamics control SRF activity by regulation of its coactivator MAL. *Cell* 113, 329-42.

Munevar, S., Wang, Y. L. and Dembo, M. (2004). Regulation of mechanical interactions between fibroblasts and the substratum by stretch-activated Ca<sup>2+</sup> entry. *J Cell Sci* 117, 85-92.

Nagai, T., Yamakawa, N., Aota, S., Yamada, S. S., Akiyama, S. K., Olden, K. and Yamada, K. M. (1991). Monoclonal antibody characterization of two distant sites required for function of the central cell-binding domain of fibronectin in cell adhesion, cell migration, and matrix assembly. *J Cell Biol* 114, 1295-305.

Nobes, C. D. and Hall, A. (1995). Rho, rac, and cdc42 GTPases regulate the assembly of multimolecular focal complexes associated with actin stress fibers, lamellipodia, and filopodia. *Cell* 81, 53-62.

Nobes, C. D. and Hall, A. (1999). Rho GTPases control polarity, protrusion, and adhesion during cell movement. *J Cell Biol* 144, 1235-44.

Pankov, R. and Yamada, K. M. (2002). Fibronectin at a glance. *J Cell Sci* 115, 3861-3.

Paszek, M. J., Zahir, N., Johnson, K. R., Lakins, J. N., Rozenberg, G. I., Gefen, A., Reinhart-King, C. A., Margulies, S. S., Dembo, M., Boettiger, D. et al. (2005). Tensional homeostasis and the malignant phenotype. *Cancer Cell* 8, 241-54.

Paterson, H. F., Self, A. J., Garrett, M. D., Just, I., Aktories, K. and Hall, A. (1990). Microinjection of recombinant p21rho induces rapid changes in cell morphology. *J Cell Biol* 111, 1001-7.

Pellegrin, S. and Mellor, H. (2007). Actin stress fibres. *J Cell Sci* 120, 3491-9.

Posern, G., Miralles, F., Guettler, S. and Treisman, R. (2004). Mutant actins that stabilise F-actin use distinct mechanisms to activate the SRF coactivator MAL. *EMBO J* 23, 3973-83.

Posern, G. and Treisman, R. (2006). Actin' together: serum response factor, its cofactors and the link to signal transduction. *Trends Cell Biol* 16, 588-96.

Ratnikov, B. I., Partridge, A. W. and Ginsberg, M. H. (2005). Integrin activation by talin. *J Thromb Haemost* 3, 1783-90.

Reichardt, L. (1999). Composition and function of the extracellular matrix. In *Extracellular Matrix, Anchor, and Adhesion Proteins*, (ed. T. a. V. Kreis, R), pp. 335-342. Oxford, UK: Sambrook & Tooze publication at Oxford University Press.

Ren, X. D., Kiosses, W. B. and Schwartz, M. A. (1999). Regulation of the small GTP-binding protein Rho by cell adhesion and the cytoskeleton. *EMBO J* 18, 578-85.

Ridley, A. J., Paterson, H. F., Johnston, C. L., Diekmann, D. and Hall, A. (1992). The small GTP-binding protein rac regulates growth factor-induced membrane ruffling. *Cell* 70, 401-10.

Riveline, D., Zamir, E., Balaban, N. Q., Schwarz, U. S., Ishizaki, T., Narumiya, S., Kam, Z., Geiger, B. and Bershadsky, A. D. (2001). Focal contacts as mechanosensors: externally applied local mechanical force induces growth of focal contacts by an mDia1-dependent and ROCK-independent mechanism. *J Cell Biol* 153, 1175-86.

Rottner, K., Hall, A. and Small, J. V. (1999). Interplay between Rac and Rho in the control of substrate contact dynamics. *Curr Biol* 9, 640-8.

Rychly, J., Pommerenke, H., Durr, F., Schreiber, E. and Nebe, B. (1998). Analysis of spatial distributions of cellular molecules during mechanical stressing of cell surface receptors using confocal microscopy. *Cell Biol Int* 22, 7-12.

Sakai, T., Johnson, K. J., Murozono, M., Sakai, K., Magnuson, M. A., Wieloch, T., Cronberg, T., Isshiki, A., Erickson, H. P. and Fassler, R. (2001). Plasma fibronectin supports neuronal

survival and reduces brain injury following transient focal cerebral ischemia but is not essential for skin-wound healing and hemostasis. *Nat Med* 7, 324-30.

Sarasa-Renedo, A., Tunc-Civelek, V. and Chiquet, M. (2006). Role of RhoA/ROCK-dependent actin contractility in the induction of tenascin-C by cyclic tensile strain. *Exp Cell Res* 312, 1361-70.

Sawada, Y., Tamada, M., Dubin-Thaler, B. J., Cherniavskaya, O., Sakai, R., Tanaka, S. and Sheetz, M. P. (2006). Force sensing by mechanical extension of the Src family kinase substrate p130Cas. *Cell* 127, 1015-26.

Schwartz, I., Seger, D. and Shaltiel, S. (1999). Vitronectin. *Int J Biochem Cell Biol* 31, 539-44.

Sinha, S. and Yang, W. (2008). Cellular signaling for activation of Rho GTPase Cdc42. *Cell Signal* 20, 1927-34.

Smith, M. L., Gourdon, D., Little, W. C., Kubow, K. E., Eguiluz, R. A., Luna-Morris, S. and Vogel, V. (2007). Force-induced unfolding of fibronectin in the extracellular matrix of living cells. *PLoS Biol* 5, e268.

Smith, P. G., Roy, C., Zhang, Y. N. and Chaudhuri, S. (2003). Mechanical stress increases RhoA activation in airway smooth muscle cells. *Am J Respir Cell Mol Biol* 28, 436-42.

Takenawa, T. and Miki, H. (2001). WASP and WAVE family proteins: key molecules for rapid rearrangement of cortical actin filaments and cell movement. *J Cell Sci* 114, 1801-9.

Tavazoie, S. F., Alarcon, C., Oskarsson, T., Padua, D., Wang, Q., Bos, P. D., Gerald, W. L. and Massague, J. (2008). Endogenous human microRNAs that suppress breast cancer metastasis. *Nature* 451, 147-52.

Wang, D., Chang, P. S., Wang, Z., Sutherland, L., Richardson, J. A., Small, E., Krieg, P. A. and Olson, E. N. (2001). Activation of cardiac gene expression by myocardin, a transcriptional cofactor for serum response factor. *Cell* 105, 851-62.

Watanabe, N., Kato, T., Fujita, A., Ishizaki, T. and Narumiya, S. (1999). Cooperation between mDia1 and ROCK in Rho-induced actin reorganization. *Nat Cell Biol* 1, 136-43.

- Wehrle, B. and Chiquet, M. (1990). Tenascin is accumulated along developing peripheral nerves and allows neurite outgrowth in vitro. *Development* 110, 401-15.
- Wenk, M. B., Midwood, K. S. and Schwarzbauer, J. E. (2000). Tenascin-C suppresses Rho activation. *J Cell Biol* 150, 913-20.
- Wheeler, A. P. and Ridley, A. J. (2004). Why three Rho proteins? RhoA, RhoB, RhoC, and cell motility. *Exp Cell Res* 301, 43-9.
- White, E. S., Baralle, F. E. and Muro, A. F. (2008). New insights into form and function of fibronectin splice variants. *J Pathol* 216, 1-14.
- Wierzbicka-Patynowski, I. and Schwarzbauer, J. E. (2003). The ins and outs of fibronectin matrix assembly. *J Cell Sci* 116, 3269-76.
- Wolfenson, H., Henis, Y. I., Geiger, B. and Bershadsky, A. D. (2009). The heel and toe of the cell's foot: a multifaceted approach for understanding the structure and dynamics of focal adhesions. *Cell Motil Cytoskeleton* 66, 1017-29.
- Woods, A. and Couchman, J. R. (1994). Syndecan 4 heparan sulfate proteoglycan is a selectively enriched and widespread focal adhesion component. *Mol Biol Cell* 5, 183-92.
- Yao, E. S., Zhang, H., Chen, Y. Y., Lee, B., Chew, K., Moore, D. and Park, C. (2007). Increased beta1 integrin is associated with decreased survival in invasive breast cancer. *Cancer Res* 67, 659-64.
- Zaidel-Bar, R., Ballestrem, C., Kam, Z. and Geiger, B. (2003). Early molecular events in the assembly of matrix adhesions at the leading edge of migrating cells. *J Cell Sci* 116, 4605-13.
- Zaidel-Bar, R., Cohen, M., Addadi, L. and Geiger, B. (2004). Hierarchical assembly of cell-matrix adhesion complexes. *Biochem Soc Trans* 32, 416-20.
- Zamir, E. and Geiger, B. (2001). Molecular complexity and dynamics of cell-matrix adhesions. *J Cell Sci* 114, 3583-90.



Zamir, E., Katz, M., Posen, Y., Erez, N., Yamada, K. M., Katz, B. Z., Lin, S., Lin, D. C., Bershadsky, A., Kam, Z. et al. (2000). Dynamics and segregation of cell-matrix adhesions in cultured fibroblasts. *Nat Cell Biol* 2, 191-6.

Zimmerman, E., Geiger, B. and Addadi, L. (2002). Initial stages of cell-matrix adhesion can be mediated and modulated by cell-surface hyaluronan. *Biophys J* 82, 1848-57.

## VI.3 Abbreviations

BSAC	basic, SAP, and coiled-coil domain
CHB	cell and heparin binding domain (of fibronectin)
Coll	collagen
COX	cyclooxygenase
DH	DBI homology
DMEM	Dulbecco's modified Eagle medium
ECM	extracellular matrix
EGFR	epidermal growth factor receptor
ERK	extracellular signal-regulated kinase
F-actin	filamentous actin
FAK	focal adhesion kinase
FCS	fetal calf serum
FN	fibronectin
FNIII13	fibronectin type III repeat nr13
G-actin	globular actin
GAG	glycosaminoglycan
GAP	GTPase-activating protein
GAPDH	glyceraldehyde 3-phosphate dehydrogenase
GDI	guanosine nucleotide dissociation inhibitor
GEF	guanine nucleotide exchange factor
IKK	I $\kappa$ B kinase
ILK	integrin linked kinase
MAL	megakaryocytic acute leukemia
MEF	mouse embryo fibroblasts
MKL1	megakaryoblastic leukemia 1
MRTF-A	myocardin-related transcription factor A
PBS	phosphate-buffered saline
PG	plain gold
PH	pleckstrin homology
PKB	protein kinase B
REF	rat embryo fibroblast
TCF	ternary complex factor
TnC	tenascin-C
WT	wild type
RGD	arginine-glycine-aspartate
SRF	serum response factor

## VI.2 Curriculum vitae

### Personal

Name, first name: Lutz, Roman  
Date of birth: 29.07.1981  
Place of Birth: Zürich, Switzerland  
Nationality: Swiss  
Marital status: Single  
Languages: German (native), English (fluent), French (intermediate)  
Home Address: Güterstrasse 180, CH-4053 Basel, Switzerland  
Phone: +78 703 40 34  
E-mail address: [roman.lutz@fmi.ch](mailto:roman.lutz@fmi.ch)

### Educational background

Oct 2006 – Jul 2010: PhD Studies in Cell Biology at the University of Basel, Switzerland  
Oct 2004 – Feb 2006: Master in Biochemistry  
Biozentrum, University of Basel, Switzerland  
Oct 2001 – Oct 2004: Bachelor in Molecular Biology  
Biozentrum, University of Basel, Switzerland  
Mai 2001 – Oct 2001: International Language School, San Diego, USA  
Aug 1997 – Mai 2001: Kantonsschule Typus C (Mathematics, Science), Zofingen AG

### Work experience

Oct 2006 – present: International PhD program at the Friedrich Miescher Institute (FMI), Basel, Switzerland, Group of Dr. Ruth Chiquet-Ehrismann  
Mar 2006 – Jun 2006: Practical in the laboratory of Prof. M. Spiess  
Oct 2004 – Feb 2005: Master Thesis at the Biozentrum, University of Basel, Switzerland, Group of Prof. M. Spiess

### Teaching experience

Oct 2009 – Jan 2010: Tutorial for biology students (Introduction in Biology), Biozentrum, Basel, Switzerland  
Feb 2005 – Mar 2006: Teaching in the Biochemistry block course for biology students, Biozentrum, Basel, Switzerland  
Dec 1998 – Feb 2001: Teaching for scholars in the subject chemistry, physics and biology

**Publications and scientific contributions:**

- Posters: Union of the Swiss Societies for Experimental Biology (USGEB)  
february 6-7 2008, Lausanne, Switzerland.  
FMI annual meeting, September 2007, Grindelwald, Switzerland  
FMI annual meeting, September 2008, Grindelwald, Switzerland  
Keystone Symposia – Mechanotransduction in Physiology and  
disease, January 2010, Taos, NM, USA  
FMI annual meeting, September 2009, Basel, Switzerland
- Talk: “Pericellular fibronectin is required for RhoA-dependent responses to  
cyclic strain in fibroblasts”,  
Cytomeet, January 2010, Bern, Switzerland
- Publications: Limiting growth of focal complexes inhibits their maturation and  
induces lamellipodia formation  
Lutz R, Pataky K, Brugger J, Chiquet M  
(Ready for submission)
- Pericellular fibronectin is required for RhoA-dependent responses to  
cyclic strain in fibroblasts.  
Lutz R, Sakai T, Chiquet M.  
J Cell Sci. 2010
- Identification of a fibronectin interaction site in the extracellular  
matrix protein ameloblastin.  
Beyeler M, Schild C, Lutz R, Chiquet M, Trueb B.  
Exp Cell Res. 2010
- From mechanotransduction to extracellular matrix gene expression in  
fibroblasts.  
Chiquet M, Gelman L, Lutz R, Maier S.  
Biochim Biophys Acta. 2008
- Tenascin-C induction by cyclic strain requires integrin-linked kinase.  
Maier S, Lutz R, Gelman L, Sarasa-Renedo A, Schenk S, Grashoff C,  
Chiquet M.  
Biochim Biophys Acta. 2008